

UNIVERSITÄTSKLINIKUM HAMBURG-EPPENDORF

Institut für Medizinische Mikrobiologie, Virologie und Hygiene

Prof. Dr. med. Martin Aepfelbacher

Visualization of effector protein
translocation and pore formation during
Yersinia enterocolitica infection of cells

Dissertation

zur Erlangung des Doktorgrades Dr. rer. biol. hum.
an der Medizinischen Fakultät der Universität Hamburg.

vorgelegt von:

Maren Rudolph

aus Bremen

Hamburg 2020

Dissertation zur Erlangung der Würde des Doktors der Humanbiologie der Medizinischen Fakultät der Universität Hamburg vorgelegt von Maren Rudolph aus Bremen. Hamburg 2020.

Angenommen von der Medizinischen Fakultät am: 06.08.2020

Veröffentlicht mit Genehmigung der Medizinischen Fakultät der Universität Hamburg

Prüfungsausschuss, der/die Vorsitzende: Prof. Dr. Martin Aepfelbacher

Prüfungsausschuss, 2. Gutachter/in: Prof. Dr. Hans-Willi Mittrücker

Table of contents

| | | |
|----------|--|----|
| 1. | Abstract | 1 |
| 1.1. | Abstract | 1 |
| 1.2. | Zusammenfassung..... | 2 |
| 2. | Introduction..... | 3 |
| 2.1. | Pathogenic <i>Yersinia</i> | 3 |
| 2.2. | Characteristics of enteropathogenic <i>Yersinia</i> | 4 |
| 2.2.1. | Classification..... | 4 |
| 2.2.2. | Yersiniosis..... | 5 |
| 2.2.3. | Pathogenesis and route of infection | 5 |
| 2.3. | Virulence strategies of pathogenic <i>Yersinia</i> | 6 |
| 2.3.1. | Chromosomal and plasmid-encoded virulence factors..... | 6 |
| 2.3.2. | The type three secretion system..... | 7 |
| 2.3.3. | Effector proteins..... | 10 |
| 2.3.4. | Regulation of translocation | 13 |
| 2.4. | Pathogen-host cell interaction | 14 |
| 2.4.1. | Interaction of host cell factors with <i>Yersinia</i> containing compartments | 14 |
| 2.5. | Protein tagging for fluorescence microscopy..... | 17 |
| 2.5.1. | Challenges and solutions for visualizing translocated bacterial proteins | 17 |
| 2.5.2. | Detection in cell lysates or entire host cell | 17 |
| 2.5.3. | Tags enabling protein localization in the host cell | 19 |
| 2.5.3.1. | Imaging limited to fixed samples..... | 19 |
| 2.5.3.2. | Protein tags compatible with live cell imaging..... | 19 |
| 2.5.4. | Selection of tag position for <i>Yersinia</i> outer proteins | 25 |
| 2.5.5. | CRISPR-Cas12a assisted recombination | 27 |
| 3. | Aims | 31 |
| 4. | Results | 33 |
| 4.1. | Tagging of effector proteins with Halo, SNAP, CLIP or split-GFP | 34 |
| 4.1.1. | Halo, SNAP and CLIP tags affect the secretion and translocation of effector proteins and thereby reduce cytotoxicity | 35 |
| 4.1.2. | YopE, YopH and YopM can be visualized with Halo, SNAP and CLIP tags within the bacterium but not in the cytosol of the host cell | 39 |

| | |
|--|----|
| 4.1.3. Split-GFP inserted between two proteins (mRFP-GFP11-Rab5) can induce a signal in GFP1-10 transfected cells | 41 |
| 4.1.4. Tagging YopE with split-GFP reveals limited effect on effector secretion | 42 |
| 4.1.5. YopE-GFP11 can be visualized in the cytosol of the host cell transfected with GFP1-10 | 43 |
| 4.1.6. A GFP signal is detectable in live imaging experiments after infection with pTTSS+YopE-GFP11 | 45 |
| 4.2. Tagging of pore proteins | 46 |
| 4.2.1. CRISPR-Cas12a is a useful tool for insertion of small DNA fragments into the virulence plasmid of <i>Yersinia enterocolitica</i> | 47 |
| 4.2.2. YopB remains functional after split-GFP insertion while YopD function is affected..... | 48 |
| 4.2.3. No fluorescent signal is detectable with split-GFP tagged YopB/D during infection of GFP1-10 expressing cells..... | 50 |
| 4.2.4. YopD is functional with the ALFA-tag inserted between amino acids 194 and 195 | 50 |
| 4.2.5. YopD in translocons can be visualized using the ALFA-tag and staining with nanobodies..... | 52 |
| 4.2.6. Pore formation can be visualized with YopD-ALFA during live imaging..... | 55 |
| 4.2.7. Translocon formation is preceded by enrichment of PI(4,5)P2 in the host membrane enclosing the bacteria | 56 |
| 4.2.8. Galectin-3 recruitment to translocon induced membrane damage | 57 |
| 5. Discussion | 61 |
| 5.1. Halo, SNAP and CLIP tags are incompatible for translocation through the needle of the injectisome | 61 |
| 5.2. GFP11 is a useful tag for visualizing effector translocation but not pore formation..... | 62 |
| 5.3. CRISPR-Cas12a is a highly efficient tool for inserting small DNA fragments into the virulence plasmid of <i>Yersinia enterocolitica</i> | 65 |
| 5.4. Varying effect of tag insertion in different sites on protein function of translocators YopB and YopD | 67 |
| 5.5. The ALFA-tag allows visualization of both intrabacterial YopD as well as YopD as part of the TTSS pore..... | 68 |
| 5.6. PI(4,5)P2 presence precedes pore formation | 69 |
| 5.7. Pore formation rapidly induces membrane damage | 70 |
| 6. Material and methods..... | 72 |
| 6.1. Materials..... | 72 |
| 6.1.1. Devices..... | 72 |
| 6.1.2. Microscopes | 73 |
| 6.1.3. Disposables..... | 75 |

| | |
|--|-----|
| 6.1.4. Buffers and reagents | 77 |
| 6.1.5. Antibodies..... | 78 |
| 6.1.6. Nanobodies, dyes and labeling substrates..... | 79 |
| 6.1.7. Growth media and additives | 80 |
| 6.1.8. Plasmids..... | 81 |
| 6.1.9. Primer | 82 |
| 6.1.10. <i>Yersinia</i> strains and eukaryotic cells..... | 85 |
| 6.1.11. Data processing | 88 |
| 6.2. Methods | 89 |
| 6.2.1. Microbiological methods..... | 89 |
| 6.2.1.1. Cultivation and strain maintenance of <i>Yersinia enterocolitica</i> | 89 |
| 6.2.1.2. Released protein assay | 89 |
| 6.2.1.3. <i>Yersinia</i> infection | 90 |
| 6.2.1.4. Preparation and transformation of chemically competent bacteria | 90 |
| 6.2.1.5. Preparation and transformation of electrocompetent bacteria | 91 |
| 6.2.2. Cell culture..... | 91 |
| 6.2.2.1. Cultivation of eukaryotic cells | 91 |
| 6.2.2.2. Cryoconservation and reactivation of eukaryotic cell lines | 92 |
| 6.2.2.3. Transfection of HeLa cells..... | 92 |
| 6.2.2.4. CNF-1 treatment of HeLa cells..... | 92 |
| 6.2.2.5. Isolation and cultivation of primary human macrophages | 92 |
| 6.2.2.6. Transfection of primary human macrophages..... | 93 |
| 6.2.3. Molecular biology techniques | 93 |
| 6.2.3.1. Isolation of plasmid DNA | 93 |
| 6.2.3.2. Determination of DNA concentration | 93 |
| 6.2.3.3. Polymerase chain reaction | 93 |
| 6.2.3.4. Restriction enzyme digest | 95 |
| 6.2.3.5. Agarose gel electrophoresis | 95 |
| 6.2.3.6. Ligation | 96 |
| 6.2.3.7. Generation of expression vectors and CRISPR vectors and fragments used in this study. | 96 |
| 6.2.3.8. CRISPR-Cas12a-assisted recombineering | 99 |
| 6.2.3.9. DNA sequencing | 101 |
| 6.2.4. Proteinbiochemical methods | 101 |

| | |
|---|-----|
| 6.2.4.1. Affinity purification of antibodies from serum | 101 |
| 6.2.4.2. Protein expression and purification | 102 |
| 6.2.4.3. Translocation assay | 102 |
| 6.2.4.4. Pull down assay | 103 |
| 6.2.4.5. Determination of protein concentration..... | 103 |
| 6.2.4.6. SDS-polyacrylamide gel electrophoresis (SDS-PAGE)..... | 104 |
| 6.2.4.7. Coomassie staining of SDS-polyacrylamide gels | 104 |
| 6.2.4.8. Western blot analysis | 104 |
| 6.2.5. Microscopy | 105 |
| 6.2.5.1. Immunofluorescence staining | 105 |
| 6.2.5.2. Substrate staining (Halo/SNAP/CLIP/ALFA)..... | 106 |
| 6.2.5.3. Confocal microscopy | 107 |
| 6.2.5.4. Live cell imaging | 107 |
| 7. Literature | 108 |
| 8. Table of figures..... | 146 |
| 9. List of tables..... | 147 |
| 10. Abbreviations | 148 |
| 11. Acknowledgement..... | 152 |
| 12. Lebenslauf | 154 |
| 13. Eidesstattliche Versicherung | 155 |

1. Abstract

1.1. Abstract

Yersinia enterocolitica employs a type three secretion system (TTSS; injectisome) in order to translocate effector proteins into host cells. The effectors (*Yersinia* outer proteins, Yops H,O,P,E,M,T and Q) manipulate host cell functions to support the infection strategy of the bacteria. Extensive research elucidated the function and structure of the TTSS and to a lesser extent of the associated translocation pore. The two pore proteins (YopB, YopD) are translocated themselves by the TTSS and then form a heterodimeric pore complex in the host cell membrane that acts as an entry gate for the bacterial effectors. Until now, a real time visualization of translocation pore formation or effector protein translocation in host cells by an active TTSS has been very challenging. Several approaches have been developed in this regard but most displayed critical limitations such as incompatibility with live cell imaging, insufficient resolution and sensitivity or disturbance of protein and TTSS function.

In this study different approaches for visualizing pore- and effector proteins of *Y. enterocolitica* injectisomes in action were investigated. Tagging of the effectors YopH, YopM and YopE with the self-labeling enzymes Halo, SNAP and CLIP showed a strong inhibitory effect on overall Yop secretion and translocation. In comparison, a split-GFP approach for tagging YopE allowed the visualization of YopE translocation into HeLa cells and primary human macrophages. However, tagging of the pore proteins YopB and YopD with the smaller part of split-GFP did not produce satisfactory results. Finally, by employing a CRISPR-Cas12a assisted recombination approach a small peptide tag (ALFA-tag) was inserted into a region of the YopD protein that is thought to lie extracellularly when Yop is integrated in the translocation pore. In a cell infection assay using *Y. enterocolitica* expressing ALFA-tagged YopD and an extracellularly applied fluorophore-labeled nanobody, the nanobody allowed live cell imaging of nascent and seemingly fully functional translocation pores. Thus, this assay allowed for the first time the visualization of injectisomes while forming translocation pores during cell infection. Onset of pore formation occurred directly after uptake of the bacteria into a PI(4,5)P₂-enriched prevacuole. After maturation of the bacteria-containing prevacuole into a phagosome, damaging of the phagosomal membrane by the bacterial pores could be visualized with help of the marker protein GFP-galectin-3. Altogether this work allowed for the first time to visualize in real time the formation of TTSS translocation pores.

1.2. Zusammenfassung

Yersinia enterocolitica verwendet ein Typ-3-Sekretionssystem (TTSS; Injektisom), um Effektorproteine in Wirtszellen zu translozieren. Die Effektoren (*Yersinia* outer proteins, Yops H,O,P,E,M,T und Q) manipulieren Funktionen der Wirtszelle, um die Infektionsstrategie des Bakteriums zu unterstützen. Umfangreiche Forschungsarbeiten haben die Funktion und Struktur des TTSS und in geringerem Maße der angehefteten Translokationspore untersucht. Die beiden Porenproteine (YopB, YopD) werden durch das TTSS selbst transloziert und bilden dann einen heterodimeren Porenkomplex in der Wirtszellmembran als der als Eintrittspforte für die bakteriellen Effektoren dient. Bisher war die Echtzeit-Visualisierung der Porenbildung bzw. der Effektorprotein-Translokation in Wirtszellen nur schwer möglich. Es wurden mehrere Ansätze entwickelt, die meisten zeigten jedoch kritische Einschränkungen wie Inkompatibilität mit der Bildgebung in lebenden Zellen, unzureichende Auflösung und Empfindlichkeit oder Störung der Protein- und TTSS-Funktionen.

In dieser Studie wurden verschiedene Ansätze zur Visualisierung von Poren- und Effektorproteinen von *Y. enterocolitica* Injektisomen untersucht. Die Markierung der Effektoren YopH, YopM und YopE mit den selbstmarkierenden Enzymen Halo, SNAP und CLIP zeigte eine starke hemmende Wirkung auf die gesamte Yop-Sekretion und -Translokation. Im Vergleich dazu erlaubte ein Split-GFP-Ansatz zur Markierung von YopE die Visualisierung der YopE-Translokation in HeLa-Zellen und primären menschlichen Makrophagen. Die Markierung der Porenproteine YopB und YopD mit dem kleineren Teil des Split-GFP erwies sich jedoch als ungeeignet. Schließlich wurde mit Hilfe eines CRISPR-Cas12a-assistierten Rekombinationsansatzes ein kleiner Peptid-Tag (ALFA-Tag) an einer Stelle von YopD eingefügt, die vermutlich im extrazellulären Teil des Proteins liegt, wenn dieses eine Translokationspore in der Wirtszellmembran gebildet hat. In einem Zellinfektionsversuch mit *Y. enterocolitica*, das ALFA-gekoppelte YopD exprimiert und einem extrazellulär applizierten Fluorophor-markierten Nanokörper, konnten naszierende und funktionelle Translokationsporen sichtbar gemacht werden. Damit ermöglichte dieser Assay zum ersten Mal die Live-Bildgebung von Injektisomen bei der Bildung von Translokationsporen während einer Zellinfektion. Der Beginn der Porenbildung erfolgte direkt nach der Aufnahme der Bakterien in eine PI(4,5)P₂-angereicherte Prä-Vakuole. Nach Reifung der bakterienhaltigen Prä-Vakuole zu einem Phagosom konnte mit Hilfe des Markerproteins GFP-Galectin-3 eine Schädigung der Phagosomenmembran durch die bakteriellen Poren sichtbar gemacht werden. Insgesamt ermöglichte diese Arbeit zum ersten Mal die Echtzeit-Visualisierung der Bildung von TTSS-Translokationsporen während der Wirtszellinfektion.

2. Introduction

2.1. Pathogenic *Yersinia*

The genus *Yersinia* belongs to the family of Yersiniaceae and comprises 18 different species of which only three are pathogenic to humans: *Yersinia pestis*, *Yersinia pseudotuberculosis* and *Yersinia enterocolitica* (Adeolu et al. 2016; McNally et al. 2016). *Y. pestis* causes bubonic, septicemic and pneumonic plague and was first isolated from human tissue in independent studies by Alexandre Yersin and Shibasaburo Kitasato in 1894 in Hongkong (Treille and Yersin 1894; Kitasato 1894; Bibel and Chen 1976). The enteropathogenic bacteria *Y. pseudotuberculosis* and *Y. enterocolitica* are transferred through contaminated food and water and cause gastrointestinal diseases (Carniel 2002). While *Y. pseudotuberculosis* is primarily found on carrots and lettuce *Y. enterocolitica* infections often originate from contaminated pork meat (Jalava et al. 2006; Bottone 1997; Grahek-Ogden et al. 2007). Enteropathogenic *Yersinia* are the third most common cause of gastroenteritis in Europe after *Campylobacter* and *Salmonella* (Rosner et al. 2010; van Pelt et al. 2003; McNally et al. 2016). The gastrointestinal symptoms resulting from an *Yersinia* infection are termed yersiniosis. The majority of recorded cases is caused by *Y. enterocolitica* while only a small number of yersiniosis cases are due to *Y. pseudotuberculosis*. The infection is usually self-limiting and rarely leads to systemic infections or sepsis.

An infection with *Y. pestis* leads to the bubonic or pneumonic plague which if untreated is fatal in 50 – 60% or 100% respectively (Groß 2006). Although the disease is no acute threat anymore, as it can be treated with antibiotics, several plague cases are recorded each year (Cornelis 2002a). The plague is a zoonotic disease with rodents as hosts and fleas as carriers (Madigan and Martinko 2009). The bite of the rat flea can transmit the disease to humans, although today infections usually arise from contact to infected or dead rodents. The bacteria can enter through skin injuries from where they colonize the lymphatic tissue which causes swelling. Via the blood circulation the infection can spread to inner organs (Kayser et al. 2001). When the lungs are infected the disease is fatal within 1-3 days and a transmission of the disease from human to human via droplet infection is possible (Cornelis 2002b).

Although *Y. pseudotuberculosis* and *Y. pestis* have different pathogenesis and routes of infection, studies of the genomes have shown they are closely related. All three pathogenic *Yersinia* species have a common ancestor from which *Y. enterocolitica* split off about 200 million years ago. *Y. pestis* developed from *Y. pseudotuberculosis* between 1 500 – 20 000 years ago (Achtman et al. 1999). This process involved the loss and gain of genes and the rearrangement of the genome (Wren 2003; Achtman et al. 1999).

All pathogenic *Yersinia* share a tropism for lymphatic tissue and are able to resist the innate immune response of the host (Cornelis and Wolf-Watz 1997). Their virulence factors are both encoded on the chromosome as well as on plasmids. The 70 kb virulence plasmid termed pYV (plasmid of *Yersinia* virulence) can be found in all three pathogenic *Yersinia* species and encodes proteins of the type three secretion system (TTSS) and the effector proteins called Yops (*Yersinia* outer proteins). The TTSS enables the translocation of effector proteins from bacteria to the cytosol of the host cell where they prevent phagocytosis and suppress the innate immune response (Viboud and Bliska 2005; Pha and Navarro 2016). *Y. pestis* possesses two additional plasmids which enable the development from a gastrointestinal pathogen to a blood-borne pathogen transmitted by a vector. The plasmid pFra/pMT1 (100 – 110 kb) encodes the F1 capsular protein and the *Yersinia* murine toxin (Ymt), which is a phospholipase D and allows the survival in the flea gut (Hu et al. 1998; Brubaker 1991). This plasmid shows a recent ancestry to *Salmonella* enterica serovar Typhimurium, an exclusively human pathogen (Prentice et al. 2001). The other plasmid pPst/pPCP1 (9.5 kb) enables the dissemination via the subcutaneous route through the plasminogen activator Pla.

2.2. Characteristics of enteropathogenic *Yersinia*

2.2.1. Classification

Yersinia are Gram negative pleomorphic rods and belong to the family of Yersiniaceae (Adeolu et al. 2016). The ubiquitous pathogens have a facultative anaerobe metabolism, are catalase positive, oxidase negative, ferment glucose and do not form endospores under starvation conditions (Fredriksson-Ahomaa 2007). *Yersinia* spp. can multiply at a wide temperature range between 0 – 40°C although optimal conditions for growth are 24 – 27°C. Studies have shown that *Yersinia* form peritrichous flagella at 22 – 30°C (Kapatral and Minnich 1995; Bleves et al. 2002; Freund et al. 2008).

Yersinia enterocolitica can be divided into 6 biovars (1A, 1B, 2-5) by different biochemical reactions and is further differentiated in 50 serotypes through antigenic variations in cell wall lipopolysaccharides (Wauters et al. 1971; Aleksić and Bockemühl 1984). This highly heterogenic species is characterized by their different geographical spread, ecological niches and pathogenic characteristics. The only apathogenic biovar is 1A which does not possess a virulence plasmid (Bottone 1999). The most common isolates from humans are serotypes O:3, O:8 and O:9 while bioserovar 4/O:3 is the most dominant yersiniosis agent in Europe and North America (Pavlidis et al. 2019). However, especially severe cases are caused by bioserovar 1B/O:8, which is endemic to North America with travel-associated cases found in Europe (Wren 2003). The highly pathogenic phenotype of this bioserovar is conveyed by a cluster of genes termed high pathogenicity island (HPI) encoding for an iron-acquisition system (Carniel et al. 1996). This system allows

bacteria to absorb and utilize iron mediated by iron-chelating compounds promoting their ability to grow under iron-limiting conditions in host tissues (Carniel 1999).

2.2.2. Yersiniosis

Y. enterocolitica mediated yersiniosis is one of the most common notifiable bacterial zoonoses in the European Union after campylobacteriosis and salmonellosis (Bottone 1997). Yersiniosis caused by *Y. enterocolitica* makes up 99% of cases while only a few cases are down to *Y. pseudotuberculosis* infections (ECDC 2019). *Y. enterocolitica* is mostly harbored by mammals including wildlife and farm animals. Thus, yersiniosis is mainly transmitted through uptake of pork and pork products, unpasteurized milk or contaminated water (Shayegani et al. 1981; Carniel et al. 2006). In rare cases yersiniosis was caused by blood transfusions (Jacobs et al. 1989; Strobel et al. 2000). An inoculum of at least 10^9 organisms is necessary to cause the disease (Schaake et al. 2014).

The clinical picture of infection depends on the age and physical condition of the patient or on the pathogenic properties of the infecting strain. Generally, symptoms develop 4-7 days after exposure lasting for 1 – 3 weeks, are usually self-limiting and do not require antibiotic treatment (Rosner et al. 2012; CDC 2016). They involve abdominal pain and a mild fever which in young children is usually accompanied by diarrhea. The cause of these symptoms is a gastrointestinal infection including enteritis, terminal ileitis or mesenteric lymphadenitis (Gurry 1974; Puylaert 1986; Galindo et al. 2011). Infections occasionally lead to extraintestinal complications such as reactive arthritis or erythema nodosum post-infection (Luqmani and Dawes 1986; Rosner et al. 2013). In immunocompromised patients or individuals with states of iron overload such as hemolytic anemia the infection can develop into septicemia resulting in an overall fatality rate for yersiniosis of 0.08% (Bottone 1997; ECDC 2019). Generally, small children under 4 years show much higher infection rates compared to adults. Yersiniosis presents throughout the year and is most common in Europe with about 7000 confirmed cases a year, the majority of which occurring in Germany (Galindo et al. 2011; ECDC 2019). Although this can be due to frequency and method of diagnosis, more accurate reporting or prevalence of *Yersinia* in animal reservoirs, the source could also be the higher consumption of meat in Germany including uncooked pork meat (Rosner et al. 2010).

2.2.3. Pathogenesis and route of infection

Infection with *Y. enterocolitica* occurs through the fecal-oral route through uptake into the gastrointestinal tract. The pathogen can protect itself against the acidic stomach environment through the production of urease, which hydrolyses urea producing carbonic acid and ammonia resulting in an increased pH level (Koning-Ward and Robins-Browne 1995; Gripenberg-Lerche et al. 2000; Bhagat and Viridi 2009). In the intestine *Yersinia* have to pass the gastrointestinal mucus and before mainly interacting with the follicle

associated epithelium (FAE) of the ileum covering Peyer's patches which are accumulated lymphoid follicles and form a part of the gut associated lymphoid tissue (Autenrieth and Firsching 1996; Autenrieth et al. 1996). The expression of the invasin and ail proteins facilitates the attachment and invasion of M-cells (microfold cells) overlaying Peyer's patches (Hanski et al. 1989; Grützkau et al. 1990; Pepe and Miller 1993; Felek and Krukonis 2008). Invasin binding to integrin receptors induces restructuring of the actin cytoskeleton enabling uptake of *Yersinia* (Pepe and Miller 1993). Mouse experiments have shown destruction of Peyer's patches and FAE after 5-7 days (Autenrieth and Firsching 1996). Through translocation of antiphagocytic effector proteins *Yersinia* manipulate the host's immune response and allow extracellular survival and replication in the lymphatic tissue. Additionally, they are known to form microcolonies resistant against phagocytosis from macrophages and neutrophils (Cornelis et al. 1998; Viboud and Bliska 2005; Aepfelbacher et al. 2007). From the Peyer's patches *Yersinia* spread to mesenteric lymph nodes via blood and lymphatics and can further disseminate to inner organs such as liver and spleen (Pepe and Miller 1993; Pepe et al. 1995; Cornelis and Wolf-Watz 1997; Trülsch et al. 2007).

2.3. Virulence strategies of pathogenic *Yersinia*

2.3.1. Chromosomal and plasmid-encoded virulence factors

Pathogenicity of *Y. enterocolitica* requires both chromosomal and plasmid encoded genes promoting bacterial survival in the host (Atkinson and Williams 2016). The expression is regulated by environmental signals such as temperature which is the main expression regulator. Lower temperatures between 25 – 28°C mostly promote expression of chromosomal genes while a shift to 37°C in the mammalian host induces expression of plasmid encoded genes (Cornelis et al. 1987; Rouvroit et al. 1992).

The chromosomal factors mediate mainly the bacterial survival during early infection stages and facilitate the invasion of the pathogen into the host cells (Straley and Perry 1995). Adhesion and bacterial uptake necessary for passage of intestinal epithelial cells is mediated by adhesins which are bacterial outer membrane proteins covering the surface of the bacterium (Grosdent et al. 2002). The adhesion protein invasin is the major bacterial factor binding to β -integrin initiating a signaling cascade resulting in actin polymerization enabling bacterial uptake into the host cell. Invasins are highly expressed at lower temperatures (25 – 28°C) while their expression is limited at higher temperatures (Simonet and Falkow 1992). Another factor mediating adhesion is the chromosome-encoded Ail (attachment invasion locus) which is expressed at 30 – 37°C (Miller and Falkow 1988; Miller et al. 1990). Ail mediates bacterial invasion and confers resistance to complement killing (Bliska and Falkow 1992; Pierson and Falkow 1993). Expression of surface virulence markers such as invasin are regulated by Hfq chaperone influencing transcription of regulator RovA which induces *invA* expression (Kakoschke et al. 2016). The *Yersinia*

chromosome also encodes for the heat-stable enterotoxin Yst (*Yersinia* stable toxin) which is possibly an endogenous activator of intestinal guanylate cyclase inducing diarrhea (Pai and Mors 1978; Delor and Cornelis 1992). Only the highly infectious *Y. enterocolitica* biotype 1B possesses the HPI mediating iron capture from the host environment (Carniel et al. 1996; Carniel 1999). The development of flagella on the bacterial surface encoded by flagellin genes *fleABC* is transcribed at 25°C but not 37°C and is relevant for establishing contact to the target cell (Kapatral and Minnich 1995; Young et al. 2000).

While chromosomal factors mediate attachment and invasion, plasmid factors establish and sustain infection. The virulence plasmid of *Y. enterocolitica* called pYV (plasmid of *Yersinia* virulence) is a 70 kb plasmid encoding for TTSS proteins Ysc (*Yersinia* secretion) and Yop (*Yersinia* outer proteins) and adhesin YadA (*Yersinia* adhesin A). These proteins are essential for pathogenicity and are regulated by temperature and calcium presence (Horne and Prüss 2006). The virulence regulon transcriptional activator VirF is expressed at 37°C and suppressed by YmoA encoded on the chromosome (Cornelis et al. 1991; Rouvroit et al. 1992; Bancercz-Kisiel et al. 2018). Ysc proteins mainly form the basal body and the needle complex of the injectisome, while the tip complex and translocon are formed by LcrV, YopB and YopD (Cornelis 2002a). The injectisome is required for Yop effector protein translocation into the host cell suppressing the host innate immune response (Cornelis 2002b; Viboud and Bliska 2005; Pujol and Bliska 2005). YadA is a plasmid-encoded adhesin expressed at 37°C which forms a fibrillar matrix on the bacterial surface (Mühlenkamp et al. 2015). It mediates the indirect binding to integrins on host cells through proteins of the extracellular matrix (Deuschle et al. 2016).

Interestingly, in *Y. pseudotuberculosis* an increase in virulence plasmids number was detected under infection conditions (Wang et al. 2016). However, only the synergy of both chromosomal as well as plasmid encoded virulence factors allows the full extent of *Yersinia* pathogenicity.

2.3.2. The type three secretion system

The type three secretion system is a bacterial nanomachine used for the injection of effector proteins from Gram-negative bacteria into host cells and is therefore called injectisome. It was first described in *Yersinia* in 1994 by Rosqvist and colleagues (Rosqvist et al. 1994). Although seven different secretion systems have been defined, TTSS has the widest prevalence among bacterial species and is the best researched in comparison (Tseng et al. 2009; Costa et al. 2015; Green and Meccas 2016). The TTSS displays a high conservation between bacteria of different species. Generally, three different versions can be distinguished including the Ysc injectisome in *Yersinia*, *Pseudomonas* and *Aeromonas*, the Inv-Mxi injectisome in *Chlamydia*, *Salmonella* SPI-1 and *Shigella* and the Ssa-Esc injectisome in *E. coli* and *Salmonella* SPI-2 (Cornelis and van Gijsegem 2000; Troisfontaines and Cornelis 2005; Mota et al. 2005;

Cornelis 2006; Diepold and Armitage 2015). Interestingly, some species possess more than one injectisome variant. *Yersinia* biovar 1B for example has a chromosomally encoded Ysa TTSS with an unidentified role in addition to its Ysc injectisome (Young and Young 2002; Foutier et al. 2003). For better comparability a unified Sct (secretion and cellular translocation) nomenclature for components of the TTSS from different bacteria strains was developed (Hueck 1998; Deng et al. 2017; Dos Santos et al. 2020). This nomenclature is used in Figure 1 showing the general structure of TTSS and a translation to the *Yersinia* Ysc nomenclature is supplied in the figure legend below.

The injectisome is evolutionarily related to the flagellum with which it shares structural and functional similarities (Diepold and Armitage 2015). It is a multiprotein structure of about 6 Mda with 20 subunits formed during the infection process (Zilkenat et al. 2016). Its major components are sorting platform, basal body, needle, tip complex and translocon. The basal body spans the inner and outer bacterial membrane with protein rings while the needle with its tip complex connects bacterium and host cell and the translocon is inserted into the hosts plasma membrane. Scaffolding proteins form the outer part of the basal body with YscC creating a ring structure in the outer bacterial membrane reaching into the periplasm and YscJ and YscD creating a ring in the inner bacterial membrane (Koster et al. 1997; Hodgkinson et al. 2009; Diepold et al. 2010; Ross and Plano 2011). The export apparatus on the inside of the basal body is assembled by YscR, YscS, YscT, YscU and YscV (Wagner et al. 2010). YscQ constitutes the cytoplasmic ring (c-ring) and YscL and YscK together the sorting platform at the cytosolic side of the TTSS responsible for recruitment of chaperone substrate complexes regulating order of export (Lara-Tejero et al. 2011). YscN forms the ATPase complex and similar to YscQ, YscL and YscK is a cytosolic component which can be both bound to the injectisome as well as free in the bacterial cytoplasm (Lara-Tejero et al. 2011; Diepold et al. 2015; Diepold et al. 2017; Zhang et al. 2017). YscI allows the transport of proteins through the inner membrane (inner rod) while YscF polymerises to a helical needle complex (Hoiczyk and Blobel 2001; Marlovits et al. 2004; Marlovits et al. 2006; Hu et al. 2018; Miletic et al. 2019). The length of the needle depends on the species and its surface proteins and can vary between 30 and 80 nm (Kubori et al. 1998; Blocker et al. 2001; Hoiczyk and Blobel 2001; Poyraz et al. 2010; Cordes et al. 2003; Marlovits et al. 2006; Miletic et al. 2019). In *Y. pestis* the needle has a length of approximately 41 nm and in *Y. enterocolitica* of 58 nm (Journet et al. 2003). The proximal end of the needle is equipped with the tip complex comprised of the hydrophilic translocator LcrV (low calcium response protein V) forming a pentameric platform for the assembly of the pore by the hydrophobic translocators YopB (42 kDa) and YopD (33 kDa) in the host plasma membrane (Håkansson et al. 1996; Blocker et al. 1999; Neyt and Cornelis 1999; Warawa et al. 1999; Mueller et al. 2005; Broz et al. 2007; Mueller et al. 2008). The complex is predicted to be hexadecameric with alternating hydrophobic translocators (Romano et al. 2016). All three translocators

and their chaperones (SycB and LcrG) are encoded on the same operon *lcrGVHyopBD* (Bergman et al. 1991; Håkansson et al. 1993; Mattei et al. 2011).

The genes encoding for the TTSS are expressed at 37°C at millimolar calcium concentrations (Straley et al. 1993). These conditions represent cell contact as the cytoplasm has lower calcium concentrations than the extracellular environment (Kim et al. 2005). The increased TTSS gene expression, decreased bacterial growth and secretion of effector proteins upon calcium depletion *in vitro* has been termed low calcium response (LCR) (Brubaker and Surgalla 1964; Straley and Bowmer 1986; Michiels et al. 1990; Straley et al. 1993; Fowler and Brubaker 1994; Fowler et al. 2009). Secretion and translocation of Yops *in vivo* is induced by cell contact. Secretion of components is highly regulated on different levels and its correct order is important for pathogenicity (Dewoody et al. 2013). The insertion of inner and outer membrane rings of the basal body into bacterial membranes requires the Sec pathway and is therefore called Sec dependent phase (Deng et al. 2017). It is characterized by cleavable amino-terminal secretion signals on the ring components (Kubori et al. 2000; Kimbrough and Miller 2000). In TTSS phase the ATPase complex localizes to export apparatus and C-Ring allowing secretion of early substrates for the formation of the inner rod and needle, the translocators as middle substrates and the effector proteins as late substrates (Dewoody et al. 2013; Dos Santos et al. 2020). Export of components of the injectisome, translocators and effector proteins is regulated by binding of chaperones in the bacterial cytoplasm (chaperone class 3, 2, 1 respectively) (Wattiau et al. 1994; Neyt and Cornelis 1999; Foultier et al. 2003; Akeda and Galán 2005). Proteins have to be released from their chaperone and unfolded by the hexamer ATPase YscN for translocation through the needle (Akeda and Galán 2005; Sorg et al. 2006; Roblin et al. 2015). Export is driven by proton motive force similar to the flagellar movement (Blair 2003; Wilharm et al. 2004). YscL has been shown to act as a negative regulator of YscN (Minamino and MacNab 2000; Blaylock et al. 2006). As both needle and pore have a small diameter (2 – 3 and 2 – 4 nm, respectively), protein unfolding is crucial for translocation (Blocker et al. 2001; Kubori et al. 1998; Hoiczky and Blobel 2001; Journet et al. 2003). The translocators are secreted irrespective of cell contact upon proteolytic cleavage of YscU through interaction with YscP after needle formation (Edqvist et al. 2003; Lavander et al. 2003; Sorg et al. 2006; Riordan and Schneewind 2008). Cell contact is required for secretion of the effector proteins as late stage Yops. Without cell contact in the presence of calcium the secretion is blocked by a “calcium plug” of YopN-TyeA-YscB-SycN (Day and Plano 1998; Ferracci et al. 2005; Joseph and Plano 2013). In an environment lacking calcium or during cell contact YopN is released removing the plug (Dewoody et al. 2013).

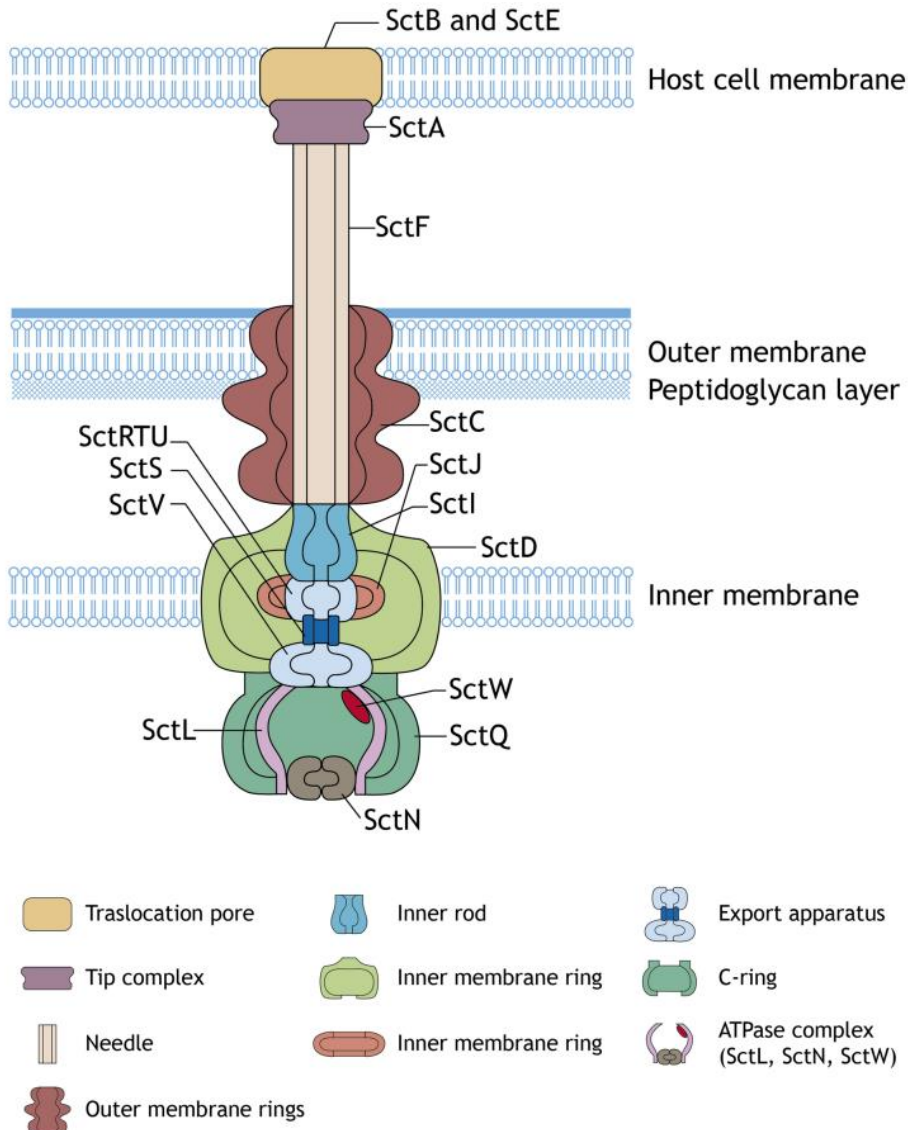


Figure 1 Structure of type three secretion system. For comparability between different strains the unified nomenclature Sct (secretion and cellular translocation (Hueck 1998)) for different TTSS components followed by a specific suffix is used. From top to bottom (protein in *Y. enterocolitica*): translocators SctB/E (YopB/D) forming the translocation pore and SctA (LcrV) the tip complex at the proximal end of a SctF needle (YscF), the outer bacterial membrane is spanned by a SctC membrane ring (YscC), the inner bacterial membrane spanned by SctD/SctJ membrane rings (YscD/YscJ), the SctI inner rod (YscI) connects the needle with the export apparatus which is formed by SctR, SctT, SctU, SctS, SctV (YscR, YscS, YscT, YscU and YscV), the SctQ C-ring (YscQ) is connected to the SctN ATPase complex with the stator SctL (YscN, YscL) and the SctW gatekeeper (YopN). This figure is adapted from (Dos Santos et al. 2020).

2.3.3. Effector proteins

Yersinia possesses six effector proteins YopE, YopH, YopM, YopT, YopO and YopP which directly interact with host proteins upon translocation (Cornelis 2002b; Fahlgren et al. 2009; Bliska et al. 2013; Pha and Navarro 2016). These effectors imitate cellular proteins such as kinases, phosphatases or proteases to

inhibit phagocytosis by manipulating the actin cytoskeletal structures and to downregulate proinflammatory responses (Pha and Navarro 2016). YopH, YopE, YopT and YopO are involved in influencing phagocytosis by manipulating the cytoskeleton. With the exception of YopH, this is mediated by direct interaction with Rho-GTPases (Barbieri et al. 2002; Grosdent et al. 2002; Aepfelbacher 2004). The effectors YopM, YopP and YopH modulate the inflammatory response (Cornelis 2002b). Similarly, the potential seventh effector YopQ known to regulate translocation by interacting with translocators, has later been shown to prevent activation of the inflammasome (Bliska et al. 2013). Together, the action of these Yops contributes to *Yersinia* resisting phagocytosis and evading the host immune response promoting bacterial survival and enabling extracellular proliferation.

As a potent protein tyrosine phosphatase **YopH** (50 kDa) has a strong antiphagocytic function and thereby promotes bacterial survival (Guan and Dixon 1990; Zhang et al. 1992; Andersson et al. 1996). The catalytic domain of YopH is located at the C-terminus and resembles eukaryotic phosphatases (Zhang 1995; Phan et al. 2003; Sun et al. 2003). It dephosphorylates adaptor proteins involved in formation of focal adhesion points including Crk associated tyrosine kinase substrate (p130^{Cas}), focal adhesion kinase (FAK), Paxillin, Fyn-binding protein (FyB) and SKAP-HOM (Andersson et al. 1996; Persson et al. 1997; Aepfelbacher 2004; Viboud and Bliska 2005). This function inhibits phagocytosis by disruption of actin structures necessary for the uptake of bacteria (Evdokimov et al. 2002; Andersson et al. 1996). The signaling cascade induced by invasin mediated binding of β 1-integrin receptors is blocked by YopH which counteracts recognition by the host (Aepfelbacher et al. 2007). Bacterial survival is further supported through inhibition of calcium signaling in neutrophils mediating degranulation of immune cells (Persson et al. 1999; Andersson et al. 1999). YopH has further been shown to prevent T-cell activation and production of cytokine CC chemokine ligand 2 produced by macrophages inhibiting proliferation of lymphocytes and recruitment of macrophages (Yao et al. 1999; Sauvonnet et al. 2002).

Leucine-rich protein **YopM** is a major conveyor of *Yersinia* virulence and is found in the cytosol and nucleus of the host cell (Leung et al. 1990; Skrzypek et al. 1998; Benabdillah et al. 2004). YopM is less conserved between *Yersinia* species compared to other Yops caused by the varying numbers of leucine-rich-repeats resulting in range of molecular weights (*Y. pestis* 41.6 kDa, *Y. enterocolitica* 56.9 kDa) (Boland et al. 1998; Cornelis et al. 1998). Although no enzymatic activity could be detected for YopM, it still proved important for the establishment of infection (Leung et al. 1990; Höfling et al. 2015). The immunosuppressive effect of YopM is mediated by its binding to host cell kinases such as the serine/threonine kinases RSK1 (p90 ribosomal S6 kinase 1; MAPKAP-K1) and PKN2 (protein kinase N2; protein kinase C related kinase2/PRK2) resulting in their activation (McDonald et al. 2003; Hentschke et al. 2010). YopM is probably transported into the nucleus by vesicle-associated transport (Skrzypek et al. 1998; Benabdillah et al. 2004). In the

nucleus YopM influences IL-10 transcription through phosphorylation of RSK and its export is regulated by interaction with DEAD-box helicase 3 (DDX3) (Berneking et al. 2016). In addition, it also reduces transcription of several other proinflammatory cytokines through an unknown mechanism (Kerschen et al. 2004; McPhee et al. 2010; Berneking et al. 2016). Interestingly, YopM has been shown to act as a caspase-1 inhibitor blocking the formation of the mature inflammasome promoting *Yersinia* survival (LaRock and Cookson 2012).

YopE (23 kDa) is a GTPase-activating effector protein which facilitates the hydrolysis of GTP to GDP with its conserved arginine finger domain mimicking the host GTPase activating protein (GAP) (Black and Bliska 2000). Binding of YopE to the plasma membrane and unidentified perinuclear compartments is mediated by a membrane localization domain (MLD) containing a hydrophobic leucine-rich motif (Krall et al. 2004; Zhang and Barbieri 2005; Isaksson et al. 2009; Auerbuch et al. 2009). While *in vivo* YopE enables inactivation of Rac1 and RhoA, an additional inhibitory effect on CDC42 was detected *in vitro* (Black and Bliska 2000; Andor et al. 2001). The YopE mediated GAP activity causes disruption of the actin cytoskeleton resulting in reduced phagocytosis (Andor et al. 2001). An additional function of YopE is the negative regulation of pore formation and translocation (Aili et al. 2006; Viboud et al. 2006; Mejía et al. 2008; Isaksson et al. 2009; Gaus et al. 2011; Aepfelbacher et al. 2011). Especially in YopE deletion mutants an uncontrolled effector expression and a strong hypertranslocation was detected under infection conditions (Aili et al. 2008; Gaus et al. 2011; Wolters et al. 2013). As no direct interaction of YopE with the translocon was detected, the effect is thought to be indirectly mediated by the manipulation of the cytoskeleton (Dewoody et al. 2013).

The cysteine protease **YopT** (35.5 kDa) mediates the release of Rho GTPases from membranes by cleaving off the C-terminus resulting in their inactivation (Black and Bliska 2000; Shao et al. 2003; Wang et al. 2014; Chung et al. 2016). This causes disruption of actin filaments and induces cytotoxicity (Iriarte and Cornelis 1998). The formation of actin cups during bacterial uptake is affected as well as the assembly of focal adhesion structures required for pseudopodia formation and migration of macrophages (Aepfelbacher 2004; Shao et al. 2003). In contrast to YopE, YopT does not inactivate Rac1 or Cdc42 *in vivo* but prefers RhoA (Aepfelbacher et al. 2003).

YopO (*Yersinia* protein kinase A (Ypka) in *Y. pestis* and *Y. pseudotuberculosis*; 81.7 kDa) is a multi-domain protein which possesses an N-terminal serine/threonine kinase module and a C-terminal GTPase interaction domain (Galyov et al. 1993; Prehna et al. 2006). Both domains mediate the inactivation of the Rho GTPases RhoA and Rac1 affecting the actin cytoskeleton (Groves et al. 2008). YopO remains inactive while inside the bacterium and is activated by binding of globular actin upon translocation into the host cell (Galyov et al. 1993; Trasak et al. 2007). Cellular factors for actin polymerization required for

phagocytosis are recruited by YopO bound to actin and are inactivated by phosphorylation (Lee et al. 2015).

YopP (YopJ in *Y. pseudotuberculosis* and *Y. pestis*; 32.5 kDa) functions as a serine/threonine/lysine acetyltransferase reducing the host inflammatory response (Paquette et al. 2012; Mittal et al. 2006; Mukherjee et al. 2006). It inhibits proinflammatory signaling by preventing NFkB and mitogen-activated protein (MAP) kinase signaling cascades (Orth et al. 2000; Zhou et al. 2005; Mittal et al. 2006; Mukherjee et al. 2006; Sweet et al. 2007). The inhibition of the MAP kinase pathway in macrophages induces apoptosis through suppression of proinflammatory cytokines (Palmer et al. 1998; Schesser et al. 1998; Orth et al. 2000; Zhang et al. 2005). YopP has also been shown to inhibit caspase-1 in macrophages preventing innate immune response (Schoberle et al. 2016). Interestingly, YopP appears conserved in many animal and plant pathogens showing the importance of its role in infection (Ma et al. 2006; Ma and Ma 2016; Lewis et al. 2011).

YopQ (YopK in *Y. pseudotuberculosis* and *Y. pestis*, 21 kDa) is a strong negative regulator of translocation. YopQ/K mutants are characterized by an accelerated cytotoxic response in cell culture infection experiments due to increased delivery of the remaining effector proteins (Holmström et al. 1997). It was shown that in *Y. pestis* YopK exerts its negative effect on Yop translocation from inside the target cell through binding of YopK to the translocon component YopD (Dewoody et al. 2011). Importantly, in mouse infection experiments YopQ/K mutants were essentially avirulent, showing severe colonization and dissemination defects (Straley and Cibull 1989; Holmström et al. 1995a, 1995b). YopK additionally displays a downregulation of caspase-1 activation and IL-1 β secretion preventing inflammasome activation similar to YopM (Brodsky et al. 2010).

2.3.4. Regulation of translocation

Several bacterial and host cellular factors have been shown to be involved in regulation of Yop translocation. While the inhibitory effect on translocation of YopQ is possibly mediated through its interaction with YopD, effectors YopE, YopT and YopO reduce translocation through their manipulation and inactivation of Rho GTPase activity. The Rho GTP-binding protein activation by the toxins cytotoxic necrotizing factor-Y (CNF-Y) of *Y. pseudotuberculosis* and CNF-1 of *E. coli* was shown to significantly increase effector translocation (Wolters et al. 2013). CNF-Y displayed a preference for RhoA, while CNF-1 was reported to activate RhoA, Rac1 and CDC42 both in cell cultures and in cells (Hoffmann et al. 2004). Interestingly, CNF-1 mediated deamination of Rac resulted in a permanent activation as it renders it resistant towards inactivation by GAPs (Schmidt et al. 1997; Flatau et al. 1997). The increased translocation due to activation of Rho GTPases was also seen in cells expressing constitutively active Rac1 (Aili et al.

2008; Wolters et al. 2013; Aepfelbacher and Wolters 2017). In addition, constitutively active Rac1 induced a significant increase in translocon forming bacteria (Nauth et al. 2018).

2.4. Pathogen-host cell interaction

2.4.1. Interaction of host cell factors with *Yersinia* containing compartments

During bacterial invasion, many host proteins regulate the uptake, internalization and clearance of the pathogen. The bacterium in turn uses effector proteins to influence cellular functions to their own advantage allowing bacterial survival and proliferation. During phagocytosis cellular receptors bind bacterial surface proteins which induces actin rearrangements allowing the cell to form protrusions engulfing the bacterium. Phospholipids in the cellular membrane, such as phosphoinositide 4,5 bisphosphate (PI(4,5)P₂) and phosphoinositide 3,4,5 trisphosphate (PI(3,4,5)P₃), have been shown to play a role in regulation of actin filament assembly (Hilpelä et al. 2004). There are seven different phosphoinositides, all serving as minor components on the cytosolic side of eukaryotic cell membranes and derive from phosphoinositols with an inositol ring phosphorylated by different kinases on the three, four and five hydroxyl groups (Di Paolo and Camilli 2006). Phosphoinositols are synthesized in the endoplasmic reticulum (ER) and transported to the plasma membrane where they serve as a signal molecules or second messengers regulated by phosphorylation and dephosphorylation. PI(4,5)P₂ is mainly produced by phosphorylation of PI(4)P by type I PIP kinases and less through phosphorylation of PI(5)P by type II PIP kinases as little PI(5)P is present in cells (Ma et al. 1998; Rameh et al. 1997; Roth 2004). PI(4,5)P₂ is either generated in the Golgi and transported to the plasma membrane or is directly produced there and has been shown to accumulate at sites of bacterial uptake (Odorizzi et al. 2000). A strong accumulation of PI(4,5)P₂ has also been observed at the *Yersinia* containing vacuole (Wong and Isberg 2003; Sarantis et al. 2012; Bahnan et al. 2015). *Yersinia* are internalized by binding of invasin to β 1-integrins which induces Rac1 activation and type I phosphatidylinositol 4-phosphate 5-kinase (PIP(5)K1 α) recruitment. PIP(5)K1 α is activated by Arf6 and phosphorylates PI(4)P to PI(4,5)P₂ (Isberg and Leong 1990; Alrutz et al. 2001; Wong and Isberg 2003; Brown et al. 2001). PI(4,5)P₂ has a variety of ways promoting actin assembly. Nucleation of actin networks is mediated through the interaction of PI(4,5)P₂ with small GTPases such as Cdc42 binding of N-WASP activating the ARP2/3 complex (Pollard and Borisy 2003; Rohatgi et al. 2000). In addition, Cdc42 and PI(4,5)P₂ together recruit other N-WASP activating proteins (Ho et al. 2004). PI(4,5)P₂ also mediates the dissociation of capping proteins gelsolin and CapZ as well as the binding to profilin preventing it from forming complexes with actin monomers (Saarikangas et al. 2010; Pollard and Borisy 2003). Actin polymerization is further facilitated by PI(4,5)P₂ binding of adaptor proteins connecting membrane and actin cytoskeleton (Di Paolo et al. 2002; Ling et al. 2002). As PI(4,5)P₂ is required for actin

polymerization, its catabolism is necessary for shedding of the actin cup and complete internalization of the bacterium into the cell (Botelho et al. 2004; Cheng et al. 2015). PI(4,5)P₂ is hydrolyzed by phospholipases such as phospholipase C (PLC) or phospholipase A₂ (PLA₂). Alternatively, phosphorylation by class I phosphoinositide (3) kinases (PI(3)K) to PI(3,4,5)P₃ further depletes PI(4,5)P₂ levels at the plasma membrane (Botelho et al. 2000; Clarke 2003). While PLC seems to play a minor role in PI(4,5)P₂ depletion during bacterial entry, PI(3)K mediated fusion of Rab5 vesicles containing lipid phosphatases ORCL and Inpp5b with the *Yersinia* containing prevacuole is required for membrane fission and internalization of the bacterium (Sarantis et al. 2012). PI(3,4,5)P₃ accumulation at the phagocytic cup seems to be required for its closure and disappears after sealing of the vacuole (Cox et al. 1999; Cox et al. 2001; Marshall et al. 2001; Cao et al. 2004).

For imaging of PI(4,5)P₂, pleckstrin homology (PH) domain of PLC δ 1 tagged with GFP (PLC δ 1-PH-GFP) has been employed as the PH domain binds PI(4,5)P₂ with high affinity (Garcia et al. 1995; Balla and Várnai 2009). The PI(4,5)P₂-rich compartment encompassing *Yersinia* during bacterial uptake has been termed prevacuole (Wong and Isberg 2003; Sarantis et al. 2012; Bahnan et al. 2015). It is further characterized by a connection to the extracellular milieu (Wong and Isberg 2003). This connection enables access of small molecules such as pHrodo, Gentamicin or pH-neutralizing reagents but not antibodies (Bahnan et al. 2015). Effector proteins in the host cell mediate the antiphagocytic effect of *Yersinia*. The manipulation of the cytoskeleton is facilitated by effector proteins YopH, YopE, YopT and YopO mainly through the interaction with Rho-GTPases (Grosdent et al. 2002; Barbieri et al. 2002; Aepfelbacher 2004). Many pathogens are known whose effector proteins directly influence PI(4,5)P₂ levels to invade the cell and guarantee survival in a pathogen-containing vacuole. For this purpose, some bacteria deliver phosphoinositide phosphatases into host cell cytoplasm. For example, the effector protein IpgD of *Shigella flexneri* serves as an inositol 4-phosphatase enabling dephosphorylation of PI(4,5)P₂ into PI(5)P (Niebuhr et al. 2002). This facilitates the internalization of the pathogen allowing subsequent lysis of the phagosomal membrane and multiplication in the cytosol. Similarly, SopB from *Salmonella* Dublin functions as an inositol phosphate polyphosphatase (Norris et al. 1998). In *Salmonella* Typhimurium infected cells SopB mediated clearing of PI(4,5)P₂ to reduce membrane rigidity and induce fission of the invaginating membranes (Terebiznik et al. 2002). SopB is possibly required for the formation of *Salmonella* containing vacuoles. Although its activity could not be characterized, BopB from *Burholderia pseudomallei* shares a phosphatase motif with SopB (Ungewickell et al. 2005). Conversely, PI(3)P is the target of lipid phosphatase SapM secreted from *Mycobacterium tuberculosis* impeding fusion of phagosome and late endosome and suspending PI(3)P mediated phagosome maturation (Vergne et al. 2005).

Another factor of the host cell interacting with *Yersinia* containing vacuoles (YCV) is galectin-3 (Feeley et al. 2017; Zwack et al. 2017). This protein belongs to the galectin family of β -galactoside-binding proteins which include 15 galectins found in mammals containing a carbohydrate-recognition domain (CRD) (Liu and Rabinovich 2005; Rabinovich and Toscano 2009). They are further classified into three groups: (1) prototype galectins with one CRD which can form homodimers; (2) tandem-repeat-type galectins with two CRDs; (3) chimeric galectins containing an N-terminal domain mediating protein oligomerization and a C-terminal CRD. Galectin-3 is the only chimeric galectin and is mainly found in the cytoplasm, nuclei and mitochondria (Davidson et al. 2002; Yu et al. 2002). Despite lacking a sequence for secretion by the classical pathway over the ER, secretion of galectin-3 has been observed (Cummings and Liu 2009). Here it binds carbohydrates presented on glycoproteins or glycolipids on the cell surface inducing multimerization which influences cellular events such as cell migration or receptor endocytosis (Cerliani et al. 2017). Extracellular galectin-3 has also been shown to play a role as a chemoattractant for immune cells during bacterial infections (Nieminen et al. 2008; Sano et al. 2000). It can also directly bind with both its N- and C-terminus to LPS of extracellular pathogens (Mey et al. 1996). Glycans usually reside on the cell surface or in the lumen of vacuoles but not on the cytosolic side of membranes. Through membrane rupture glycans become exposed to the cytosol and can be bound by galectin-3 (Boyle and Randow 2013). Vacuole rupture induced by *Shigella flexneri* and *Listeria monocytogenes* invading the cytosol was detected by galectin-3 binding to exposed N-acetyllactosamine (Paz et al. 2010). Galectin-3 has therefore been used as a marker for membrane damage induced by intracellular pathogens. It also has been shown to be a regulator of inflammation directly impacting infection (Baum et al. 2014; Vasta 2009; Liu et al. 2012). Galectin-3 was shown to recruit guanylate-binding proteins (GBP) to *Legionella* and *Yersinia* containing vacuoles which resulted in ubiquitination (Feeley et al. 2017). GBPs belong to a family of GTPases which are induced by interferon-gamma and are linked to intracellular defense mechanisms (Tripal et al. 2007). Studies in *Y. pseudotuberculosis* have shown that YopB and YopD direct galectin-3 to *Yersinia* containing vacuoles inducing recruitment of GBPs (Feeley et al. 2017; Zwack et al. 2017). GBP recruitment also activates the caspase-11 pathway resulting in plasma membrane pores through gasdermin D cleavage inducing potassium efflux and subsequent NLRP3 inflammasome activation (Baker et al. 2015; Schmid-Burgk et al. 2015; Rühl and Broz 2015). This can lead to the destruction of the intracellular bacterium and reduce overall infection load *in vivo*.

2.5. Protein tagging for fluorescence microscopy

2.5.1. Challenges and solutions for visualizing translocated bacterial proteins

To analyze the function of bacterial translocators and their effector proteins, time resolved detection is an important source of information. Systems enabling reliable, specific detection in fixed and live cells without interfering with the protein function are required. However, many approaches display limitations preventing a proper spatio-temporal resolution of protein translocation. Methods for the detection of translocated effector proteins can be classified into resolution on cell population level (e.g. Digitonin lysis), single cell level (e.g. β -lactamase) or subcellular level (e.g. immunofluorescence). Antibodies against the native protein or an epitope tag allow effector protein localization within the host cell but are generally not suitable for live imaging (Lee and Schneewind 1999; Nauth et al. 2018). GFP tagging proved unsuitable for analysis of secretion or translocation of effector proteins as it prevents secretion (Akeda and Galán 2005). Several other approaches have been tested for the visualization of bacterial proteins including self-labeling enzyme tags, fluorescent complementation of split fluorophores or artificially designed epitope tags in combination with specific nanobodies (van Engelenburg and Palmer 2010; Liss et al. 2015; Young et al. 2017; Götzke et al. 2019). The application of these approaches and their constraints for visualization of effector proteins are reviewed below.

2.5.2. Detection in cell lysates or entire host cell

Due to the difficulty to precisely differentiate between intrabacterial and translocated effector protein, tags only detectable in the host cell were of interest. Some reporter systems facilitating this requirement involve tag phosphorylation inside the host cell and its subsequent detection using phosphospecific antibodies. One example is the ELK tag which is derived from the eukaryotic transcription factor Elk-1 fused to the simian virus 40 (SV40) large tumor antigen nuclear localization sequence (NLS) (Day et al. 2003). The 35 residue ELK tag was used to label parts of YopN and YopE of *Y. pestis*, YopE in *Y. pseudotuberculosis* and several effectors in *Salmonella enterica* (Day et al. 2003; Day and Lee 2003; Rosenzweig et al. 2005; Garcia et al. 2006). Because fusion to the ELK tag impeded translocation, the glycogen synthase kinase (GSK) tag was tested which is similarly phosphorylatable and is comprised of merely 13 residues. It was shown that GSK tagging enabled detection of translocated effectors in *Y. pestis* infected HeLa cells (Garcia et al. 2006). Other methods tested involved the fusion of effector proteins to enzymes which allowed detection through their activity in the host cell. For instance, the adenylate cyclase A (CyA) from *Bordetella pertussis* was fused to effector proteins which induces conversion of adenosine triphosphate (ATP) to 3',5'-cyclic AMP (cAMP) and pyrophosphate in the host cell which could be quantitated by ELISA. Accordingly, the N-

terminus of YopE was fused to adenylate cyclase A and detected in the cytosol of the host cell (Sory and Cornelis 1994). The translocation of the fusion protein was possible despite the considerable molecular weight of 200 kDa for CyA (398 aa fusion protein) (Bellalou et al. 1990). This method served to identify the minimal N-terminal sequence necessary for secretion of YopE and YopH (Sory et al. 1995).

A different mechanism allows detection of proteins fused to the bacteriophage P1 Cre site-specific recombinase which catalyzes the excision or inversion between two 34 bp sequences called *loxP*. This excision of another reporter gene and a transcriptional stop signal induces expression of GFP or luciferase encoded outside the *loxP* sites. Thus, translocation of an N-terminal SopE fragment from *Salmonella* fused to the Cre recombinase was detected in the host cell (Briones et al. 2006). This approach also enabled detection of VirB secreted over a type four secretion system from *Agrobacterium tumefaciens* (Vergunst et al. 2005).

A widely applied principle is tagging with β -lactamase (*bla*), which cleaves coumarin cephalosporin fluorescein (CCF2AM) inducing a fluorescence shift from green to blue in the host cell (Zlokarnik et al. 1998). In this manner, EHEC and EPEC effector proteins Cif, Tir, Map and EspF fused to β -lactamase were used for identification of the N-terminal sequence necessary for secretion and translocation (Charpentier and Oswald 2004). Following these first experiments, immune cell targeting by YopM from *Y. pestis* and YopE from *Y. enterocolitica* was identified with the β -lactamase tag (Marketon et al. 2005; Köberle et al. 2009), while cell specific targeting of YopE-*bla* and YopH-*bla* was analyzed in *Y. pseudotuberculosis* (Durand et al. 2010). In addition, YopH-*bla* and YopJ-*bla* translocation was shown to originate specifically from macrophage phagosomes (Zhang et al. 2011). An increased translocation was shown for both a YopE deletion mutant in *Y. enterocolitica* as well as for treatment with cytotoxic necrotizing factor-Y using YopE-*bla* (Viboud and Bliska 2001; Viboud and Bliska 2005; Viboud et al. 2006; Aili et al. 2006; Aili et al. 2008; Mejía et al. 2008; Wolters et al. 2013; Wolters et al. 2015).

Although enzyme tagging of effector proteins has been shown to enable general detection of translocation in the host cell, enzyme reactions are difficult to quantify, are delayed by enzyme kinetics and give limited information about the location of the protein. Besides, CyA, ELK and GSK tags rely on cell lysates which only provide information about the whole cell population at specific time points. While Cre and β -lactamase tagged to effector proteins induce fluorescent signals when translocated, these are freely distributed within the host cell and deliver no detailed information about protein localization.

2.5.3. Tags enabling protein localization in the host cell

2.5.3.1. Imaging limited to fixed samples

Antibodies against Yops have been applied widely and resulted in a considerable gain of knowledge (Rosqvist et al. 1994; Lee and Schneewind 1999; Nauth et al. 2018). For example, antibodies enabled visualization of assembled injectisomes including the translocon and the needle complex and their localization in the PI(4,5)P₂ enriched prevacuole membrane (Nauth et al. 2018). However, there are no commercial antibodies against Yops available, their self-production is cumbersome and the resulting antibodies are of varying quality. In general, immunostainings only provide snapshots of complex dynamic processes as they are unsuitable for live imaging. This limits the ability to analyze time resolved processes. Conventional epitope tags such as FLAG, HA, myc or poly-Histidine tag might allow translocation due to their small size and lack of complex folding (8 – 10 amino acids, 1.1 – 1.4 kDa, 2.2 – 2.8 nm), but generally do not allow detection of proteins in live cells as they require binding by antibodies to be visualized (Porath et al. 1975; Wilson et al. 1984; Evan et al. 1985; Hochuli et al. 1987; Hopp et al. 1988). Additionally, the morphology and protein localization can be affected by the required fixation and permeabilization. Nevertheless, C-terminal FLAG tags allowed localization of SopE, SopE₂, SopB and SptP of *Salmonella enterica* in infected cells (Cain et al. 2004). The same method was applied to reveal a cooperative function for SipA-FLAG, SifA-HA and PipB₂-HA in later studies (Brawn et al. 2007). A repeat of 3xFLAG was used for labeling PipB₂ showing accumulation at the *Salmonella* containing compartment and associated tubules (van Engelenburg and Palmer 2010).

2.5.3.2. Protein tags compatible with live cell imaging

Previous studies have shown that conventional bulky fluorescent protein tags are unsuitable for visualization of effector protein translocation during infection. In translocation studies with SptP, an effector protein of *Salmonella enterica* serovar Typhimurium, it was shown that unfolding in an ATPase dependent manner is essential for secretion (Akeda and Galán 2005). When tagged with **GFP** the effector was not secreted while tagging with the thermodynamically less stable PhoA (alkaline phosphatase) allowed secretion. Apparently the high thermodynamic stability of folded GFP prevents unfolding by ATPases (Penna et al. 2004; Jackson et al. 2006; Pitman et al. 2015). This was further validated using electron microscopy of *Salmonella* which showed with the N-terminus of SptP₃-GFP outside the tip complex of the TTSS but the GFP stuck at the basal body of the injectisome (Radics et al. 2014). Similarly, translocator IpaB of *Shigella flexneri* fused to a knot forming protein was shown to be stuck in the needle channel (Dohlich et al. 2014). Besides issues with unfolding, fusion to GFP can result in misfolding of bacterial proteins as demonstrated for randomly selected proteins from *Pyrobaculum aerophilum*

expressed in *E. coli* (Waldo et al. 1999). As translocation of GFP tagged effector proteins into the host cell has proven unsuccessful, GFP tagged effector proteins were expressed directly in the host to identify where they would accumulate. A localization to the Golgi has been revealed in studies analysing GFP or mCherry tagged YopE expressed in HUVECs (Roppenser et al. 2009). However, ectopic expression likely leads to unphysiological effector protein levels, localization and function. This was illustrated by expression of GFP tagged effector protein PipB2 from *Salmonella* SPI2 accumulating at the cell periphery compared to translocated PipB2 localizing to the tubular network (van Engelenburg and Palmer 2010). Despite the numerous applications of GFP revolutionizing the possibilities of microscopy, GFP-tagging does not seem the right approach for analysis of translocated effector proteins.

An alternative offer **GFP-tagged chaperones** binding their native effector proteins. The specific interaction of the effector protein and its cognate chaperone is utilized for protein detection by ectopically expressing the GFP-tagged chaperone in the host cell where it binds the translocated effector protein. The resulting accumulation of GFP signal should allow detection of the effector protein. However, so far it could only be applied for the strongly accumulating SipA from *Salmonella* and its chaperone InvB (Schlumberger et al. 2005). For other more diffusely localized effectors detection was not successful due to the high background signal such as shown for SopE. Furthermore, this approach is only applicable for effectors that have a chaperone, which is not always the case.

Another tool applied in recent years to study effector translocation is the **light, oxygen and voltage-sensing (LOV) domain** from *Arabidopsis thaliana*, which binds flavin mononucleotides in the host cell resulting in green fluorescence. In comparison to GFP it has several advantages including the size (10 kDa), the stability in different environments, a rapid maturation and the suitability for super resolution and electron microscopy (Buckley et al. 2015; Shu et al. 2011). Since its discovery it has been optimised regarding brightness, fluorophore stability, recovery after bleaching, expression rate and codon selection resulting in the phiLOV2.1 tag (Gawthorne et al. 2016). The phiLOV tag enabled visualization of IpaB from *Shigella* and real-time translocation of Tir from *E. coli* during infection (Gawthorne et al. 2016). Moreover, it allowed quantification of caspase-3 activation by SipA (McIntosh et al. 2017) as well as its cleavage of SifA-phiLOV in *Salmonella* infected cells (Patel et al. 2019). Recently, phiLOV was applied for the visualization of VirE2 from *Agrobacterium tumefaciens* (Roushan et al. 2018). The major drawback of phiLOV2.1 is the low fluorescence intensity, which is threefold lower than GFP and therefore requires a strongly translocated effector translocated and a localized accumulation in the cell. Additionally, as the tag already fluoresces in the bacterium it can be difficult to differentiate between intrabacterial and translocated effector signal.

Translocated effector proteins have been successfully imaged using a **tetracysteine hairpin loop (4Cys)**. The fluorescein based biarsenical dye (FIAsH) becomes fluorescent upon binding the 4Cys tag thereby allowing tracking of effector proteins from the bacterium into the host cell (Hoffmann et al. 2010). The tag and the FIAsH dye provide the advantage of a relatively small size compared to other labeling approaches (12 aa 4Cys tag; 0.7 kDa FIAsH dye). Thus, it was possible to label 4Cys-tagged *S. flexneri* effectors IpaB and IpaC intrabacterially with the FIAsH compound before their translocation (Enninga et al. 2005). The same approach was used for effector proteins SopE and SptP from *Salmonella* (van Engelenburg and Palmer 2008). Here the signal was increased by using 3x4Cys resulting in a stronger signal suitable for live imaging experiments. However, the general signal quality using FIAsH staining of 4Cys is relatively poor and the dye itself has a cytotoxic effect limiting the time for live imaging (Gaietta et al. 2002). These disadvantages prevented the technique from becoming more broadly applied.

As previous attempts for fluorescent labeling of bacterial proteins have demonstrated limited suitability for advanced microscopy, alternative tags were investigated. One category are **self-labeling enzymes** including the Halo-, SNAP- and CLIP-tag, which covalently bind to synthetic ligands available coupled to a variety of labels (Los et al. 2005; Keppler et al. 2003; Gautier et al. 2008). They display a high specificity to their ligand and the irreversible attachment occurs rapidly both in live and fixed cell samples. The tags are suited for expression in eukaryotic and prokaryotic cells. The Halo-tag is a mutated 34 kDa haloalkane dehalogenase from *Rhodococcus rhodochrous* which covalently binds primary alkylhalides ligands (Encell et al. 2012). The SNAP-tag is derived from the 20 kDa human repair protein O⁶-alkylguanine-DNA-alkyltransferase and reacts irreversibly with O⁶-benzylguanine derivatives while the CLIP-tag is a O²-alkylcytosine-DNA-alkyltransferase mutated from the SNAP-tag and binds O²-benzylcytosine derivatives (Keppler et al. 2003; Gautier et al. 2008). The specific ligands can be labeled with fluorophores or affinity tags allowing imaging and localization of cellular proteins as well as their purification. The red fluorescent rhodamine derivative tetramethylrhodamine (TMR; 555 nm excitation, 585 nm emission; 430 Da; 636 Da with ligand) coupled to a ligand enables super resolution microscopy as well as transmission electron microscopy (Liss et al. 2015). TMR photooxidizes diaminobenzidine to an osmiophilic polymer visible on TEM sections. In addition, TMR tagged ligands show no cytotoxicity and permeate both eukaryotic cells as well as bacteria making it suitable for live imaging and single molecular tracking (Los et al. 2005; Perkovic et al. 2014; Barlag et al. 2016; Banaz et al. 2019). The self-labeling enzymes have found broad application in eukaryotic cells including imaging of proteins in the cytoplasm, nucleus, mitochondrial matrix and endoplasmic reticulum (Singh et al. 2013; Grimm et al. 2015; Stagge et al. 2013; Raina et al. 2014). The suitability of self-labeling enzyme tags in bacteria has been established on both intra- and extrabacterial proteins. The SNAP-tag has been used to visualize the protease Clp in fixed *E. coli* (Landgraf et al. 2012)

while the cytoplasmic ClpP and the periplasmic DsbA have been live imaged as fusions with the Halo-tag (Ke et al. 2016). The Halo-tag has been employed for microarrays to investigate protein-protein interactions of the TTSS in *Y. pestis* (Peterson and Kwon 2012). Dual color super resolution imaging has been performed on Halo and SNAP fusion proteins for interaction analysis between chemotaxis response regulator CheY and its phosphatase CheZ (Wille et al. 2015) and for different proteins of *Salmonella enterica* including subunits of the TTSS (Barlag et al. 2016). Intensive comparisons of conventional photoactivatable fluorophore tags with the Halo-tag for single molecular tracking has been performed for MukB, a structural maintenance of chromosomes protein and DNA polymerase I in *E. coli*, with overall positive results for the self-labeling enzyme tag (Banaz et al. 2019). The application of self-labeling enzyme tags for secreted bacterial proteins has been demonstrated for imaging of *Salmonella* effector proteins including live cell imaging, super resolution microscopy and single-molecular tracking (Göser et al. 2019). They also investigated YopM from *Y. enterocolitica* with Halo, SNAP and CLIP tag but visualization proved more challenging although some signal was detected.

The principle of **fluorophore complementation** has been applied broadly to investigate protein interaction or protein transport (Kodama and Hu 2012; Romei and Boxer 2019). It is based on separate expression of parts of fluorescent proteins and their subsequent complementation restoring fluorescence (Figure 2B). For GFP this system is widely established and has been used to analyze protein interaction in vitro or in vivo both in prokaryotic and eukaryotic cells (Avilov and Aleksandrova 2018; Pedelacq and Cabantous 2019). The GFP molecule has a barrel shape made up of 11 β -strands. For split-GFP complementation β -strands 1-10 (GFP1-10) are expressed separate from the 11th β -strand (GFP11 or split-GFP) and can be fused to proteins of interest (Cabantous et al. 2005). Both parts are not fluorescent on their own but able to self-ligate when in close proximity and restore fluorescence. GFP11 is comprised of just 16 amino acid residues offering advantages compared to tagging with conventional GFP fluorophores comprised of 238 amino acids (Prasher et al. 1992; Cabantous et al. 2005). Due to its small size GFP11 can avoid misfolding or functional interference occurring for proteins tagged with GFP (Waldo et al. 1999). Its properties have been proven suitable for tagging of effector proteins translocated via a variety of secretion systems of different species into both mammalian and plant cells in fixed and live samples. The successful application of split-GFP for visualization of effector protein translocation through type three secretion systems has been demonstrated with effector proteins PipB2, SteA and SteC from *Salmonella enterica* labeled with GFP11 (van Engelenburg and Palmer 2010). While all three effectors generally accumulated at tubules on *Salmonella*-containing vacuoles in HeLa cells, PipB2 colocalized additionally with endo- and exocytic markers, SteA with Golgi markers and SteC with actin. Later studies showed *Salmonella* effector proteins SseF, SseG, and SlrP tagged with split-GFP in live imaging experiments accumulating in different

compartments when infecting macrophages, HeLa cells or RAW cell lines (Young et al. 2017). Infection with *Chlamydia trachomatis* expressing GFP11 tagged proteins allowed their localization in the GFP1-10 expressing HeLa cells (Wang et al. 2018b). It revealed effector protein IncA localization to both the inclusion membrane and in the inclusion lumen while CT005 was only detected at the inclusion membrane and CT694 at the plasma membrane. Deubiquitinases CT867 and CT868 were enriched at the inclusion membrane however CT867 later localized to the plasma membrane. When analysing plant pathology of *Arabidopsis* infected with *Pseudomonas syringae*, split-GFP tagged effectors AvrB and AvrRps4 were visualized in specific subcellular localizations with GFP1-10 targeted to these organelles (Park et al. 2017; Lee et al. 2018). However, employing the split-GFP system for visualization of effector translocation is not limited to type three secretion systems. For example, the delivery of VirE2, an effector protein of *Agrobacterium tumefaciens*, via the type four secretion system into plant cells was shown using a leaf-infiltration assay (Li et al. 2014b) and the same approach enabled examination of VirE2 trafficking along the ER and actin network (Yang et al. 2017). Besides, *Listeria monocytogenes* secreting InIC over the Sec pathway into the host was visualized using both red and green split-fluorescent proteins and a signal accumulation over time could be observed in primary bone-marrow-derived macrophages (Batan et al. 2018). Even protein export of Hsp40 co-chaperone PFE55 of *Plasmodium falciparum*, a unicellular protozoan parasite of humans, into erythrocytes was imaged live by GFP11 labeling (Külzer et al. 2013). Together these studies demonstrate that split-GFP is a versatile marker for protein secretion over different pathways during infection enabling the visualization of effector protein dynamics, their localization within the host cell as well as their accumulation after infection.

In recent years the application of **nanobodies** has expanded from biotechnological uses to diagnostic and therapeutic advances. Nanobodies are a new class of antibodies found in different camelid species including llamas and alpacas (Muyldermans 2013). They lack the light chains of antibodies and have only a single fragment-antigen-binding (Fab) domain called variable heavy domain of heavy chain antibodies (VHH) or nanobody (Hamers-Casterman et al. 1993). Nanobodies are ten times smaller than IgG antibodies with a molecular weight of 15 kDa compared to 150 kDa (see Figure 2), can be expressed in bacteria and are very stable in a wide range of conditions. When labeled with fluorophores nanobodies can be used for immunofluorescent imaging (Rothbauer et al. 2006). The combination with epitope tagging allows use of the same nanobody for different proteins of interest with a strong affinity increasing the versatility of the application.

A novel candidate is the **ALFA-tag**, a rationally designed 15 residue epitope tag derived from an artificial peptide which was shown to form a stable α -helix in solution (Petukhov et al. 2009; Götzke et al. 2019). A specific anti-ALFA nanobody was developed with a low picomolar affinity towards the tag which can be

labeled with fluorophores or enzymes for detection in Western blot, be mounted on solid surfaces or beads and be expressed in living cells. Labeling with the ALFA-tag appears functional in different positions of proteins in prokaryotic and eukaryotic cells and allowed immunostaining of different cellular proteins such as Tom70, Vimentin, or a transmembrane domain in fixed cells (Götzke et al. 2019). The staining proved suitable for super resolution microscopy, as demonstrated with ALFA-Vimentin and expression of fluorescently tagged nanobody enabled visualization of ALFA-Vimentin in living cells. In Western blots ALFA-Vimentin could be detected in cell lysates using labeled nanobody and a FLAG-HA-myc-ALFA-tagged maltose-binding protein expressed in *E. coli* was used to illustrate to higher sensitivity of ALFA detection compared to the established epitope tags. ALFA tagged GFP from eukaryotic and prokaryotic lysates was pulled down using nanotag labeled beads. This study demonstrated the broad range of application for the ALFA-tag with its anti-ALFA nanobody. Due to the novelty of the tag and its nanobody the published research is limited. The only published application generated switchable nanobodies using the anti-ALFA nanobody as an example (Farrants et al. 2020). They inserted a circularly permuted bacterial dihydrofolate reductase (cpDHFR) close to the complementary-determining region 2 (CDR2) of the nanobody mediating affinity towards their target. Addition of NADPH or DHFR inhibitors resulted in the inhibition of nanobody binding further expanding the applicability of the ALFA-tag. Overall, these results indicate the ALFA-tag to be an interesting candidate for labeling of bacterial proteins.

A comparison of the size and structural differences of probes for protein visualization relevant in this study is displayed in Figure 2 compared to GFP for orientation.

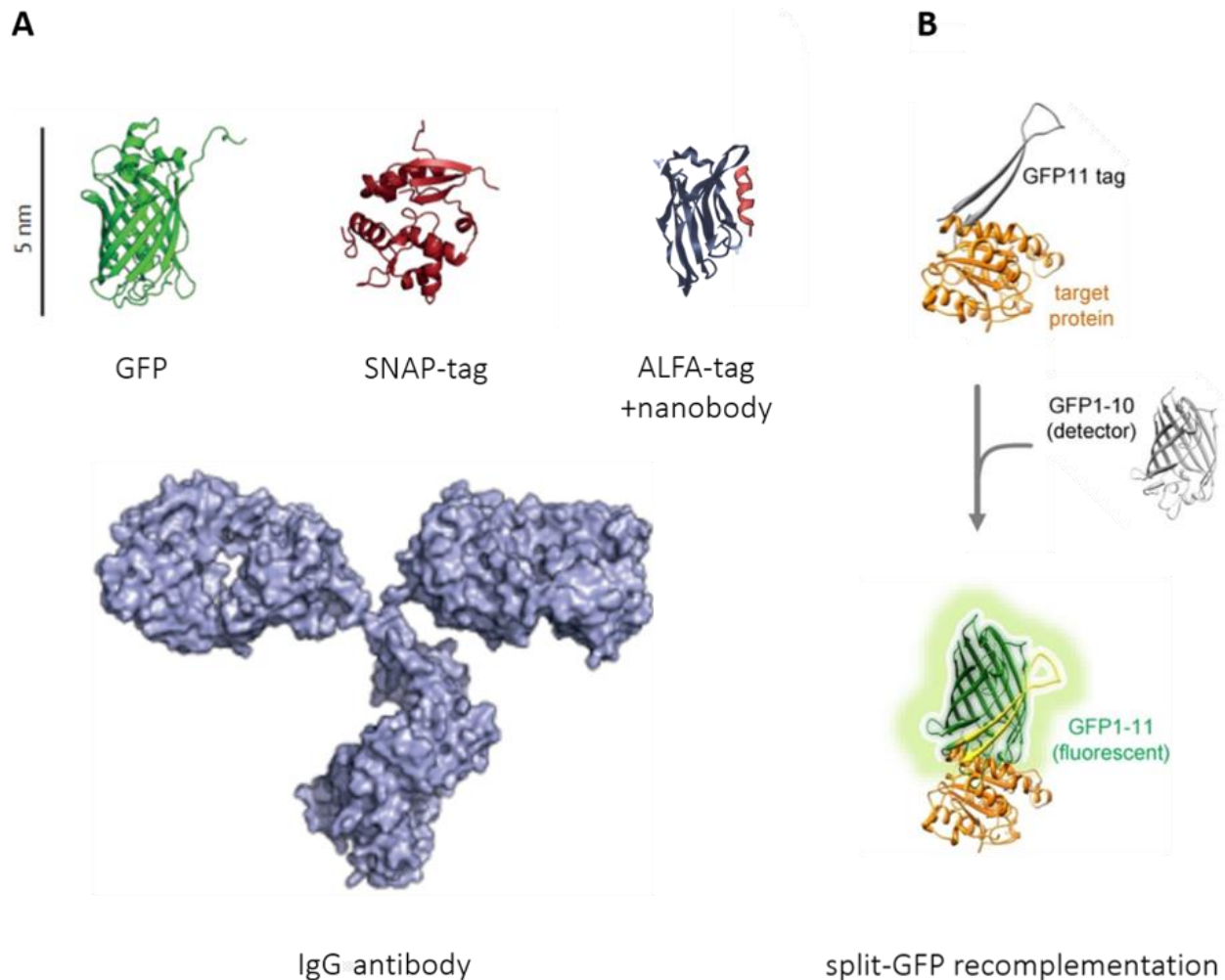


Figure 2 A structure and size comparison of conventional and advanced visualization approaches. A: Different probes for imaging of proteins. GFP, SNAP-tag, ALFA-tag and its nanobody (ALFA-tag in red) and IgG antibody are shown to the same scale. Figure is adapted from (Sahl et al. 2017). Structures were obtained from the Protein Data Bank (PDB). PDB entries: 5dty (green fluorescent protein, GFP), 3kzy (SNAP-tag), 1igt (IgG), 6i2g (ALFA-tag binding nanobody (NbALFA) bound to ALFA-tag peptide). **B: Detection of target proteins using split-GFP recombination.** The target protein is labeled with the 11th β -strand of GFP. A fluorescent signal is induced upon restoration of the GFP barrel complex. Figure is adapted from (Knapp et al. 2017).

2.5.4. Selection of tag position for *Yersinia* outer proteins

The position of a tag on a protein of interest requires careful consideration to prevent interference with protein function. *Yersinia* outer proteins are generally tagged at the C-terminus. Although Yops do not share a consensus sequence at the N-terminus, its presence appears necessary for secretion (Michiels and Cornelis 1991). Mutation experiments have led to the theory that the secretion signal depends rather on physical or chemical properties than on the sequence of amino acids, although specific proof is still needed (Amer et al. 2011). The length of the secretion signal has been widely discussed and varies between

studies. Early studies showed that the first 48, 78 and 98 residues of YopH, YopQ and YopE respectively are required for secretion (Michiels and Cornelis 1991). Later, 15 N-terminal residues for YopE and 17 for YopH proved to be sufficient for protein secretion but the first 50 and 71, respectively, were necessary for translocation into the host cell (Sory et al. 1995). A short signal of 7-15 residues was confirmed by further studies for YopE in *Y. pseudotuberculosis* (Schesser et al. 1996; Anderson and Schneewind 1997; Lloyd et al. 2001). In addition, amino acids 15-100 of YopE showed to serve as a second independent secretion signal when bound to its chaperone SycE in *Y. enterocolitica* (Woestyn et al. 1996; Cheng et al. 1997). Generally, it has to be considered that detectable secretion does not necessarily imply successful translocation (Sory et al. 1995). Due to the importance of the N-terminal secretion signal, tagging is generally conducted at the C-terminus of effector proteins not relevant for secretion or translocation.

The tagging of the translocators YopB and YopD is more complex compared to effector protein tagging as they are a membrane-associated part of the tightly packed TTSS machinery which is indispensable for effector delivery into the host cell. Therefore, insertion of a tag should not disrupt any functional domains of the translocator proteins and should not affect their structure allowing formation of a functional TTSS. The knowledge of functional domains or the structure of pore proteins YopB and YopD is limited. Nevertheless, several functional domains shared by both translocators have been discovered including the N-terminal secretion signal (Amer et al. 2011), hydrophobic transmembrane domains (Tardy et al. 1999) and interaction sites with their chaperone SycD (Neyt and Cornelis 1999) as well as each other while YopD additionally possesses a binding site to the tip complex protein LcrV (Tengel et al. 2002). Moreover, the *lcrGVHyopBD* operon encoding for both YopB and YopD is highly conserved in many bacterial pathogens allowing predictions about their properties (Matteï et al. 2011). For instance, *pcrGVHpopBD* from *P. aeruginosa* was able to complement deletion of its homologue *lcrGVHyopBD* in *Y. pseudotuberculosis* (Bröms et al. 2003). It is therefore possible to transfer functional and structural information available for homologous translocator proteins PopB and PopD to the translocators in *Y. enterocolitica* (Frithz-Lindsten et al. 1998).

The secretion of YopB is assumed to be mediated by residues 2-15 (Amer et al. 2011). YopB has two predicted, hydrophobic transmembrane domains towards the center of the protein sequence (aa 166 – 188; aa 228 – 250) and two coiled-coil domains – one before the first transmembrane domain and another towards the C-terminus (Pallen et al. 1997; Frithz-Lindsten et al. 1998; Ryndak et al. 2005; Matteï et al. 2011). Data for PopB suggests both N- and C-terminus facing the extracellular milieu after protein insertion into the hosts membrane following translocation (Discola et al. 2014; Armentrout and Rietsch 2016). Interestingly, the transmembrane domains and the loop in between display a strong sequence identity

between species indicating a significant functional importance for this region (Blocker et al. 1999; McGhie et al. 2002; Hume et al. 2003; Ryndak et al. 2005; Schroeder and Hilbi 2007).

The secretion of YopD relies on an intact N-terminus with the first 5 residues sufficient for low level YopD-secretion while the first 10-15 residues are necessary for efficient secretion (Amer et al. 2011). YopD has a single predicted transmembrane domain (Mattei et al. 2011), a putative C-terminal coiled-coil domain (Pallen et al. 1997) and an α -helical amphipathic domain (Håkansson et al. 1993). The transmembrane domain is predicted to span amino acids 128-149, with the N-terminus towards the cytosol and the C-terminus towards the extracellular matrix. The coiled-coil domain from residues 248-277 displayed no functional role while the amphipathic domain encompassing residues 278-292 revealed to be vital for the formation of YopD-oligomers and the binding of LcrV (Costa et al. 2010). Together with residues 53-149, the amphipathic domain is responsible for binding of SycD the cognate chaperone of YopB and YopD (Francis et al. 2000). Also, a conserved six amino acid sequence for the chaperone binding domain of different translocators has been identified in *Shigella*, *Salmonella* and *Yersinia* (Lunelli et al. 2009). The interaction with the chaperone SycD is mediated by the chaperone binding domain between residues 50-55 of YopB and 58-63 YopD in *Y. enterocolitica* (Lunelli et al. 2009). This binding motive and its similarity to the interaction between PopD and its chaperone PcrH in *Pseudomonas* as well as IpaB to its chaperone IpgC in *Shigella* was confirmed for YopD and SycD in *Y. enterocolitica* through structural analysis (Schreiner and Niemann 2012). The C-terminus of YopD likely faces the extracellular milieu as shown in studies of PopD (Armentrout and Rietsch 2016). Additionally, hybrid experiments with YopD/PopD and YopB/PopB showed an interaction site between PopD (aa 228-245) and PopB (aa 274-297) located in the C-terminal half of the proteins in the extracellular milieu (Armentrout and Rietsch 2016). The final selection of the tag position on the translocators is determined by functional domains and accessibility to potential binding partners of the tag mediating fluorescence.

2.5.5. CRISPR-Cas12a assisted recombination

For direct insertion of tags into bacterial genomes or plasmids different approaches have been applied. Homologous recombination has been a popular tool for genetic manipulation although it has a limited efficiency and usually relies on the insertion of a resistance cassette or requires intensive screening to identify positive clones (Yu et al. 2000; Sharan et al. 2009; Thomason et al. 2014). In recent years the CRISPR-Cas system (clustered regularly interspaced short palindromic repeats - CRISPR associated protein) has become widely used for gene editing both in eukaryotes (Adli 2018) as well as prokaryotes (Yao et al. 2018). It originates from an antiviral defense mechanism of prokaryotes allowing the organisms to detect and cleave bacteriophage DNA (Pourcel et al. 2005; Mojica et al. 2005; Bolotin et al. 2005). Parts of viral

mechanisms for double-strand breaks. In eukaryotes both non-homologous end joining (NHEJ) or homology directed repair (HDR) are involved (Koonin et al. 2017; Mitsunobu et al. 2017), while most prokaryotes only employ HDR, which has been proven to be more precise (Bowater and Doherty 2006; Tian et al. 2017; Selle and Barrangou 2015).

Both Cas9 and Cas12a systems have been used for genome editing in prokaryotes including *E. coli*, *Cyanobacteria*, *Streptomyces*, *Clostridium* and *Corynebacterium* (Yao et al. 2018). In pathogenic bacteria such as *Staphylococcus aureus* (Gu et al. 2018; Chen et al. 2017; Dong et al. 2017), *Mycobacterium tuberculosis* (Choudhary et al. 2015; Rock et al. 2017; Singh et al. 2016), *Pseudomonas aeruginosa* (Tan et al. 2018) and *Klebsiella pneumoniae* (Wang et al. 2018a) Cas9 has been used for genetic modifications. In addition, CRISPR interference (CRISPRi) has been established as a tool for protein knockdown through small guide RNAs allowing a catalytically dead Cas9 to bind to target DNA sterically hindering RNA polymerases access preventing transcription of the target gene (Larson et al. 2013; Qi et al. 2013; Hawkins et al. 2015; Plagens et al. 2015). This method has been used for reversible gene silencing of proteins both in the genome as well as on the virulence plasmid of *Y. pestis* (Wang et al. 2019).

Recently, recombineering approaches facilitating genome editing using homologous recombination were combined in prokaryotes with CRISPR-Cas mediated DNA cleavage allowing selection for recombinant clones (Oh and van Pijkeren 2014). The efficiency of introducing modifications has been significantly increased by combining CRISPR-Cas9 with the lambda red recombinase system (Jiang et al. 2013; Jiang et al. 2015; Pyne et al. 2015; Li et al. 2015; Liang et al. 2017). The lambda red system comprises the phage recombination genes *gam*, *exo* and *beta* (Yu et al. 2000). The polypeptide Gam prevents digestion of linear DNA by nucleases, the exonuclease Exo digests dsDNA to produce a linear ssDNA oligo and the Beta binds ssDNA and promotes its annealing to a complementary target (Sharan et al. 2009). In the presence of DNA fragments with sequences homologous to the target sequence these properties can be used to delete, insert or exchange DNA. For deletions the DNA fragment needs to be homologous to the sequences framing the DNA to be deleted while insertions require homologous arms to both sides of the insert site with the insert in the middle.

The red recombinase together with endonuclease Cas9 showed high efficiency in inducing allelic exchange, single or multiple gene deletions and insertions in *E. coli* (Jiang et al. 2013; Jiang et al. 2015). The combined system further enabled deletions up to 19.4 kb and insertions up to 3 kb in *E. coli* (Pyne et al. 2015). It was also used for metabolic engineering in *E. coli* optimizing the production of β -carotene and isopropanol (Li et al. 2015; Liang et al. 2017). Subsequently, Cas12a-assisted recombineering was shown to successfully generate point mutations, deletions, insertions, and replacements in *E. coli*, *Mycobacterium smegmatis* and *Y. pestis* (Yan et al. 2017). Two point mutations were introduced into the chromosome of *Y. pestis*

while an arginine to alanine mutation was performed on the native pMT1 plasmid and effective curation of the pMT1 plasmid was achieved. This study demonstrated that CRISPR-Cas12a-assisted recombineering is a useful method for modification of both chromosome and native plasmid in *Y. pestis*.

3. Aims

A broad range of Gram-negative bacteria use a protein delivery machine for the translocation of effector proteins into host cells (Galán and Waksman 2018). For pathogenic bacteria the majority of machines are type three, four or six secretion systems. In *Y. enterocolitica* the TTSS-mediated translocation of effector proteins has been shown to be a requirement for its virulence (Bölin et al. 1982; Brubaker 1991; Viboud and Bliska 2005). For a detailed understanding of bacterial pathogenicity, it is crucial to elucidate how effector proteins manipulate target cell functions. Knowledge about these processes can be advanced through the analysis of translocation dynamics, subcellular distribution of effector proteins as well as their interaction with host cell factors. Although the tools for imaging of translocated effector proteins are abundant, many display limitations (O'Boyle et al. 2018). For instance the use of antibodies allows direct detection of translocated effector proteins or introduced epitope tags, but their application is restricted to fixed samples (Rosqvist et al. 1994; Mounier et al. 1997; Cain et al. 2004; Nauth et al. 2018). Fluorescent proteins, which are generally well applicable for live cell imaging, affect protein translocation as they prevent the unfolding required for subsequent translocation into the target host cell (Akedo and Galán 2005; Radics et al. 2014). Self-labeling enzyme tags have provided promising results for advanced microscopy (Liss et al. 2015), while fluorescent complementation has become a widely applied tool specifically for visualizing effector proteins in the host cell. A novel approach is the labeling of proteins with a small artificial epitope called ALFA-tag which can be stained with fluorophore labeled nanobodies (Götzke et al. 2019). These systems are tested and compared in the present thesis.

In addition, the common approach for expression of tagged versions of effector proteins is the introduction of artificial vectors (Sory and Cornelis 1994; Marketon et al. 2005; Köberle et al. 2009; Wolters et al. 2013; Göser et al. 2019). However, these vectors result in an unphysiological overexpression of the protein. Although direct insertion of a tag into the virulence plasmid using homologous recombination in *Yersinia* results in native expression, it involves an elaborate process of recombinant selection with a low success rate. Therefore, a new approach for genetic recombineering needed to be established in *Y. enterocolitica* enabling adaptable, rapid and reliable insertion of protein tags into the virulence plasmid.

The following aims are center of the present thesis:

- Identification of a versatile tag suitable for fluorescent microscopy of fixed and live samples visualizing
 - effector protein translocation and localization in the host cell.
 - pore formation and its interaction with host cell factors.
- Establishment of CRISPR-Cas12a assisted recombineering for editing of the virulence plasmid of *Y. enterocolitica*.

- Determination of the onset and cellular compartment of pore formation during cell infection.
- Analysis of the role of translocon insertion for vacuolar membrane damage.

4. Results

Table 1 Overview of experimental results using tagged *Yersinia* outer proteins

| Method: | Protein analysis | | | | Microscopy | | |
|--------------------------|-------------------------|------------------------------|------------------------------|---------------|-------------------------|-------------------------|------------------------|
| | Protein expression | Released proteins | | Translocation | Cytotoxicity | Fixed samples | Live samples |
| | WB | Coomassie | WB | WB | light microscope | confocal imaging | spinning disc/confocal |
| control | WA-314/ <i>ΔYopH</i> | WA-314/ <i>ΔYopH</i> | WA-314/ <i>ΔYopH</i> | | WA-314/ <i>ΔYopH</i> | WA-314 | |
| ΔYopH+YopH-Halo | ++ | -- | -- | √ | -- | intrabact. signal | n.d. |
| ΔYopH+YopH-SNAP | + | -- | -- | √ | -- | intrabact. signal | n.d. |
| ΔYopH+YopH-CLIP | + | -- | -- | √ | -- | intrabact. signal | n.d. |
| control | <i>pTTSS+YopH</i> | <i>pTTSS+YopH</i> | <i>pTTSS+YopH</i> | | | <i>pTTSS+YopH</i> | |
| pTTSS+YopH-Halo | - | --- | --- | 0 | n.d. | intrabact. signal | n.d. |
| pTTSS+YopH-SNAP | - | --- | -- | √ | n.d. | intrabact. signal | intrabact. signal |
| pTTSS+YopH-CLIP | -- | --- | -- | √ | n.d. | intrabact. signal | intrabact. signal |
| control | | WA-314 | | | | WA-314 | |
| ΔYopM+YopM-Halo | n.d. | --- | n.d. | n.d. | n.d. | intrabact. signal | n.d. |
| ΔYopM+YopM-SNAP | n.d. | --- | n.d. | n.d. | n.d. | intrabact. signal | n.d. |
| ΔYopM+YopM-CLIP | n.d. | --- | n.d. | n.d. | n.d. | intrabact. signal | n.d. |
| control | | <i>pTTSS+YopM</i> | | | | <i>pTTSS+YopM</i> | |
| pTTSS+YopM-Halo | n.d. | --- | n.d. | n.d. | n.d. | intrabact. signal | n.d. |
| pTTSS+YopM-SNAP | n.d. | --- | n.d. | n.d. | n.d. | intrabact. signal | n.d. |
| pTTSS+YopM-CLIP | n.d. | --- | n.d. | n.d. | n.d. | intrabact. signal | n.d. |
| control | | WA-314 | WA-314 | | WA-314/ <i>ΔYopE</i> | WA-314/ <i>ΔYopE</i> | |
| ΔYopE+YopE-Halo | n.d. | 0 | 0 | n.d. | -- | intrabact. signal | intrabact. signal |
| ΔYopE+YopE-SNAP | n.d. | - | --- | n.d. | -- | intrabact. signal | n.d. |
| ΔYopE+YopE-CLIP | n.d. | - | --- | n.d. | -- | intrabact. signal | n.d. |
| control | | <i>pTTSS+YopE</i> | <i>pTTSS+YopE</i> | | | <i>pTTSS+YopE</i> | |
| pTTSS+YopE-Halo | n.d. | - | 0 | n.d. | n.d. | n.d. | n.d. |
| pTTSS+YopE-SNAP | n.d. | - | 0 | n.d. | n.d. | intrabact. signal | n.d. |
| pTTSS+YopE-CLIP | n.d. | - | 0 | n.d. | n.d. | intrabact. signal | n.d. |
| control | | WA-314/ <i>ΔYopE+YopE</i> | WA-314/ <i>ΔYopE+YopE</i> | | <i>ΔE</i> | | |
| ΔYopE+YopE-GFP11 | n.d. | --- / = | --- / -- | n.d. | - | cytosolic signal | n.d. |
| control | | <i>pTTSS+YopE</i> | <i>pTTSS+YopE</i> | | | | |
| pTTSS+YopE-GFP11 | n.d. | ++ | +++ | n.d. | n.d. | cytosolic signal | cytosolic signal |
| control | | <i>pTTSS</i> | <i>pTTSS</i> | | | <i>pTTSS</i> | |
| pTTSS YopD-GFP11 | n.d. | = | = | n.d. | n.d. | unspecific signal | unspecific signal |
| pTTSS YopB-GFP11 | n.d. | = | - | n.d. | n.d. | unspecific signal | n.d. |
| control | | WA-314 | WA-314 | WA-314 | WA-314 | WA-314 | |
| WA-314 YopD-GFP11 | n.d. | -- | - | -- | -- | unspecific signal | n.d. |
| WA-314 YopB-GFP11 | n.d. | = | = | = | = | unspecific signal | n.d. |
| control | | WA-314 | WA-314 | WA-314 | WA-314 | WA-314 | |
| WA-314 YopD-ALFA | n.d. | = | = | = | = | specific signal | specific signal |

Table legend:

| | |
|------|---------------------------------------|
| +++ | strong increase compared to control |
| ++ | moderate increase compared to control |
| + | small increase compared to control |
| = | same as control |
| - | small decrease compared to control |
| -- | moderate decrease compared to control |
| --- | strong decrease compared to control |
| 0 | no signal |
| √ | signal detected |
| n.d. | no data |

4.1. Tagging of effector proteins with Halo, SNAP, CLIP or split-GFP

In order to establish a method that allows for imaging of translocated effector proteins, different tags were fused to *Yersinia* effector proteins and validated regarding their suitability for this specific application. Self-labeling enzyme (Halo, SNAP, CLIP) and split-GFP tags were coupled to effector proteins YopE, YopH and YopM on existing pACYC184 (Cm^R) vectors encoding for the effector proteins under control of their native promoters and in case of YopE and YopH also their respective chaperones SycE and SycH (Trülsch et al. 2003). As the N-terminus of Yops contains the secretion signal required for recognition by the TTSS, all effector proteins were tagged at their C-terminus (Michiels and Cornelis 1991; Sory et al. 1995; Schesser et al. 1996; Anderson and Schneewind 1997; Lloyd et al. 2001). Halo, SNAP and CLIP were additionally labeled with an HA-tag for detection in immunoblots. The newly constructed plasmids were introduced into *Yersinia* WA-314 carrying pYV with deletions of YopE, YopH or YopM (called WA-314ΔYopE/ΔYopH/ΔYopM, respectively) to complement the deleted Yop or WA-C carrying a plasmid encoding only for the TTSS (WA-C pTTSS) resulting in strains secreting only the tagged Yop (Table 1). Staining of Halo, SNAP or CLIP tagged Yops, is conducted by fluorophore coupled ligands that permeate both eukaryotic plasma membranes as well as the cell wall of Gram-negative bacteria. For the split-GFP approach a non-fluorescent, truncated form of GFP (GFP1-10) is expressed in host cells. Translocated GFP11-tagged Yops are then detected by complementation of GFP1-10.

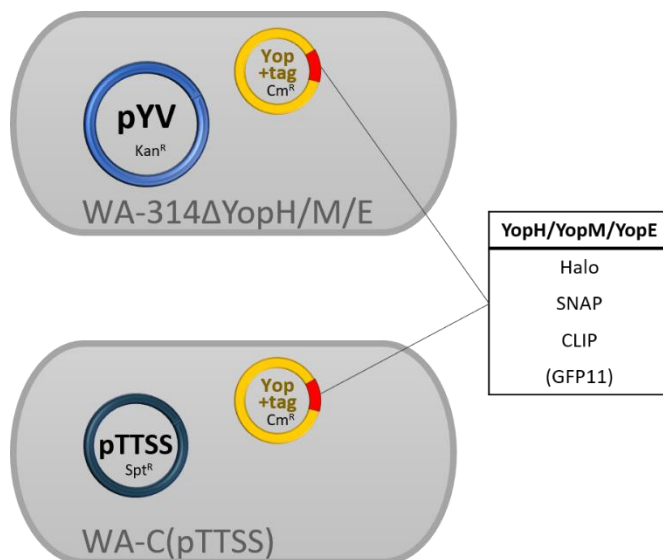


Figure 4 Schematic of the strains expressing Halo, SNAP, CLIP, and split-GFP tagged effector Yops. WA-314ΔYopE/ΔYopH/ΔYopM containing the *Yersinia* virulence plasmid (pYV) or WA-C pTTSS were transformed with the pACYC184 bacterial expression plasmid containing the tagged Yops.

4.1.1. Halo, SNAP and CLIP tags affect the secretion and translocation of effector proteins and thereby reduce cytotoxicity

It is well established that heterologous proteins fused to TTSS substrates may be resistant to TTSS mediated unfolding and get trapped in the secretion path (Akedo and Galán 2005). Blockage of the secretion path by heterologous substrates may also prevent subsequent secretion of natural substrates. Therefore, the new fusion constructs had to be thoroughly validated. The strains carrying the YopH fusion constructs were analyzed regarding protein expression, secretion, translocation into HeLa cells and cytotoxicity.

To analyze the expression of YopH tagged with Halo, SNAP or CLIP, lysates of bacteria grown at 37°C were analyzed by Western blot with anti-YopH and anti-HA antibodies. YopH is a 51 kDa protein, the Halo, SNAP and CLIP tag add 33 kDa, 20 kDa and 20 kDa, respectively. All samples revealed bands corresponding to the expected molecular weight and several degradation bands. In the Δ YopH background Halo, SNAP and CLIP fusions of YopH encoded on pACYC184 were expressed at higher levels compared to native YopH encoded on pYV in WAP (Figure 5A). In the pTTSS background expression of the tagged YopH constructs was compared to wildtype YopH encoded on pACYC184. In this case the levels of native and tagged YopH appeared similar and at increased levels compared to native YopH expressed from pYV, indicating that expression is generally increased from pACYC184.

To analyze whether Halo, SNAP and CLIP affect TTSS substrate secretion, the low calcium response was induced. This response triggers secretion of Yops into the supernatant, when *Yersinia* are placed at 37°C and calcium is depleted from the growth medium (Brubaker and Surgalla 1964; Michiels et al. 1990; Straley et al. 1993). The released proteins were precipitated from the medium and analyzed by SDS gel. One gel was stained with Coomassie to visualize all secreted proteins and the other was blotted on a PVDF membrane for staining with YopH and HA antibodies. Yop secretion was readily detectable by Coomassie (Figure 5B; Yops as indicated by the labels). Native YopH related to a clear band running at the expected molecular weight of 51 kDa, which was not present in the Δ YopH mutant. For the tagged versions of YopH no clear bands were detectable at the expected molecular weight (expected position marked by black asterisks). Further, it was apparent that the secretion levels for the untagged Yops in the Δ YopH mutant expressing YopH-Halo/SNAP/CLIP were decreased compared to the wild type and in the pTTSS strains with tagged YopH no bands were discernible. In immunoblots probed with YopH antibody less YopH secretion was observed in the Δ YopH mutants complemented with tagged YopH compared to the wild type control. The same could be seen for the pTTSS strain with tagged compared to untagged YopH. Probing the blot with HA antibody confirmed that YopH-Halo secretion was the lowest both in complemented Δ YopH and pTTSS. Besides, more YopH-SNAP and YopH-CLIP were secreted in the pTTSS compared to the Δ YopH

expressing these proteins. Together these results suggest that the effectors coupled to self-labeling enzyme tags are not efficiently secreted and apparently also partly block the secretion path for export of natural substrates.

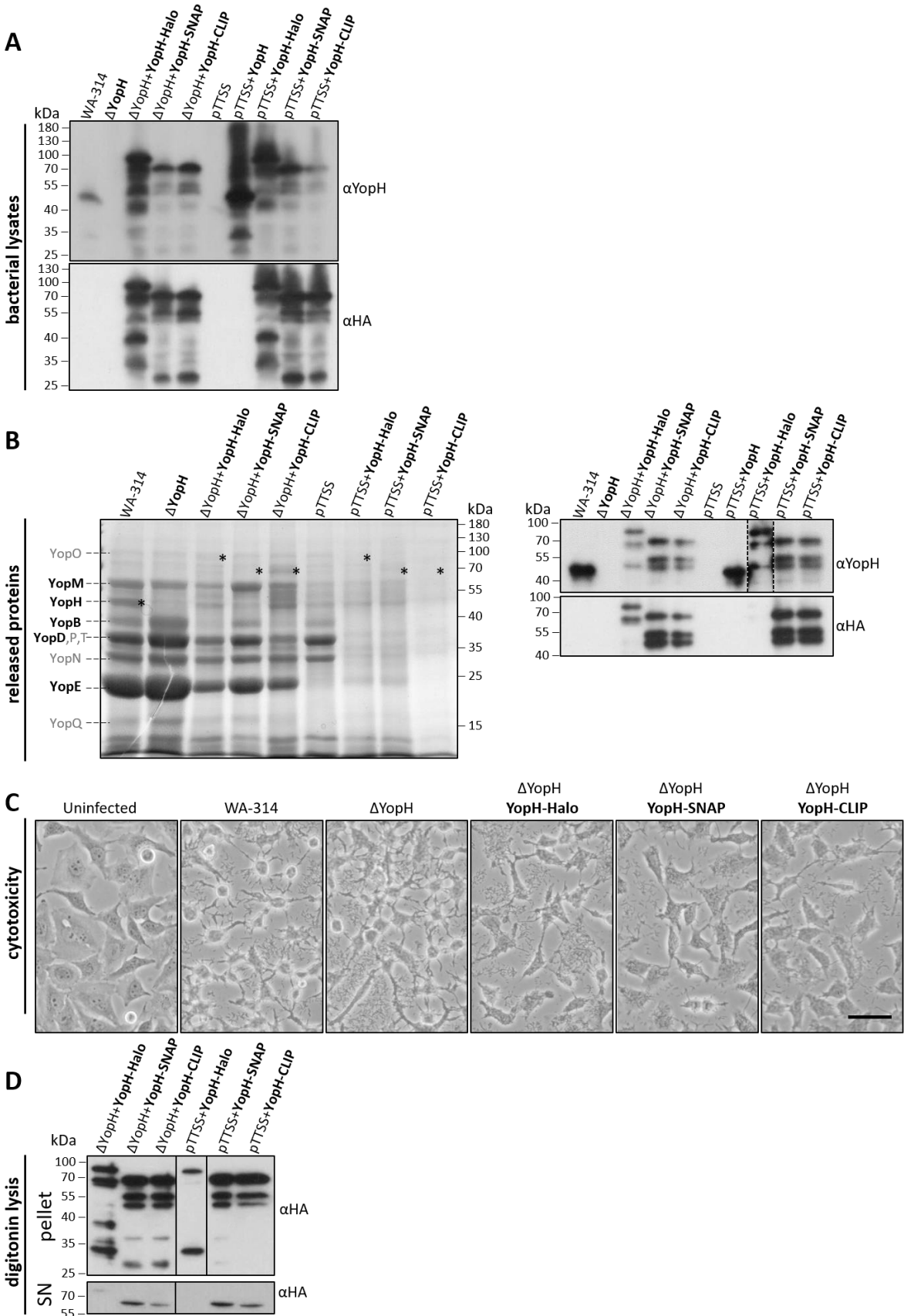


Figure 5 Effect of tagging YopH with Halo, SNAP and CLIP on expression, secretion, cytotoxicity and translocation.

(A) Comparison of untagged and tagged YopH expression in different *Yersinia* strains. Overnight *Yersinia* cultures were diluted 1:20 and placed at 37°C for 1.5 h. The same number of bacteria for each strain was lysed and analysed with Western blot for their YopH content using YopH antibody in the upper panel and HA antibody in the lower panel.

(B) Released proteins from different *Yersinia* strains expressing tagged YopH under calcium depletion conditions. Proteins from the supernatant of bacterial cultures under calcium depletion conditions were analysed on a Coomassie stained gel (left) for their overall protein secretion properties and in Western blot (right) for their YopH content using YopH antibody in the upper panel and HA antibody in the lower panel. Black asterisks indicate the expected position of YopH bands in the Coomassie gel. The dashed line around the pTSS+YopH-Halo lane in the Western blot indicates an increased exposure time.

(C) Cytotoxic effect of different *Yersinia* strains expressing tagged YopH on HeLa cells. HeLa cells were infected for 1 h with WA-314, Δ YopH, Δ YopH+YopH-Halo, Δ YopH+YopH-SNAP and Δ YopH+YopH-CLIP at an MOI of 50. Samples were imaged with the light microscope and compared to uninfected cells. Scale bar: 20 μ m.

(D) Translocation of tagged YopH using digitonin extraction. HeLa cells were infected for 1 h at an MOI of 50 with different *Yersinia* strains expressing Halo, SNAP or CLIP tagged YopH. HeLa cells were lysed with digitonin and the complete resulting supernatants (upper panel) and 10% of each cell pellet (lower panel) were analysed with Western blot for HA labeled tags.

To further assess the functionality of the strains, cytotoxicity was tested by observing the phenotype of infected HeLa cells by phase contrast light microscopy. While uninfected cells were spread out, cells infected with the wild type were uniformly rounded after 1 hour of infection due to the cytotoxic effect of translocated effector proteins (Figure 5C). Cells infected with Δ YopH also lead to rounding. This phenotype was clearly attenuated when infected with Δ YopH carrying the Halo, SNAP or CLIP tagged fusions of YopH again indicating blockage of the secretion path for export of native Yops.

To quantify the amount of translocated YopH, cells were lysed with digitonin after one hour of infection. Digitonin lyses eukaryotic cells but not bacteria, which allows separation by centrifugation of the cytoplasmic fraction containing membrane integrated and soluble Yops in the host cells from a pellet containing insoluble cell components and bacteria (Nordfelth and Wolf-Watz 2001). When comparing the amount of tagged YopH in the pellet and the supernatant by immunoblot with an HA antibody, very little tagged YopH was detected in the digitonin soluble fraction, while a much stronger signal was detected in the pellet fraction (Figure 5D). Halo tagged YopH appears to be translocated in even lower levels compared to SNAP and CLIP tagged YopH.

Table 1 gives an overview of the conducted experiments and results with all strains used in this study. It also summarizes the results for the analyses of the Halo, SNAP and CLIP tagged YopM and YopE strains. The performed experiments show similar results as seen in the strains expressing tagged YopH. Overall, it can be stated that although effector proteins tagged with either Halo, SNAP or CLIP are expressed in sufficient amounts the secretion and translocation of both tagged and untagged Yops is impaired by this approach.

4.1.2. YopE, YopH and YopM can be visualized with Halo, SNAP and CLIP tags within the bacterium but not in the cytosol of the host cell

To get an idea of the distribution of translocated YopH in the infected host cell a YopH antibody was used for immunofluorescence staining. HeLa cells transfected with myc-Rac1Q61L to increase overall translocation (Wolters et al. 2013) were infected with WA-314, Δ YopH and pTTSS+YopH. The Δ YopH mutant was used as a negative control to assess the background signal created by the YopH or secondary antibody staining. In WA-314 infected cells no signal above background could be detected in the host (Figure 6A). A YopH signal from the host cell was only detectable in cells infected with the pTTSS strain expressing YopH from pACYC184 with signal intensity increasing at higher MOIs. The immunofluorescence staining of YopH revealed a rather homogeneous cytosolic distribution of YopH in the host cell.

In HeLa cells transfected with myc-Rac1Q61L and infected with pTTSS+YopH-Halo a strong YopH-Halo signal is detectable within bacteria after staining with TMR-Halo substrate, but no signal can be found in the cytosol of the host cell (Figure 6B). The same distribution was observed in cells infected with strains expressing SNAP or CLIP tagged YopH or Halo tagged YopM. No cytosolic but an intrabacterial signal was confirmed for SNAP and CLIP-tagged YopM expressed in the pTTSS as well as Halo, SNAP and CLIP tagged YopH, YopM and YopE introduced into the deletion mutants Δ YopH, Δ YopM and Δ YopE, respectively (data not shown; see overview in Table 1). Altogether these results indicate a strongly impaired translocation of Halo, SNAP or CLIP tagged effector proteins irrespective of tag, Yop or strain used and demonstrate incompatibility of these tags with TTSS mediated protein transport in *Y. enterocolitica*.

In fixed samples of cells infected with strains overexpressing Halo, SNAP or CLIP tagged effector proteins the intrabacterial signals showed different levels of fluorescence intensity. Live imaging of selected mutants was used to determine whether a decrease or loss of signal could be observed during cell infection, which could indicate the depletion of the intrabacterial pools of tagged YopH due to secretion of the protein. When examining myc-Rac1Q61L transfected HeLa cells infected with SNAP-Cell TMR-Star pre-stained pTTSS+YopH-SNAP a signal could be observed concentrated at the poles of the bacteria, which did not change in intensity over time (Figure 6C). The same observation was made in pTTSS+YopH-CLIP and Δ YopE+YopE-Halo infected cells (data not shown; see Table 1). This confirms the impaired Yop translocation observed in fixed samples (Figure 6B) and immunoblots of translocated proteins (Figure 5D).

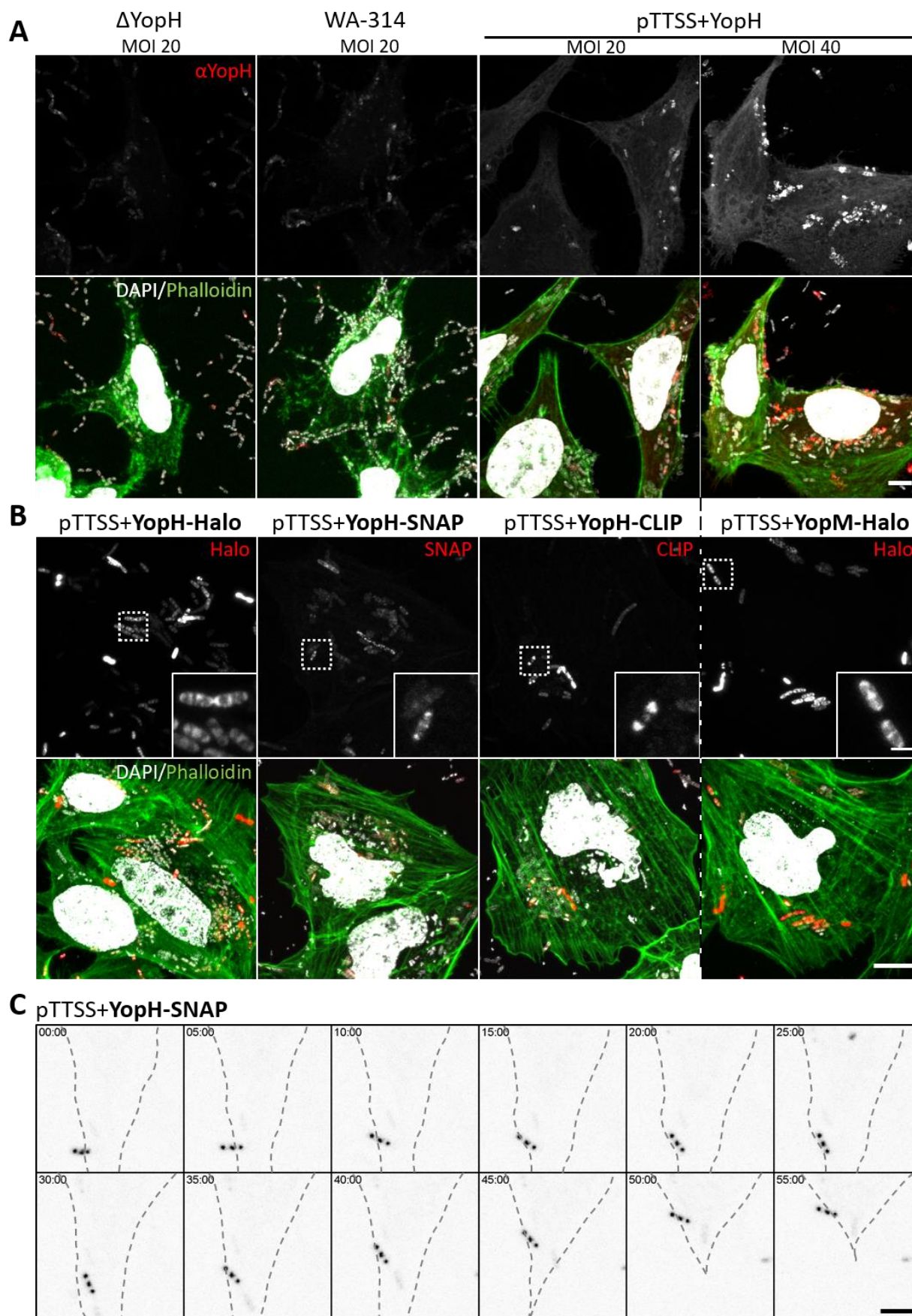


Figure 6 Comparison of effector protein visualization using antibody staining and self-labeling enzyme tags. (A) YopH staining with anti-YopH antibody in infected cells. HeLa cells transfected with myc-Rac1Q61L were infected with WA-314, Δ YopH and pTTSS+YopH (from left to right) for 90 min at an MOI of 20 and an MOI of 40 for the last panel. Cells were stained with anti-YopH antibody (white in upper panel, red in lower panel), AlexaFluor633 phalloidin (displayed in green) and DAPI. Upper panels show the anti-YopH antibody stain and lower panels the overviews with phalloidin and DAPI stain. Scale bars: 10 μ m (YopH antibody stain and overviews). **(B) Comparison of different self-labeling enzymes tagged to YopH and YopM.** HeLa cells transfected with myc-Rac1Q61L were infected with pTTSS+YopH-Halo, pTTSS+YopH-SNAP, pTTSS+YopH-CLIP and pTTSS+YopM-Halo (from left to right) for 90 min at an MOI of 20. Cells were stained with HaloTag TMR Ligand, SNAP-Cell TMR-Star or CLIP-Cell TMR-Star as indicated (555 nm, white in upper panel, red in lower panel), AlexaFluor633 phalloidin (displayed in green) and DAPI. The upper panels show the TMR Ligand stain alone and the lower panels the overviews with phalloidin and DAPI stain. Boxed regions in the upper panels are depicted as enlargements at the lower right corner of each image. Scale bars: 10 μ m (TMR substrate stain and overviews) and 2 μ m (enlargements). **(C) Live imaging of pTTSS+YopH-SNAP infection.** HeLa cells transfected with myc-Rac1Q61L were infected with SNAP-Cell TMR-Star pre-stained pTTSS+YopH-SNAP for 1 h at an MOI of 20. The cells were imaged under the spinning disk microscope and every 30 sec a z-stack of 15 images was taken with an interval of 0.5 μ m between each slice. The z-stacks for each time point were combined to one image using maximum intensity projection and one image every 5 min is shown to generate an overview of fluorescence intensity over time. The dashed line shows the outline of the cell. Scale bar: 5 μ m.

4.1.3. Split-GFP inserted between two proteins (mRFP-GFP11-Rab5) can induce a signal in GFP1-10 transfected cells

As Halo, SNAP and CLIP tags appeared inapplicable for analysis of TTSS substrates, split-GFP was tested as an alternative tool to monitor effector translocation. To confirm the functionality of the split-GFP system in our hands, GFP11 was inserted between RFP and Rab5 on an mRFP-N1 (Kan^R) vector and co-transfected with GFP1-10/BFP into HeLa cells. The cells were fixed 24 h after transfection and imaged with the confocal microscope. The transfected cells could be identified by the BFP signal (vector: pMax_GFP1-10_IRES-NLS_tagBFP). A clear complemented GFP (GFP_{comp}) signal colocalized with the RFP signal indicating a successful complementation of split-GFP inserted into the RFP/Rab5 fusion protein and GFP1-10 expressed in the cytosol (Figure 7). When cells were not expressing GFP1-10 no GFP signal was detectable showing that GFP11 alone is not fluorescent.

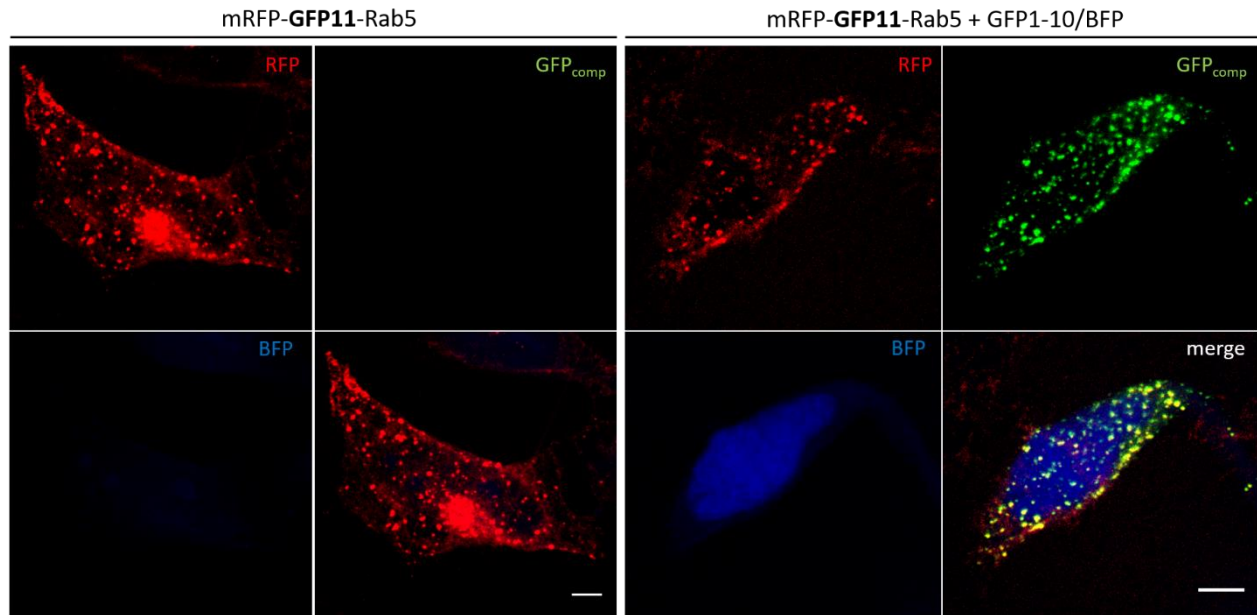


Figure 7 Complementation of GFP11 labeled mRFP-Rab5 and GFP1-10 as proof of principle. HeLa cells were transfected with mRFP-GFP11-Rab5 and GFP1-10/BFP (right) for 24 h. Cells not transfected with GFP1-10/BFP serve as a negative control for GFP complementation (left). Confocal microscopy of the RFP, GFP_{comp} and BFP channels are shown as indicated. Scale bars: 5 μ m (left and right).

4.1.4. Tagging YopE with split-GFP reveals limited effect on effector secretion

The split-GFP approach appeared a possible alternative to the tagging of effector proteins with self-labeling enzymes due to its small size and successful application for tagging effector proteins in *Salmonella* (van Engelenburg and Palmer 2008, 2010). YopE C-terminally tagged with the 11th β -strand of GFP (GFP11) should restore fluorescence when complemented with GFP1-10 expressed in the host cell if efficiently translocated. To test secretion properties of YopE tagged with split-GFP in Δ YopE and pTTSS, the strains were cultured in low calcium medium and the protein from the supernatant was analyzed in Coomassie stained SDS gels and Western blot. In comparison to the wild type overall protein release in Δ YopE+YopE-GFP11 was affected (Figure 8). The YopE band was the largest band in secreted proteins of the wild type in Coomassie gels compared to the other Yops (white asterisk for YopE band). This band was faintly discernible in the Δ YopE mutants complemented with split-GFP tagged YopE. A stronger YopE-GFP11 band was visible in the pTTSS+YopE-GFP11. These observations were confirmed in the Western blot probed with YopE antibody. A strong YopE secretion was visible in the wild type with much less secreted YopE in Δ YopE+YopE-GFP11 but a considerable amount in pTTSS+YopE-GFP11. Together this shows that GFP11 tagged YopE can be secreted although the analysis indicates a general effect of unphysiological expression of tagged effector proteins on overall secretion.

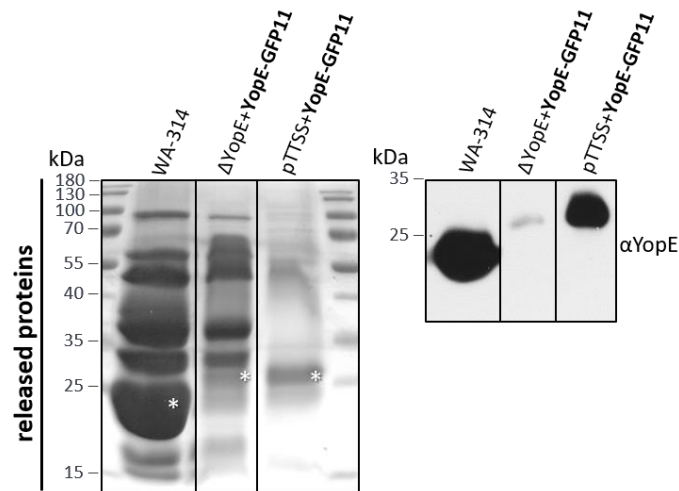


Figure 8 Effect of split-GFP tagging YopE on protein secretion from *Yersinia* strains compared to the wild type. Proteins from the supernatant of bacterial cultures under calcium depletion conditions were analyzed on a Coomassie stained SDS gel (left) for their overall protein secretion properties and in Western blot (right) for their YopE content using YopE antibody. White asterisks indicate the expected position of YopE bands in the Coomassie stained gel.

4.1.5. YopE-GFP11 can be visualized in the cytosol of the host cell transfected with GFP1-10
 Although YopE secretion in strains overexpressing YopE-GFP11 was below wild type level, these strains were used for imaging experiments of GFP1-10 transfected cells to determine whether GFP reconstitution could be observed. When HeLa cells co-transfected with myc-Rac1Q61L and GFP1-10/BFP were infected for 4 h with Δ YopE+YopE-GFP11, a strong fluorescent GFP signal was visible in the host cell (Figure 9A). Only background signal could be seen in cells transfected with myc-Rac1Q61L and GFP1-10 and infected with Δ YopE or in cells not transfected with GFP1-10 and infected with Δ YopE+YopE-GFP11. This again demonstrates that GFP11 and GFP1-10 alone are not fluorescent.

As an alternative to Rac1 induced increase in translocation CNF-1 treatment has been shown to increase translocation in *Yersinia enterocolitica* through the activation of Rho GTPases in eukaryotic cells (Wolters et al. 2013). When Rho GTPases were activated with CNF-1 2 h before infection of GFP1-10 transfected cells with Δ YopE+YopE-GFP11 or pTTSS+YopE-GFP11, a substantial GFP signal was detectable for both strains (Figure 9B). These results indicate that split-GFP could be a useful tool for visualization of translocated effectors.

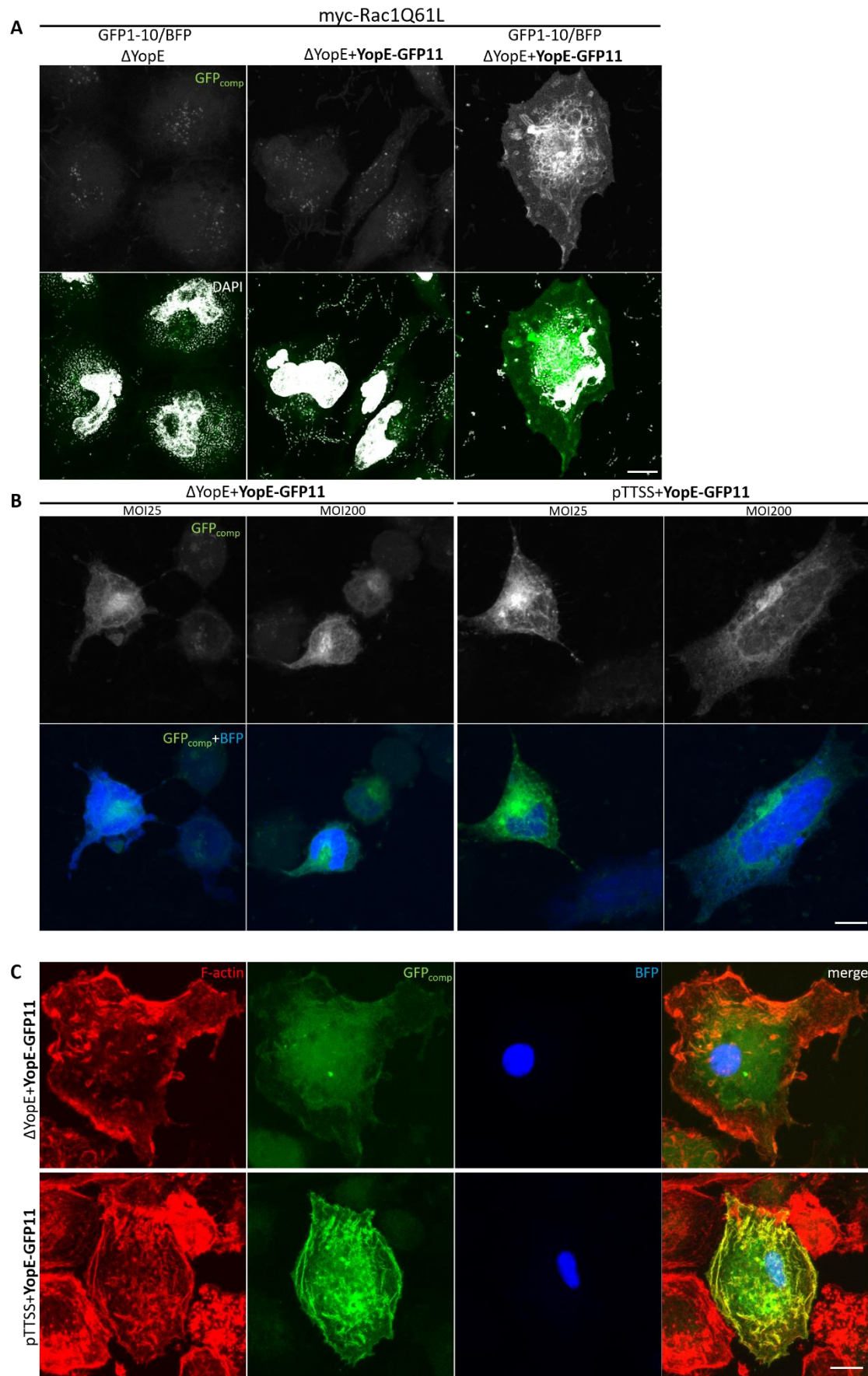


Figure 9 YopE-GFP11 visualization in the cytosol of the host. (A) YopE-GFP11 membrane localization in myc-Rac1Q61L transfected cells. HeLa cells transfected with myc-Rac1Q61L and GFP1-10/BFP were infected with Δ YopE (as a negative control, first panel) and Δ YopE+YopE-GFP11 for 4 h at an MOI of 20. As an additional negative control cells not transfected with GFP1-10 are shown in the middle panel. Samples were stained with DAPI. Upper panels show the GFP_{comp}-channel and lower panels overviews with DAPI stain. Scale bar: 10 μ m. **(B) YopE-GFP11 localization in CNF-1 treated cells.** HeLa cells transfected with GFP1-10/BFP and treated with 1 μ g/ml CNF-1 for 2 h pre-infection were infected with Δ YopE+YopE-GFP11 (left) and pTTSS+YopE-GFP11 (right) for 2 h at an MOI of 25 and 200 as indicated. Upper panels show the GFP_{comp}-channel and lower panels superimposed images of GFP_{comp} and BFP-channels as a transfection control. Scale bar: 10 μ m. **(C) YopE-GFP11 visualization in primary human macrophages.** Primary human macrophages transfected with GFP1-10/BFP were infected with Δ YopE+YopE-GFP11 (upper panel) and pTTSS+YopE-GFP11 (lower panel) for 4 h at an MOI of 100. Cells were stained with AlexaFluor568 phalloidin (displayed in red). The panels show actin signal, GFP_{comp}-channel, BFP-channel and a merge of all channels (from left to right). Scale bar: 10 μ m.

The YopE-GFP11 strains allowing effector translocation in HeLas cells were tested in primary human macrophages, a more physiological target cell for TTSS mediated effector translocation during *Yersinia* infection. When primary human macrophages were transfected with GFP1-10 and infected with Δ YopE+YopE-GFP11 and pTTSS+YopE-GFP11 for 4 h, a diffuse perinuclear signal and a signal colocalizing with the F-actin staining was detectable (Figure 9C). The signal in the pTTSS+YopE-GFP11 infected cells was considerably brighter compared to the complemented deletion mutant. This observation agrees with the stronger YopE band in immunoblots of secreted YopE-GFP11 protein in the pTTSS strain (Figure 8). In addition, the fluorescent GFP signal appears significantly brighter compared to HeLas infected with pTTSS+YopE-GFP11 (Figure 9A-B), which indicates an overall high level of translocation in macrophages. Altogether these findings confirm split-GFP as a useful tool for visualizing effector protein translocation during *Yersinia* infection.

4.1.6. A GFP signal is detectable in live imaging experiments after infection with pTTSS+YopE-GFP11

The suitability of the split-GFP system was tested in live samples as it proved functional in fixed cells. For this, HeLa cells treated with CNF-1, transfected with GFP1-10 and infected with pTTSS+YopE-GFP11 were observed live with a confocal microscope. A detectable GFP signal appeared 40-50 min after infection which continued to increase in the perinuclear region over time (Figure 10). These results show that split-GFP can be used for live cell imaging of YopE translocation.

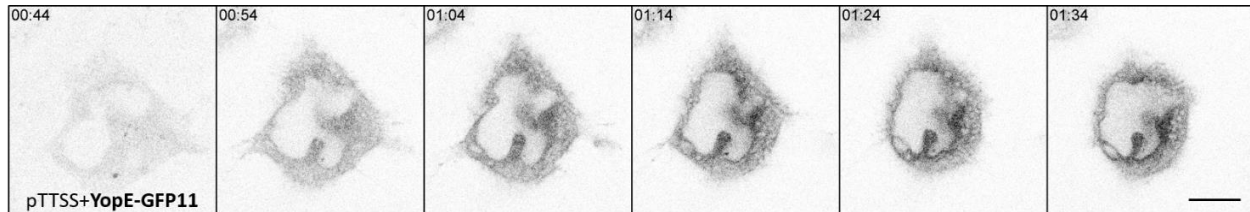


Figure 10 GFP complementation after pTTSS+YopE-GFP11 infection in live imaging. HeLa cells transfected with GFP1-10/BFP and treated with 1 $\mu\text{g/ml}$ CNF-1 for 2 h pre-infection were infected with pTTSS+YopE-GFP11) at an MOI of 200. Cells were imaged with the confocal microscope. Every 2 min one image was acquired and one image every 10 min is shown starting at 44 min to generate an overview of fluorescence increase over time. Scale bar: 10 μm .

4.2. Tagging of pore proteins

Due to the predicted transmembrane topology of the translocators YopB and YopD and the presence of several functionally important domains such as the N-terminal secretion signal and chaperone or tip complex interaction sites, the insertion site for tags into the translocators must be well considered. GFP11 was inserted between amino acids 50-51 of YopD located after the N-terminal secretion signal and directly before a SycD interaction site. For YopB the predicted intracellular loop was targeted for insertion of split-GFP (aa 216-217). These sites were selected as they are expected to be located inside the target cell to enable interaction with GFP1-10 expressed within the cytosol of the host cell. The predicted orientation of C- and N-terminus in relation to the plasma membrane is based on a genetic study of the homologous translocator proteins PopD and PopB in *Pseudomonas aeruginosa* (Armentrout and Rietsch 2016; Discola et al. 2014). The ALFA-tag was inserted into a position of YopD which faces the extracellular side when the protein is inserted into the plasma membrane, so it could be bound by extracellular added nanobody. The insertion between amino acids 194 and 195 is based on deletion experiments in *Y. pseudotuberculosis* (Olsson et al. 2004) and personal communication with Tomas Edgren.

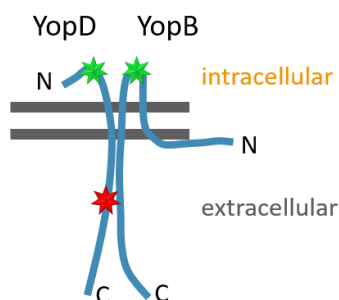


Figure 11 Tag insertion positions for YopB and YopD in the host cell membrane. The graph is derived from predicted membrane orientations of PopB/D (Armentrout and Rietsch 2016). The green stars indicate insertion positions for GFP11 on the intracellular side and the red star indicates the insertion site for the ALFA-tag on the extracellular side.

4.2.1. CRISPR-Cas12a is a useful tool for insertion of small DNA fragments into the virulence plasmid of *Yersinia enterocolitica*

As passage of Yops tagged with GFP11 through the injectosome needle proved successful, split-GFP was evaluated also for tagging of YopB and YopD. However, YopB and YopD are encoded on the large and complex *lcrGVHyopBD* translocon operon (Bergman et al. 1991). Cloning of a single gene of this operon into an expression vector would likely result in unphysiological protein expression levels. Therefore, CRISPR-Cas12a assisted recombineering was applied to introduce GFP11 directly into the native virulence plasmid of *Yersinia* in order to support physiological protein expression and function.

Coupling a CRISPR-Cas system with recombineering was shown to be a simple and efficient tool for genome editing in bacteria (Yan et al. 2017). By combining the CRISPR-Cas12a system with lambda Red recombineering, highly efficient genome editing was demonstrated in *Yersinia pestis*, using single-stranded DNA (ssDNA-oligonucleotides) or double-stranded DNA (dsDNA) generated by PCR as templates for homologous recombination (Zhao and Sun 2018). As the method was newly introduced in our laboratory during this study both approaches (ssDNA oligonucleotides and dsDNA generated by PCR) were evaluated in parallel for the insertion of GFP11 into the translocators. To this end, double-stranded DNAs with 500 bp homologous arms to both sides of the insert site and split-GFP in the middle framed by two different linkers were generated by overlap extension PCR. In addition, single stranded oligos with 50 bp homologous arms on each side of split-GFP and its linkers were designed and ordered.

Cas12a-Kan and Cas12a-Spt encoding Cas12a and the lambda red recombinase were introduced in the pTTSS and WA-314, respectively. Afterwards, the specific crRNA plasmids in combination with either the ssDNA-oligonucleotide or dsDNA PCR product were transformed into the strains. The bacterial suspensions were then streaked on LB plates selecting for bacteria containing an intact pTTSS or pYV as well as for the Cas12a plasmid and the crRNA plasmid. The resulting colonies were tested by colony-PCR for presence of the insertion of GFP11.

The resulting Table 2 shows the success rate of each approach. For the pTTSS the insertion of GFP11 into YopD with the dsDNA PCR product was the most efficient (53%), followed by inserting GFP11 into YopB with the dsDNA PCR product (25%). The ssDNA oligonucleotide did not work for insertion with YopD and very limited with YopB (4%). While inserting split-GFP into YopD with the dsDNA PCR product was highly efficient (70%), the insertion with the ssDNA oligonucleotide did not work. For inserting split-GFP into YopB on the virulence plasmid both dsDNA PCR product and ssDNA oligonucleotide worked well with the latter even showing a higher success rate (50%) compared to the dsDNA PCR product (20%). Overall, the success rate was fivefold higher when using the 500 bp dsDNA PCR product compared to 50 bp ssDNA oligonucleotide (52.1% average vs. 10.8%). In general, it could be shown that small DNA fragments can be

efficiently inserted into the virulence plasmid (or plasmids derived from it e.g. pTTSS) of *Yersinia* using the CRISPR-Cas12a assisted recombineering approach.

Table 2 Efficiency of CRISPR-Cas12a assisted recombineering in *Y. enterocolitica*

| strain | target protein | insert vehicle | total colony count | positive colony PCR | |
|--------|----------------|----------------|--------------------|---------------------|------------|
| | | | | total number | percentage |
| pTTSS | YopD | HDR | 40 | 21 | 53% |
| | | oligo | 13 | 0 | 0% |
| | YopB | HDR | 8 | 2 | 25% |
| | | oligo | 27 | 1 | 4% |
| WA-314 | YopD | HDR | 20 | 14 | 70% |
| | | oligo | 20 | 0 | 0% |
| | YopB | HDR | 5 | 1 | 20% |
| | | oligo | 14 | 7 | 50% |

4.2.2. YopB remains functional after split-GFP insertion while YopD function is affected

Yersinia strains with GFP11 inserted into YopB and YopD were analyzed regarding secretion properties, cytotoxicity, translocation and pore formation. Overall Yop secretion levels of WA-314 YopB-GFP11 were equal to those of the wild type as demonstrated by Coomassie staining of precipitated released proteins (Figure 12A). This was confirmed in Western blots when probing specifically for YopB and YopD in the released proteins. In contrast, in WA-314 YopD-GFP11 overall Yop secretion was reduced and less YopD was detected by immunoblot compared to the wild type, while the amount of secreted YopB was not reduced. For testing the cytotoxicity of the split-GFP mutants, HeLa cells were infected for 1 h with an MOI of 100. While cells infected with the wild type and WA-314 YopB-GFP11 showed similar cytotoxicity, WA-314 YopD-GFP11 infected cells did not show rounding, indicating a decreased overall Yop translocation (Figure 12 B). Infected cells were lysed with digitonin and the supernatant containing the translocated Yop fraction was probed for YopH as an indicator for a functional pore. Less YopH could be detected with YopD-GFP11 while YopB-GFP11 enabled YopH translocation comparable to the wild type (Figure 12 C). The formation of pores during infection was analyzed using HeLa cells transfected with myc-Rac1Q61L, infected for 1 h and stained separately with YopD and YopB antibody (Figure 12 D). The wild type displayed YopD and YopB as spots surrounding the bacterial surface as observed previously (Nauth et al. 2018). Although some spot-like YopB signal could be seen in cells infected with WA-314 YopD-GFP11, the YopD signal looked much fainter and more evenly distributed. WA-314 YopB-GFP11 showed the wild type-like

spots both in YopD and YopB staining. The results for the analyses performed for pTTSS YopD-GFP11 and pTTSS YopB-GFP11 are summarized in Table 1.

Overall, these results demonstrated that the insertion of GFP11 between amino acids 216-217 of YopB does not interfere with major aspects of TTSS function, while GFP11 inserted between amino acids 50-51 of YopD impairs T3SS function in different assays.

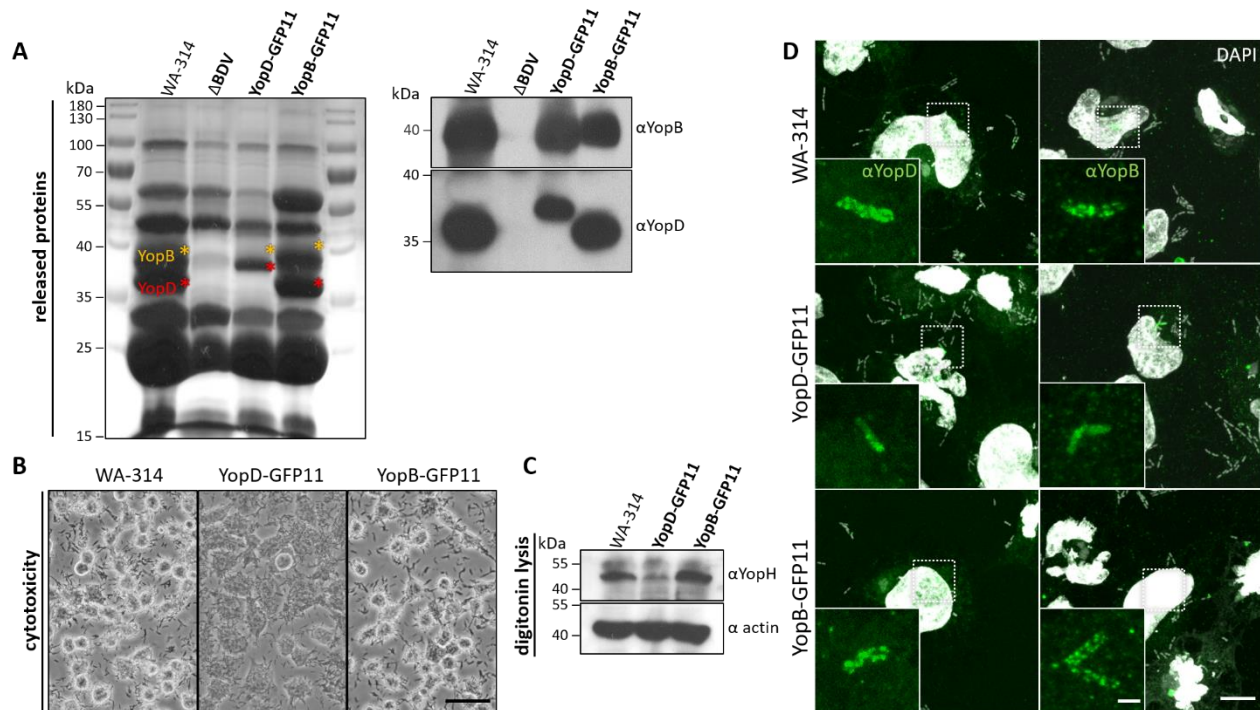


Figure 12 Effect of GFP11 insertion in YopD and YopB on expression, secretion, cytotoxicity, translocation and immunofluorescence staining. **(A)** Released proteins from WA-314 expressing YopD-GFP11 and YopB-GFP11. Proteins from the supernatant of bacterial cultures under calcium depletion conditions were analyzed on a Coomassie stained gel (left) for their overall protein secretion properties and in Western blot (right) for their YopD (upper panel) and YopB (lower panel) content using specific antibodies. Red and yellow asterisks indicate the expected position of the YopD and YopB bands, respectively. WA-314 serves as a positive control and WA-314 Δ BDV as a negative control. **(B)** Cytotoxic effect of WA-314 expressing YopD and YopB with GFP11 insertion. HeLa cells were infected for 1 h with WA-314, WA-314 YopD-GFP11 and WA-314 YopB-GFP11 at an MOI of 100. Cells were imaged with the light microscope. Scale bar: 20 μ m. **(C)** Comparison of effector protein translocation after digitonin extraction. HeLa cells were infected for 1 h at an MOI of 100 with WA-314, WA-314 YopD-GFP11 and WA-314 YopB-GFP11. Cells were lysed with digitonin and resulting supernatants (upper panel) were analyzed with Western blot for YopH. YopH serves as marker for effector translocation and actin serves as host cell loading control. **(D)** YopD and YopB antibody stain in YopD-GFP11 and YopB-GFP11 mutant strains compared to the wild type. HeLa cells transfected with myc-Rac1Q61L were infected with WA-314, WA-314 YopD-GFP11 and WA-314 YopB-GFP11 (from upper to lower panel) for 1 h at an MOI of 30. Cells were stained with anti-YopD antibody (left) and anti-YopB antibody (right) both displayed in green and combined with DAPI. Boxed regions are depicted as enlargements of the antibody signal in the lower left corner of each overview image. Enlargements show representative images of stained bacteria. Scale bars: 10 μ m (overviews) and 2 μ m (enlargements).

4.2.3. No fluorescent signal is detectable with split-GFP tagged YopB/D during infection of GFP1-10 expressing cells

The functional analysis of split-GFP tagged translocators revealed issues with the function of tagged YopD, while the tagged YopB was functional in all control experiments. Still, the ability of both mutants to reconstitute GFP1-10 and induce GFP fluorescence was assessed. When WA-314 YopB-GFP11 and WA-314 YopD-GFP11 were used to infect cells transfected with GFP1-10 for 1 h, no GFP signal was detectable in the host cell apart from some background signal also present in wild type infected control samples (Figure 13). The same result was shown for the pTTSS strains expressing YopD or YopB tagged with GFP11 (data summarized in Table 1). It appears that although split-GFP enables imaging of effector proteins and YopB is functional after GFP11 insertion, it does not allow for visualization of translocon components.

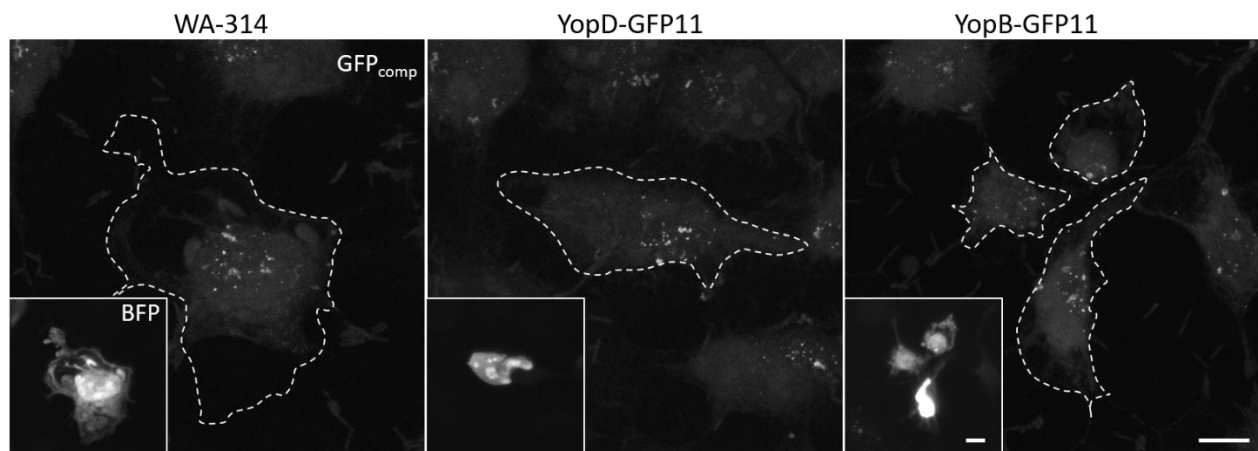


Figure 13 Lack of GFP signal at split-GFP tagged pore proteins. HeLa cells transfected with GFP1-10/BFP were infected with WA-314, WA-314 YopD-GFP11 and WA-314 YopB-GFP11 (from left to right) for 1 h at an MOI of 30. Upper panel show the GFP signal for each condition and lower panel show BFP signal of transfected cells. Scale bars: 10 μm .

4.2.4. YopD is functional with the ALFA-tag inserted between amino acids 194 and 195

The split-GFP approach was not expedient for visualizing pore proteins of *Yersinia* translocons even though the secretion and translocation of the GFP11-tagged effectors and translocators seemed not to be generally hindered. Therefore, we rationalized that small peptide or epitope tags might be an alternative option for visualizing the translocation pore. The ALFA-tag is a short artificially designed peptide tag of 13 amino acids. ALFA-tagged proteins can be detected by high-affinity binding of available anti-ALFA nanobodies labeled with different fluorophores (Götzke et al. 2019). Due to its small size and simple alpha helical structure the ALFA-tag was considered a promising candidate. The small size of the tag also rendered it a suitable for CRISPR-Cas12a mediated insertion into the virulence plasmid. The ALFA-tag was successfully inserted into *YopD* between amino acids 194 and 195 predicted to be on the extracellular part

of the pore complex. To assess if insertion of ALFA into YopD alters the functionality of the protein, the YopD-ALFA mutant was analyzed regarding its secretion and translocation properties as well as its cytotoxic effect and protein interaction. When examining the overall secretion by Coomassie staining as well as probing Western blots of secreted proteins for YopD and YopB no difference was found in WA-314 YopD-ALFA compared to the wild type (Figure 14 A). Digitonin lysis experiments revealed normal effector Yop translocation (Figure 14 B), which was confirmed also in light microscopy images showing regular cytotoxicity comparable to wild type (Figure 14 C). As YopD and YopB are supposed to physically interact in the pore complex, binding of YopD-ALFA to YopB was tested in a pull-down experiment. For this, beads functionalized with anti-ALFA nanobody were loaded with lysates of infected HeLa cells to precipitate YopD-ALFA and potential interaction partners from the membrane inserted pore complexes. In one condition the HeLa cells were treated with CNF-1 to increase the overall translocation rate. The lysates of infected cells before and after incubation with the beads as well as the pull down fraction were tested by immunoblot for their YopB and YopD content (Figure 14 D). ALFA-tagged YopD was readily detectable in pull downs of WA-314 YopD-ALFA infected cells with increased signal intensity in the CNF-1 treated cells, while lysate samples before and after incubation with beads exhibited only unspecific background signal. YopB could be detected in lysates before and after incubation with the ALFA-beads with increased signal intensity in the CNF-1 treated cells. Importantly, YopB could also be detected in the pull down fraction of CNF-1 treated cells indicating an intact interaction of ALFA-tagged YopD and YopB. In summary, ALFA insertion into YopD seems not to interfere with YopD protein function.

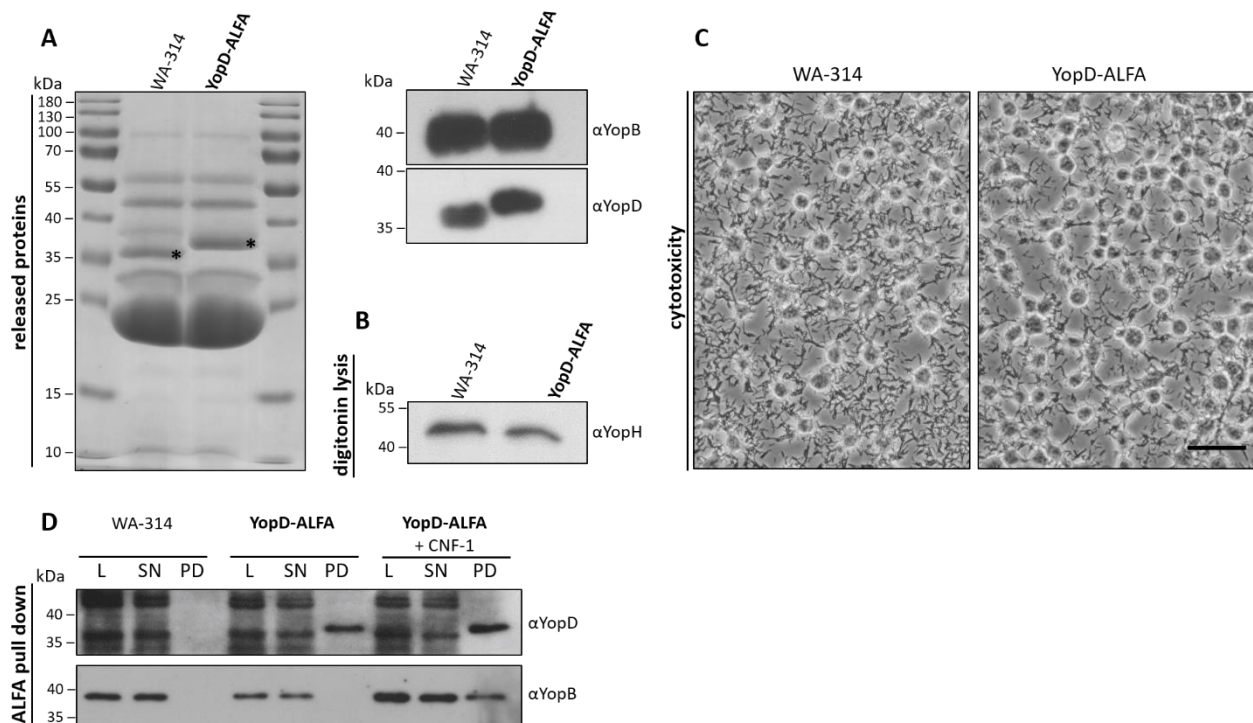


Figure 14 Effect of ALFA-tag insertion in YopD on expression, secretion, translocation, cytotoxicity and protein interaction. (A) Released proteins from WA-314 expressing YopD-ALFA. Proteins from the supernatant of bacterial cultures under calcium depletion conditions were analyzed on a Coomassie stained SDS gel (left) for their overall protein secretion properties and in Western blot (right) for their YopB (upper panel) and YopD (lower panel) content using specific antibodies. Black asterisks indicate the expected position of the YopD bands in the SDS gel. WA-314 serves as a control. **(B) Comparison of effector protein translocation after digitonin extraction.** HeLa cells were infected for 1 h at an MOI of 100 with WA-314 and WA-314 YopD-ALFA. Cells were lysed with digitonin and resulting supernatants were analyzed with Western blot for YopH. **(C) Cytotoxic effect of WA-314 expressing YopD with ALFA insertion.** HeLa cells were infected for 1 h with WA-314 and WA-314 YopD-ALFA at an MOI of 100. The cells were imaged with the light microscope. Scale bar: 20 μ m. **(D) Pull down experiment of YopD-ALFA and YopB from cell lysates of WA-314 YopD-ALFA infected cells.** HeLa cells were infected for 1 h with WA-314 and WA-314 YopD-ALFA at an MOI of 100. In addition, HeLas pre-treated with 1 μ g/ml CNF-1 for 2 h were infected with WA-314 YopD-ALFA. Cells were lysed using digitonin and beads functionalized with anti-ALFA nanobody were used to isolate YopD-ALFA and its interaction partners. The Western blot shows cell lysates before (L = lysate) and after (SN = supernatant) incubation with the beads and pull-down eluates compared in the three different conditions stained with anti-YopD and anti-YopB antibody.

4.2.5. YopD in translocons can be visualized using the ALFA-tag and staining with nanobodies

To test the staining of ALFA-tagged YopD with anti-ALFA nanobody in fluorescence microscopy, HeLa cells transfected with myc-Rac1Q61L were infected for 1 h with WA-314 YopD-ALFA. The cells were fixed and stained overnight with the anti-ALFA nanobody (FluoTag-X2 anti-ALFA, Abberior® Star 580; NbALFA-Ab580) without prior permeabilization. Permeabilization was generally omitted for translocon staining with the nanobody because preliminary investigations indicated that standard permeabilization with 0.1 % Triton X-100 lead to partial staining of intrabacterial YopD, which is evidently not intended in our attempt of specifically visualizing the translocon.

First, for evaluation of specificity, the nanobody stain of YopD-ALFA was compared to the established antibody stain of YopD after permeabilization. The fluorescent signal of the ALFA nanobody stain revealed the same spotty pattern as seen in the YopD antibody staining (Figure 15 A). Additionally, all bacteria with a nanobody stained pore also had a YopD antibody signal showing a high degree of colocalization, confirming the specificity of the nanobody stain. The same results were seen with the ALFA nanobody stain in combination with a YopB antibody stain after permeabilization, demonstrating the presence of YopB together with YopD-ALFA at the translocon. Interestingly, some bacteria displayed an antibody signal but lacked a nanobody signal, indicating that some of the translocation pores are formed in a compartment not accessible by the nanobody without prior permeabilization. It was previously shown that *Yersinia* enters an intermediate host cell compartment, called prevacuole, where formation of the translocation pore is triggered. This compartment is characterized by a narrow connection to the extracellular space,

which allows smaller proteins like streptavidin with an approximate size of 50 kDa to enter (Sarantis et al. 2012; Nauth et al. 2018). Accordingly, the nanobody with just 15 kDa is apparently able to enter the prevacuole and stain the translocon but cannot stain translocons associated with entirely internalized bacteria.

Subsequently, to further confirm the localization of the nanobody stained, translocon forming bacteria in the prevacuole, the nanobody staining of YopD-ALFA was combined with an antibody inside-outside staining using anti-O8 antibodies. This experiment revealed nanobody signal only on bacteria inaccessible to outside staining by anti-O8 antibodies (Figure 15 B), indicating that the nanobody stained bacteria most likely reside in the prevacuole compartment.

Preliminary investigations indicated that the bacteria are permeabilized by 0.1 % Triton X-100 to become accessible by the ALFA-nanobody for staining of intrabacterial proteins. This finding lead us to the idea that it should be possible to distinguish the intra- and extrabacterial pool of YopD-ALFA by nanobody-based inside-outside staining of the bacteria. To test this, cells infected with WA-314 YopD-ALFA were stained with NbALFA-Ab580 before permeabilization and NbALFA-Ab635P after permeabilizing both bacterial and host cell membranes and using 0.05% Triton X-100 in the staining solution. With this approach the signal of extrabacterial translocons could be clearly distinguished from the intrabacterial pool of YopD-ALFA. While all bacteria showed an intrabacterial signal of YopD-ALFA that appeared to increase towards the periphery of the cell, only a subset of the bacteria showed the characteristic pore staining. Interestingly, bacteria displaying pores appeared to have a stronger intrabacterial YopD signal indicating increased YopD expression in these bacteria. In summary, these findings clearly demonstrate that the ALFA-tag is a suitable tool for visualizing the translocon in fixed HeLa cells.

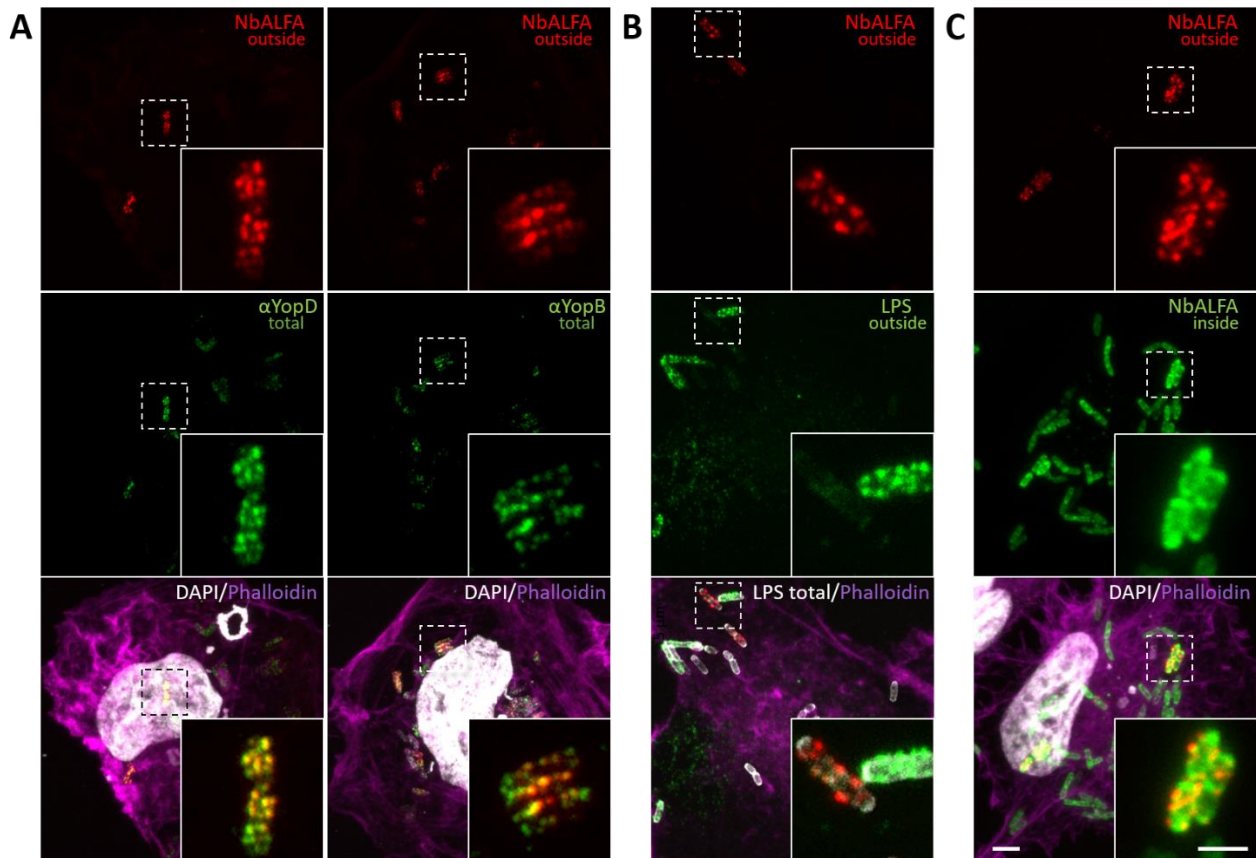


Figure 15 Immunofluorescence staining of YopD-ALFA with the anti-ALFA nanobody in infected cells. (A) Pore protein visualization using ALFA tagged YopD compared to YopD and YopB antibody staining. HeLa cells transfected with myc-Rac1Q61L were infected with WA-314 YopD-ALFA for 1 h at an MOI of 10. Cells were stained with anti-ALFA nanobody (α ALFA nb; displayed in red) before permeabilization, with YopD (left) and YopB antibody (right) after permeabilization (displayed in green), AlexaFluor633 phalloidin (displayed in magenta) and DAPI. The upper panels show the nanobody stain, the middle panels the YopD and YopB antibody stain and the lower panels the superimposed overview images. Boxed regions in the images are depicted enlarged at the lower right corner of each image. Enlargements in the superimposed images only show an overlay of nanobody and antibody channel. Scale bars: 5 μ m (overviews) and 2 μ m (enlargements). **(B) Localization of YopD-ALFA signal before permeabilization of the host cell.** Experimental conditions as in (A). Cells were stained with anti-ALFA nanobody (displayed in red) and LPS antibody (displayed in green) before permeabilization and with LPS (displayed in white) and AlexaFluor633 phalloidin (displayed in magenta) after permeabilization. Upper panels show the extrabacterial nanobody stain, middle panels the LPS outside signal and lower panels the superimposed overview images. Boxed regions in the images are depicted enlarged at the lower right corner of each image. Enlargements in the superimposed images only show overlays of nanobody, outside and total LPS signals. Scale bars: 5 μ m (overviews) and 2 μ m (enlargements). **(C) Localization of YopD-ALFA signal before and after bacterial permeabilization.** Experimental conditions as in (A). Cells were stained with NbALFA-Ab580 (displayed in red) before permeabilization, anti-ALFA nanobody NbALFA-Ab635P (displayed in green) after permeabilization and AlexaFluor633 phalloidin (displayed in magenta) and DAPI. Upper panels show the extrabacterial nanobody stain, middle panels the intrabacterial YopD-ALFA signal and lower panels the superimposed overview images. Boxed regions in the images are depicted enlarged at the lower right corner of each image. Enlargements in the superimposed images only show overlays of the extra- and intrabacterial nanobody signal. Scale bars: 5 μ m (overviews) and 2 μ m (enlargements).

4.2.6. Pore formation can be visualized with YopD-ALFA during live imaging

The excellent results of YopD-ALFA stainings with the fluorescently labeled nanobody in fixed but not permeabilized cells lead us to pursue the adoption of this approach for live cell imaging of pores formed by bacteria in the prevacuole. For this, HeLa cells transfected with myc-Rac1Q61L and GFP-Lifeact were infected with WA-314 YopD-ALFA. The GFP-Lifeact signal showing the actin cytoskeleton of the cell served as a guide visualizing the entry and outline of cell-associated bacteria (Figure 16). NbALFA-580 was diluted 1:300 in cell culture medium which resulted in very low background signal. The images shown are representative of several videos acquired. As observed previously, only some bacteria developed pores (Nauth et al. 2018). When focusing on a specific pair of bacteria, a rapid increase of ALFA nanobody signal was observed. Pores formed right after disappearance of an actin cup surrounding the bacterium - likely indicating the time point of entry of the bacteria into the prevacuole. The signal increased over the first 15 min and disappeared about 30 min after first signal detection. However, pore formation did not always occur instantly after entry and some pore signals took longer to disappear while other signals remained on the bacteria until the end of acquisition. The video shows both the live formation of *Yersinia* translocons as well as their following disappearance. These results demonstrate that the established method is a useful tool for live imaging of pore formation.

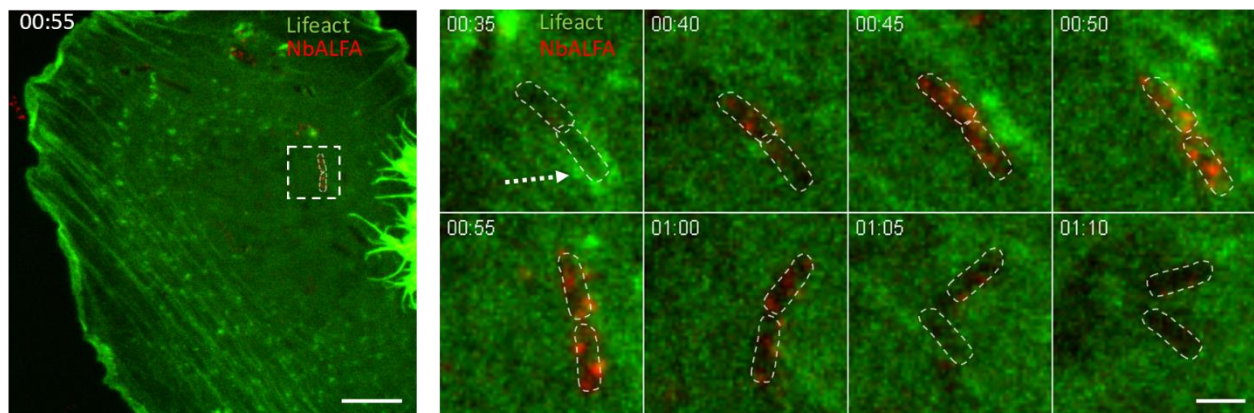


Figure 16 Live imaging of pore formation using nanobody staining for ALFA tagged YopD. HeLa cells transfected with myc-Rac1Q61L and GFP-Lifeact were infected with WA-314 YopD-ALFA at an MOI of 20 and stained with NbALFA-Ab580 diluted in cell culture medium. Cells were imaged with the spinning disk microscope and every minute one z-stack of 15 slices was taken with an interval of 0.5 μm between each slice. The left panel shows a representative overview image from 00:55 h with Lifeact as a marker for F-actin showing the outline of the cell. Stacks for each time point were combined to one image using maximum intensity projection and one image every 5 min is shown (right) starting at 35 min to generate an overview of fluorescence YopD-ALFA signal over time. Dashed lines indicate the outline of the bacteria of interest, dashed arrow indicates actin cup. The boxed region in the overview image shows the area of the video depicted in still frames to the right. Scale bars: 10 μm (overview) and 2 μm (still frames).

4.2.7. Translocon formation is preceded by enrichment of PI(4,5)P2 in the host membrane enclosing the bacteria

Previous studies have shown that the PI(4,5)P2 sensor PLC δ -PH is enriched in the prevacuole membrane. Further, the scission of the prevacuole to form a sealed vacuole was shown to coincide with PI(4,5)P2 hydrolysis. Hence, loss of PI(4,5)P2 indicates the completion of the *Yersinia* entry process (Sarantis et al. 2012; Bahnan et al. 2015). The presence of PI(4,5)P2 enriched membranes around the majority of pore forming bacteria has been demonstrated so far only in fixed cells and as a result lacks information about the dynamics of this relationship (Nauth et al. 2018). Therefore, we aimed at analyzing the precise time point of pore formation in relation to the appearance of PI(4,5)P2 in the membranes enveloping the bacteria. For live imaging myc-Rac1Q61L and PLC δ -PH-GFP transfected HeLa cells were infected with WA-314 YopD-ALFA. The anti-ALFA nanobody was added directly to the culture medium during infection. By this approach a total of 45 events of pore formation were recorded. In all cases the PLC δ -PH-GFP signal appeared either before or virtually at the same time point as pores were formed (Figure 17A). On average the PLC δ -PH-GFP signal appeared 3.8 min (\pm SD of 4.6) before pore formation (Figure 17B). Interestingly, after insertion of the translocon the PLC δ -PH-GFP signal was frequently observed to disappear and reappear around the bacteria (Figure 17A). The underlying mechanisms of this observation are not understood. It could be speculated that this phenomenon represents incomplete scission of *Yersinia* containing prevacuoles related to the antiphagocytic action of translocated Yops. Overall, these results clearly show that pore formation is initiated only after uptake of the bacteria into the PI(4,5)P2 enriched prevacuole.

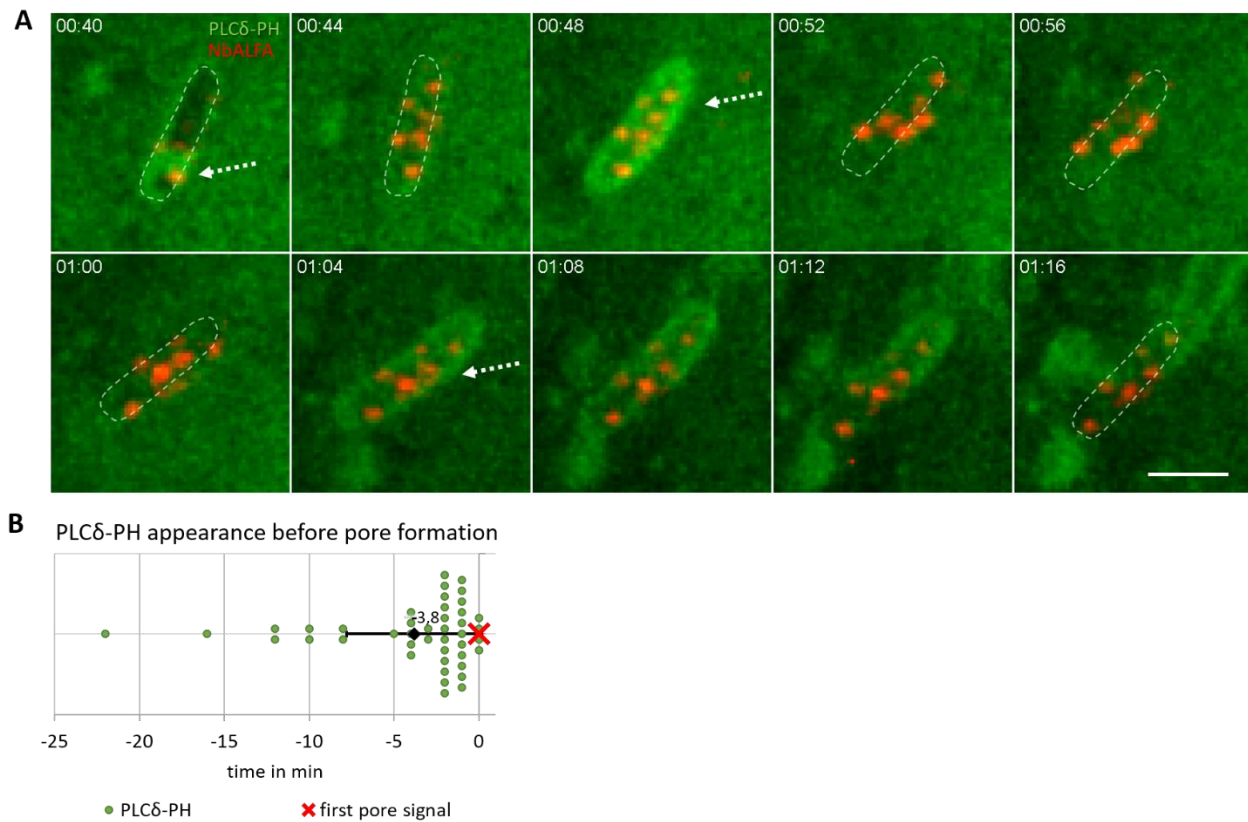


Figure 17 Analysis of signal appearance of PLCδ-PH prior to YopD-ALFA detection. (A) PLCδ-PH signal appears with or before YopD-signal. HeLa cells transfected with myc-Rac1Q61L and PLCδ-PH-GFP were infected with WA-314 YopD-ALFA at an MOI of 20 and stained with NbALFA-Ab580 diluted in cell culture medium. Cells were imaged with the spinning disk microscope and every minute one z-stack of 15 slices was taken with an interval of 0.5 μm between each slice. Stacks for each time point were combined to one image using maximum intensity projection and one image every 4 min is shown starting at 40 min. Arrows indicate the appearance of PLCδ-PH-GFP and dashed lines show the outline of the bacteria when no GFP signal is present. Scale bar: 2 μm . **(B) Dot plot of PLCδ-PH and YopD-ALFA signal appearance at single bacteria.** Based on live imaging experiments performed as in (A) calculations of time passing between the appearance of the different signals. Each dot represents one measurement in relation to YopD-signal appearance (set to 0 min; red cross), bars represent mean \pm SD of $n = 45$ bacteria for PLCδ-PH-GFP (3 different experiments, 13 different cells; \pm SD 4.6).

4.2.8. Galectin-3 recruitment to translocon induced membrane damage

Galectin-3 is a cytosolic carbohydrate-binding protein, which was recently characterized as a sensor of endosomal membrane rupture (Paz et al. 2010). It was shown previously that galectin-3 is recruited to pathogen-containing vacuoles (PCV) in a TTSS dependent manner, pointing towards a role for the translocator proteins in inducing membrane damage (Feeley et al. 2017; Zwack et al. 2017). To test whether pore formation during *Yersinia* infection eventually leads to disruption of the vacuolar membranes and subsequent recruitment of galectin-3, GFP-galectin-3 was co-transfected with myc-Rac1Q61L into HeLa cells. After infecting the cells with WA-314 YopD-ALFA for 1h, fixation and staining

with NbALFA-Ab580 without permeabilization, four different populations of bacteria were regularly identified (Figure 18A): Bacteria with pore signal (1), bacteria with GFP-galectin-3 signal (3), bacteria with both signals (2) and bacteria without any signal (4). These results indicate that apparently membrane damage is induced in a subset of bacteria containing compartments but allow no clear conclusion if GFP-galectin-3 recruitment is directly related to pore formation. However, it must be considered, that in fixed cells the nanobody only stains pores formed by bacteria which still reside in the prevacuole, but pores on bacteria that already proceeded into a sealed vacuole will not be detected. Also, it could be expected that membrane damage happens with some delay after insertion of the translocon. Therefore, live imaging of pore formation appeared as a promising tool to resolve these issues. Hence, HeLa cells expressing myc-Rac1Q61L and GFP-galectin-3 were infected with WA-314 YopD-ALFA and used for live imaging by adding NbALFA-Ab580 to the medium. By this approach a total of 21 events of GFP-galectin-3 recruitment to bacteria containing compartments were recorded. Importantly GFP-galectin-3 recruitment was preceded by pore formation in all recorded events (see representative movie in still frames in Figure 18B). GFP-galectin-3 appeared on average 13.6 min (\pm SD of 7.3) after formation of a detectable translocon (Figure 18C). In conclusion, these results suggest that formation of the translocon in the host membrane induces membrane damage revealed by the presence of GFP-galectin-3, although this hypothesis requires further research.

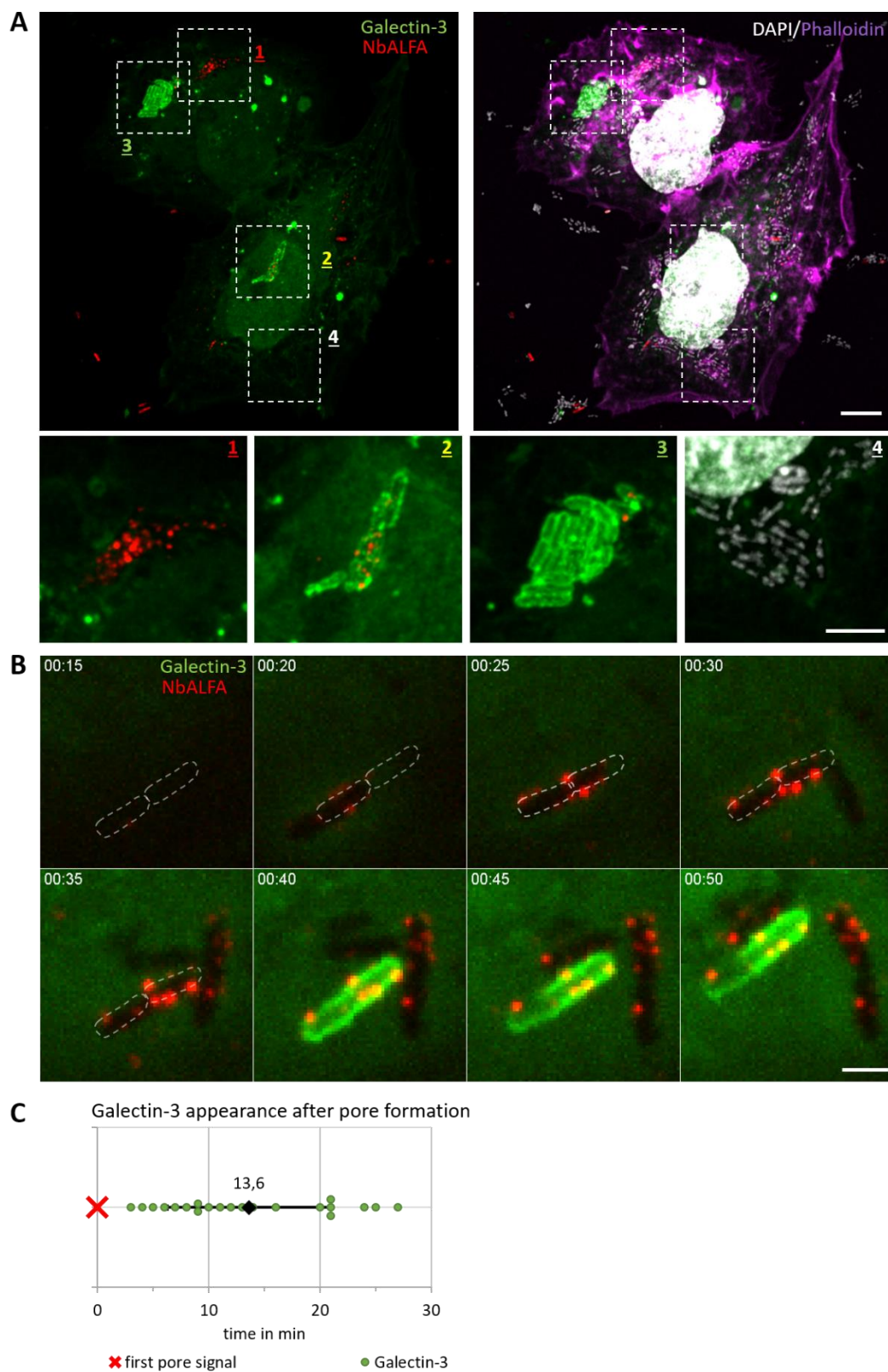


Figure 18 Analysis of galectin-3 signal appearance relative to YopD-ALFA detection. (A) Galectin-3 signal in relation to YopD-ALFA positive bacteria in fixed samples. HeLa cells transfected with myc-Rac1Q61L and GFP-galectin-3 were infected with WA-314 YopD-ALFA for 1 h at an MOI of 20. Cells were stained with NbALFA-Ab580 (displayed in red),

AlexaFluor633 phalloidin (displayed in magenta) and DAPI. The upper panels show the overview images. The left image shows the nanobody stain together with galectin-3 signal and the right image phalloidin and DAPI signal in addition. Boxed regions in the upper panels are shown enlarged below. The enlargements show four different bacteria populations (labeled 1, 2, 3, 4) with overlays of nanobody and galectin-3 signal (additional DAPI in image 4). Scale bars: 10 μm (overviews) and 5 μm (enlargements). **(B) Pore dependent appearance of galectin-3 signal at bacteria during infection.** HeLa cells transfected with myc-Rac1Q61L and GFP-galectin-3 were infected with WA-314 YopD-ALFA at an MOI of 20 and stained with NbALFA-Ab580 diluted in cell culture medium. Cells were imaged with the spinning disk microscope and every minute one z-stack of 15 slices was taken with an interval of 0.5 μm . The z-stacks for each time point were combined to one image using maximum intensity projection and one image every 5 min is representatively shown starting at 15 min showing the appearance of stained YopD-ALFA pores before galectin-3 signal. Dashed lines show the outline of the bacterium when no GFP signal is present. Scale bar: 2 μm . **(C) Dot plot of YopD-ALFA and galectin-3 signal appearance at single bacteria.** Based on live imaging experiments performed as in (B) calculations of time passing between the appearance of the different signals. Each dot represents one measurement in relation to YopD-signal appearance (set to 0 min; red cross), bars represent mean \pm SD of $n = 21$ for galectin-3 (3 different cells; \pm SD 7.3).

5. Discussion

The TTSS is a complex bacterial nanomachine enabling control of the host's immune response through translocation of effector proteins. It has been found in several pathogenic bacteria and extensive research has been performed to elucidate its function to the molecular level (Cornelis and van Gijsegem 2000; Mota et al. 2005; Troisfontaines and Cornelis 2005; Cornelis 2006; Diepold and Armitage 2015). Nevertheless, due to its complex structure and specific environment it has been a challenge to investigate the molecular machinery and effector proteins involved. Studies using antibodies offer snapshots of complex processes with limited temporal resolution (Nauth et al. 2018). However, conventional methods of tagging effector proteins with fluorophores such as GFP have been unsuccessful as proteins have to be unfolded for passage through the needle, which is prevented by the thermostability of the fluorescent proteins (Akeda and Galán 2005; Radics et al. 2014; Dohlich et al. 2014). Additionally, proteins of the injectisome are highly structured and tightly packed which can be disrupted by tagging in an unsuitable location. To allow live imaging of pore formation and effector translocation during cell infection, tags including self-labeling enzymes, split fluorescent protein and an artificial epitope tag were tested, and their application will be discussed in the following.

5.1. Halo, SNAP and CLIP tags are incompatible for translocation through the needle of the injectisome

Overall, visualization of *Yersinia* outer proteins with functional tags in their physiological environment poses a multitude of challenges. Despite many proposed approaches to the task, the majority resulted in limited success. So far translocation of effector proteins has been widely observed using Western blots of lysed host cells which provide information about general translocation at specific time points but do not offer spatial information and have a limited sensitivity (Abrahams et al. 2006; Kubori and Galán 2003). Others have used enzymatic labels which result in indirect signals in the host cell and lack spatial resolution (Sory and Cornelis 1994; Marketon et al. 2005; Garcia et al. 2006). Unfortunately, the conventional labeling of effectors with fluorescent proteins has been shown to hinder the secretion processes (Akeda and Galán 2005). Therefore, we tested self-labeling enzymes Halo, SNAP and CLIP which can be fused to a protein of interest and can be visualized by covalently binding a ligand coupled to a small fluorophore (Los et al. 2005; Keppler et al. 2003; Gautier et al. 2008). When fused to YopM, YopH and YopE and stained with a TMR labeled ligand, a strong intrabacterial signal was seen (Figure 6). The ability of visualizing the intrabacterial Yop pool is in accordance with other studies analyzing intrabacterial protein movement or protein interaction in live bacteria using self-labeling enzymes (Landgraf et al. 2012; Ke et al. 2016). The staining

showed low background signal due to the high specificity towards their ligand and enabled live imaging of intrabacterial Yops. However, the signal detected after staining of YopH-, YopM- and YopE-fusion proteins was limited to bacteria and not detectable in the cytosol of the host cell. Even during live imaging experiments no signal depletion was visible in single bacteria during infection which could have served as an indirect indication of protein translocation (Figure 6C). The limited overall secretion and low translocation detected in Western blots despite an increased expression (Figure 5) supported the conclusion that the tagging with self-labeling enzymes prevents Yop transport through the TTSS. This was further supported by the decreased cytotoxic effect compared to controls indicating a lack of effector proteins delivered to the cells. It is likely that Halo, SNAP or CLIP tags cannot be unfolded blocking the injectisome like a plug impairing overall translocation of all Yops as seen for GFP tagged effector protein SptP from *Salmonella* (Radics et al. 2014). As impaired secretion and translocation was observed regardless of which Yop was tagged or which tag was used it appears to be a general issue of incompatibility between self-labeling enzymes and the TTSS in *Y. enterocolitica*.

Studies with Halo, SNAP and CLIP tagged effector proteins in *Salmonella enterica* showed successful translocation and visualization within the host cell (Göser et al. 2019). YopM tagged with Halo, SNAP and CLIP was also investigated but performed poorly in comparison. Interestingly, tagged effector proteins from *Salmonella* pathogenicity island 2 (SPI2) translocated better than proteins from *Salmonella* pathogenicity island 1 (SPI1). Effectors encoded on SPI1 are required for bacterial uptake into the host cell while proteins from SPI2 are synthesized upon arrival in the phagosome (LaRock et al. 2015). Proteins of the SPI1 as well as the *Yersinia* outer proteins are expressed before cell contact and are subsequently translocated upon establishment of a connection. As SPI2 proteins are immediately delivered after expression without storage, there might be a different underlying mechanism of secretion involved allowing delivery of Halo, SNAP and CLIP tagged effectors. It is possible that prestored proteins are at a different level of protein folding compared to proteins which are instantly translocated after expression. Further investigations would be required to resolve this question.

5.2. GFP11 is a useful tag for visualizing effector translocation but not pore formation

The split-GFP system is based on the separate expression of GFP1-10 and GFP11 and its ability to self-complement when in close proximity. It has become a useful tool in recent years allowing analysis of protein interaction, transport and location in *in vitro* experiments as well as in eukaryotic cells and bacteria (Avilov and Aleksandrova 2018; Pedelacq and Cabantous 2019). Due to the small size of GFP11 it has been used by several groups and in different organisms to visualize effector proteins translocated into host cells

through type three and type four secretion systems (van Engelenburg and Palmer 2010; Young et al. 2017; Wang et al. 2018b; Park et al. 2017; Li et al. 2014b; Yang et al. 2017).

In this study split-GFP has allowed visualization of *Y. enterocolitica* effector translocation into HeLa cells and primary human macrophages (Figure 9A-C). YopE was chosen as it is secreted in the largest amount compared to other Yops (Straley and Cibull 1989; Lee et al. 1998). However, HeLa cells required an artificial increase of translocation through transfection with constitutively active Rac1 or treatment with CNF-1 to gain a detectable GFP signal. In contrast, infected primary human macrophages did not require any manipulation to allow for visualization of translocated YopE (Figure 9C). Possibly, this is connected to the previously observed higher percentage of bacteria displaying a pore in macrophages compared to HeLa cells resulting in increased translocation of effector proteins (Nauth et al. 2018).

YopE tagged with split-GFP has been shown to induce a fluorescent signal 40-50 min after infection in live imaging experiments with HeLa cells (Figure 10). However, it provides limited information about the beginning of YopE translocation as YopE can only be detected when the GFP11 tag and GFP1-10 expressed in the host cell restore GFP fluorescence and enough signal is generated to pass the detection threshold. This depends on the speed of translocation, the strain used, the time GFP11 and GFP1-10 take to complement, the number of GFP molecules necessary for signal detection, the level of infection, and the amount of GFP1-10 expressed in the host cell.

The higher fluorescence intensity in primary human macrophages infected with pTTSS+YopE-GFP11 compared to the YopE mutant expressing YopE-GFP11 could be explained by the presence of other Yops which have to be expressed and secreted while the pTTSS only expresses the machinery necessary for translocation. Besides, YopK, which is known to downregulate overall translocation limiting the possible fluorescence intensity, is not present in the pTTSS (Aili et al. 2008).

It is likely that YopE is present at very early stages of infection as phagocytosis is a rapid process and can only be prevented by immediate translocation of anti-phagocytic effector proteins. Accordingly, previous studies showed the cytotoxic effect of YopE in form of cell rounding 15 min after infection caused by the inactivation of GTPases involved in the polymerization of actin causing disruption of the cytoskeleton (Straley and Cibull 1989; Rosqvist et al. 1991; Black and Bliska 2000; Pawel-Rammingen et al. 2000; Aili et al. 2006). This shows that a considerable amount of YopE would be present at this time point. Other anti-phagocytic Yops are translocated immediately after cell contact. Specifically, YopH-mediated dephosphorylation was detected within 30 s after onset of infection and subsequently found at focal adhesion points in host cells (Andersson et al. 1996; Andersson et al. 1999; Pettersson et al. 1999). In addition, YopH was detectable in Western blot after only 15 min of infection (Wolters et al. 2013). Using YopH(1-17) tagged with β -lactamase showed secretion within the first 5 min upon calcium depletion from

the medium (Milne-Davies et al. 2019). Overall, these studies indicate YopE presence in the host cell significantly before its detection using GFP complementation.

The kinetics of reassociation of GFP11 and GFP1-10 *in vitro* are estimated to range between 15-30 min (Rodrigues and Enninga 2010; Avilov and Aleksandrova 2018). However, *in vitro* experiments have been performed at room temperature and experiments in live cells could result in faster self-assembly. However, no data have been published on the specific kinetics of GFP fluorescence restoration in live cells. In infection experiments using split-GFP for effector visualization, the time until detection varies greatly. For instance, the *Salmonella* effector protein PipB2 labeled with split-GFP induced fluorescence earliest 4 h post infection, while PipB2 was detectable in WB after 2 h post infection (van Engelenburg and Palmer 2010; Young et al. 2017). Split-GFP labeled effectors AvrB and AvrRps4 from *Pseudomonas syringae* were detected 3 and 6 hours post infection, respectively, in specific subcellular localizations of *Arabidopsis* (Park et al. 2017). An even longer time frame was found for the detection of the effector protein VirE2 in *Agrobacterium tumefaciens*. A fluorescent signal was induced 32 h after infiltration into the leaf tissues of transgenic tobacco (Yang et al. 2017).

GFP detection relies not only on fluorophore restoration but also on the amount of GFP molecules necessary for visualization. Analyses of protein abundance in *Saccharomyces cerevisiae* revealed that 1 400 GFP molecules per cell allowed reliable detection above cellular autofluorescence using flow cytometry and confocal live microscopy (Ho et al. 2018), although this number could be lower for proteins accumulating in a specific location. Nevertheless, the delay of YopE-GFP11 translocation and detection can be explained by the kinetics of GFP reassociation and the number of GFP molecules necessary for detection.

The GFP11 labeling of pore proteins YopB and YopD did not result in a detectable fluorescence signal (Figure 13). Possibly, split-GFP is prevented from complementing with GFP1-10 as it is either not translocated properly, not correctly inserted into the hosts membrane or sterically inaccessible due to protein folding or interaction with other proteins. Otherwise, the amount of complemented GFP present could be insufficient to generate a GFP signal above the background level. For GFP11 inserted into YopD, lack of GFP detection is likely caused by functional impairment of YopD seen in control experiments (Figure 12). Presumably, no functional pore is formed preventing contact of GFP11 to GFP1-10. As YopB tagging with GFP11 results in unaffected secretion and translocation of other Yops is comparable to the wild type under infection conditions (Figure 12), a functional problem seems unlikely in this case. However, inaccessibility and a signal below detection threshold could be the cause.

In general, a disadvantage of the split-GFP approach is that both pathogen and host require genetic modification, which limits the application to transfectable cells and poses the danger of interference with

native function of the cell or the pathogen. Additionally, complemented GFP is not as bright as GFP requiring more molecules before detection is possible. There are several options to optimize imaging quality of GFP11 tagged Yops during infection. Firstly, the generation of stable cell lines expressing GFP1-10 might improve the probability to image fluorescent complementation of GFP11 tagged Yops. In addition, the use of superfolder GFP, which has improved properties since the discovery in *Aequorea victoria* in regard to brightness, and the precision and speed in which it folds, could enhance signal detection (Pédélec et al. 2006). Another interesting approach has been the use of nanobodies against GFP inducing conformational changes which increase the fluorescence intensity of the molecule. These enhancer nanobodies allow the fourfold fluorescent enhancement of split-GFP and even the 1.5-fold increase in fluorescence of recombinantly purified eGFP (Kirchhofer et al. 2010). The co-expression of anti-GFP nanobody resulted in a 5-8-fold fluorescent enhancement for split-GFP (Koraïchi et al. 2018). However, this approach requires additional treatment or transfection of cells. Other groups have tested repeated GFP11 tags to increase signal intensity. These tandem arrangements of 3x, 4x, or 7xGFP11 resulted in proportional increase in fluorescence tested for the *Salmonella* effector protein SteA and β -tubulin (Kamiyama et al. 2016; Young et al. 2017). The latest attempt to increase the speed of self-association and fluorescence intensity of split-GFP was the use of GFP1-10 pre-maturation (Lundqvist et al. 2019). Recombinantly expressed GFP1-10 was pre-folded by the interaction with GFP11 coated beads which later increased fluorescent complementation 150-fold and reduced the amount of GFP1-10 necessary for detection of fluorescence above the background signal. Despite the impressive increase, this approach involves an additional elaborate assay and GFP1-10 would have to be added to the medium of the cells instead of expression in the cell requiring a change of GFP11 insertion site to an extracellular position. Overall, despite successful application of split-GFP for the visualization of translocated YopE, fluorescent complementation appears to be unsuitable for detection of translocon formation.

5.3. CRISPR-Cas12a is a highly efficient tool for inserting small DNA fragments into the virulence plasmid of *Yersinia enterocolitica*

In our hands, CRISPR-Cas12a assisted recombineering achieved efficient insertion of small DNA sequences into the virulence plasmid of *Y. enterocolitica*. The method offers a variety of advantages and prospects for future research. By combining basic research methods such as PCR and electroporation of bacteria, which are inexpensive, fast and reliable, a positive result was realized with an efficiency of about 30%. Due to the 5'-TTN-3' PAM of Cas12a insertion sites can be chosen flexibly as many such sequences are available enabling effortless crRNA design.

The direct insertion of tags into genes encoded on the pYV in *Yersinia* allows for physiological regulation of gene expression. Increased effector protein expression as observed for example using the pACYC184 encoded effectors may result in increased translocation and interfere with *Yersinia* pathogenicity. A tight regulation of Yop translocation during infection was shown to be necessary for the inhibition of key innate defense mechanisms to prevent the detection of bacteria by the host. For example YopK and YopE downregulate Yop translocation (Aili et al. 2008). A limited amount of YopD in the host cell prevents inflammasome activation which is induced through YopD hypertranslocation (Brodsky et al. 2010). YopE and YopT activate the pyrin inflammasome while YopM inactivates pyrin by binding to protein kinase C-related kinases (PRKs) which induces phosphorylation and inactivation (Chung et al. 2016). Therefore, the absence or hypertranslocation of a Yop affects other Yops and interferes with overall *Yersinia* pathogenicity implicating the importance of a correct level of expression and translocation.

Conventional homologous recombination is an effective way to manipulate bacterial genomes but usually relies on the insertion of a resistance cassette for selection of recombinants. To cure resistance genes site-specific recombinases or resolvases can be used although they cause chromosomal scarring (Datsenko and Wanner 2000; Malaga et al. 2003; Song and Niederweis 2007; Shenkerman et al. 2014). The plasmids used for CRISPR-Cas12a assisted recombineering encoding Cas12a, lambda red recombinase and the crRNA can be easily cured from the strains due to their sucrose and heat sensitivity. No additional resistance cassette must be inserted into pYV as selection is based on the activity of Cas12a cutting the virulence plasmid which conveys kanamycin resistance preventing growth on kanamycin containing LB plates. However, it is possible for bacteria to evade this through spontaneous point mutations or partial deletions of the PAM or protospacer sequence region. This could account for colonies present on LB plates containing kanamycin but lacking an insert.

The length of homology arms seemed relevant to the level of effective insertion of split-GFP into YopB and YopD genes on pYV. The insertion using 500 bp homology arms compared to 50 bp homology arms was five times more successful (Table 2). Although it must be considered that the longer homology arms were PCR-generated and therefore double stranded while the shorter homology arms were single stranded which could affect the outcome. For both the ssDNA oligo as well as the dsDNA PCR product 700 ng were used which results in 1 pmol of 1090 bp dsDNA and about 11 pmol of 190 bp ssDNA. Besides, the shorter synthesized oligos were probably purer compared to the PCR fragments isolated from agarose gels. These differences must be taken into account when looking at the efficiency comparison of both DNA fragments. However, as a larger number of purer DNA was used for the synthesized oligos, this should increase the insertion efficiency. Possibly, this explains the merely fivefold higher efficiency when using the tenfold longer homology arms. The effect of longer homology arms was shown in previous studies. For example,

gene replacements in the chromosome of *E. coli* were performed using Cas12a and double stranded PCR products with 45 and 500 bp homology arms (Yan et al. 2017). With the 45 bp homology arms only 0.4% were positive while 59% with 500 bp homology arms showing homology arm length positively correlates with successful recombination. The relevance of homology arm length was also shown for Cas9 in *Clostridium cellulolyticum* inserting antisense RNA for gene repression (Xu et al. 2017).

As only inserts of a similar size were used in this study (GFP11: 87 bp; ALFA: 84 bp), it is not possible to say whether insert size affects recombination efficiency as demonstrated in other studies. Insertions in the chromosome of *M. smegmatis* were more likely to occur with decreased insert size (Yan et al. 2017). The same study showed a decreased efficiency with increased deletion size and additionally a relevance of homology arm length (79 bp homology arms: 418 bp deletion 17.4%, 1000 bp deletion 8.2%; 59 bp homology arms: 1000 bp deletion 0%). The importance of insert size and homology arm length for recombination was also shown in eukaryotic cells using Cas9 (Li et al. 2014a). Interestingly, in *Y. pestis*, *E. coli* and *M. smegmatis* targeting of the lagging strand showed a higher efficiency than targeting of the leading strand, which moves in the same direction as the helicase during replication (Yan et al. 2017).

Overall, CRISPR Cas12a assisted recombineering is a precise, cost- and time-efficient tool for bacterial genome editing enabling native expression of tagged proteins but is dependent on insert and homology arm size.

5.4. Varying effect of tag insertion in different sites on protein function of translocators YopB and YopD

Tag insertion into proteins always poses a risk as disruption of protein sequence can affect their structure and function or lead to obstruction of interaction sites. If structural information through analysis of crystallography data is available and interaction sites with other proteins are clearly defined, these issues can be avoided through precise selection of insertion sites. In the case of YopB and YopD the information available is limited to knowledge about N-terminal secretion signals, predicted transmembrane domains, chaperone and translocator interaction sites, and YopD binding to the tip complex. This information formed the basis for the selection of insertion sites. For GFP11 insertion into YopD the secretion signal within the first 10-15 residues was considered as well as amino acids 53-149 essential for SycD binding (Lunelli et al. 2009). Besides, regions including the transmembrane domain (aa 128-149) and the amphipathic domain (aa 278-292) were avoided (Mattei et al. 2011; Costa et al. 2010). As only the N-terminal side of YopD is predicted to face the cytosol when inserted into the host membrane, GFP11 was inserted after amino acid 50 before the SycD interaction domain. Although expression and secretion of this construct appeared functional, the pore forming function of YopD seemed impaired. This was evident

as YopD and YopB antibody staining did not result in spots on the bacterial surface under infection conditions and less translocation was observed resulting in reduced cytotoxicity (Figure 12). As deletion mutants of sequences adjacent to the selected insert site in YopD in *Y. pseudotuberculosis* impaired SycD binding, secretion and translocation, the issues with GFP11 insertion were predictable (Olsson et al. 2004). However, no better site could be identified based on the present information.

Insertion of the ALFA-tag between amino acids 194 and 195 of YopD was chosen as it is predicted to face the extracellular milieu when inserted into the plasma membrane of the host and avoided the interaction sites with LcrV and YopB (Costa et al. 2010; Armentrout and Rietsch 2016). The insertion resulted in an overall functional protein, acting as the wild type in secretion, translocation and cytotoxicity (Figure 14). This is in accordance with data of *Y. pseudotuberculosis* YopD deletion mutants indicating the selected region of limited functional relevance (Olsson et al. 2004). The study demonstrated that deletion of amino acids 174-198 allowed efficient secretion, translocation and cytotoxicity.

For the insertion of GFP11 into YopB a site between the transmembrane domains (aa 166-188; aa 228-250) was chosen as it is supposed to face the intracellular milieu when YopB is inserted into the host membrane (Matteï et al. 2011). GFP11 insertion between amino acids 216 and 217 of YopB allowed normal secretion, translocation and pore formation (Figure 12) indicating that no functional domain was disrupted at the selected site. This finding was in a way surprising as the high degree of conservation of this region between different species suggested an important functional role (Matteï et al. 2011).

5.5. The ALFA-tag allows visualization of both intrabacterial YopD as well as YopD as part of the TTSS pore

Tagging YopD with the artificial epitope tag ALFA in a position which faces the extracellular side of the translocon allows visualization of the pore during *Yersinia* infection using fluorescently labeled nanobodies. The staining pattern strongly resembles the pattern observed when using YopD antibody and colocalizes with both YopD and YopB antibody when applied to the same sample (Figure 15). Compared to antibodies it offers the advantage that the nanobody is small enough to enter the prevacuole in fixed cells. Besides, it enables staining of intrabacterial YopD using only mild permeabilization with 0.1% Triton X-100 compared to 2% SDS treatment necessary for staining intrabacterial protein with antibodies (Nauth et al. 2018). The observation that mainly bacteria with a bright intrabacterial YopD pool display pores on their surface points to the existence of different subpopulations among *Yersinia*. Either some *Yersinia* are programmed to express more YopD resulting in pore formation on their surface or the pore formation and translocation itself induces a positive feedback loop increasing YopD expression. Why some bacteria display translocons while others stay inactive remains an intriguing topic for future research.

Due to its specificity and high affinity the nanobody stain displays little to no background signal even without washing steps. This enables imaging of live pore formation during infection by adding anti-ALFA nanobody to the medium. During live imaging the nanobody can enter the prevacuole encompassing *Yersinia*, it can stain the pore when it is formed and is subsequently transported into the host cell allowing visualization of live intracellular pores and their ensuing degradation (Figure 16). This allows the analysis of pore formation dynamics in combination with fluorescently labeled marker proteins.

In general, the anti-ALFA nanobody stain is highly suited for super resolution microscopy due to its specific binding and small size (Götzke et al. 2019). Nanobodies with about 15 kDa are already 10 times smaller than an antibody and 20-30 times smaller than a primary-secondary antibody complex (Sahl et al. 2017). With a decreased distance between epitope and label a much higher resolution is reached. Although multiple polyclonal secondary antibodies increase the signal intensity this impairs resolution as the fluorophore is displaced from the target. This was shown in comparisons of nanobody and antibody stains using tightly packed microtubules. When comparing nanobody to a staining of primary and secondary antibody complex the fluorophore displacement was reduced about 11 times (Ries et al. 2012). When the nanobody signal was compared to a fluorescently labeled primary antibody the displacement was still 5 times lower (Mikhaylova et al. 2015). If the ALFA tag would be applied for effector proteins, fixed samples of infected cells would need to be carefully permeabilized as to allow staining of the tag but prevent intrabacterial stainings. Another option would be to use an anti-ALFA nanobody fused to a fluorophore expressed in the host cell. The fusion of mScarlet-I28 to the ALFA nanobody allowed the visualization of ALFA-vimentin with limited background signal in COS-7 cells (Götzke et al. 2019). Another possibility would be using the ALFA tag for multicolor imaging in combination with another epitope tag. A likely candidate would be the BC2 or SPOT-tag which has been developed during a search for a beta-catenin nanobody and has a similar size (12 aa, 1.4 kDa, 3.3 nm) (Traenkle et al. 2015; Braun et al. 2016). Although the anti-BC2 nanobody has been shown to possess a lower affinity compared to the anti-ALFA nanobody, it has proven to be suitable for super resolution microscopy and single-particle tracking in live HeLa cells (Virant et al. 2018). Therefore, the SPOT-tag could be combined with the ALFA-tag to analyze pore formation in combination with parts of the TTSS machinery or effector proteins during live imaging or super resolution microscopy. Overall, the ALFA-tag has proven to be highly suitable for visualization of pore formation and poses a variety of interesting opportunities for future research.

5.6. PI(4,5)P2 presence precedes pore formation

During bacterial uptake a rapid recruitment of PI(4,5)P2 to membranes enclosing the bacteria was observed by live imaging using PLC δ 1-PH-GFP as a marker. A subset of bacteria in this compartment was

shown to form translocation pores shortly after accumulation of PI(4,5)P₂ (Figure 17). PI(4,5)P₂ is known to accumulate at sites of bacterial uptake due to activation of PIP(5)Ks by Rac and Arf6 (Wong and Isberg 2003). Actin-remodeling proteins are recruited by PI(4,5)P₂ facilitating membrane extension and engulfment of the bacterium (Pollard and Borisy 2003; Ho et al. 2004; Saarikangas et al. 2010). The hydrolysis of PI(4,5)P₂ is a requirement for vacuolar fission and internalization of the bacterium (Botelho et al. 2000; Sarantis et al. 2012). One important factor likely influencing PI(4,5)P₂ accumulation at the *Yersinia* containing compartment in our experimental setup is the overexpression of constitutively active Rac1 in HeLa cells (Figure 17) inducing PI(4,5)P₂ synthesis through the recruitment of PIP(5)K α (Wong and Isberg 2003). The activity of Rac1 has been demonstrated to increase the number of bacteria taken up into the prevacuole and as a result to stimulate pore formation and translocation in HeLa cells (Nauth et al. 2018).

Although, PI(4,5)P₂ accumulation always precedes pore formation during *Yersinia* uptake into the host cell, there is no evidence showing that enrichment of PI(4,5)P₂ itself is the trigger for pore formation. This is illustrated by the finding that a relevant subset of bacteria residing in a PI(4,5)P₂ enriched prevacuole seems not to form translocons. Interestingly, the translocon is often formed by groups of adjacent bacteria. This finding might point towards an additional stimulus present in only a subset of PI(4,5)P₂ enriched compartments triggering pore formation. Thus, the identification of this stimulus should be investigated in future studies.

Another interesting observation was the repeated disappearance and re-appearance of the PLC δ 1-PH-GFP signal around the bacteria. This flickering PLC δ 1-PH-GFP signal has not been described in the literature and might be related to the onset of effector protein translocation into the host cell, mediating the antiphagocytic effect of *Yersinia*. It could well be imagined that manipulation of the actin cytoskeleton facilitated by the effector proteins YopH, YopE, YopT and YopO might hinder the vacuolar fission and completion of internalization (Grosdent et al. 2002; Barbieri et al. 2002; Aepfelbacher 2004). On the other hand overexpression of constitutively active Rac1 alone could play a role in this phenotype because as mentioned above active Rac1 is known to be involved in the recruitment of PIP(5)K. This mechanism might also counteract the required depletion of PI(4,5)P₂ for vacuolar fission.

5.7. Pore formation rapidly induces membrane damage

Live imaging of pore formation and galectin-3 recruitment to *Yersinia* containing compartments showed that galectin-3 was only recruited to bacteria displaying a YopD pore signal (Figure 18B). Conversely, not all bacteria developing a translocon recruited galectin-3 during the covered time span of the live imaging experiments. Nonetheless, pore formation seems to be a prerequisite for galectin-3 enrichment.

Interestingly, galectin-3 recruitment was not limited to fully internalized compartments but could also be detected on putative prevacuoles. This was concluded from the observation that galectin-3 enrichment was detectable on compartments that stained positive for pores by nanobody in unpermeabilized fixed samples (Figure 18A), indicating the presence of a conduit to the extracellular space.

Galectin-3 binds β -galactosides which are mainly present on the cell surface or in the lumen of vacuoles and are accessible only through membrane damage. Recruitment of galectin-3 to membranes disrupted by intracellular pathogens has previously been observed on *Y. pseudotuberculosis* containing vacuoles (Feeley et al. 2017). Additionally, galectin-3 accumulation has been detected on a number of intracellular pathogen-containing compartments including *Shigella* and *Salmonella* possessing TTSS but also on bacteria using alternative secretion approaches such as the T4SS in *Coxiella* and *Legionella* or the Sec pathway in *Listeria* (Dupont et al. 2009; Paz et al. 2010; Thurston et al. 2012; Mansilla Pareja et al. 2017; Feeley et al. 2017). Galectin-3 binding to damaged bacterial vacuoles has been connected to reduction of bacterial load in infected cells through its recruitment of GBPs inducing autophagy (Baker et al. 2015; Schmid-Burgk et al. 2015; Rühl and Broz 2015; Feeley et al. 2017).

HeLa cells infected with *Y. enterocolitica* WA-314 YopD-ALFA recruit galectin-3 about 14 minutes after pores were formed under hypertranslocating conditions (Figure 18B). The presence of constitutively active Rac1 results in a higher number of bacteria displaying pores and in an increased level of effector protein translocation which could affect membrane damage (Nauth et al. 2018). The specific mechanism by which *Yersinia* disrupts the membrane structure has not been uncovered so far. Previously shown infection studies with *Y. pseudotuberculosis* revealed damage at YopD-containing compartments (Zwack et al. 2017). This could be either due to the insertion of pore proteins into the membrane or indirectly through a cellular response to pore formation or translocated effector proteins. Studies with *Y. pseudotuberculosis* showed that no effector proteins were necessary for galectin-3 recruitment which indicates that the membrane damage is caused by the translocator proteins alone (Zwack et al. 2017). Although in infection studies using *Yersinia* lacking the virulence plasmid, galectin-3 was recruited as well but only very late and to a rather low degree (Valencia Lopez et al. 2019). Notably, several studies have shown that the needle is directly connected to the translocon and forms a sealed connection between the bacterium and the host cell preventing exchange with the extracellular milieu (Hu et al. 2018; Nans et al. 2015). This tight connection does not appear to allow for galectins to access β -galactosides on the insides of vacuolar membranes. Nevertheless, pore formation of *Yersinia* seems to directly or indirectly induce membrane damage. However, the exact mechanism of how YopB and YopD cause disruption of membrane structures remains elusive.

6. Material and methods

6.1. Materials

6.1.1. Devices

Table 3 Devices

| Device | Manufacturer |
|-----------------------------|--|
| Accu-Jet | Accu-jet pro, Brand, Wertheim, Germany |
| Agarose gel electrophoresis | Agarose gel chamber: Roth, Karlsruhe; Germany |
| Blotting chamber | OWL HEP-1, Thermo Fisher Scientific, Waltham, USA |
| Cell counting chamber | Neubauer-Zellzählkammer, Hartenstein, Würzburg, Germany |
| Cell incubator | CB Series, Binder, Tuttlingen, Germany |
| Centrifuges | Sorvall RC-5B, Thermo Fisher Scientific, Waltham, USA; 5417R and 5810R, Eppendorf, Hamburg, Germany; biofuge pico, Heraeus instruments, Hanau, Germany; Sigma 3-18K, Sigma-Aldrich, St. Louis, Missouri, USA Sarstedt MC 6 Centrifuge, Nümbrecht, Germany Strip rotor MC 6 – 0.2 ml, 2 x 8f, Sarstedt, Nümbrecht, Germany |
| Clean bench | Hera Safe, Thermo Fisher Scientific, Waltham, USA |
| Developer for X-ray films | Curix 60, Agfa, Mortsel, Belgium |
| Electroporator | Gene Pulser II electroporator with Puls controller Plus, Biorad |
| Electrophoresis | Mini-Protean II, Biorad, Munich, Germany |
| Film cassette | Hartenstein, Würzburg, Germany |
| Freezer | -80°C: HERA freezer, Heraeus, Kendro Laboratory, Hanau, Germany -20 °C: comfort, Liebherr-International AG, Bulle, Switzerland |
| Freezing containers | Cryo freezing containers, Nalgene Scientific, Rockford, USA |
| Incubator shaker | Certomat BS-1, Sartorius, Göttingen, Germany |
| Magnetic stirrer | RCT-Basic, IKA-Labortechnik, Staufen, Germany |
| NanoDrop® ND-1000 | PeqLab, Erlangen, Germany |
| pH meter | Seven easy, Mettler-Toledo, Giessen, Germany |
| Photometer | Ultrospec 3000 pro, Amersham/GE Healthcare Europe, Munich, Germany |
| Pipettes | 2, 10, 100, 200, 1000 µl, Research Plus, Eppendorf, Hamburg, Germany |
| Power supply unit | Power Pac 2000, BioRad, Munich, Germany |
| Refrigerator | 4-8°C, Liebherr Premium, Liebherr-International AG, Bulle, Switzerland |

| | |
|----------------------------------|---|
| SDS-PAGE electrophoresis cell | SDS-PAGE: Mini-Protean II Biorad, Munich, Germany |
| Scanner | CanoScan 4400F, Canon, Amsterdam, Niederlande |
| Sonifier | Digital Sonifier 250-D, Branson, Danbury, USA |
| Thermocycler | Thermocycler peqStar, PeqLab, Erlangen, Germany |
| Thermoblock | DRI-Block DB3 Techne, Bibby Scientific Limited, Staffordshire, UK |
| Transilluminator | Vilber Lourmat, ETX, Eberhardzell, Germany |
| UV-Transilluminator and Detector | Chemidoc XRS, Biorad, Hercules, Californien, USA |
| Vortex | REAX Topo, Heidolph Instruments, Schwabach, Germany |
| Water bath | GFL Typ 1013, GFL, Burgwedel, Germany |
| Weighing scales | 440-47N, Kern, Balingen-Frommern, Germany |

6.1.2. Microscopes

Table 4 Technical data for the Laser-Scanning-microscope (Leica TCS SP8 X)

| Laser-Scanning microscope | Product, manufacturer |
|---------------------------|--|
| Microscope | Leica DMI8, Leica, Wetzlar, Germany |
| Objectives | 63x HC PL APO Oil CS2; NA: 1.40; WD (mm): 0.14 |
| Detectors | 2x HyD, 2x PMT, 1x Trans-PMT |
| Laser lines (nm) | White light laser, pulsed (WLL): 470-670; Diode: 405; Multi-Ar: 458 / 476 / 488 / 496 / 514; DPSS: 561; HeNe: 594 / 633 |
| Filters for fluorescence | Filtersystem (em.-color, dye): excitation beamsplitter emission L5 ET (green; AF488, GFP): BP 480/40 FP 505 em. BP 527/30 A (blue; DAPI): BP 340-380 FP LP 425 I 3 (green; AF488, GFP): BP 450-490 FP LP 515 N 2.1 (red; AF568, mCherry): BP 515-560 FP LP 590 |
| UV-lamp | EL 6000 120W (LQHXP 120 LEJ) |
| Halogen lamp | 100 W, 12 V |
| Further features | Piezo Focus drive: SuperZ Galvo type H |
| Software | Leica LAS X SP8 |

Table 5 Technical data for the spinning disk microscope (Visitron SD-TIRF)

| Laser-Scanning microscope | Product, manufacturer |
|---|---|
| Microscope | Nikon Eclipse TiE, Nikon, Tokio, Japan |
| Objectives | 60x Apo TIRF (corr.) Oil NA: 1.49 WD (mm): 0.13 (CS: 0.10-0.22 @ 23 or 37 °C) |
| Cameras | 2x evolve-EM 512 (back-illuminated EM-CCD, 16µm pixel-size) |
| Laser lines (nm) | Solid-state: 405 / 445 / 488 / 515 / 561 / 640 |
| Spinning Disk unit | Yokogawa CSU W-1 in dual-camera configuration |
| Emission filters spinning disk (for laser-related fluorescence) | Camera 1: DAPI, ET460 (W50) CFP ET470 (W24) GFP, ET525 (W50) Camera 2: YFP ET535 (W30) mCherry, ET609 (W54) CY5 ET700 (W75) |
| Dichroic in spinning disk unit | 405/488/561/640 (used with the respective channels) 445/515/640 (used for 445, 515 and 640 channels) |
| Dichroic for dual camera mode | 561LP 514LP |
| Fluorescence filters in microscope stand | Filtersystem (em.-color, dye): excitation beamsplitter emission DAPI (blue; DAPI): BP 325-375 DM 400 BP 435-485 GFP (green; AF488, GFP): BP 450-490 DM 495 BP 500-550 TxRed (red; AF568, mCherry): BP 540-580 DM 585 BP 593-668 |
| UV-lamp | SOLA-SM Light Engines, white light LED, 380-680nm |
| Transmitted light lamp | precisExcite, High-Power 525nm LED |
| Incubation unit | okolab bold line |
| Piezo focus drive | Ludl NanoPrecision PiezoZ, 350µm travel range |
| Motorized XY stage | Ludl BioPrecision2 |
| Auto-focus | Nikon PerfectFocus system |
| Actively damped optical table | Newport |

Table 7 Kits, enzymes, reagents

| Kits, enzymes, reagents | Manufacturer |
|---|---|
| 16% paraformaldehyde | Electron Microscopy Science, Hatfield, USA |
| Accutase, Enzyme Cell Detachment Medium | eBioscience, San Diego, California, USA |
| ALFA Selector ST slurry | NanoTag Biotechnologies, Göttingen, Germany |
| BioRad Protein Assay | BioRad, Munich, Germany |
| CD 14 Microbeads, human | MACS, Milteny Biotec GmbH, Bergisch Gladbach, Germany |
| Complete Protease Inhibitor | Sigma-Aldrich, St. Louis, USA |
| Digitonin | Sigma-Aldrich, St. Louis, USA |
| dNTPs 10 mM Mix | Invitrogen, Life Technologies, Carlsbad, USA |
| EZ-Link Sulfo-NHS-SS-Biotin | Thermo Fisher Scientific, Waltham, USA |
| FastDigest® restriction enzymes | Fermentas, St. Leon-Rot, Germany |
| GoTaq® G2 polymerase | Promega, Madison, Wisconsin, USA |
| Isopropyl β -D-1-thiogalactopyranoside (IPTG) | Sigma-Aldrich, St. Louis, USA |
| NucleoBond® Xtra Maxi EF | Macherey-Nagel, Düren, Germany |
| NucleoSpin® Gel and PCR Clean-up | Macherey-Nagel, Düren, Germany |
| Neon transfection system | Invitrogen, Life Technologies, Carlsbad, USA |
| Opti-MEM™ I Reduced Serum Medium | Gibco, Carlsbad, Californien, USA |
| PageRuler Prestained Protein Ladder | Thermo Fisher Scientific, Waltham, USA |
| Phenylmethylsulfonylfluid (PMSF) | Roth, Karlsruhe, Germany |
| Phusion™ high-fidelity DNA polymerase | Thermo Fisher Scientific, Waltham, USA |
| Phosphate buffered saline | Sigma-Aldrich, St. Louis, Missouri, USA |
| Plasmid miniprep kit I (C-Line) | Qiagen, Erlangen, Germany |
| ProLong Diamond | Thermo Fisher Scientific, Waltham, USA |
| Proteinase K | Roche, Mannheim, Germany |
| Rapid DNA Ligation Kit | Thermo Fisher Scientific, Waltham, USA |
| SuperSignal West Femto/ Pico detection | Thermo Fisher Scientific, Waltham, USA |
| Trypsin 0.05%, 0.53 mM EDTA | Invitrogen, Life Technologies, Carlsbad, USA |
| Trypsin 0.05%, 0.53 mM EDTA x 4Na with phenol red | Invitrogen, Life Technologies, Carlsbad, USA |
| TurboFect Transfection Reagent | Thermo Fisher Scientific, Waltham, USA |

6.1.4. Buffers and reagents

Chemicals were obtained from Amersham/GE Healthcare, Munich (Germany), BD Biosciences, Heidelberg (Germany), Biozyme, Oldendorf (Germany), Dianova, Hamburg (Germany), Fermentas, St. Leon-Rot (Germany), Invitrogen/Life Technologies, Carlsbad (USA), Merck, Darmstadt (Germany), PAA, Pasching (Austria), PromoCell, Heidelberg (Germany), Roche, Mannheim (Germany), Roth, Karlsruhe (Germany) and Sigma-Aldrich, St. Louis (USA). Buffers were autoclaved for 20 min at 121 °C and 1.4 bar or sterile filtered.

Table 8 Buffer composition

| Buffers | Concentration | Components |
|--|----------------------|---------------------------------|
| Permeabilization buffer for immunofluorescence | 0.1 % (v/v) | Triton X-100 |
| Digitonin-lysis-buffer | 0.5 % (w/v) | Digitonin in 1xPBS |
| Elution buffer | 30 mM | Glutathione |
| | 50 mM | Tris pH 8.8 |
| PBS (10x) | 137 mM | NaCl |
| | 2.7 mM | KClNa ₂ |
| | 14.4 g | HPO ₄ |
| | 2.3 mM | KH ₂ PO ₄ |
| SDS-PAGE/Western Blot | | |
| 4x Lämmli (sample buffer for SDS-PAGE) | 240 mM | Tris pH 6.8 |
| | 8% (w/v) | SDS |
| | 40% (w/v) | Glycerol |
| | 5% (v/v) | β-mercaptoethanol |
| | 0.04% (w/v) | Bromphenol blue |
| Resolving buffer | 1.5 M | Tris-HCl pH 8.8 |
| | 0.1% (w/v) | SDS |
| Stacking buffer | 0.5 M | Tris-HCl pH 6.8 |
| | 0.1% (w/v) | SDS |
| SDS-PAGE running buffer | 25 mM | Tris |
| | 190 mM | Glycine |
| | 0.1% (w/v) | SDS |
| Transfer buffer | 150 mM | Tris |
| | 25 mM | Glycine |
| | 20% (v/v) | Methanol |
| TBS-T | 1x | TBS |

| | | |
|-----------------------------|------------|--------------------------------|
| | 0.1% (v/v) | Tween20 |
| Coomassie staining solution | 0.1% (w/v) | Coomassie Brilliant Blue R-250 |
| | 25% (w/v) | Methanol |
| | 10% (w/v) | Acetic acid |
| | | ddH ₂ O |
| Coomassie destain solution | 25% (w/v) | Methanol |
| | 10% (w/v) | Acetic acid |
| | | ddH ₂ O |
| Electrophoresis | | |
| TAE(50x) pH 7.4 | 40 mM | Tris-Acetate pH 8.3 |
| | 10 mM | EDTA |
| | | ddH ₂ O |

6.1.5. Antibodies

The antibodies used for immunofluorescence staining were diluted in 3% BSA (bovine serum albumin in 1xPBS). The antibodies used for Western Blot were diluted in 5% milk powder in TBS-T. The anti-YopE, anti-YopH and anti-YopM rabbit polyclonal sera were a gift from Jürgen Heesemann (Max von Pettenkofer-Institute, München, Germany) (Heesemann and Laufs 1983; Jacobi et al. 1998).

Table 9 Primary antibodies

| Antigen | Species | Dilution IF | Dilution WB | Origin |
|------------------------------|---------|-------------|-------------|--------------------------------|
| Actin (monoclonal) | Mouse | - | 1:10000 | Millipore, Schwalbach, Germany |
| Calnexin (polyclonal) | Rabbit | - | 1:2000 | Enzo, Lörrach, Germany |
| Myc-tag | Rabbit | 1:200 | 1:1000 | Cell Signaling, Cambridge, UK |
| <i>Y. enterocolitica</i> O:8 | Rabbit | 1:50 | - | Sifin, Berlin, Germany |
| YopH | Rabbit | - | 1:5000 | Serum |
| YopB (1-168) | Rabbit | 1:50 | 1:1000 | Serum |
| YopB (1-168) | Rat | 1:50 | 1:1000 | Serum |
| YopD (150-287) | Rabbit | 1:50 | 1:1000 | Serum |
| YopE (polyclonal) | Rabbit | - | 1:1000 | Serum |
| YopH (polyclonal) | Rabbit | - | 1:1000 | Serum |
| YopM (polyclonal) | Rabbit | - | 1:1000 | Serum |
| anti-HA (monoclonal) | Rat | - | 1:1000 | Santa Cruz, Dallas, Texas, USA |

Table 10 Secondary antibodies

| Secondary antibody | Dilution in 3% BSA | Manufacturer |
|--|--------------------|---------------|
| AlexaFluor-488 chicken anti-rabbit IgG | 1:200 | Invitrogen |
| AlexaFluor-488 goat anti-rat IgG | 1:200 | Invitrogen |
| AlexaFluor-568 goat anti-rabbit IgG | 1:200 | Invitrogen |
| AlexaFluor-568 goat anti-rat IgG | 1:200 | Invitrogen |
| AlexaFluor-568 donkey anti-mouse IgG | 1:200 | Invitrogen |
| AlexaFluor-594 chicken anti-rat IgG | 1:200 | Invitrogen |
| AlexaFluor-647 goat anti-rabbit | 1:200 | Invitrogen |
| Abberior donkey anti-rabbit Star580 | 1:200 | Abberior |
| Abberior goat anti-rabbit IgG Star635P | 1:200 | Abberior |
| Abberior goat anti-rabbit IgG Star | 1:200 | Abberior |
| Abberior goat anti-rat IgG Star | 1:200 | Abberior |
| rabbit anti-Biotin IgG | 1:10 000 | Rockland |
| <u>Western Blot: HRP-conjugated secondary antibodies</u> | | |
| sheep anti-mouse IgG | 1: 50 000 | GE Healthcare |
| donkey anti-rabbit IgG | 1: 50 000 | GE Healthcare |
| goat anti-rat IgG | 1: 50 000 | GE Healthcare |

6.1.6. Nanobodies, dyes and labeling substrates

Table 11 Nanobodies, dyes and labeling substrates

| Name | Target | Fluorophore | Dilution IF | Origin |
|----------------------------|----------|--------------------------|-------------|---|
| <u>Labeling substrates</u> | | | | |
| HaloTag TMR Ligand | Halo-tag | Tetramethylrhodamine | 1:500 | Promega, Madison, Wisconsin, USA |
| SNAP-Cell TMR-Star | SNAP-tag | Tetramethylrhodamine | 1:500 | New England Biolabs, Massachusetts, USA |
| CLIP-Cell TMR-Star | CLIP-tag | Tetramethylrhodamine | 1:500 | New England Biolabs, Massachusetts, USA |
| <u>Nanobody</u> | | | | |
| FluoTag-X2 anti-ALFA | ALFA-tag | Abberior® Star 580, 635P | 1:500 | NanoTag Biotechnologies, Göttingen, Germany |
| <u>Dyes</u> | | | | |
| Phalloidin | F-Actin | AlexaFluor-488, 568, 647 | 1:200 | Invitrogen, Carlsbad, USA |
| 300 nM DAPI | DNA | 405 | 1:5000 | Invitrogen, Carlsbad, USA |

6.1.7. Growth media and additives

Media were sterilized by autoclaving for 20 min, 121°C, and 1.4 bar. Supplements, which could not be autoclaved, were sterile filtered.

Table 12 Growth media for the cultivation of *Y. enterocolitica*

| Medium | Concentration | Component |
|---|---------------|---------------|
| LB (Luria-Bertani)-Medium, pH 7.5 (Roth, Karlsruhe, Germany) | 10 g/l | Tryptone |
| | 5 g/l | Yeast extract |
| | 10 g/l | NaCl |
| LB (Luria-Bertani)-Agar, pH 7.0 (Roth, Karlsruhe, Germany) | 10 g/l | Tryptone |
| | 5 g/l | Yeast extract |
| | 10 g/l | NaCl |
| | 15 g/l | Agar |

Table 13 Antibiotics and additives for the cultivation and selection of *Y. enterocolitica*

| Antibiotic | Dissolved in | Final concentration | Manufacturer |
|-----------------|--------------------|---------------------|-------------------------------|
| Nalidixic acid | 1 M NaOH | 100 µg/ml | Sigma-Aldrich, St. Louis, USA |
| Kanamycin | ddH ₂ O | 50 µg/ml | Sigma-Aldrich, St. Louis, USA |
| Spectinomycin | ddH ₂ O | 50 µg/ml | Sigma-Aldrich, St. Louis, USA |
| Chloramphenicol | 10% EtOH | 20 µg/ml | Roth, Karlsruhe, Germany |

Table 14 Growth media for the cultivation of eukaryotic cells

| Medium | Concentration | Component | Manufacturer |
|--|---------------|-------------------------|-------------------------------------|
| Dulbecco's Modified Eagle Medium (DMEM) | | | Gibco, Carlsbad, California, USA |
| | 10% (v/v) | Fetal calf serum | Gibco, Carlsbad, California, USA |
| RPMI Medium 1640 | | | Gibco, Carlsbad, California, USA |
| | 20% (v/v) | Autologous serum | |
| | 1% (v/v) | Penicillin/Streptomycin | Gibco, Carlsbad, California, USA |

6.1.8. Plasmids

Table 15 Expression plasmids

| Plasmid | Vector | Origin |
|--------------------------------|---|---|
| myc-Rac1Q61L | pRK5-myc, constitutively active Rac1 | Pontus Aspenström, Uppsala, Sweden (Aspenström et al. 2004) |
| pYopE/SycE | pACYC184; Cm ^R | (Trülzsch et al. 2003) |
| pYopM-Halo | pACYC184; Cm ^R | Michael Hensel, Osnabrück, Germany (Göser et al. 2019) |
| pYopM-CLIP | pACYC184; Cm ^R | Michael Hensel, Osnabrück, Germany (Göser et al. 2019) |
| pYopM-SNAP | pACYC184; Cm ^R | Michael Hensel, Osnabrück, Germany (Göser et al. 2019) |
| pYopH-Halo | pACYC184; Cm ^R | Michael Hensel, Osnabrück, Germany |
| pYopH-CLIP | pACYC184; Cm ^R | Michael Hensel, Osnabrück, Germany |
| pYopH-SNAP | pACYC184; Cm ^R | Michael Hensel, Osnabrück, Germany |
| pYopE-Halo | pACYC184; Cm ^R | This study |
| pYopE-CLIP | pACYC184; Cm ^R | This study |
| pYopE-SNAP | pACYC184; Cm ^R | This study |
| pMax-GFP1-10-IRES-NLS-mTagBFP2 | blue nuclear marker (NLS-mTagBFP2) inserted downstream of GFP1-10; separated by internal ribosomal entry site (IRES) | Amy Palmer, Denver, USA (Young et al. 2017) |
| SteAprom_SteA_GFP11_R3_ACYC177 | SteA promotor and <i>steA</i> gene tagged with GFP11 on pACYC177 (Amp ^R) | Amy Palmer, Denver, USA (Young et al. 2017) |
| mRFP-GFP11-Rab5 | mRFP-N1; Kan ^R | This study |
| pYopE-GFP11 | pACYC184; Cm ^R | This study |
| pKD46-Cas12a_Kan | temperature-sensitive replicon; encoding for the recombination genes <i>gam</i> , <i>bet</i> , and <i>exo</i> , as well as Cas12a; curation by incubation at 42°C (Kan ^R) | Yi-Cheng Sun, Beijing, China (Zhao and Sun 2018) |
| pKD46-Cas12a_Amp | temperature-sensitive replicon; encoding for the recombination genes <i>gam</i> , <i>bet</i> , and <i>exo</i> , as well as Cas12a; curation by incubation at 42°C (Amp ^R) | Yi-Cheng Sun, Beijing, China (Zhao and Sun 2018) |
| pKD46-Cas12a_Spt | temperature-sensitive replicon; encoding for the recombination genes <i>gam</i> , <i>bet</i> , and <i>exo</i> , as well as Cas12a; curation by incubation at 42°C (Spt ^R) | This study |

| | | |
|------------------|--|---|
| pAC-crRNA_Kan | Encoding pre-crRNA cassettes, the <i>sacB</i> gene (sucrose sensitivity) and the <i>gfp</i> gene as a selection marker (flanked by BpmI and BsaI restriction enzyme sites) | Yi-Cheng Sun, Beijing, China (Zhao and Sun 2018) |
| pAC-crRNA_Cm | Encoding pre-crRNA cassettes, the <i>sacB</i> gene (sucrose sensitivity) and the <i>gfp</i> gene as a selection marker (flanked by BpmI and BsaI restriction enzyme sites) | Yi-Cheng Sun, Beijing, China (Zhao and Sun 2018) |
| pEGFP-galectin-3 | pEGFP-C1; Kan ^R | Addgene #73080 (Maejima et al. 2013) |
| PLCδ1-PH-GFP | pEGFP-N1, plasma membrane marker, PI(4,5)P2 indicator; Kan ^R | Tamas Balla, National Institutes of Health, Bethesda, USA (Balla and Várnai 2009) |
| GST-CNF-1 | CNF-1 cloned into the bacterial expression vector pGEX-4T-1 at the C-terminus of GST; Amp ^R | (Essler et al. 2003) |

6.1.9. Primer

Table 16 Primer and sequences

| Name | Sequence 5'-3' |
|-----------------------------------|--|
| <u>pYopE-Halo</u> | |
| YopE fwd | TTGACAGCTTATCATCGATATGATATTGCTGGCACCAC |
| YopE rev (+Halo overlap) | CCGCAGAGCCCATCAATGACAGTAATTGATGC |
| Halo fwd (+YopE overlap) | GTCATTGATGGGCTCTGCGGCGTCTGCG |
| Halo rev | GTGATAAACTACCGCATTAAATTAAGCGTAGTCTGGGACGTCGTATGG |
| <u>pYopE-SNAP</u> | |
| pACYC184-YopE/SycE fwd (+SmaI) | GTTAGACCCGGGTTAATGCGGTAGTTTATC |
| pACYC184-YopE/SycE rev (+HindIII) | AGAGCCAAGCTTCATCAATGACAGTAATTG |
| SNAP fwd (+HindIII) | TTGATGAAGCTTGGCTCTGCGGCGTCTGCG |
| SNAP rev (+SmaI) | CATTAACCCGGGTCTAACCCAGCCCAGGCT |
| <u>pYopE-CLIP</u> | |
| CLIP fwd (+HindIII) | TTGATGAAGCTTGGCTCTGCGGCGTCTGCG |
| CLIP rev (+SmaI) | CATTAACCCGGGTTAAGCGTAGTCTGGGAC |
| <u>pYopE-GFP11</u> | |
| GFP11 fwd (+HindIII) | TCAGATAAGCTTGGGAGTAGTGGTGGTAGT |

| | |
|-----------------------------|--|
| GFP11 rev (+SmaI) | AATTCGCCCCGGGTCATGTAATCCCAGCAGCATT |
| | |
| <u>mRFP-GFP11-Rab5</u> | |
| GFP11 Rab5 oligo fwd | TCAGATCTCGAGGGGAGTAGTGGTGGTAGTAGCGGGCGTGACCACATGG TCCTTCATGAGTATGTAAATGCTGCTGGGATTACAGGTGGCGGCAAATTC AAGCTTCGAATT |
| GFP11 Rab5 oligo rev | AATTCGAAGCTTGAATTTGCCGCCACCTGTAATCCCAGCAGCATTTACATA CTCATGAAGGACCATGTGGTCACGCCGCTACTACCACCACTACTCCCCTC GAGATCTGA |
| | |
| <u>pKD46-Cas12a-Spt</u> | |
| Cas12a-Spt ^R fwd | TTTTTCTAAATACATTCAAATATGTATCCGCTCATGAGACAATAACCCTG AAGCTTTATGCTTGTAACCGTTTT |
| Cas12a-Spt ^R rev | TACCAATGCTTAATCAGTGAGGCACCTATCTCAGCGATCTGTCTATTTTCG GGCGTCGGCTTGAACGAATT |
| | |
| <i>crRNA oligos</i> | |
| YopD-crRNA oligo fwd | TAGATTGACCGAGATAAGCTTGCCTCGCTA |
| YopD-crRNA oligo rev | AGACTAGCGAGGCAAGCTTATCTCGGTCAA |
| YopB-crRNA oligo fwd | TAGATCCTCTTGGGATATCAGGCCATCTTC |
| YopB-crRNA oligo rev | AGACGAAGATGGCCTGATATCCCAAGAGGA |
| YopD-Xcell-crRNA oligo fwd | TAGATCATATTCTCCCGATATCCTC |
| YopD-Xcell-crRNA oligo rev | AGACGAGGATATCGGGAGAATATGA |
| | |
| <i>HDR primers</i> | |
| <u>YopD-HDR primers</u> | |
| YopD HomA fwd | AATTCTTTATCCAATAATGCC |
| YopD-GFP11 HomA rev | CATATGGTACTGCATGAATATGTGAACGCGGGCGGCATTACCGGTGGCG GCAAATTCAGCTTATCTCGGTACAGGTGCC |
| YopD-GFP11 HomB fwd | CACATATTCATGCAGTACCATATGATCACGTCCGCTACTACCACCACTACT TCCTGCCTCGCTACTCTTTATTGCTT |
| YopD HomB rev | CGGTGACTAAATTAGGGGGCA |
| YopD-GFP11 50 bp HDR | ATTCCTGACTCGGTTTGATCAATTCAGGCACCTGTGACCGAGATAAGCT GAATTTGCCGCCACCGGTAATGCCCGCCGTTTCACATATTCATGCAGTAC CATATGATCACGTCCGCTACTACCACCACTACTTCTGCCTCGCTACTCTTT ATTGCTTGCTTCATGACGGGTGTCTTCTGTTT |
| | |
| <u>YopB-HDR primers</u> | |
| YopB HomA fwd | TACAGCTCCCTGCACCACTAG |

| | |
|---------------------|--|
| YopB-GFP11 HomA rev | G TTCACATATTCATGCAGTACCATATGATCACGTCCGCTACTACCACCACT ACTTCCCAGGCCATCTTCCGCCGCTTGTT |
| YopB-GFP11 HomB fwd | A TGGTACTGCATGAATATGTGAACGCGGGCATTACCGGTGGCGGCA AATTCATATCCCAAGAGGCAATGCA |
| YopB HomB rev | A TCTGAAAAATCAGTTCCATC |
| YopB-GFP11 50bp HDR | T CAATCGCAGTGAGTATCGGCCCTAATACTTGCATTGCCTCTTGGGATATG AATTTGCCGCCACCGGTAATGCCCGCCGCTTACATATTCATGCAGTACC ATATGATCACGTCCGCTACTACCACCACTACTTCCCAGGCCATCTTCCGCC GCTTGTTTCACAGCCATATTCGCCATCCCAATTA |

YopB-ALFA HDR primers

| | |
|--------------------|--|
| YopB-ALFA HomA rev | C GTTTGAAGAGGAACTGAGACGCCGCTTA ACTGAACCAGGCGGAGGTG GATCTATATCCCAAGAGGCAATGCA |
| YopB-ALFA HomB fwd | G CGTCTCAGTTCCTCTTCCAAACGGCTCGGGCCACCAGACCCGCCCGAAC CACCCAGGCCATCTTCCGCCGCTTGTT |

YopD-Xcell HDR primers

| | |
|--------------------------|---|
| YopD-Xcell HomA fwd | T ATTATCCTAACTTATTATTTTTAATTTAATAATAAAAAGCCCTGGATTACCA TTAGTTAA |
| YopD-Xcell-ALFA HomA rev | T TGGAAGAGGAACTGAGACGCCGCTTA ACTGAACCAGGCGGAGGTGGAT CTATCGGGAGAATATGGAAACCAGA |
| YopD-Xcell-ALFA HomB fwd | G CGGCGTCTCAGTTCCTCTTCCAAACGGCTCGGGCCACCAGACCCGCCCG AACCACCATCCTCTCTGCTTACCGCTTTAT |
| YopD-Xcell HomB rev | A AAGCGGTGAGGTTAAAAAAA |

Colony PCR primers binding close to the insert site

| | |
|----------------|------------------------|
| YopD fwd | C TGGCTTTTACTCAGTAATGC |
| YopD rev | A TCACTACAGAGACAGTCGGG |
| YopB fwd | C TACAGTCAATGCGACTTCAA |
| YopB rev | A ATGATGATTGCCTCAGGCGT |
| YopD-Xcell fwd | T GGCTTTTGAGTCGGTCA |
| YopD-Xcell rev | A TATTGCTGGCCGCGATC |

Sequencing primers binding outside the homology arms

| | |
|----------|------------------------|
| YopD fwd | C GTTGCGGCATTAACGCATT |
| YopD rev | G TTGCCCAAATTCGACAGGC |
| YopB fwd | G GGGTCTGCCGGCCAAATTAT |
| YopB rev | A GACCCAACAAGTCGCGGGAG |

| | |
|-------------------------|-----------------------|
| YopD-Xcell fwd | CAACAACCGGTAAGTCTGTC |
| YopD-Xcell rev | CAGCCCAATTATCACGAC |
| crRNA sequencing primer | TGTTTGACAGCTTATCATCGA |

6.1.10. *Yersinia* strains and eukaryotic cells

Table 17 *Yersinia enterocolitica* strains

| Strain | Features | Reference |
|--------------------|--|---|
| WA-314 | Wild type strain carrying the virulence plasmid pYV; serogroup O8; kanamycin resistance cassette (Kan ^R) | (Heesemann and Laufs 1983; Oellerich et al. 2007) |
| WA-C | pYV-cured derivative of WA-314 | (Heesemann and Laufs 1983) |
| WA-C(pTTSS) | WA-C harboring pTTSS encoding the TTSS secretion/translocation apparatus of WA-314 but no Yop effector genes; Spt ^R | (Heesemann and Laufs 1983; Trülsch et al. 2003) |
| WA-314ΔYopE | WA-C harboring pYVΔyopE; Kan ^R | (Trülsch et al. 2004) |
| WA-314ΔYopH | WA-C harboring pYVΔyopH; Kan ^R | (Wiedmaier et al. 2008) |
| WA-314ΔYopM | WA-C harboring pYVΔyopM; Kan ^R | (Trülsch et al. 2004) |
| WA-314ΔYopE(pYopE) | WA-C harboring pYVΔyopE; Kan ^R ; complemented with YopE in pACYC184; CM ^R | This study |
| WA-314ΔYopH(pYopH) | WA-C harboring pYVΔyopH; Kan ^R ; complemented with YopH in pACYC184; CM ^R | (Trülsch et al. 2004) |
| WA-314ΔYopM(pYopM) | WA-C harboring pYVΔyopM; Kan ^R ; complemented with YopM in pACYC184; CM ^R | (Trülsch et al. 2004) |
| WA-C(pTTSS+pYopE) | WA-C harboring pTTSS; Spt ^R ; complemented with YopE in pACYC184; CM ^R | (Trülsch et al. 2003) |

| | | |
|--------------------------|---|---------------------------|
| WA-C(pTTSS+pYopH) | WA-C harboring pTTSS; Spt ^R ; complemented with YopH in pACYC184; CM ^R | (Trülzsch et al. 2003) |
| WA-C(pTTSS+pYopM) | WA-C harboring pTTSS; Spt ^R ; complemented with YopM in pACYC184; CM ^R | (Trülzsch et al. 2003) |
| WA-314ΔYopE(pYopE-Halo) | WA-C harboring pYVΔyopE; Kan ^R ; complemented with YopE-Halo-HA in pACYC184; CM ^R | This study |
| WA-314ΔYopE(pYopE-CLIP) | WA-C harboring pYVΔyopE; Kan ^R ; complemented with YopE-CLIP-HA in pACYC184; CM ^R | This study |
| WA-314ΔYopE(pYopE-SNAP) | WA-C harboring pYVΔyopE; Kan ^R ; complemented with YopE-SNAP in pACYC184; CM ^R | This study |
| WA-314ΔYopE(pYopE-GFP11) | WA-C harboring pYVΔyopE; Kan ^R ; complemented with YopE-GFP11 in pACYC184; CM ^R | This study |
| WA-314ΔYopH(pYopH-Halo) | WA-C harboring pYVΔyopH; Kan ^R ; complemented with YopH-Halo-HA in pACYC184; CM ^R | This study |
| WA-314ΔYopH(pYopH-CLIP) | WA-C harboring pYVΔyopH; Kan ^R ; complemented with YopH-CLIP-HA in pACYC184; CM ^R | This study |
| WA-314ΔYopH(pYopH-SNAP) | WA-C harboring pYVΔyopH; Kan ^R ; complemented with YopH-SNAP-HA in pACYC184; CM ^R | This study |
| WA-314ΔYopM(pYopM-Halo) | WA-C harboring pYVΔyopM; Kan ^R ; complemented with YopM-Halo-HA in pACYC184; CM ^R | This study |
| WA-314ΔYopM(pYopM-CLIP) | WA-C harboring pYVΔyopM; Kan ^R ; complemented with YopM-CLIP-HA in pACYC184; CM ^R | This study |
| WA-314ΔYopM(pYopM-SNAP) | WA-C harboring pYVΔyopM; Kan ^R ; complemented with YopM-SNAP-HA in pACYC184; CM ^R | This study |
| WA-C(pTTSS+pYopE-Halo) | WA-C harboring pTTSS; Spt ^R ; complemented with YopE-Halo-HA in pACYC184; CM ^R | This study |

| | | |
|-------------------------|--|------------|
| WA-C(pTTSS+pYopE-CLIP) | WA-C harboring pTTSS; Spt ^R ; complemented with YopE-CLIP-HA in pACYC184; CM ^R | This study |
| WA-C(pTTSS+pYopE-SNAP) | WA-C harboring pTTSS; Spt ^R ; complemented with YopE-SNAP in pACYC184; CM ^R | This study |
| WA-C(pTTSS+pYopE-GFP11) | WA-C harboring pTTSS; Spt ^R ; complemented with YopE-GFP11 in pACYC184; CM ^R | This study |
| WA-C(pTTSS+pYopH-Halo) | WA-C harboring pTTSS; Spt ^R ; complemented with YopH-Halo-HA in pACYC184; CM ^R | This study |
| WA-C(pTTSS+pYopH-CLIP) | WA-C harboring pTTSS; Spt ^R ; complemented with YopH-CLIP-HA in pACYC184; CM ^R | This study |
| WA-C(pTTSS+pYopH-SNAP) | WA-C harboring pTTSS; Spt ^R ; complemented with YopH-SNAP-HA in pACYC184; CM ^R | This study |
| WA-C(pTTSS+pYopM-Halo) | WA-C harboring pTTSS; Spt ^R ; complemented with YopM-Halo-HA in pACYC184; CM ^R | This study |
| WA-C(pTTSS+pYopM-CLIP) | WA-C harboring pTTSS; Spt ^R ; complemented with YopM-CLIP-HA in pACYC184; CM ^R | This study |
| WA-C(pTTSS+pYopM-SNAP) | WA-C harboring pTTSS; Spt ^R ; complemented with YopM-SNAP-HA in pACYC184; CM ^R | This study |
| WA-C(pTTSS YopD-GFP11) | WA-C harboring pTTSS; Spt ^R ; with GFP11 inserted between amino acid 50-51 | This study |
| WA-C(pTTSS YopB-GFP11) | WA-C harboring pTTSS; Spt ^R ; with GFP11 inserted between amino acid 216-217 | This study |
| WA-314 YopD-GFP11 | Wild type strain carrying the virulence plasmid pYV (Kan ^R) with GFP11 inserted between amino acid 50-51 | This study |
| WA-314 YopB-GFP11 | Wild type strain carrying the virulence plasmid pYV (Kan ^R) with GFP11 inserted between amino acid 216-217 | This study |

| | | |
|------------------|---|------------|
| WA-314 YopD-ALFA | Wild type strain carrying the virulence plasmid pYV (Kan ^R) with ALFA inserted between amino acid 194-195 | This study |
|------------------|---|------------|

Table 18 Eukaryotic cells

| Name | Features | Origin |
|---------------------------|---|--|
| HeLa | human cervical carcinoma cell line | ACC# 57, DSMZ-Deutsche Sammlung von Mikroorganismen und Zellkulturen GmbH, Braunschweig, Germany |
| Primary human macrophages | Isolated peripheral blood monocytes, differentiated to macrophages through addition of growth factors within 6-8 days | Weekly isolation from buffy-coats supplied by Frank Bentzien, Institut für Transfusionsmedizin, Universitätsklinikum Hamburg-Eppendorf, Hamburg, Germany |

6.1.11. Data processing

Table 19 Software

| Software | Manufacturer |
|--------------------------|---------------|
| FijiVersion 1.51n/ImageJ | Bethesda, USA |

6.2. Methods

All experiments performed in this study were done in safety level 2 (S2) laboratories.

6.2.1. Microbiological methods

6.2.1.1. Cultivation and strain maintenance of *Yersinia enterocolitica*

The *Yersinia enterocolitica* strains used in this study were cultivated from frozen stocks at 27°C for 24-48 hours on Luria Bertani (LB) plates containing the specific antibiotics and could be stored at 4°C for up to 4 weeks. Liquid bacteria culture in the exponential growth phase was mixed in equal proportions with 40% glycerol in LB medium and frozen at -80°C for long term storage. For experiments, bacteria were inoculated from either LB plates in 3 ml LB medium in test tubes with suitable antibiotics added and were grown overnight at 27°C in a shaker incubator.

6.2.1.2. Released protein assay

The released protein assay is used to analyze Yop secretion to the culture medium, which is induced by depletion of calcium. This is achieved by adding EGTA to the medium which chelates calcium inducing the low-calcium response in *Yersinia*. *Yersinia* overnight cultures were diluted 1:20 in 40 ml LB medium and placed at 37°C for 1.5 h. The OD₆₀₀ was measured before addition of 15 nM MgCl₂, 5 nM EGTA und 0.2% glucose. A further 3 h incubation at 37°C allowed secretion of proteins to the medium which was separated from the bacteria by centrifugation (10 min, 5000 x g, 4°C). For fluorescence staining of bacteria under secretion conditions the bacterial pellet was resuspended in ice-cold 1xPBS and some drops placed on a coverslip. The droplets were incubated at room temperature for 10 min before removing the liquid and fixing the sample with 4% paraformaldehyde (PFA) for 5-10 min at room temperature. The coverslips were washed twice with 1xPBS and were stained as described in section 6.2.5.1.

The supernatant was sterile filtered to avoid contamination with bacteria from the pellet and 10% trichloroacetic acid (TCA) was added for protein precipitation. After a 4 h incubation at 4°C or an overnight incubation at -20°C the supernatant was centrifuged (1 h, 20 000 x g, 4°C) and the resulting pellet scraped in 1.5 ml ice-cold acetone and transferred to a 2 ml reaction tube. After centrifugation (10 min, 10 000 x g, 4°C) the acetone supernatant was discarded and the tube placed under the fume hood for evaporation of the remaining liquid. The protein pellet was resuspended in 100 µl 1xSDS sample buffer, incubated at 95°C for 5-10 min and stored at -20°C. The measurement of OD₆₀₀ after the 37°C incubation was used to normalize the volume of sample loaded on the SDS gel.

6.2.1.3. *Yersinia* infection

For infection experiments *Yersinia* overnight cultures were diluted 1:20 and grown at 37°C for 1.5 h in a shaker incubator to induce expression of the virulence plasmid. The bacteria were pelleted by centrifugation (10 min, 5000 x *g*, 4°C) and the pellet was resuspended in 4 ml ice-cold 1xPBS. The OD₆₀₀ was set to 3.6 and depending on the experiment further adjusted to a lower OD₆₀₀ (0.36 or 0.72). Cell culture medium containing antibiotics was replaced by antibiotic free medium at least 2 hours before infection. The number of bacteria used for infection was adjusted depending on the area of the culture dish seeded with cells and the multiplicity of infection (MOI) intended for the experiment. The cell culture dishes were spun down (1 min, 200 x *g*, RT) to synchronize the beginning of infection before being placed into the 37°C incubator with 5% CO₂. The duration of infection varied between experiments. The infected cells were washed twice with 1xPBS to remove unattached bacteria. Afterwards the cells were fixed with 4% PFA for immunofluorescence staining or harvested for translocation assays (see section 6.2.5.1 or 6.2.4.3, respectively).

6.2.1.4. Preparation and transformation of chemically competent bacteria

To introduce plasmids into *E. coli* Top10 for cloning or plasmid production, bacteria were made chemically competent. This was achieved by washing the bacteria with calcium chloride promoting the binding of plasmid DNA to lipopolysaccharides (LPS) on the bacterial surface. The negatively charged DNA and the negatively charged LPS interacts with the positively charged calcium chloride while the applied heat shock strongly depolymerizes the membrane potential allowing the entry of the DNA into the cell.

For this, bacteria were grown overnight at 37°C. The overnight culture was diluted 1:100 in 100 ml LB medium and grown until OD₆₀₀ of 0.6-0.8. The bacteria were pelleted by centrifugation (10 min, 5000 x *g*, 4°C) and resuspended in 100 ml ice-cold 50 mM CaCl₂. The suspension was incubated for 10 min at 4°C before further centrifugation (10 min, 5000 x *g*, 4°C). The resulting pellet was resuspended in 50 ml ice-cold CaCl₂ and incubated on ice for 2 h. After centrifugation (10 min, 5000 x *g*, 4°C) bacteria were resuspended in 4 ml ice-cold CaCl₂ with 15% glycerol. Aliquots of 50-100 µl were flash frozen in liquid nitrogen and stored at -80°C. For introducing plasmids, the aliquots were thawed on ice and incubated with 1 µg DNA for 30 min. The tubes were placed at 42°C for 1 min and on ice for 2 min before incubation at 37°C for 1.5 h in a shaker incubator. Afterwards 200 µl bacterial suspension was plated on LB plates containing the specific antibiotics. For ligation experiments the bacterial suspension was centrifuged (2 min, 10 000 x *g*, RT), the pellet resuspended in 150 µl and completely plated on LB plates.

6.2.1.5. Preparation and transformation of electrocompetent bacteria

For introduction of artificial plasmids into bacteria, which do not allow chemical transformation, electrical pulses can be used to create holes in the bacterial membrane. To avoid short circuits, all salts must be removed from the bacterial suspension. Overnight cultures of the specific strain were diluted 1:10 in 100 ml LB medium and grown to OD₆₀₀ of 0.8 at 27°C in a shaker incubator. The bacteria were pelleted by centrifugation (10 min, 5000 x *g*, 4°C) and washed thrice in 40 ml ice-cold sterile ddH₂O (centrifugation: 5 min, 5000 x *g*, 4°C). In the last washing step, the pellet was washed with 10 ml 10% glycerol. After further centrifugation, all liquid was removed from the resulting pellet before resuspension in 200 µl 10% glycerol which was aliquoted in 35 µl in pre-chilled reaction tubes. For normal transformation of single plasmids, storage at -80°C was possible after freezing the aliquots in liquid nitrogen. However, when performing the CRISPR-Cas assisted recombination experiments the aliquots were immediately used to increase transformation efficiency.

Before electroporation the bacteria were thawed on ice and 10-1000 ng salt-free DNA was added. The mixture was transferred to a pre-chilled electroporation cuvette with 1 mm electrode gap. The cuvettes were carefully dried on the outside to avoid short circuits and directly placed into the BioRad Gene Pulser II (Elektroporator, BioRad, Germany) for electroporation at 100 Ω (low range), 50 µF and 1.8 kV. Immediately after electroporation 1 ml LB medium was added and the suspension transferred to a 1.5 ml reaction tube. The tubes were placed in a shaking heat block at 850 rpm and 27°C for 2 h to allow recovery of the electroporated bacteria. Afterwards 250 µl of the bacterial suspension was plated on selective LB plates containing the specific antibiotics. For CRISPR-Cas experiments the bacteria were pelleted by centrifugation (2 min, 10 000 x *g*, RT) and resuspended in 150 µl LB medium before plating.

6.2.2. Cell culture

All cell culture experiments were performed at clean benches under sterile conditions.

6.2.2.1. Cultivation of eukaryotic cells

The HeLa cells used for the majority of experiments were cultivated in DMEM (Dulbeco's Modified Eagle Medium, Gibco, USA) supplemented with 10% (v/v) FCS (Gibco, USA) in a humidified incubator at 37°C and 5% CO₂. The cells were passaged when becoming fully confluent. For this, cells growing in 10 cm dishes were washed with 5 ml sterile 1xPBS and 1 ml 0.05% Trypsin was added for 5 min at 37°C to detach cells from the dish. The cells were resuspended in pre-warmed DMEM and their density was determined using a counting chamber. The suspension was diluted either for further cultivation in 10 cm dishes or for seeding on coverslips or in live imaging dishes for microscopy experiments (approximately 2.5-3.5x10⁴ cells/cm²).

6.2.2.2. Cryoconservation and reactivation of eukaryotic cell lines

For cryoconservation, HeLa cells were resuspended in 1.5 ml FCS with 10% (v/v) DMSO preventing the formation of crystals damaging the cells. The suspension was transferred to a cryo-tube which was placed in an isopropanol filled cryocontainer (Nalgene Scientific, USA). The container was frozen overnight at -80°C and the tubes transferred to the liquid nitrogen storage containers.

For reactivation HeLa cells were thawed and immediately resuspended in pre-warmed cell culture medium. Centrifugation (5 min, 200 x *g*, RT) allowed the removal of DMSO used for cryo conservation. The cells were resuspended in 10 ml cell culture medium and transferred to a cell culture dish for further cultivation.

6.2.2.3. Transfection of HeLa cells

HeLa cells were transfected using Turbofect (Thermo Fisher Scientific, USA) as a transfection reagent. For each 24-well 0.5 µg DNA for myc-Rac1Q61L or 1 µg for other plasmids was diluted in 100 µl Opti-MEM (Gibco, USA) and mixed with 2 µl Turbofect. After 20 min incubation at room temperature, the solution was added dropwise to HeLa cells seeded on coverslips and incubated at 37°C and 5% CO₂ for 16 h. At least 2 h before infection the medium was replaced to prevent the transfection reagent interfering with infection or affecting immunofluorescence staining.

6.2.2.4. CNF-1 treatment of HeLa cells

Cytotoxin necrotizing factor 1 (CNF-1) is a toxin produced by some *E. coli* strains which deamidates a glutamine residue resulting in the permanent activation of Rho GTPases such as Rho, Rac and Cdc42 in eukaryotic cells. CNF-1 treatment has been shown to increase translocation in *Yersinia enterocolitica* (Wolters et al. 2013). Recombinantly expressed and purified GST-tagged CNF-1 can be aliquoted and stored at -80°C (see below 6.2.4.2) for long term storage. For cell treatment, the protein was thawed on ice and diluted to 1 µg/ml in DMEM with 10% FCS and added to the cells 2 h before infection.

6.2.2.5. Isolation and cultivation of primary human macrophages

Human peripheral blood monocytes were isolated from buffy coats as described by Kopp and colleagues (Kopp et al. 2006). They were cultivated in RPMI Medium 1640 (Gibco, USA) supplemented with 20% human serum, penicillin and streptomycin. The growth factors from the human serum allow the differentiation of the monocytes to macrophages within 6 days. For detaching macrophages from the dish, they were washed with 1xPBS and incubated at 37°C and 5% CO₂ for 30 min. The cells were carefully scraped and resuspended in RPMI. The cell density was determined using a counting chamber and 1x10⁵ cells were seeded on a coverslip for microscopy experiments.

6.2.2.6. Transfection of primary human macrophages

For transfection of primary human macrophages an electrical pulse was applied to induce temporary pores in the cell membrane allowing the uptake of DNA. For each transfection 1×10^6 cells were washed with 1xPBS and resuspended in R-buffer supplied by the Neon transfection system (Invitrogen, USA). For the expression of GFP1-10/BFP 5 μg plasmid DNA was added. Two pulses of 1000 V were applied for 40 ms with the Neon electroporation device (Invitrogen, USA) as indicated by the manufacturer. The suspension was immediately resuspended in pre-warmed RPMI and 1×10^5 cells were seeded on coverslips. After 1 h RPMI with 20% human serum, penicillin and streptomycin was added. Before infection the medium had to be changed to antibiotic-free medium for at least 2 h.

6.2.3. Molecular biology techniques

6.2.3.1. Isolation of plasmid DNA

Plasmid isolations were performed using the Plasmid miniprep kit I (C-Line, Peqlab, Germany) and 10 ml *E. coli* Top10 overnight culture following the manufacturer's instructions. For cloning experiments or the transfection of mammalian cells, larger amounts of DNA were necessary. These were acquired using the NucleoBond® Xtra Maxi EF kit (Macherey-Nagel, Germany) according to the protocol supplied by the manufacturer. All DNA was stored at -20°C .

6.2.3.2. Determination of DNA concentration

To determine the concentration of dsDNA in solution, the absorption at 260 nm was measured using the NanoDrop® ND-1000 spectrophotometer with the ND-1000 V 3.1.0 software (PeqLab, Germany). Following the manufacturer's instructions, the samples were measured against a blank containing ddH₂O. By looking at the ratio of absorption OD_{260}/OD_{280} the solution was tested for contamination with protein or phenol. Values between 1.8 and 2 show the lowest level of contaminants.

6.2.3.3. Polymerase chain reaction

The PCR allows the amplification of DNA fragments. Phusion® polymerase (Thermo Fisher Scientific, USA) was used for cloning experiments due to the higher proof-reading capacity, while GoTaq G2 polymerase (Promega, USA) was used for colony PCR. All primers used were ordered from Eurofins (Munich, Germany). The PCR was performed following the manufacturer's instructions. The following tables show the general set ups and thermocycler programs used. The annealing temperatures depend on the primer length and composition while the elongation time depends on the length of the DNA fragment and the polymerase used.

The pYVO:8 plasmid DNA isolated from *Yersinia enterocolitica* WA-314 was used as a template for cloning experiments. It was isolated by resuspending a colony in ddH₂O, incubating it at 95°C for 10 min and centrifuging it at 10 000 x *g* for 2 min at 4°C. The supernatant containing the DNA was transferred to a reaction tube and stored at -20°C.

For cloning experiments the PCR products were run on an agarose gel (0.8-2% depending on the fragment size) to check whether they have the appropriate size. The band with the correct size was cut from the gel and purified as described in section 6.2.3.5.

Table 20 Phusion PCR reaction mix

| Component | Volume | Final concentration |
|-------------------------|-----------------|---------------------|
| DNA template | variable | <250 ng |
| 5x Phusion HF Buffer | 10 µl | 1x |
| Forward primer | 2.5 µl | 0.5 µM |
| Reverse primer | 2.5 µl | 0.5 µM |
| 10 mM dNTPs | 1 µl | 200 µM |
| Phusion® DNA polymerase | 0.5 µl | 1.0 u |
| DMSO | 1.5 µl | 3% |
| ddH ₂ O | Add up to 50 µl | |

Table 21 Phusion thermocycler program

| Step | Temperature | Time | Cycles |
|-------------------------|-------------|-------------|--------|
| 1. Initial denaturation | 98°C | 30 s | 1 |
| 2. Denaturation | 98°C | 10 s | 30-35 |
| 3. Annealing | 40-72°C | 30 s | |
| 4. Extension | 72°C | 30 s/kb DNA | |
| 5. Final elongation | 72°C | 10 min | 1 |
| 6. Storage | 8°C | forever | 1 |

Table 22 GoTaq G2 PCR reaction mix

| Component | Final volume | Final concentration |
|-----------------------------------|--------------|--------------------------------|
| DNA template | variable | < 0.1 µg/µl |
| 5x Green GoTaq reaction buffer | 2 µl | 1x (1.5 mM MgCl ₂) |
| Forward primer | 0.5 µl | 0.5 µM |
| Reverse primer | 0.5 µl | 0.5 µM |
| 10 mM dNTPs | 0.2 µl | 0.2 mM |
| GoTaq® G2 DNA polymerase (5 u/µl) | 0.05 µl | 1.25 u |

solved in 1xTAE buffer and RedSAFE (Intron Biotechnology, Korea) was added according to the manufacturer's protocol. The GeneRuler 1 kb Plus DNA Ladder (Thermo Fisher Scientific, USA) was used to determine the size of the DNA fragments. The samples were mixed with Orange DNA loading dye (6x, Fermentas, USA) before loading them on a gel unless the buffer of the sample already contained a loading dye (colony PCR, restriction digest). A voltage of 8 V/cm was applied for 45 min to 1 h before visualizing the DNA by UV-light on a Transilluminator (BioRad, Germany). For colony PCR, an image of the DNA bands illuminated by UV light was acquired for selecting the right colony. For cloning experiments, the DNA bands of the correct size were cut from the gel and purified using the NucleoSpin® Gel and PCR Clean-up Kit (Macherey-Nagel, Germany).

6.2.3.6. Ligation

During ligation phosphodiester bonds are formed between the digested ends of vector and insert DNA. This occurs between compatible DNA ends resulting from digests with the same restriction enzyme. Digested and purified vector and insert were combined in a molecular ratio of 1:3 – 1:5 for most experiments and 1:20 for crRNA ligation. The T4 DNA ligase from the Rapid DNA Ligation Kit (Thermo Fisher Scientific, USA) was used for all ligations. The ligation was set up as described in the manufacturer's protocol (see Table 25) and incubated for 30 min at room temperature before using it for transformation in *E. coli* Top10.

Table 25 Ligation

| Component | Volume/amount |
|--------------------------|---|
| Linearised vector | 50-100 ng |
| DNA insert | (molecular ratio to vector of 1:3 – 1:5) |
| 5x Rapid Ligation Buffer | 2 µl |
| T4 DNA Ligase, 5u/µl | 1 µl |
| ddH ₂ O | Add ddH ₂ O to total volume of 20 µl |

6.2.3.7. Generation of expression vectors and CRISPR vectors and fragments used in this study

Eukaryotic expression

The mRFP-GFP11-Rab5 plasmid was created by inserting GFP11 with linkers on both sides into the mRFP-Rab5 plasmid between the fluorophore and the protein. For this, *GFP11 Rab5 oligo fwd* and *GFP11 Rab5 oligo rev* ordered from Eurofins were annealed (as performed for the crRNA oligos in section 6.2.3.8). The oligos contain GFP11 (RDHMLVHEYVNAAGIT) with flexible linkers at both sides (linker A: GSSGGSSG; linker B: GGGKF) and lack the start and stop codon. At the ends are restriction sites (XhoI and HindIII) compatible to the restriction sites between mRFP (XhoI) and Rab5 (HindIII). Both plasmid and annealed oligos were

digested, run on an agarose gel and purified before ligation. After transformation a colony containing the correct plasmid was identified using colony PCR and sequencing. All primers used are listed in Table 16.

Bacterial expression

The pYopE-Halo plasmid was generated by digesting the empty pACYC184 vector with HindIII and amplifying YopE, its chaperone SycE and their promoter region (YopE/SycE) from the pYV plasmid and Halo_HA from the YopM-Halo plasmid. The primers introduced overlaps of the YopE/SycE fragment to the vector and the Halo tag and overlaps of the Halo tag fragment to YopE/SycE and the vector. The ligation of vector and fragments was achieved by combining all parts in a Phusion PCR as described in Table 21 using circular polymerase extension cloning with an annealing temperature of 58°C and 3 min extension time (Quan and Tian 2011). The overlaps of the inserts with each other and with the vector serve as primers which anneal to each other and allow ligation of the inserts into the vector.

The plasmids pYopE-CLIP and well as pYopE-SNAP and pYopE-GFP11 were generated using restriction enzymes. The pACYC184-YopE/SycE plasmid (Trülzsch et al. 2003) was amplified with primers introducing a HindIII restriction site and removing the stop codon at the C-terminus of YopE and adding a SmaI restriction site at the beginning of the plasmid linearizing it. The inserts CLIP, SNAP and GFP11 were amplified from template vectors with primers adding the HindIII restriction site to the N-terminus and the SmaI restriction site to the C-terminus. The template vectors were pYopH-CLIP, pYopH-SNAP and SteAprom_SteA_GFP11_R3_ACYC177 (Young et al. 2017). Both Halo and CLIP have a human influenza hemagglutinin (HA) tag (YPYDVPDYA). The tag enables the detection, isolation and purification of a protein of interest. GFP11 has a flexible linker (GSSGGSSG) at its N-terminus and a stop codon at the C-terminus. All primers used are listed in Table 16.

CRISPR vectors and fragments

The pKD46-Cpf1_Spt plasmid was created by using the pKD46-Cas12a_Amp plasmid and replacing the ampicillin resistance cassette with the spectinomycin resistance cassette from the pTTSS plasmid. The spectinomycin resistance cassette was amplified from the pTTSS using primers with short (50/51 bp) homology sequences to the pKD46-Cas12a_Amp. Top10 *E. coli* were transformed with pKD46-Cas12a_Amp using the heat shock protocol without the 42°C incubation due to the heat-sensitivity of the plasmid and were plated on LB plates containing ampicillin (see section 6.2.1.4). An overnight culture was prepared from this plate and the bacteria made electrocompetent as described in section 6.2.1.5. The expression of the red recombinase was induced by adding arabinose to a final concentration of 0.2% when the culture reached an OD₆₀₀ of 0.2. the electrocompetent bacteria were aliquoted and the spectinomycin PCR product was introduced by electroporation. The bacteria suspension was plated on LB plates

containing spectinomycin. A resulting clone was picked and used for a plasmid purification as described in section 6.2.3.1. All primers used are listed in Table 16.

The crRNAs used for targeting insertion sites in YopB and YopD sequences were designed based on the 20 bp protospacer following the 3'-end of a PAM (5'-TTN-3'). It is important that the insert site disrupts either a PAM itself or the protospacer sequence proximal to the PAM. Two complementary oligonucleotides with the protospacer sequence were designed with Eco31L overhangs at the 5'- and 3'-ends and ordered from Eurofins (all sequences can be found in Table 16). For annealing 22.5 µl of each oligonucleotide (100 pmol/µl in ddH₂O) and 5 µl of annealing buffer were mixed in 1.5 ml reaction tubes, placed in boiling water of at least 95°C and left in the water until it reaches room temperature. The original pAC-crRNA plasmid contains a chromo-red fluorescent GFP-like reporter gene (from *Echinopora forskaliana*) flanked by Eco31L restriction sites resulting in light pink colonies when transformed into bacteria (Gurskaya et al. 2001). It serves as a negative control indicating no crRNA has been inserted instead of the reporter gene. The plasmid was digested by Eco31L (see Table 24) for 15 min at 37°C, inactivated for 5 min at 65°C and run on a 0.8% agarose gel to separate the cut plasmid from the uncut plasmid. The cut plasmid was extracted from the gel using the NucleoSpin® Gel and PCR Clean-up kit (Macherey-Nagel, Germany). The annealed crRNA oligonucleotides were ligated into the cut vector using T4 DNA ligase from the Rapid DNA Ligation Kit (Thermo Fisher Scientific, USA). For this, 45 ng of digested vector was mixed with the annealed oligonucleotide at a molar ratio of 1:20, 4 µl of 5x Rapid Ligation Buffer and 1 µl T4 DNA ligase were added and filled up with ddH₂O to a total volume of 20 µl. The reaction was incubated at room temperature for 30 min. Afterwards 5-10 µl of the ligation products were transformed into chemically competent *E. coli* Top10 by heat shock (see section 6.2.1.4). The suspension was resuspended in 1 ml of LB medium and incubated for 1.5 h at 37°C and 850 rpm. The bacteria were pelleted by centrifugation (2 min, 10 000 x g, RT) and resuspended in 150 µl LB medium before plating on LB plates containing chloramphenicol. The plates were incubated overnight at 37°C and three resulting colonies were picked for sequencing. For this, the colonies were inoculated in 10 ml LB medium containing chloramphenicol and placed in a shaker incubator overnight at 37°C. The plasmid DNA was isolated with a Plasmid miniprep kit I (C-Line, Peqlab, Germany) and send for sequencing. Glycerol stocks were made of correctly sequenced colonies.

The HDR fragments used for insertion of GFP11 or the ALFA-tag were either a ssDNA oligo with short homology arms or a double-stranded PCR product with long homology arms (Figure 19). GFP11 was inserted between amino acids 50-51 of YopD and 216-217 of YopB and the ALFA-tag between amino acids 194-195 of YopD. The homology arms were designed based on the 50/500 bp 3' and 5' of the insertion site. GFP11 (16 aa: RDHMLVHEYVNAAGIT) and ALFA (15 aa: PSRLEEELRRRLTEP) were flanked by flexible

linkers at both sides (linker A: GSSGGSSG; linker B: GGGKF) and lacked the start and stop codon (GFP11 with linkers: 87 bp; ALFA with linkers: 84 bp). The single-stranded HDR fragment used in this study had 50 bp homology arms framing the insert sequence homologous to the sequence around the insert site and could be ordered from Eurofins (Munich Germany). Alternatively, one 500 bp homology arm (HomA) was amplified from the virulence plasmid with the reverse primer including part of the insert. The other homology arm (HomB) was amplified with a forward primer including the remaining part of the insert with an overlap to the previous reverse primer. Both arms were fused together in a PCR using the outer primers (HomA fwd and HomB rev) and the overlapping regions serving as additional primers. This procedure can only be performed with inserts below 100 bp due to the limited length of primers for the PCR. For larger inserts the insert must be separately amplified with overlaps to HomA and HomB. All primers for the HDR fragment amplification as well as single stranded oligo sequences with short homology arms can be found in Table 16 (all primers or oligos used for insertion are labeled with *Xcell*).

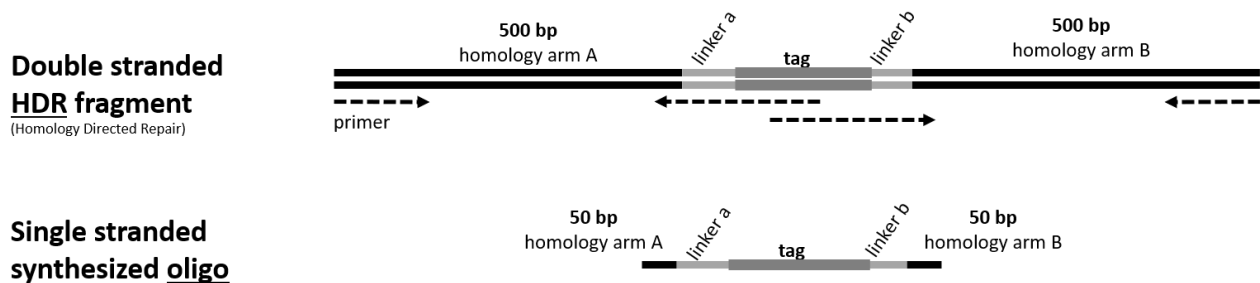


Figure 19 Comparison of double stranded HDR fragment and single stranded oligo for insertion of a tag into YopB and YopD. The double stranded HDR fragment has 500 bp homology arms and is generated by PCR using overlapping primers to generate the insert. The single stranded synthesized oligo has 50 bp homology arms and is entirely ordered.

6.2.3.8. CRISPR-Cas12a-assisted recombineering

The CRISPR-Cas protocol used in this study is based on a protocol published in *Yersinia Pestis Protocols* (Zhao and Sun 2018) and the related paper (Yan et al. 2017). Here, the bacteriophage lambda red system allowing homologous recombination was combined with the Cas12a-mediated double strand cleavage at a specific target sequence. We used this genome editing tool for the insertion of GFP11 and the ALFA-tag into the virulence plasmid of *Yersinia enterocolitica*.

For this, WA-314 was transformed with the temperature-sensitive pKD46-Cas12a plasmid which encodes for the lambda red system with an arabinose-inducible promoter, the endonuclease Cas12a and a spectinomycin resistance gene. The lambda red system includes the phage recombination genes *gam*, *exo*

and *beta* which prevent digestion of linear DNA, digest dsDNA to produce a linear ssDNA oligo and protect this ssDNA promoting its annealing to a complementary target. This allows the insertion of an introduced single- or double-stranded DNA fragment into the virulence plasmid via homologous recombination. The DNA fragment used is called homology directed repair (HDR) fragment. Cas12a proteins bind specific PAM sites in the DNA and induce cleavage through a conformational change caused by binding of crRNAs homologous to the target protospacer. The insertion of a DNA fragment alters the PAM or protospacer sequence recognised by the crRNA-Cas12a complex. Sequences where no insertion occurred are cleaved. The virulence plasmid in *Yersinia* WA-314 used in this study confers kanamycin resistance. Only bacteria survive in the presence of kanamycin where the PAM or protospacer has been changed by insertion of a DNA fragment preventing cleavage of the plasmid. The HDR fragments used were either a ssDNA oligo with 50 bp homology arms or a double-stranded PCR product with 500 bp homology arms. For the insertion of GFP11 both approaches were compared while the ALFA-tag was inserted using the double-stranded PCR product with long homology arms. The crRNA is encoded on the pAC-crRNA plasmid which also contains a chloramphenicol resistance cassette and the *sacB* gene conferring sucrose sensitivity. The crRNA and HDR fragments were generated as described in section 6.2.3.7.

Both crRNA and the HDR were transformed into the WA-314 containing the Cas12a plasmid. For this, the WA-314+pKD46-Cas12a was made electrocompetent as described in section 6.2.1.5. At OD₆₀₀ of 0.2 L-arabinose was added to a final concentration of 0.2% to induce the expression of the lambda red recombinase. The bacterial suspension was aliquoted on ice and 350 ng crRNA and 700 ng HDR fragment was electroporated into the WA-314+pKD46-Cas12a. After recovery at 27°C for 2 h, the bacteria were pelleted by centrifugation (2 min, 10 000 x *g*, RT) and resuspended in 150 µl LB medium. The suspension was plated on LB plates containing spectinomycin, chloramphenicol and kanamycin for the pKD46-Cas12, the crRNA and the pYV plasmid respectively. The plates were incubated at 27°C for 2 days before checking the resulting colonies for the insert. Each colony was streaked on an LB plate containing spectinomycin, chloramphenicol and kanamycin labeled with a numbered grid. Part of each colony was dissolved in 10 µl ddH₂O in a PCR tube, incubated at 95°C for 10 min in a thermocycler and spun down for 5 min in a tabletop centrifuge. The supernatant was used as a template for a colony PCR as described in section 6.2.3.3. Colony PCR primers binding on each side close to the insert site were used. The samples were run on a 2% agarose gel and compared to the wild-type control. Three positive colonies were selected and the sequencing primers binding outside the homology arms used to amplify a larger fragment for sequencing. A colony with a positive sequencing result was streaked on an LB plate containing 5% sucrose and kanamycin to cure the crRNA plasmid from the strain. The resulting colonies were checked for the crRNA-plasmid by streaking them on an LB plate with a numbered grid containing nalidixic acid and kanamycin and on an LB

plate with a numbered grid containing nalidixic acid, kanamycin and chloramphenicol. One colony not growing on the LB plate containing chloramphenicol was streaked on an LB plate containing nalidixic acid and kanamycin, wrapped in parafilm and a glove, sealed with tape and placed in a 42°C incubator for 3 days. One of the resulting colonies was streaked on an LB plate containing nalidixic acid and kanamycin. Colonies from this plate were checked for the pKD46-Cas12a plasmid by streaking them on an LB plate with a numbered grid containing nalidixic acid and kanamycin and on an LB plate with a numbered grid containing nalidixic acid, kanamycin and spectinomycin. A colony not growing on the LB plate containing spectinomycin was used for further experiments and a glycerol stock was prepared.

6.2.3.9. DNA sequencing

For sequencing of targets on the virulence plasmid, the region of interest was amplified using primers, while artificial plasmids were entirely isolated using Plasmid miniprep kit I (C-Line, Peqlab, Germany). Sequencing was performed by SeqLab (Göttingen, Germany). The PCR products or plasmids were mixed with the suitable primer according to the sample requirements of the company and send for sequencing. The results were compared to sequences in databases (NCBI-database, www.ncbi.nlm.nih.gov) or in CLC Genomics Workbench (CLC bio; Denmark).

6.2.4. Proteinbiochemical methods

6.2.4.1. Affinity purification of antibodies from serum

The primary antibodies against YopB and YopD used in this study were produced and tested for specificity by Franziska Huschka (Huschka 2017). Serum containing the specific antibodies was obtained through the repeated injection of purified protein into laboratory animals. The sera were run over affinity columns coated with the native immobilized antigen for purification.

Further purification steps were necessary to prepare antibodies for immunofluorescence. Secreted proteins from WA-314 (as described in section 6.2.1.2) were separated on an SDS-polyacrylamide gel and blotted on a PVDF membrane. The membrane was stained with Coomassie for 1 min before a brief washing step with destain buffer. The specific bands of YopB or YopD were cut from the membrane, completely destained using methanol and washed thrice with TBS-T (1xTBS with 0.1% Tween20). After blocking of unspecific binding sites with 5% (w/v) milk powder in TBS-T, the stripes were washed again and cut into smaller pieces. The serum was diluted 1:3 in 1xPBS and incubated with the membrane pieces in 2 ml reaction tubes overnight at 4°C on a rotator. On the following day the serum was removed, sterile filtered and stored at -20°C for further use. The membrane pieces were washed thrice with TBS-T and were thoroughly vortexed with 100-200 µl 0.1 M glycine-HCL (pH 2.5). The pH was immediately neutralized using

5.5 µl 1 M Tris-Base. BSA (2% final concentration) and glycerol (50% final concentration) were added to the antibody solution for stabilization during cryo conservation.

6.2.4.2. Protein expression and purification

For the purification of CNF-1 the protein was expressed in *E. coli* tagged with glutathione-S-transferase (GST). GST has a high affinity for glutathione (GSH) and can be used for purification of proteins in combination with GSH coupled beads.

GST-CNF-1 in the expression vector pGEX-4T-1 was transformed into the protease-deficient *E. coli* strain BL21-AI. For the overnight culture 50 ml LB medium with ampicillin was used to grow BL21-AI+GST-CNF-1 at 37°C in a shaker incubator. On the following day the culture was diluted 1:20 in 1000 ml LB medium with ampicillin and grown until an OD₆₀₀ of 0.5-0.7. Protein expression was induced by adding 400 µl 1 M IPTG and the culture was further incubated for 4 h at 37°C. Bacteria were pelleted by centrifugation (15 min, 6000 x g, 4°C) and were stored at -20°C.

Polypropylene columns (Qiagen, Germany) were prepared by adding 1 ml GSH-bead slurry and washing it twice with 10 ml ice-cold 1xPBS. The pellet was resuspended in 5 ml 0.1 mM PMSF and sonicated 10x10 s with an amplitude of 43% (Digital Sonifier 250-D, Branson, USA). Cell debris was removed by centrifugation (30 min, 20 000 x g, 4°C) and the supernatant transferred to the columns. The columns were rotated for 1 h at 4°C before being washed four times with 10 ml 1xPBS. The GST fusion proteins were eluted by incubation for 1 h with 500 µl elution buffer at 4°C and an additional overnight incubation with 500 µl elution buffer at 4°C. At each step a sample was taken and analyzed with SDS-PAGE and Coomassie staining. To remove surplus GSH, the eluted protein was dialyzed against 1xPBS. The protein was transferred to a Slide-A-Lyzer cassette (Thermo Fisher Scientific, USA) and placed under stirring in 3 L pre-cooled 1xPBS overnight at 4°C. The next day the protein was extracted from the cassette and the protein concentration measured using Bradford reagent (as described in section 6.2.4.5). The protein was aliquoted, flash frozen in liquid nitrogen and stored at -80°C.

6.2.4.3. Translocation assay

The effector proteins translocated into the host cell during infection with *Yersinia* were analyzed using the translocation assay. For this, 3x10⁵ HeLa cells were seeded in 6-well plates and overnight cultures of the *Yersinia* strains of interest were prepared. The next day *Yersinia* were prepared for infection as described in section 6.2.1.3 and the cells infected with an MOI of 100 for 1 h. The wells were carefully washed with ice-cold 1xPBS before adding 60 µl of proteinase K solution (500 µg/ml in 1xPBS) to cleave extracellular effector proteins. The solution was removed after 30 s and the protease activity was blocked after 20 min by adding 60 µl PMSF (phenylmethylsulfonyl fluoride, 4 mM in 1xPBS). The eukaryotic cells were lysed by

adding 60 μ l 0.5% (w/v) digitonin in 1xPBS. A cell scraper was used to detach the cells from the dish. The solution was transferred to a 1.5 ml reaction tube and incubated at room temperature for 20 min with vortexing every 10 min. Afterwards the cytosolic fraction was separated from the cell membranes and bacteria, which are not lysed by digitonin, by centrifugation (10 000 \times *g*, 4°C, 10 min). The supernatant was transferred to a 1.5 ml reaction tube and the protein concentration determined as described in section 6.2.4.5. The sample was mixed 3:1 with sample buffer and boiled for 5 min at 95°C before storage at -20°C. The samples were analyzed using SDS-polyacrylamide gel electrophoresis and Western blot.

6.2.4.4. Pull down assay

To test the protein properties of YopD-ALFA, beads labeled with anti-ALFA nanobody were used to pull interaction partners from cell lysates. For this, 90 μ l ALFA Selector ST slurry (30 μ l per condition; NanoTag Biotechnologies, Germany) were washed with 1 ml 1xPBS containing 1x complete mini protease inhibitor (1 tablet in 50 ml 1xPBS). After centrifugation (1000 \times *g*, 4°C, 2 min) the beads were resuspended in 600 μ l 0.5% digitonin in 1xPBS containing protease inhibitor. This solution was split in 200 μ l aliquots per condition in 1.5 ml reaction tubes. For each condition two 10 cm dishes were used, each with 3×10^5 HeLa cells and infected with WA-314 YopD-ALFA and WA-314 as a control for 1h with an MOI of 100. Another 2 dishes were treated with 1 μ g/ml CNF-1 for 2 h before infection with WA-314 YopD-ALFA. The infected cells were washed once with 1xPBS before adding 750 μ l 0.5% digitonin in 1xPBS containing protease inhibitor. The cells were scraped from the dish and transferred to 1.5 ml reaction tubes. After centrifugation (14 000 \times *g*, 4°C, 10 min) a sample of 60 μ l was taken and the remaining supernatant was transferred to the prepared beads. The lysate was incubated with the beads for 1.5 h at 4°C on a rotor to allow the nanobody to bind the ALFA-tag. The solution was centrifuged (1000 \times *g*, 4°C, 2 min) and a 60 μ l sample taken before discarding the remaining supernatant. The beads were resuspended in 1 ml 1xPBS containing protease inhibitor and transferred to a fresh 1.5 ml reaction tube where they were washed three times with 1 ml 1xPBS containing protease inhibitor. The remaining beads as well as supernatant samples were resuspended in 60 μ l and 20 μ l 4xSDS sample buffer, respectively and incubated for 7 min at 95°C. All samples were analyzed by immunoblot for their protein content.

6.2.4.5. Determination of protein concentration

The concentration of solubilized protein was determined by using Bradford reagent from the BioRad Protein-Assay-Kit (BioRad, Germany). The Bradford reagent was diluted 1:5 in ddH₂O. To 1 ml diluted reagent 2 μ l sample was added and vortexed. After 10 min the absorbance at 595 nm was measured in a photometer against a blank value. A standard curve based on different BSA concentrations (1-20 μ g/ml) was used to calculate the protein concentration of each sample.

6.2.4.6. SDS-polyacrylamide gel electrophoresis (SDS-PAGE)

The separation of proteins based on their molecular weight in an electric field using denaturing sodium dodecyl sulphate polyacrylamide gel electrophoresis (SDS-PAGE) is an analytical procedure developed by Lämmli (Laemmli 1970). Chemically inert acrylamide-bisacrylamide gels were prepared based on Table 26. The samples were incubated at 95°C for 5 min with SDS-PAGE loading buffer, which denatures the protein and covers it with a strong negative charge. This negative charge allows proteins to move towards the anode and separation is achieved because smaller proteins travel faster through the molecular net formed by acrylamide. The gel combines a short stacking gel (4% acrylamide, Tris HCL pH 6.8) with a larger resolving gel (7-17% acrylamide, Tris HCL pH 8.8). The gels were placed in the SDS-PAGE electrophoresis cell (Biorad, Germany) filled with SDS-PAGE running buffer. The samples were loaded into the wells of the stacking gel and run at 80 V for 30 min allowing the proteins to focus at the edge to the resolving gel. Afterwards a current of 150 V was applied until the desired separation in the resolving gel was reached.

Table 26 Composition of a 10% acrylamide SDS-PAGE mini gel

| Component/buffer | 10 % Resolving gel | 4 % Stacking gel |
|-------------------------|---------------------------|-------------------------|
| ddH ₂ O | 4.2 ml | 1.55 ml |
| Resolving Buffer pH 8.8 | 2.5 ml | - |
| Stacking Buffer pH 6.8 | - | 625 µl |
| Acrylamide 30% | 3.3 ml | 325 µl |
| APS (10 mg/ml) | 50 µl | 12.5 µl |
| TEMED | 5 µl | 2.5 µl |

6.2.4.7. Coomassie staining of SDS-polyacrylamide gels

Proteins separated by SDS-PAGE can be fixed and visualized using the Coomassie staining solution. For this, the stacking gel was discarded and the resolving gel was incubated with the Coomassie staining solution for 1 h on a shaker. Afterwards the gel was destained by incubating in Coomassie destain solution. The solution was exchanged several times until the protein bands were clearly visible. For documentation gels were scanned. The composition of all buffers can be found in Table 8.

6.2.4.8. Western blot analysis

Semidry protein blot systems were used to transfer proteins separated by SDS-PAGE to a polyvinylidene difluoride (PVDF) membrane (Immobilion-P, Millipore, Germany). The PVDF membrane was activated by a brief incubation in 100% methanol. Three filter papers (Whatman, Hartenstein, Germany) soaked in transfer buffer were placed on the cathode of the blotting chamber (OWL HEP-1, Thermo Fisher Scientific,

USA) and the SDS-PAGE gel was placed on top followed by the PVDF membrane. Another stack of three filter papers soaked in transfer buffer was placed on the stack before closing the blotting apparatus with the anode lid. A constant amperage of 1.2 mA/cm² was applied for 70 min allowing the transfer of proteins to the PVDF membrane. To block free protein-binding domains the membrane was incubated with 5% milk solution (5% (w/v) milk powder in TBS-T) for 1 h on a shaker. Afterwards primary antibody diluted in 5% milk solution was added either for 1 h at room temperature or overnight at 4°C. The membrane was washed thrice with TBS-T for 10 min before adding secondary antibody coupled to horseradish peroxidase (HRP) diluted in 5% milk solution for 45 min at room temperature. The membranes were washed again four times with TBS-T for 10 min to remove all unbound secondary antibody. Depending on the signal intensity expected either SuperSignal West Pico or SuperSignal West Femto Maximum (Thermo Fisher Scientific, USA) was used to detect the antibody signal. These solutions were used according to the manufacturer's instructions and allow the oxidization of luminol in the presence of HRP and peroxide. The resulting chemiluminescent signal was detected using X-ray films (Super RX, Fuji medical X-ray film, Japan) and developed in the Curix 60 (Agfa, Belgium). The films were scanned for documentation. All antibodies and their dilutions used can be found in Table 9 and Table 10.

6.2.5. Microscopy

6.2.5.1. Immunofluorescence staining

HeLa cells or primary human macrophages seeded on coverslips were infected with *Yersinia* as described in section 6.2.1.3. After infection for the required time the cells were washed thrice with 1xPBS, fixed with 4% PFA in 1xPBS for 5-10 min and washed again thrice with 1xPBS. Permeabilization was achieved using 0.1% Triton X-100 for 15 min. To avoid unspecific binding, the cells were blocked with 3% BSA in 1xPBS for 1 h before incubation with primary antibody diluted in 3% BSA for 1 h. Unbound antibody was removed by washing with 1xPBS three times. The fluorophore coupled secondary antibodies were also diluted in 3% BSA and added to the coverslips for 45 min. After washing three times with 1xPBS the coverslips were mounted on microscope slides using Prolong Diamond (Thermo Fisher Scientific, USA). The slides were incubated in the dark at room temperature for the mounting medium to set and were kept at 4°C for long term storage.

To determine whether bacteria are on the outside or the inside of cells, a staining step was added before permeabilization. Directly after fixation the cells were blocked with 3% BSA and incubated with an LPS antibody. This was followed by a specific secondary antibody before the cells were permeabilized and the steps were repeated using a secondary antibody with a different wavelength to distinguish between bacteria accessible before permeabilization and after permeabilization.

All PBS used for immunofluorescence staining was bought from Sigma-Aldrich (USA) and all antibodies and their dilutions can be found in Table 9 and Table 10.

6.2.5.2. Substrate staining (Halo/SNAP/CLIP/ALFA)

The same staining protocol was used for the fluorescent substrates of the Halo, SNAP and CLIP-tag. The substrates HaloTag TMR Ligand, SNAP-Cell TMR-Star and CLIP-Cell TMR-Star (New England Biolabs, USA) were diluted in DMSO to a working dilution of 500 μ M which was further diluted 1:1000 with DMEM with 10% FCS to a final concentration of 500 nM. HeLa cells were infected with the different *Yersinia* strains containing additional plasmids of YopH/YopM/YopE tagged with either Halo, SNAP or CLIP (as described in section 6.2.1.3). After 45 min of infection the medium was removed and 200 μ l of DMEM containing 500 nM substrate was added and incubated at 37°C and 5% CO₂ for another 15 min. Afterwards the cells were washed five times with cell culture medium and once with 1xPBS before fixation with 4% PFA for 5-10 min. The following steps including additional immunofluorescence staining were performed as described in section 6.2.5.1.

For live imaging bacteria had to be stained before infection. The bacteria were prepared as described in section 6.2.1.1 but set to an OD of 3.6 in 200 μ l LB medium. After centrifugation (5000 x *g*, 5 min, RT) the bacterial pellet was resuspended in 200 μ l LB medium containing 500 nM substrate. The solution was incubated at 37°C for 15 min, centrifuged (5000 x *g*, 5 min, 4°C) and resuspended in 1 ml ice-cold 1xPBS. An incubation step on ice for 5 min was followed by another centrifugation (5000 x *g*, 5 min, 4°C) and another 5 min incubation on ice. The bacteria were pelleted by centrifugation (5000 x *g*, 5 min, 4°C) and resuspended in 200 μ l 1xPBS. This bacterial suspension was used to infect HeLa cells seeded in MatTek dishes for live imaging. The dishes were placed in an incubation chamber of the Visitron SD-TRIF (Nikon Eclipse TiE, Nikon, Japan) providing a temperature of 37°C and 5% CO₂.

The FluoTag-X2 anti-ALFA nanobody in either Abberior® Star 580 or 635P (NanoTag Biotechnologies, Germany) was diluted 1:500 in 3% BSA. The cells infected with WA-314 YopD-ALFA were treated as for immunofluorescence staining including the blocking step with 3% BSA (in some experiments excluding the permeabilization step). The cells were incubated with the nanobody solution either at room temperature for 1-2 h or overnight at 4°C before washing for four times with 1xPBS. For staining of intrabacterial YopD-ALFA the nanobody was diluted in 0.05% Triton X-100 in 3% BSA and incubated overnight at 4°C. Additional immunofluorescence staining was performed afterwards as described in section 6.2.5.1.

For live imaging the cells were seeded in 8-well dishes and placed in the prewarmed chamber supplied with 5% CO₂ of the Visitron SD-TIRF. The nanobody was diluted 1:300 in 200 μ l DMEM with 10 % FCS and mixed with the WA-314 YopD-ALFA. The number of bacteria was chosen according to the intended MOI.

The medium was removed from the cells and the 200 μ l medium containing nanobody and bacteria was added. The imaging process was started immediately.

6.2.5.3. Confocal microscopy

The microscopy samples were observed using the laser scanning microscope Leica TCS SP8 with a 63x oil immersion objective (NA 1.4) and the LAS X SP8 software (Leica Microsystems, Germany).

6.2.5.4. Live cell imaging

Some live imaging was performed using the laser scanning microscope Leica TCS SP8 under the same set up as described in section 6.2.5.3 or the spinning disc microscope Visitron SD-TRIF (Nikon Eclipse TiE, Nikon, Japan) with a 60x oil immersion objective (NA 1.49) and the VisiView software (Visitron Systems, Germany).

7. Literature

Abrahams, Garth L.; Müller, Petra; Hensel, Michael (2006): Functional dissection of SseF, a type III effector protein involved in positioning the salmonella-containing vacuole. In *Traffic (Copenhagen, Denmark)* 7 (8), pp. 950–965. DOI: 10.1111/j.1600-0854.2006.00454.x.

Achtman, M.; Zurth, K.; Morelli, G.; Torrea, G.; Guiyoule, A.; Carniel, E. (1999): *Yersinia pestis*, the cause of plague, is a recently emerged clone of *Yersinia pseudotuberculosis*. In *Proceedings of the National Academy of Sciences of the United States of America* 96 (24), pp. 14043–14048. DOI: 10.1073/pnas.96.24.14043.

Adeolu, Mobolaji; Alnajjar, Seema; Naushad, Sohail; S Gupta, Radhey (2016): Genome-based phylogeny and taxonomy of the 'Enterobacteriales': proposal for Enterobacterales ord. nov. divided into the families Enterobacteriaceae, Erwiniaceae fam. nov., Pectobacteriaceae fam. nov., Yersiniaceae fam. nov., Hafniaceae fam. nov., Morganellaceae fam. nov., and Budviciaceae fam. nov. In *International journal of systematic and evolutionary microbiology* 66 (12), pp. 5575–5599. DOI: 10.1099/ijsem.0.001485.

Adli, Mazhar (2018): The CRISPR tool kit for genome editing and beyond. In *Nature communications* 9 (1), p. 1911. DOI: 10.1038/s41467-018-04252-2.

Aepfelbacher, M. (2004): Modulation of Rho GTPases by type III secretion system translocated effectors of *Yersinia*. In *Reviews of physiology, biochemistry and pharmacology* 152, pp. 65–77. DOI: 10.1007/s10254-004-0035-3.

Aepfelbacher, Martin; Roppenser, Bernhard; Hentschke, Moritz; Ruckdeschel, Klaus (2011): Activity modulation of the bacterial Rho GAP YopE: an inspiration for the investigation of mammalian Rho GAPs. In *European journal of cell biology* 90 (11), pp. 951–954. DOI: 10.1016/j.ejcb.2010.12.004.

Aepfelbacher, Martin; Trasak, Claudia; Ruckdeschel, Klaus (2007): Effector functions of pathogenic *Yersinia* species. In *Thrombosis and haemostasis* 98 (3), pp. 521–529.

Aepfelbacher, Martin; Trasak, Claudia; Wilharm, Gottfried; Wiedemann, Agnès; Trulzsch, Konrad; Krauss, Kristina et al. (2003): Characterization of YopT effects on Rho GTPases in *Yersinia enterocolitica*-infected cells. In *The Journal of biological chemistry* 278 (35), pp. 33217–33223. DOI: 10.1074/jbc.M303349200.

Aepfelbacher, Martin; Wolters, Manuel (2017): Acting on Actin: Rac and Rho Played by *Yersinia*. In *Current topics in microbiology and immunology* 399, pp. 201–220. DOI: 10.1007/82_2016_33.

Aili, Margareta; Isaksson, Elin L.; Carlsson, Sara E.; Wolf-Watz, Hans; Rosqvist, Roland; Francis, Matthew S. (2008): Regulation of *Yersinia* Yop-effector delivery by translocated YopE. In *International journal of medical microbiology : IJMM* 298 (3-4), pp. 183–192. DOI: 10.1016/j.ijmm.2007.04.007.

Aili, Margareta; Isaksson, Elin L.; Hallberg, Bengt; Wolf-Watz, Hans; Rosqvist, Roland (2006): Functional analysis of the YopE GTPase-activating protein (GAP) activity of *Yersinia pseudotuberculosis*. In *Cellular microbiology* 8 (6), pp. 1020–1033. DOI: 10.1111/j.1462-5822.2005.00684.x.

Akeda, Yukihiro; Galán, Jorge E. (2005): Chaperone release and unfolding of substrates in type III secretion. In *Nature* 437 (7060), pp. 911–915. DOI: 10.1038/nature03992.

Aleksić, S.; Bockemühl, J. (1984): Proposed revision of the Wauters et al. antigenic scheme for serotyping of *Yersinia enterocolitica*. In *Journal of Clinical Microbiology* 20 (1), pp. 99–102.

Alrutz, M. A.; Srivastava, A.; Wong, K. W.; D'Souza-Schorey, C.; Tang, M.; Ch'Ng, L. E. et al. (2001): Efficient uptake of *Yersinia pseudotuberculosis* via integrin receptors involves a Rac1-Arp 2/3 pathway that bypasses N-WASP function. In *Molecular microbiology* 42 (3), pp. 689–703. DOI: 10.1046/j.1365-2958.2001.02676.x.

Amer, Ayad A. A.; Åhlund, Monika K.; Bröms, Jeanette E.; Forsberg, Åke; Francis, Matthew S. (2011): Impact of the N-terminal secretor domain on YopD translocator function in *Yersinia pseudotuberculosis* type III secretion. In *Journal of bacteriology* 193 (23), pp. 6683–6700. DOI: 10.1128/JB.00210-11.

Anderson, D. M.; Schneewind, O. (1997): A mRNA signal for the type III secretion of Yop proteins by *Yersinia enterocolitica*. In *Science* 278 (5340), pp. 1140–1143. DOI: 10.1126/science.278.5340.1140.

Andersson, K.; Carballeira, N.; Magnusson, K. E.; Persson, C.; Stendahl, O.; Wolf-Watz, H.; Fällman, M. (1996): YopH of *Yersinia pseudotuberculosis* interrupts early phosphotyrosine signalling associated with phagocytosis. In *Molecular microbiology* 20 (5), pp. 1057–1069. DOI: 10.1111/j.1365-2958.1996.tb02546.x.

Andersson, K.; Magnusson, K. E.; Majeed, M.; Stendahl, O.; Fällman, M. (1999): *Yersinia pseudotuberculosis*-induced calcium signaling in neutrophils is blocked by the virulence effector YopH. In *Infection and immunity* 67 (5), pp. 2567–2574.

Andor, A.; Trülzsch, K.; Essler, M.; Roggenkamp, A.; Wiedemann, A.; Heesemann, J.; Aepfelbacher, M. (2001): YopE of *Yersinia*, a GAP for Rho GTPases, selectively modulates Rac-dependent actin structures in endothelial cells. In *Cellular microbiology* 3 (5), pp. 301–310. DOI: 10.1046/j.1462-5822.2001.00114.x.

Armentrout, Erin I.; Rietsch, Arne (2016): The Type III Secretion Translocation Pore Senses Host Cell Contact. In *PLoS Pathogens* 12 (3). DOI: 10.1371/journal.ppat.1005530.

Aspenström, Pontus; Fransson, Asa; Saras, Jan (2004): Rho GTPases have diverse effects on the organization of the actin filament system. In *The Biochemical journal* 377 (Pt 2), pp. 327–337. DOI: 10.1042/BJ20031041.

Atkinson, Steve; Williams, Paul (2016): *Yersinia* virulence factors - a sophisticated arsenal for combating host defences. In *F1000Research* 5. DOI: 10.12688/f1000research.8466.1.

Auerbuch, Victoria; Golenbock, Douglas T.; Isberg, Ralph R. (2009): Innate immune recognition of *Yersinia pseudotuberculosis* type III secretion. In *PLoS Pathogens* 5 (12), e1000686. DOI: 10.1371/journal.ppat.1000686.

Autenrieth, I. B.; Firsching, R. (1996): Penetration of M cells and destruction of Peyer's patches by *Yersinia enterocolitica*: an ultrastructural and histological study. In *Journal of medical microbiology* 44 (4), pp. 285–294. DOI: 10.1099/00222615-44-4-285.

Autenrieth, I. B.; Kempf, V.; Sprinz, T.; Preger, S.; Schnell, A. (1996): Defense mechanisms in Peyer's patches and mesenteric lymph nodes against *Yersinia enterocolitica* involve integrins and cytokines. In *Infection and immunity* 64 (4), pp. 1357–1368.

- Avilov, Sergiy V.; Aleksandrova, Nataliia (2018): Fluorescence protein complementation in microscopy: applications beyond detecting bi-molecular interactions. In *Methods and applications in fluorescence* 7 (1), p. 12001. DOI: 10.1088/2050-6120/aaef01.
- Bahnan, Wael; Boettner, Douglas R.; Westermark, Linda; Fällman, Maria; Schesser, Kurt (2015): Pathogenic *Yersinia* Promotes Its Survival by Creating an Acidic Fluid-Accessible Compartment on the Macrophage Surface. In *PLoS one* 10 (8), e0133298. DOI: 10.1371/journal.pone.0133298.
- Baker, Paul J.; Boucher, Dave; Bierschenk, Damien; Tebartz, Christina; Whitney, Paul G.; D'Silva, Damian B. et al. (2015): NLRP3 inflammasome activation downstream of cytoplasmic LPS recognition by both caspase-4 and caspase-5. In *European journal of immunology* 45 (10), pp. 2918–2926. DOI: 10.1002/eji.201545655.
- Balla, Tamas; Várnai, Péter (2009): Visualization of cellular phosphoinositide pools with GFP-fused protein-domains. In *Current protocols in cell biology* Chapter 24, Unit 24.4. DOI: 10.1002/0471143030.cb2404s42.
- Banaz, Nehir; Mäkelä, Jarno; Uphoff, Stephan (2019): Choosing the right label for single-molecule tracking in live bacteria: side-by-side comparison of photoactivatable fluorescent protein and Halo tag dyes. In *Journal of physics D: Applied physics* 52 (6), p. 64002. DOI: 10.1088/1361-6463/aaf255.
- Bancerz-Kisiel, Agata; Pieczywek, Marta; Łada, Piotr; Szweda, Wojciech (2018): The Most Important Virulence Markers of *Yersinia enterocolitica* and Their Role during Infection. In *Genes* 9 (5). DOI: 10.3390/genes9050235.
- Barbieri, Joseph T.; Riese, Matthew J.; Aktories, Klaus (2002): Bacterial toxins that modify the actin cytoskeleton. In *Annual review of cell and developmental biology* 18, pp. 315–344. DOI: 10.1146/annurev.cellbio.18.012502.134748.
- Barlag, Britta; Beutel, Oliver; Janning, Dennis; Czarniak, Frederik; Richter, Christian P.; Kommnick, Carina et al. (2016): Single molecule super-resolution imaging of proteins in living *Salmonella enterica* using self-labelling enzymes. In *Scientific reports* 6, p. 31601. DOI: 10.1038/srep31601.
- Batan, Dilara; Braselmann, Esther; Minson, Michael; Nguyen, Dieu My Thanh; Cossart, Pascale; Palmer, Amy E. (2018): A Multicolor Split-Fluorescent Protein Approach to Visualize *Listeria* Protein Secretion in Infection. In *Biophysical journal* 115 (2), pp. 251–262. DOI: 10.1016/j.bpj.2018.03.016.
- Baum, Linda G.; Garner, Omai B.; Schaefer, Katrin; Lee, Benhur (2014): Microbe-Host Interactions are Positively and Negatively Regulated by Galectin-Glycan Interactions. In *Frontiers in immunology* 5, p. 284. DOI: 10.3389/fimmu.2014.00284.
- Bellalou, J.; Ladant, D.; Sakamoto, H. (1990): Synthesis and secretion of *Bordetella pertussis* adenylate cyclase as a 200-kilodalton protein. In *Infection and immunity* 58 (5), pp. 1195–1200.
- Benabdillah, Rachid; Mota, Luís Jaime; Lützelshwab, Silke; Demoinet, Emilie; Cornelis, Guy R. (2004): Identification of a nuclear targeting signal in YopM from *Yersinia* spp. In *Microbial pathogenesis* 36 (5), pp. 247–261. DOI: 10.1016/j.micpath.2003.12.006.

- Bergman, T.; Håkansson, S.; Forsberg, A.; Norlander, L.; Macellaro, A.; Bäckman, A. et al. (1991): Analysis of the V antigen *lcrGVH-yopBD* operon of *Yersinia pseudotuberculosis*: evidence for a regulatory role of LcrH and LcrV. In *Journal of bacteriology* 173 (5), pp. 1607–1616. DOI: 10.1128/jb.173.5.1607-1616.1991.
- Berneking, Laura; Schnapp, Marie; Rumm, Andreas; Trasak, Claudia; Ruckdeschel, Klaus; Alawi, Malik et al. (2016): Immunosuppressive *Yersinia* Effector YopM Binds DEAD Box Helicase DDX3 to Control Ribosomal S6 Kinase in the Nucleus of Host Cells. In *PLoS Pathogens* 12 (6). DOI: 10.1371/journal.ppat.1005660.
- Bhagat, Neeru; Viridi, Jugsharan S. (2009): Molecular and biochemical characterization of urease and survival of *Yersinia enterocolitica* biovar 1A in acidic pH in vitro. In *BMC Microbiology* 9, p. 262. DOI: 10.1186/1471-2180-9-262.
- Bibel, D. J.; Chen, T. H. (1976): Diagnosis of plaque: an analysis of the Yersin-Kitasato controversy. In *Bacteriological Reviews* 40 (3), pp. 633–651.
- Black, D. S.; Bliska, J. B. (2000): The RhoGAP activity of the *Yersinia pseudotuberculosis* cytotoxin YopE is required for antiphagocytic function and virulence. In *Molecular microbiology* 37 (3), pp. 515–527. DOI: 10.1046/j.1365-2958.2000.02021.x.
- Blair, David F. (2003): Flagellar movement driven by proton translocation. In *FEBS letters* 545 (1), pp. 86–95. DOI: 10.1016/s0014-5793(03)00397-1.
- Blaylock, Bill; Riordan, Kelly E.; Missiakas, Dominique M.; Schneewind, Olaf (2006): Characterization of the *Yersinia enterocolitica* type III secretion ATPase YscN and its regulator, YscL. In *Journal of bacteriology* 188 (10), pp. 3525–3534. DOI: 10.1128/JB.188.10.3525-3534.2006.
- Bleves, Sophie; Marenne, Marie-Noëlle; Detry, Gautier; Cornelis, Guy R. (2002): Up-regulation of the *Yersinia enterocolitica* yop regulon by deletion of the flagellum master operon *flhDC*. In *Journal of bacteriology* 184 (12), pp. 3214–3223. DOI: 10.1128/jb.184.12.3214-3223.2002.
- Bliska, J. B.; Falkow, S. (1992): Bacterial resistance to complement killing mediated by the Ail protein of *Yersinia enterocolitica*. In *Proceedings of the National Academy of Sciences of the United States of America* 89 (8), pp. 3561–3565. DOI: 10.1073/pnas.89.8.3561.
- Bliska, James B.; Wang, Xiaoying; Viboud, Gloria I.; Brodsky, Igor E. (2013): Modulation of innate immune responses by *Yersinia* type III secretion system translocators and effectors. In *Cellular microbiology* 15 (10), pp. 1622–1631. DOI: 10.1111/cmi.12164.
- Blocker, A.; Gounon, P.; Larquet, E.; Niebuhr, K.; Cabiaux, V.; Parsot, C.; Sansonetti, P. (1999): The tripartite type III secretion system of *Shigella flexneri* inserts IpaB and IpaC into host membranes. In *The Journal of cell biology* 147 (3), pp. 683–693. DOI: 10.1083/jcb.147.3.683.
- Blocker, A.; Jouihri, N.; Larquet, E.; Gounon, P.; Ebel, F.; Parsot, C. et al. (2001): Structure and composition of the *Shigella flexneri* "needle complex", a part of its type III secretion system. In *Molecular microbiology* 39 (3), pp. 652–663. DOI: 10.1046/j.1365-2958.2001.02200.x.
- Boland, A.; Havaux, S.; Cornelis, G. R. (1998): Heterogeneity of the *Yersinia* YopM protein. In *Microbial pathogenesis* 25 (6), pp. 343–348. DOI: 10.1006/mpat.1998.0247.

- Bölin, I.; Norlander, L.; Wolf-Watz, H. (1982): Temperature-inducible outer membrane protein of *Yersinia pseudotuberculosis* and *Yersinia enterocolitica* is associated with the virulence plasmid. In *Infection and immunity* 37 (2), pp. 506–512.
- Bolotin, Alexander; Quinquis, Benoit; Sorokin, Alexei; Ehrlich, S. Dusko (2005): Clustered regularly interspaced short palindrome repeats (CRISPRs) have spacers of extrachromosomal origin. In *Microbiology (Reading, England)* 151 (Pt 8), pp. 2551–2561. DOI: 10.1099/mic.0.28048-0.
- Botelho, R. J.; Scott, C. C.; Grinstein, S. (2004): Phosphoinositide involvement in phagocytosis and phagosome maturation. In *Current topics in microbiology and immunology* 282, pp. 1–30. DOI: 10.1007/978-3-642-18805-3_1.
- Botelho, R. J.; Teruel, M.; Dierckman, R.; Anderson, R.; Wells, A.; York, J. D. et al. (2000): Localized biphasic changes in phosphatidylinositol-4,5-bisphosphate at sites of phagocytosis. In *The Journal of cell biology* 151 (7), pp. 1353–1368. DOI: 10.1083/jcb.151.7.1353.
- Bottone, E. J. (1997): *Yersinia enterocolitica*: the charisma continues. In *Clinical microbiology reviews* 10 (2), pp. 257–276.
- Bowater, Richard; Doherty, Aidan J. (2006): Making ends meet: repairing breaks in bacterial DNA by non-homologous end-joining. In *PLoS genetics* 2 (2), e8. DOI: 10.1371/journal.pgen.0020008.
- Boyle, Keith B.; Randow, Felix (2013): The role of 'eat-me' signals and autophagy cargo receptors in innate immunity. In *Current opinion in microbiology* 16 (3), pp. 339–348. DOI: 10.1016/j.mib.2013.03.010.
- Braun, Michael B.; Traenkle, Bjoern; Koch, Philipp A.; Emele, Felix; Weiss, Frederik; Poetz, Oliver et al. (2016): Peptides in headlock--a novel high-affinity and versatile peptide-binding nanobody for proteomics and microscopy. In *Scientific reports* 6, p. 19211. DOI: 10.1038/srep19211.
- Brawn, Lyndsey C.; Hayward, Richard D.; Koronakis, Vassilis (2007): Salmonella SPI1 effector SipA persists after entry and cooperates with a SPI2 effector to regulate phagosome maturation and intracellular replication. In *Cell host & microbe* 1 (1), pp. 63–75. DOI: 10.1016/j.chom.2007.02.001.
- Briones, Gabriel; Hofreuter, Dirk; Galán, Jorge E. (2006): Cre Reporter System To Monitor the Translocation of Type III Secreted Proteins into Host Cells. In *Infection and immunity* 74 (2), pp. 1084–1090. DOI: 10.1128/IAI.74.2.1084-1090.2006.
- Brodsky, Igor E.; Palm, Noah W.; Sadanand, Saheli; Ryndak, Michelle B.; Sutterwala, Fayyaz S.; Flavell, Richard A. et al. (2010): A *Yersinia* effector protein promotes virulence by preventing inflammasome recognition of the type III secretion system. In *Cell host & microbe* 7 (5), pp. 376–387. DOI: 10.1016/j.chom.2010.04.009.
- Bröms, Jeanette E.; Sundin, Charlotta; Francis, Matthew S.; Forsberg, Ake (2003): Comparative analysis of type III effector translocation by *Yersinia pseudotuberculosis* expressing native LcrV or PcrV from *Pseudomonas aeruginosa*. In *The Journal of infectious diseases* 188 (2), pp. 239–249. DOI: 10.1086/376452.

- Brown, Fraser D.; Rozelle, Andrew L.; Yin, Helen L.; Balla, Tamás; Donaldson, Julie G. (2001): Phosphatidylinositol 4,5-bisphosphate and Arf6-regulated membrane traffic. In *The Journal of cell biology* 154 (5), pp. 1007–1018. DOI: 10.1083/jcb.200103107.
- Broz, Petr; Mueller, Catherine A.; Müller, Shirley A.; Philippsen, Ansgar; Sorg, Isabel; Engel, Andreas; Cornelis, Guy R. (2007): Function and molecular architecture of the *Yersinia* injectisome tip complex. In *Molecular microbiology* 65 (5), pp. 1311–1320. DOI: 10.1111/j.1365-2958.2007.05871.x.
- Brubaker, R. R. (1991): Factors promoting acute and chronic diseases caused by yersiniae. In *Clinical microbiology reviews* 4 (3), pp. 309–324. DOI: 10.1128/cmr.4.3.309.
- Brubaker, R. R.; Surgalla, M. J. (1964): The effect of Ca⁺⁺ and Mg⁺⁺ on lysis, growth, and production of virulence antigens by *Pasteurella pestis*. In *The Journal of infectious diseases* 114, pp. 13–25. DOI: 10.1093/infdis/114.1.13.
- Buckley, Anthony M.; Petersen, Jan; Roe, Andrew J.; Douce, Gillian R.; Christie, John M. (2015): LOV-based reporters for fluorescence imaging. In *Current opinion in chemical biology* 27, pp. 39–45. DOI: 10.1016/j.cbpa.2015.05.011.
- Cabantous, Stéphanie; Terwilliger, Thomas C.; Waldo, Geoffrey S. (2005): Protein tagging and detection with engineered self-assembling fragments of green fluorescent protein. In *Nature biotechnology* 23 (1), pp. 102–107. DOI: 10.1038/nbt1044.
- Cain, Robert J.; Hayward, Richard D.; Koronakis, Vassilis (2004): The target cell plasma membrane is a critical interface for *Salmonella* cell entry effector-host interplay. In *Molecular microbiology* 54 (4), pp. 887–904. DOI: 10.1111/j.1365-2958.2004.04336.x.
- Cao, Xianhua; Wei, Guo; Fang, Huiqing; Guo, Jianping; Weinstein, Michael; Marsh, Clay B. et al. (2004): The inositol 3-phosphatase PTEN negatively regulates Fc gamma receptor signaling, but supports Toll-like receptor 4 signaling in murine peritoneal macrophages. In *Journal of immunology (Baltimore, Md. : 1950)* 172 (8), pp. 4851–4857. DOI: 10.4049/jimmunol.172.8.4851.
- Carniel, E. (1999): The *Yersinia* high-pathogenicity island. In *International microbiology : the official journal of the Spanish Society for Microbiology* 2 (3), pp. 161–167.
- Carniel, E. (2002): Plasmids and pathogenicity islands of *Yersinia*. In *Current topics in microbiology and immunology* 264 (1), pp. 89–108.
- Carniel, E.; Guilvout, I.; Prentice, M. (1996): Characterization of a large chromosomal "high-pathogenicity island" in biotype 1B *Yersinia enterocolitica*. In *Journal of bacteriology* 178 (23), pp. 6743–6751. DOI: 10.1128/jb.178.23.6743-6751.1996.
- Carniel, Elisabeth; Autenrieth, Ingo; Cornelis, Guy; Fukushima, Hiroshi; Guinet, Françoise; Isberg, Ralph et al. (2006): *Y. enterocolitica* and *Y. pseudotuberculosis*. In Martin Dworkin, Stanley Falkow, Eugene Rosenberg, Karl-Heinz Schleifer, Erko Stackebrandt (Eds.): *The Prokaryotes*, vol. 157: Springer New York, pp. 270–398.
- CDC (2016): *Yersinia enterocolitica*. Edited by Centers for Disease Control and Prevention. Available online at Available online: <https://www.cdc.gov/yersinia>.

- Cerliani, Juan P.; Blidner, Ada G.; Toscano, Marta A.; Croci, Diego O.; Rabinovich, Gabriel A. (2017): Translating the 'Sugar Code' into Immune and Vascular Signaling Programs. In *Trends in biochemical sciences* 42 (4), pp. 255–273. DOI: 10.1016/j.tibs.2016.11.003.
- Charpentier, Xavier; Oswald, Eric (2004): Identification of the secretion and translocation domain of the enteropathogenic and enterohemorrhagic *Escherichia coli* effector Cif, using TEM-1 beta-lactamase as a new fluorescence-based reporter. In *Journal of bacteriology* 186 (16), pp. 5486–5495. DOI: 10.1128/JB.186.16.5486-5495.2004.
- Chen, Weizhong; Zhang, Yifei; Yeo, Won-Sik; Bae, Taeok; Ji, Quanjiang (2017): Rapid and Efficient Genome Editing in *Staphylococcus aureus* by Using an Engineered CRISPR/Cas9 System. In *Journal of the American Chemical Society* 139 (10), pp. 3790–3795. DOI: 10.1021/jacs.6b13317.
- Cheng, L. W.; Anderson, D. M.; Schneewind, O. (1997): Two independent type III secretion mechanisms for YopE in *Yersinia enterocolitica*. In *Molecular microbiology* 24 (4), pp. 757–765. DOI: 10.1046/j.1365-2958.1997.3831750.x.
- Cheng, Shiya; Wang, Kun; Zou, Wei; Miao, Rui; Huang, Yaling; Wang, Haibin; Wang, Xiaochen (2015): PtdIns(4,5)P₂ and PtdIns3P coordinate to regulate phagosomal sealing for apoptotic cell clearance. In *The Journal of cell biology* 210 (3), pp. 485–502. DOI: 10.1083/jcb.201501038.
- Choudhary, Eira; Thakur, Preeti; Pareek, Madhu; Agarwal, Nisheeth (2015): Gene silencing by CRISPR interference in mycobacteria. In *Nature communications* 6, p. 6267. DOI: 10.1038/ncomms7267.
- Chung, Lawton K.; Park, Yong Hwan; Zheng, Yueting; Brodsky, Igor E.; Hearing, Patrick; Kastner, Daniel L. et al. (2016): The *Yersinia* Virulence Factor YopM Hijacks Host Kinases to Inhibit Type III Effector-Triggered Activation of the Pyrin Inflammasome. In *Cell host & microbe* 20 (3), pp. 296–306. DOI: 10.1016/j.chom.2016.07.018.
- Clarke, Jonathan H. (2003): Lipid signalling: picking out the PIPs. In *Current biology : CB* 13 (20), R815-7. DOI: 10.1016/j.cub.2003.09.054.
- Cordes, Frank S.; Komoriya, Kaoru; Larquet, Eric; Yang, Shixin; Egelman, Edward H.; Blocker, Ariel; Lea, Susan M. (2003): Helical structure of the needle of the type III secretion system of *Shigella flexneri*. In *The Journal of biological chemistry* 278 (19), pp. 17103–17107. DOI: 10.1074/jbc.M300091200.
- Cornelis, G. R.; Sluiter, C.; Delor, I.; Geib, D.; Kaniga, K.; Lambert de Rouvroit, C. et al. (1991): ymoA, a *Yersinia enterocolitica* chromosomal gene modulating the expression of virulence functions. In *Molecular microbiology* 5 (5), pp. 1023–1034. DOI: 10.1111/j.1365-2958.1991.tb01875.x.
- Cornelis, G. R.; van Gijsegem, F. (2000): Assembly and function of type III secretory systems. In *Annual review of microbiology* 54, pp. 735–774. DOI: 10.1146/annurev.micro.54.1.735.
- Cornelis, G. R.; Wolf-Watz, H. (1997): The *Yersinia* Yop virulon: a bacterial system for subverting eukaryotic cells. In *Molecular microbiology* 23 (5), pp. 861–867. DOI: 10.1046/j.1365-2958.1997.2731623.x.
- Cornelis, Guy; Vanootegem, J.-C.; Sluiter, C. (1987): Transcription of the yop regulon from *Y. enterocolitica* requires trans acting pYV and chromosomal genes. In *Microbial pathogenesis* 2 (5), pp. 367–379. DOI: 10.1016/0882-4010(87)90078-7.

- Cornelis, Guy R. (2002a): The Yersinia Ysc-Yop 'type III' weaponry. In *Nature reviews. Molecular cell biology* 3 (10), pp. 742–752. DOI: 10.1038/nrm932.
- Cornelis, Guy R. (2002b): Yersinia type III secretion: send in the effectors. In *The Journal of cell biology* 158 (3), pp. 401–408. DOI: 10.1083/jcb.200205077.
- Cornelis, Guy R. (2006): The type III secretion injectisome. In *Nature reviews. Microbiology* 4 (11), pp. 811–825. DOI: 10.1038/nrmicro1526.
- Cornelis, Guy R.; Boland, Anne; Boyd, Aoife P.; Geuijen, Cecile; Iriarte, Maite; Neyt, Cécile et al. (1998): The Virulence Plasmid of Yersinia, an Antihost Genome. In *Microbiology and molecular biology reviews* : *MMBR* 62 (4), pp. 1315–1352.
- Costa, Tiago R. D.; Edqvist, Petra J.; Bröms, Jeanette E.; Ahlund, Monika K.; Forsberg, Ake; Francis, Matthew S. (2010): YopD self-assembly and binding to LcrV facilitate type III secretion activity by Yersinia pseudotuberculosis. In *The Journal of biological chemistry* 285 (33), pp. 25269–25284. DOI: 10.1074/jbc.M110.144311.
- Costa, Tiago R. D.; Felisberto-Rodrigues, Catarina; Meir, Amit; Prevost, Marie S.; Redzej, Adam; Trokter, Martina; Waksman, Gabriel (2015): Secretion systems in Gram-negative bacteria: structural and mechanistic insights. In *Nature reviews. Microbiology* 13 (6), pp. 343–359. DOI: 10.1038/nrmicro3456.
- Cox, D.; Dale, B. M.; Kashiwada, M.; Helgason, C. D.; Greenberg, S. (2001): A regulatory role for Src homology 2 domain-containing inositol 5'-phosphatase (SHIP) in phagocytosis mediated by Fc gamma receptors and complement receptor 3 (alpha(M)beta(2); CD11b/CD18). In *The Journal of experimental medicine* 193 (1), pp. 61–71. DOI: 10.1084/jem.193.1.61.
- Cox, D.; Tseng, C. C.; Bjekic, G.; Greenberg, S. (1999): A requirement for phosphatidylinositol 3-kinase in pseudopod extension. In *The Journal of biological chemistry* 274 (3), pp. 1240–1247. DOI: 10.1074/jbc.274.3.1240.
- Cummings, R. D.; Liu, FT. (Eds.) (2009): Galectins. Essentials of Glycobiology. 2. In: Varki A, Cummings RD, Esko JD, Freeze HH, Stanley P, Bertozzi CR, Hart GW, Etzler ME, editors.: Cold Spring Harbor (NY).
- Datsenko, K. A.; Wanner, B. L. (2000): One-step inactivation of chromosomal genes in Escherichia coli K-12 using PCR products. In *Proceedings of the National Academy of Sciences of the United States of America* 97 (12), pp. 6640–6645. DOI: 10.1073/pnas.120163297.
- Davidson, Peter J.; Davis, Michael J.; Patterson, Ronald J.; Ripoche, Marie-Anne; Poirier, Françoise; Wang, John L. (2002): Shuttling of galectin-3 between the nucleus and cytoplasm. In *Glycobiology* 12 (5), pp. 329–337. DOI: 10.1093/glycob/12.5.329.
- Day, J. B.; Plano, G. V. (1998): A complex composed of SycN and YscB functions as a specific chaperone for YopN in Yersinia pestis. In *Molecular microbiology* 30 (4), pp. 777–788. DOI: 10.1046/j.1365-2958.1998.01110.x.
- Day, James B.; Ferracci, Franco; Plano, Gregory V. (2003): Translocation of YopE and YopN into eukaryotic cells by Yersinia pestis yopN, tyeA, sycN, yscB and lcrG deletion mutants measured using a phosphorylatable peptide tag and phosphospecific antibodies. In *Molecular microbiology* 47 (3), pp. 807–823. DOI: 10.1046/j.1365-2958.2003.03343.x.

- Day, James B.; Lee, Catherine A. (2003): Secretion of the orgC gene product by *Salmonella enterica* serovar Typhimurium. In *Infection and immunity* 71 (11), pp. 6680–6685. DOI: 10.1128/iai.71.11.6680-6685.2003.
- Delor, I.; Cornelis, G. R. (1992): Role of *Yersinia enterocolitica* Yst toxin in experimental infection of young rabbits. In *Infection and immunity* 60 (10), pp. 4269–4277.
- Deng, Wanyin; Marshall, Natalie C.; Rowland, Jennifer L.; McCoy, James M.; Worrall, Liam J.; Santos, Andrew S. et al. (2017): Assembly, structure, function and regulation of type III secretion systems. In *Nature reviews. Microbiology* 15 (6), pp. 323–337. DOI: 10.1038/nrmicro.2017.20.
- Deuschle, Eva; Keller, Birgit; Siegfried, Alexandra; Manncke, Birgit; Spaeth, Tanja; Köberle, Martin et al. (2016): Role of β 1 integrins and bacterial adhesins for Yop injection into leukocytes in *Yersinia enterocolitica* systemic mouse infection. In *International journal of medical microbiology : IJMM* 306 (2), pp. 77–88. DOI: 10.1016/j.ijmm.2015.12.001.
- Dewoody, Rebecca; Merritt, Peter M.; Houppert, Andrew S.; Marketon, Melanie M. (2011): YopK regulates the *Yersinia pestis* type III secretion system from within host cells. In *Molecular microbiology* 79 (6), pp. 1445–1461. DOI: 10.1111/j.1365-2958.2011.07534.x.
- Dewoody, Rebecca S.; Merritt, Peter M.; Marketon, Melanie M. (2013): Regulation of the *Yersinia* type III secretion system: traffic control. In *Frontiers in cellular and infection microbiology* 3, p. 4. DOI: 10.3389/fcimb.2013.00004.
- Di Paolo, Gilbert; Camilli, Pietro de (2006): Phosphoinositides in cell regulation and membrane dynamics. In *Nature* 443 (7112), pp. 651–657. DOI: 10.1038/nature05185.
- Di Paolo, Gilbert; Pellegrini, Lorenzo; Letinic, Kresimir; Cestra, Gianluca; Zoncu, Roberto; Voronov, Sergei et al. (2002): Recruitment and regulation of phosphatidylinositol phosphate kinase type 1 gamma by the FERM domain of talin. In *Nature* 420 (6911), pp. 85–89. DOI: 10.1038/nature01147.
- Diepold, Andreas; Amstutz, Marlise; Abel, Sören; Sorg, Isabel; Jenal, Urs; Cornelis, Guy R. (2010): Deciphering the assembly of the *Yersinia* type III secretion injectisome. In *The EMBO journal* 29 (11), pp. 1928–1940. DOI: 10.1038/emboj.2010.84.
- Diepold, Andreas; Armitage, Judith P. (2015): Type III secretion systems: the bacterial flagellum and the injectisome. In *Philosophical transactions of the Royal Society of London. Series B, Biological sciences* 370 (1679). DOI: 10.1098/rstb.2015.0020.
- Diepold, Andreas; Kudryashev, Mikhail; Delalez, Nicolas J.; Berry, Richard M.; Armitage, Judith P. (2015): Composition, formation, and regulation of the cytosolic c-ring, a dynamic component of the type III secretion injectisome. In *PLoS biology* 13 (1), e1002039. DOI: 10.1371/journal.pbio.1002039.
- Diepold, Andreas; Sezgin, Erdinc; Huseyin, Miles; Mortimer, Thomas; Eggeling, Christian; Armitage, Judith P. (2017): A dynamic and adaptive network of cytosolic interactions governs protein export by the T3SS injectisome. In *Nature communications* 8, p. 15940. DOI: 10.1038/ncomms15940.
- Discola, Karen F.; Förster, Andreas; Boulay, François; Simorre, Jean-Pierre; Attree, Ina; Dessen, Andréa; Job, Viviana (2014): Membrane and chaperone recognition by the major translocator protein PopB of the

- type III secretion system of *Pseudomonas aeruginosa*. In *The Journal of biological chemistry* 289 (6), pp. 3591–3601. DOI: 10.1074/jbc.M113.517920.
- Dohlich, Kim; Zumsteg, Anna Brotcke; Goosmann, Christian; Kolbe, Michael (2014): A substrate-fusion protein is trapped inside the Type III Secretion System channel in *Shigella flexneri*. In *PLoS Pathogens* 10 (1), e1003881. DOI: 10.1371/journal.ppat.1003881.
- Dong, Xiaoyun; Jin, Yingli; Di Ming; Li, Bangbang; Dong, Haisi; Wang, Lin et al. (2017): CRISPR/dCas9-mediated inhibition of gene expression in *Staphylococcus aureus*. In *Journal of microbiological methods* 139, pp. 79–86. DOI: 10.1016/j.mimet.2017.05.008.
- Dos Santos, Anamaria M. P.; Ferrari, Rafaela G.; Conte-Junior, Carlos A. (2020): Type three secretion system in *Salmonella Typhimurium*: the key to infection. In *Genes & genomics* 42 (5), pp. 495–506. DOI: 10.1007/s13258-020-00918-8.
- Dupont, Nicolas; Lacas-Gervais, Sandra; Bertout, Julie; Paz, Irit; Freche, Barbara; van Nhieu, Guy Tran et al. (2009): *Shigella* phagocytic vacuolar membrane remnants participate in the cellular response to pathogen invasion and are regulated by autophagy. In *Cell host & microbe* 6 (2), pp. 137–149. DOI: 10.1016/j.chom.2009.07.005.
- Durand, Enrique A.; Maldonado-Arocho, Francisco J.; Castillo, Cynthia; Walsh, Rebecca L.; Mecsas, Joan (2010): The presence of professional phagocytes dictates the number of host cells targeted for Yop translocation during infection. In *Cellular microbiology* 12 (8), pp. 1064–1082. DOI: 10.1111/j.1462-5822.2010.01451.x.
- ECDC (2019): Yersiniosis. Annual epidemiological report for 2018. In *European Centre for Disease Prevention and Control*. (Stockholm).
- Edqvist, Petra J.; Olsson, Jan; Lavander, Moa; Sundberg, Lena; Forsberg, Ake; Wolf-Watz, Hans; Lloyd, Scott A. (2003): YscP and YscU regulate substrate specificity of the *Yersinia* type III secretion system. In *Journal of bacteriology* 185 (7), pp. 2259–2266. DOI: 10.1128/jb.185.7.2259-2266.2003.
- Encell, Lance P.; Friedman Ohana, Rachel; Zimmerman, Kris; Otto, Paul; Vidugiris, Gediminas; Wood, Monika G. et al. (2012): Development of a dehalogenase-based protein fusion tag capable of rapid, selective and covalent attachment to customizable ligands. In *Current chemical genomics* 6, pp. 55–71. DOI: 10.2174/1875397301206010055.
- Enninga, Jost; Mounier, Joëlle; Sansonetti, Philippe; van Tran Nhieu, Guy (2005): Secretion of type III effectors into host cells in real time. In *Nature methods* 2 (12), pp. 959–965. DOI: 10.1038/NMETH804.
- Essler, Markus; Linder, Stefan; Schell, Barbara; Hufner, Katharina; Wiedemann, Agnès; Randhahn, Katharina et al. (2003): Cytotoxic necrotizing factor 1 of *Escherichia coli* stimulates Rho/Rho-kinase-dependent myosin light-chain phosphorylation without inactivating myosin light-chain phosphatase in endothelial cells. In *Infection and immunity* 71 (9), pp. 5188–5193. DOI: 10.1128/IAI.71.9.5188-5193.2003.
- Evan, G. I.; Lewis, G. K.; Ramsay, G.; Bishop, J. M. (1985): Isolation of monoclonal antibodies specific for human c-myc proto-oncogene product. In *Molecular and Cellular Biology* 5 (12), pp. 3610–3616.

- Evdokimov, Artem G.; Tropea, Joseph E.; Routzahn, Karen M.; Waugh, David S. (2002): Crystal structure of the *Yersinia pestis* GTPase activator YopE. In *Protein science : a publication of the Protein Society* 11 (2), pp. 401–408. DOI: 10.1110/ps.34102.
- Fahlgren, Anna; Westermark, Linda; Akopyan, Karen; Fällman, Maria (2009): Cell type-specific effects of *Yersinia pseudotuberculosis* virulence effectors. In *Cellular microbiology* 11 (12), pp. 1750–1767. DOI: 10.1111/j.1462-5822.2009.01365.x.
- Farrants, Helen; Tarnawski, Miroslaw; Müller, Thorsten G.; Otsuka, Shotaro; Hiblot, Julien; Koch, Birgit et al. (2020): Chemogenetic Control of Nanobodies. In *Nature methods*. DOI: 10.1038/s41592-020-0746-7.
- Feeley, Eric M.; Pilla-Moffett, Danielle M.; Zwack, Erin E.; Piro, Anthony S.; Finethy, Ryan; Kolb, Joseph P. et al. (2017): Galectin-3 directs antimicrobial guanylate binding proteins to vacuoles furnished with bacterial secretion systems. In *Proceedings of the National Academy of Sciences of the United States of America* 114 (9), E1698-E1706. DOI: 10.1073/pnas.1615771114.
- Felek, Suleyman; Krukonis, Eric S. (2008): The *Yersinia pestis* Ail Protein Mediates Binding and Yop Delivery to Host Cells Required for Plague Virulence ∇ . In *Infection and immunity* 77 (2), pp. 825–836. DOI: 10.1128/IAI.00913-08.
- Ferracci, Franco; Schubot, Florian D.; Waugh, David S.; Plano, Gregory V. (2005): Selection and characterization of *Yersinia pestis* YopN mutants that constitutively block Yop secretion. In *Molecular microbiology* 57 (4), pp. 970–987. DOI: 10.1111/j.1365-2958.2005.04738.x.
- Flatau, G.; Lemichez, E.; Gauthier, M.; Chardin, P.; Paris, S.; Fiorentini, C.; Boquet, P. (1997): Toxin-induced activation of the G protein p21 Rho by deamidation of glutamine. In *Nature* 387 (6634), pp. 729–733. DOI: 10.1038/42743.
- Foultier, Boris; Troisfontaines, Paul; Vertommen, Didier; Marenne, Marie-Noëlle; Rider, Mark; Parsot, Claude; Cornelis, Guy R. (2003): Identification of Substrates and Chaperone from the *Yersinia enterocolitica* 1B Ysa Type III Secretion System. In *Infection and immunity* 71 (1), pp. 242–253. DOI: 10.1128/IAI.71.1.242-253.2003.
- Fowler, J. M.; Brubaker, R. R. (1994): Physiological basis of the low calcium response in *Yersinia pestis*. In *Infection and immunity* 62 (12), pp. 5234–5241.
- Fowler, Janet M.; Wulff, Christine R.; Straley, Susan C.; Brubaker, Robert R. (2009): Growth of calcium-blind mutants of *Yersinia pestis* at 37 degrees C in permissive Ca²⁺-deficient environments. In *Microbiology (Reading, England)* 155 (Pt 8), pp. 2509–2521. DOI: 10.1099/mic.0.028852-0.
- Francis, M. S.; Aili, M.; Wiklund, M. L.; Wolf-Watz, H. (2000): A study of the YopD-IcrH interaction from *Yersinia pseudotuberculosis* reveals a role for hydrophobic residues within the amphipathic domain of YopD. In *Molecular microbiology* 38 (1), pp. 85–102. DOI: 10.1046/j.1365-2958.2000.02112.x.
- Fredriksson-Ahomaa, Maria (2007): *Yersinia enterocolitica* and *Yersinia pseudotuberculosis*. In Shabbir Simjee (Ed.): *Foodborne Diseases*, vol. 98. Totowa, NJ: Humana Press, pp. 79–113.
- Freund, Sandra; Czech, Beate; Trülsch, Konrad; Ackermann, Nikolaus; Heesemann, Jürgen (2008): Unusual, virulence plasmid-dependent growth behavior of *Yersinia enterocolitica* in three-dimensional collagen gels. In *Journal of bacteriology* 190 (12), pp. 4111–4120. DOI: 10.1128/JB.00156-08.

- Frithz-Lindsten, E.; Holmström, A.; Jacobsson, L.; Soltani, M.; Olsson, J.; Rosqvist, R.; Forsberg, A. (1998): Functional conservation of the effector protein translocators PopB/YopB and PopD/YopD of *Pseudomonas aeruginosa* and *Yersinia pseudotuberculosis*. In *Molecular microbiology* 29 (5), pp. 1155–1165. DOI: 10.1046/j.1365-2958.1998.00994.x.
- Gaietta, Guido; Deerinck, Thomas J.; Adams, Stephen R.; Bouwer, James; Tour, Oded; Laird, Dale W. et al. (2002): Multicolor and electron microscopic imaging of connexin trafficking. In *Science* 296 (5567), pp. 503–507. DOI: 10.1126/science.1068793.
- Galán, Jorge E.; Waksman, Gabriel (2018): Protein-Injection Machines in Bacteria. In *Cell* 172 (6), pp. 1306–1318. DOI: 10.1016/j.cell.2018.01.034.
- Galindo, Cristi L.; Rosenzweig, Jason A.; Kirtley, Michelle L.; Chopra, Ashok K. (2011): Pathogenesis of *Y. enterocolitica* and *Y. pseudotuberculosis* in Human Yersiniosis. In *Journal of pathogens* 2011, p. 182051. DOI: 10.4061/2011/182051.
- Galyov, E. E.; Håkansson, S.; Forsberg, A.; Wolf-Watz, H. (1993): A secreted protein kinase of *Yersinia pseudotuberculosis* is an indispensable virulence determinant. In *Nature* 361 (6414), pp. 730–732. DOI: 10.1038/361730a0.
- Garcia, Julie Torruellas; Ferracci, Franco; Jackson, Michael W.; Joseph, Sabrina S.; Pattis, Isabelle; Plano, Lisa R. W. et al. (2006): Measurement of effector protein injection by type III and type IV secretion systems by using a 13-residue phosphorylatable glycogen synthase kinase tag. In *Infection and immunity* 74 (10), pp. 5645–5657. DOI: 10.1128/IAI.00690-06.
- Garcia, P.; Gupta, R.; Shah, S.; Morris, A. J.; Rudge, S. A.; Scarlata, S. et al. (1995): The pleckstrin homology domain of phospholipase C-delta 1 binds with high affinity to phosphatidylinositol 4,5-bisphosphate in bilayer membranes. In *Biochemistry* 34 (49), pp. 16228–16234. DOI: 10.1021/bi00049a039.
- Gasiunas, Giedrius; Barrangou, Rodolphe; Horvath, Philippe; Siksnys, Virginijus (2012): Cas9-crRNA ribonucleoprotein complex mediates specific DNA cleavage for adaptive immunity in bacteria. In *Proceedings of the National Academy of Sciences of the United States of America* 109 (39), E2579-86. DOI: 10.1073/pnas.1208507109.
- Gaus, Kristin; Hentschke, Moritz; Czymmeck, Nicole; Novikova, Lena; Trülzsch, Konrad; Valentin-Weigand, Peter et al. (2011): Destabilization of YopE by the ubiquitin-proteasome pathway fine-tunes Yop delivery into host cells and facilitates systemic spread of *Yersinia enterocolitica* in host lymphoid tissue. In *Infection and immunity* 79 (3), pp. 1166–1175. DOI: 10.1128/IAI.00694-10.
- Gautier, Arnaud; Juillerat, Alexandre; Heinis, Christian; Corrêa, Ivan Reis; Kindermann, Maik; Beaufile, Florent; Johnsson, Kai (2008): An engineered protein tag for multiprotein labeling in living cells. In *Chemistry & biology* 15 (2), pp. 128–136. DOI: 10.1016/j.chembiol.2008.01.007.
- Gawthorne, Jayde A.; Audry, Laurent; McQuitty, Claire; Dean, Paul; Christie, John M.; Enninga, Jost; Roe, Andrew J. (2016): Visualizing the Translocation and Localization of Bacterial Type III Effector Proteins by Using a Genetically Encoded Reporter System. In *Applied and environmental microbiology* 82 (9), pp. 2700–2708. DOI: 10.1128/AEM.03418-15.

- Göser, Vera; Kommnick, Carina; Liss, Viktoria; Hensel, Michael (2019): Self-Labeling Enzyme Tags for Analyses of Translocation of Type III Secretion System Effector Proteins. In *mBio* 10 (3). DOI: 10.1128/mBio.00769-19.
- Götzke, Hansjörg; Kilisch, Markus; Martínez-Carranza, Markel; Sograte-Idrissi, Shama; Rajavel, Abirami; Schlichthaerle, Thomas et al. (2019): The ALFA-tag is a highly versatile tool for nanobody-based bioscience applications. In *Nature communications* 10 (1), p. 4403. DOI: 10.1038/s41467-019-12301-7.
- Grahek-Ogden, Danica; Schimmer, Barbara; Cudjoe, Kofitsyo S.; Nygård, Karin; Kapperud, Georg (2007): Outbreak of *Yersinia enterocolitica* serogroup O:9 infection and processed pork, Norway. In *Emerging infectious diseases* 13 (5), pp. 754–756. DOI: 10.3201/eid1305.061062.
- Green, Erin R.; Meccas, Joan (2016): Bacterial Secretion Systems: An Overview. In *Microbiology spectrum* 4 (1). DOI: 10.1128/microbiolspec.VMBF-0012-2015.
- Grimm, Jonathan B.; English, Brian P.; Chen, Jiji; Slaughter, Joel P.; Zhang, Zhengjian; Revyakin, Andrey et al. (2015): A general method to improve fluorophores for live-cell and single-molecule microscopy. In *Nature methods* 12 (3), 244-50, 3 p following 250. DOI: 10.1038/nmeth.3256.
- Gripenberg-Lerche, C.; Zhang, L.; Ahtonen, P.; Toivanen, P.; Skurnik, M. (2000): Construction of urease-negative mutants of *Yersinia enterocolitica* serotypes O:3 and o:8: role of urease in virulence and arthritogenicity. In *Infection and immunity* 68 (2), pp. 942–947. DOI: 10.1128/IAI.68.2.942-947.2000.
- Grosdent, Nadine; Maridonneau-Parini, Isabelle; Sory, Marie-Paule; Cornelis, Guy R. (2002): Role of Yops and adhesins in resistance of *Yersinia enterocolitica* to phagocytosis. In *Infection and immunity* 70 (8), pp. 4165–4176. DOI: 10.1128/iai.70.8.4165-4176.2002.
- Groß, Uwe (Ed.) (2006): Kurzlehrbuch Medizinische Mikrobiologie und Infektiologie. [nach neuer AO mit den Fächern: Mikrobiologie, Virologie, Hygiene sowie Infektiologie und Immunologie]. 202f., 364. 3rd ed.: Georg Thieme Verlag, 2013.
- Groves, E.; Dart, A. E.; Covarelli, V.; Caron, E. (2008): Molecular mechanisms of phagocytic uptake in mammalian cells. In *Cellular and molecular life sciences : CMLS* 65 (13), pp. 1957–1976. DOI: 10.1007/s00018-008-7578-4.
- Grützkau, A.; Hanski, C.; Hahn, H.; Riecken, E. O. (1990): Involvement of M cells in the bacterial invasion of Peyer's patches: a common mechanism shared by *Yersinia enterocolitica* and other enteroinvasive bacteria. In *Gut* 31 (9), pp. 1011–1015.
- Gu, Tongnian; Zhao, Siqi; Pi, Yishuang; Chen, Weizhong; Chen, Chuanyuan; Liu, Qian et al. (2018): Highly efficient base editing in *Staphylococcus aureus* using an engineered CRISPR RNA-guided cytidine deaminase. In *Chemical science* 9 (12), pp. 3248–3253. DOI: 10.1039/C8SC00637G.
- Guan, K. L.; Dixon, J. E. (1990): Protein tyrosine phosphatase activity of an essential virulence determinant in *Yersinia*. In *Science* 249 (4968), pp. 553–556. DOI: 10.1126/science.2166336.
- Gurry, J. F. (1974): Acute Terminal Ileitis and *Yersinia* Infection. In *British Medical Journal* 2 (5913), pp. 264–266.

- Gurskaya, N. G.; Fradkov, A. F.; Terskikh, A.; Matz, M. V.; Labas, Y. A.; Martynov, V. I. et al. (2001): GFP-like chromoproteins as a source of far-red fluorescent proteins. In *FEBS letters* 507 (1), pp. 16–20. DOI: 10.1016/s0014-5793(01)02930-1.
- Håkansson, S.; Bergman, T.; Vanooteghem, J. C.; Cornelis, G.; Wolf-Watz, H. (1993): YopB and YopD constitute a novel class of Yersinia Yop proteins. In *Infection and immunity* 61 (1), pp. 71–80.
- Håkansson, S.; Schesser, K.; Persson, C.; Galyov, E. E.; Rosqvist, R.; Homblé, F.; Wolf-Watz, H. (1996): The YopB protein of Yersinia pseudotuberculosis is essential for the translocation of Yop effector proteins across the target cell plasma membrane and displays a contact-dependent membrane disrupting activity. In *The EMBO journal* 15 (21), pp. 5812–5823. DOI: 10.1002/j.1460-2075.1996.tb00968.x.
- Hamers-Casterman, C.; Atarhouch, T.; Muyldermans, S.; Robinson, G.; Hamers, C.; Songa, E. B. et al. (1993): Naturally occurring antibodies devoid of light chains. In *Nature* 363 (6428), pp. 446–448. DOI: 10.1038/363446a0.
- Hanski, C.; Kutschka, U.; Schmoranzler, H. P.; Naumann, M.; Stallmach, A.; Hahn, H. et al. (1989): Immunohistochemical and electron microscopic study of interaction of Yersinia enterocolitica serotype O8 with intestinal mucosa during experimental enteritis. In *Infection and immunity* 57 (3), pp. 673–678.
- Hawkins, John S.; Wong, Spencer; Peters, Jason M.; Almeida, Ricardo; Qi, Lei S. (2015): Targeted Transcriptional Repression in Bacteria Using CRISPR Interference (CRISPRi). In *Methods in molecular biology (Clifton, N.J.)* 1311, pp. 349–362. DOI: 10.1007/978-1-4939-2687-9_23.
- Heesemann, J.; Laufs, R. (1983): Construction of a mobilizable Yersinia enterocolitica virulence plasmid. In *Journal of bacteriology* 155 (2), pp. 761–767.
- Hentschke, Moritz; Berneking, Laura; Belmar Campos, Cristina; Buck, Friedrich; Ruckdeschel, Klaus; Aepfelbacher, Martin (2010): Yersinia virulence factor YopM induces sustained RSK activation by interfering with dephosphorylation. In *PLoS one* 5 (10). DOI: 10.1371/journal.pone.0013165.
- Hilpelä, P.; Vartiainen, M. K.; Lappalainen, P. (2004): Regulation of the actin cytoskeleton by PI(4,5)P2 and PI(3,4,5)P3. In *Current topics in microbiology and immunology* 282, pp. 117–163. DOI: 10.1007/978-3-642-18805-3_5.
- Ho, Brandon; Baryshnikova, Anastasia; Brown, Grant W. (2018): Unification of Protein Abundance Datasets Yields a Quantitative Saccharomyces cerevisiae Proteome. In *Cell systems* 6 (2), 192–205.e3. DOI: 10.1016/j.cels.2017.12.004.
- Ho, Hsin-yi Henry; Rohatgi, Rajat; Lebensohn, Andres M.; Le Ma; Li, Jiaxu; Gygi, Steven P.; Kirschner, Marc W. (2004): Toca-1 mediates Cdc42-dependent actin nucleation by activating the N-WASP-WIP complex. In *Cell* 118 (2), pp. 203–216. DOI: 10.1016/j.cell.2004.06.027.
- Hochuli, E.; Döbeli, H.; Schacher, A. (1987): New metal chelate adsorbent selective for proteins and peptides containing neighbouring histidine residues. In *Journal of Chromatography A* 411, pp. 177–184. DOI: 10.1016/S0021-9673(00)93969-4.
- Hodgkinson, Julie L.; Horsley, Ashley; Stabat, David; Simon, Martha; Johnson, Steven; da Fonseca, Paula C. A. et al. (2009): Three-dimensional reconstruction of the Shigella T3SS transmembrane regions reveals

12-fold symmetry and novel features throughout. In *Nature structural & molecular biology* 16 (5), pp. 477–485. DOI: 10.1038/nsmb.1599.

Hoffmann, Carsten; Gaietta, Guido; Zürn, Alexander; Adams, Stephen R.; Terrillon, Sonia; Ellisman, Mark H. et al. (2010): Fluorescent labeling of tetracysteine-tagged proteins in intact cells. In *Nature protocols* 5 (10), pp. 1666–1677. DOI: 10.1038/nprot.2010.129.

Hoffmann, Claudia; Pop, Marius; Leemhuis, Jost; Schirmer, Jörg; Aktories, Klaus; Schmidt, Gudula (2004): The Yersinia pseudotuberculosis cytotoxic necrotizing factor (CNFY) selectively activates RhoA. In *The Journal of biological chemistry* 279 (16), pp. 16026–16032. DOI: 10.1074/jbc.M313556200.

Höfling, Sabrina; Grabowski, Benjamin; Norkowski, Stefanie; Schmidt, M. Alexander; Rüter, Christian (2015): Current activities of the Yersinia effector protein YopM. In *International journal of medical microbiology : IJMM* 305 (3), pp. 424–432. DOI: 10.1016/j.ijmm.2015.03.009.

Hoiczky, E.; Blobel, G. (2001): Polymerization of a single protein of the pathogen Yersinia enterocolitica into needles punctures eukaryotic cells. In *Proceedings of the National Academy of Sciences of the United States of America* 98 (8), pp. 4669–4674. DOI: 10.1073/pnas.071065798.

Holmström, A.; Petterson, J.; Rosqvist, R.; Håkansson, S.; Tafazoli, F.; Fällman, M. et al. (1997): YopK of Yersinia pseudotuberculosis controls translocation of Yop effectors across the eukaryotic cell membrane. In *Molecular microbiology* 24 (1), pp. 73–91. DOI: 10.1046/j.1365-2958.1997.3211681.x.

Holmström, A.; Rosqvist, R.; Wolf-Watz, H.; Forsberg, A. (1995a): Virulence plasmid-encoded YopK is essential for Yersinia pseudotuberculosis to cause systemic infection in mice. In *Infection and immunity* 63 (6), pp. 2269–2276.

Holmström, A.; Rosqvist, R.; Wolf-Watz, H.; Forsberg, A. (1995b): YopK, a novel virulence determinant of Yersinia pseudotuberculosis. In *Contributions to microbiology and immunology* 13, pp. 239–243.

Hopp, Thomas P.; Prickett, Kathryn S.; Price, Virginia L.; Libby, Randell T.; March, Carl J.; Pat Cerretti, Douglas et al. (1988): A Short Polypeptide Marker Sequence Useful for Recombinant Protein Identification and Purification. In *Nature biotechnology* 6 (10), pp. 1204–1210. DOI: 10.1038/nbt1088-1204.

Horne, Shelley M.; Prüss, Birgit M. (2006): Global gene regulation in Yersinia enterocolitica: effect of FliA on the expression levels of flagellar and plasmid-encoded virulence genes. In *Archives of microbiology* 185 (2), pp. 115–126. DOI: 10.1007/s00203-005-0077-1.

Hu, J.; Worrall, L. J.; Hong, C.; Vuckovic, M.; Atkinson, C. E.; Caveney, N. et al. (2018): Cryo-EM analysis of the T3S injectisome reveals the structure of the needle and open secretin. In *Nature communications* 9 (1), p. 3840. DOI: 10.1038/s41467-018-06298-8.

Hu, Ping; Elliott, Jeffrey; McCready, Paula; Skowronski, Evan; Garnes, Jeffrey; Kobayashi, Arthur et al. (1998): Structural organization of virulence-associated plasmids of Yersinia pestis. In *Journal of bacteriology* 180 (19), pp. 5192–5202.

Hueck, Christoph J. (1998): Type III Protein Secretion Systems in Bacterial Pathogens of Animals and Plants. In *Microbiology and molecular biology reviews : MMBR* 62 (2), pp. 379–433.

- Hume, Peter J.; McGhie, Emma J.; Hayward, Richard D.; Koronakis, Vassilis (2003): The purified Shigella IpaB and Salmonella SipB translocators share biochemical properties and membrane topology. In *Molecular microbiology* 49 (2), pp. 425–439. DOI: 10.1046/j.1365-2958.2003.03559.x.
- Huschka, Franziska (2017): Visualisierung des Typ III Translokator-Komplexes von *Yersinia enterocolitica* während der Wirtszellinfektion. Dissertation, Universität Hamburg, Hamburg.
- Iriarte, M.; Cornelis, G. R. (1998): YopT, a new *Yersinia* Yop effector protein, affects the cytoskeleton of host cells. In *Molecular microbiology* 29 (3), pp. 915–929. DOI: 10.1046/j.1365-2958.1998.00992.x.
- Isaksson, Elin L.; Aili, Margareta; Fahlgren, Anna; Carlsson, Sara E.; Rosqvist, Roland; Wolf-Watz, Hans (2009): The membrane localization domain is required for intracellular localization and autoregulation of YopE in *Yersinia pseudotuberculosis*. In *Infection and immunity* 77 (11), pp. 4740–4749. DOI: 10.1128/IAI.00333-09.
- Isberg, R. R.; Leong, J. M. (1990): Multiple beta 1 chain integrins are receptors for invasin, a protein that promotes bacterial penetration into mammalian cells. In *Cell* 60 (5), pp. 861–871. DOI: 10.1016/0092-8674(90)90099-z.
- Jackson, Sophie E.; Craggs, Timothy D.; Huang, Jie-rong (2006): Understanding the folding of GFP using biophysical techniques. In *Expert review of proteomics* 3 (5), pp. 545–559. DOI: 10.1586/14789450.3.5.545.
- Jacobi, C. A.; Roggenkamp, A.; Rakin, A.; Zumbihl, R.; Leitritz, L.; Heesemann, J. (1998): In vitro and in vivo expression studies of yopE from *Yersinia enterocolitica* using the gfp reporter gene. In *Molecular microbiology* 30 (4), pp. 865–882. DOI: 10.1046/j.1365-2958.1998.01128.x.
- Jacobs, J.; Jamaer, D.; Vandeven, J.; Wouters, M.; Vermeylen, C.; Vandepitte, J. (1989): *Yersinia enterocolitica* in donor blood: a case report and review. In *Journal of Clinical Microbiology* 27 (5), pp. 1119–1121.
- Jalava, Katri; Hakkinen, Marjaana; Valkonen, Miia; Nakari, Ulla-Maija; Palo, Taito; Hallanvuori, Saija et al. (2006): An outbreak of gastrointestinal illness and erythema nodosum from grated carrots contaminated with *Yersinia pseudotuberculosis*. In *The Journal of infectious diseases* 194 (9), pp. 1209–1216. DOI: 10.1086/508191.
- Jiang, Wenyan; Bikard, David; Cox, David; Zhang, Feng; Marraffini, Luciano A. (2013): RNA-guided editing of bacterial genomes using CRISPR-Cas systems. In *Nature biotechnology* 31 (3), pp. 233–239. DOI: 10.1038/nbt.2508.
- Jiang, Yu; Chen, Biao; Duan, Chunlan; Sun, Bingbing; Yang, Junjie; Yang, Sheng (2015): Multigene editing in the *Escherichia coli* genome via the CRISPR-Cas9 system. In *Applied and environmental microbiology* 81 (7), pp. 2506–2514. DOI: 10.1128/AEM.04023-14.
- Jinek, Martin; Chylinski, Krzysztof; Fonfara, Ines; Hauer, Michael; Doudna, Jennifer A.; Charpentier, Emmanuelle (2012): A programmable dual-RNA-guided DNA endonuclease in adaptive bacterial immunity. In *Science* 337 (6096), pp. 816–821. DOI: 10.1126/science.1225829.

- Joseph, Sabrina S.; Plano, Gregory V. (2013): The SycN/YscB chaperone-binding domain of YopN is required for the calcium-dependent regulation of Yop secretion by *Yersinia pestis*. In *Frontiers in cellular and infection microbiology* 3, p. 1. DOI: 10.3389/fcimb.2013.00001.
- Journet, Laure; Agrain, Céline; Broz, Petr; Cornelis, Guy R. (2003): The needle length of bacterial injectisomes is determined by a molecular ruler. In *Science* 302 (5651), pp. 1757–1760. DOI: 10.1126/science.1091422.
- Kakoschke, Tamara Katharina; Kakoschke, Sara Carina; Zeuzem, Catharina; Bouabe, Hicham; Adler, Kristin; Heesemann, Jürgen; Rossier, Ombeline (2016): The RNA Chaperone Hfq Is Essential for Virulence and Modulates the Expression of Four Adhesins in *Yersinia enterocolitica*. In *Scientific reports* 6, p. 29275. DOI: 10.1038/srep29275.
- Kamiyama, Daichi; Sekine, Sayaka; Barsi-Rhyne, Benjamin; Hu, Jeffrey; Chen, Baohui; Gilbert, Luke A. et al. (2016): Versatile protein tagging in cells with split fluorescent protein. In *Nature communications* 7, p. 11046. DOI: 10.1038/ncomms11046.
- Kapatral, V.; Minnich, S. A. (1995): Co-ordinate, temperature-sensitive regulation of the three *Yersinia enterocolitica* flagellin genes. In *Molecular microbiology* 17 (1), pp. 49–56. DOI: 10.1111/j.1365-2958.1995.mmi_17010049.x.
- Kayser, Fritz H.; Böttger, Erik Christian; Zinkernagel, Rolf M. (Eds.) (2001): *Medizinische Mikrobiologie: Georg Thieme*.
- Ke, Na; Landgraf, Dirk; Paulsson, Johan; Berkmen, Mehmet (2016): Visualization of Periplasmic and Cytoplasmic Proteins with a Self-Labeling Protein Tag. In *Journal of bacteriology* 198 (7), pp. 1035–1043. DOI: 10.1128/JB.00864-15.
- Keppler, Antje; Gendreizig, Susanne; Gronemeyer, Thomas; Pick, Horst; Vogel, Horst; Johnsson, Kai (2003): A general method for the covalent labeling of fusion proteins with small molecules in vivo. In *Nature biotechnology* 21 (1), pp. 86–89. DOI: 10.1038/nbt765.
- Kerschen, Edward J.; Cohen, Donald A.; Kaplan, Alan M.; Straley, Susan C. (2004): The plague virulence protein YopM targets the innate immune response by causing a global depletion of NK cells. In *Infection and immunity* 72 (8), pp. 4589–4602. DOI: 10.1128/IAI.72.8.4589-4602.2004.
- Kim, Jaewha; Ahn, Kyungseop; Min, Sungran; Jia, Jinghua; Ha, Unhwan; Wu, Donghai; Jin, Shouguang (2005): Factors triggering type III secretion in *Pseudomonas aeruginosa*. In *Microbiology (Reading, England)* 151 (Pt 11), pp. 3575–3587. DOI: 10.1099/mic.0.28277-0.
- Kimbrough, T. G.; Miller, S. I. (2000): Contribution of *Salmonella typhimurium* type III secretion components to needle complex formation. In *Proceedings of the National Academy of Sciences of the United States of America* 97 (20), pp. 11008–11013. DOI: 10.1073/pnas.200209497.
- Kirchhofer, Axel; Helma, Jonas; Schmidhals, Katrin; Frauer, Carina; Cui, Sheng; Karcher, Annette et al. (2010): Modulation of protein properties in living cells using nanobodies. In *Nature structural & molecular biology* 17 (1), pp. 133–138. DOI: 10.1038/nsmb.1727.
- Kitasato, S. (1894): THE BACILLUS OF BUBONIC PLAGUE. In *The Lancet* 144 (3704), pp. 428–430. DOI: 10.1016/S0140-6736(01)58670-5.

- Knapp, Andreas; Rippahn, Myriam; Volkenborn, Kristina; Skoczinski, Pia; Jaeger, Karl-Erich (2017): Activity-independent screening of secreted proteins using split GFP. In *Journal of biotechnology* 258, pp. 110–116. DOI: 10.1016/j.jbiotec.2017.05.024.
- Köberle, Martin; Klein-Günther, Annegret; Schütz, Monika; Fritz, Michaela; Berchtold, Susanne; Tolosa, Eva et al. (2009): Yersinia enterocolitica targets cells of the innate and adaptive immune system by injection of Yops in a mouse infection model. In *PLoS Pathogens* 5 (8), e1000551. DOI: 10.1371/journal.ppat.1000551.
- Kodama, Yutaka; Hu, Chang-Deng (2012): Bimolecular fluorescence complementation (BiFC): a 5-year update and future perspectives. In *BioTechniques* 53 (5), pp. 285–298. DOI: 10.2144/000113943.
- Koning-Ward, T. F. de; Robins-Browne, R. M. (1995): Contribution of urease to acid tolerance in Yersinia enterocolitica. In *Infection and immunity* 63 (10), pp. 3790–3795.
- Koonin, Eugene V.; Makarova, Kira S.; Zhang, Feng (2017): Diversity, classification and evolution of CRISPR-Cas systems. In *Current opinion in microbiology* 37, pp. 67–78. DOI: 10.1016/j.mib.2017.05.008.
- Kopp, Petra; Lammers, Reiner; Aepfelbacher, Martin; Woehlke, Günther; Rudel, Thomas; Machuy, Nikolaus et al. (2006): The kinesin KIF1C and microtubule plus ends regulate podosome dynamics in macrophages. In *Molecular biology of the cell* 17 (6), pp. 2811–2823. DOI: 10.1091/mbc.e05-11-1010.
- Koraïchi, Faten; Gence, Rémi; Bouchenot, Catherine; Grosjean, Sarah; Lajoie-Mazenc, Isabelle; Favre, Gilles; Cabantous, Stéphanie (2018): High-content tripartite split-GFP cell-based assays to screen for modulators of small GTPase activation. In *Journal of cell science* 131 (1). DOI: 10.1242/jcs.210419.
- Koster, M.; Bitter, W.; Cock, H. de; Allaoui, A.; Cornelis, G. R.; Tommassen, J. (1997): The outer membrane component, YscC, of the Yop secretion machinery of Yersinia enterocolitica forms a ring-shaped multimeric complex. In *Molecular microbiology* 26 (4), pp. 789–797. DOI: 10.1046/j.1365-2958.1997.6141981.x.
- Krall, Rebecca; Zhang, Yue; Barbieri, Joseph T. (2004): Intracellular membrane localization of pseudomonas ExoS and Yersinia YopE in mammalian cells. In *The Journal of biological chemistry* 279 (4), pp. 2747–2753. DOI: 10.1074/jbc.M301963200.
- Kubori, T.; Matsushima, Y.; Nakamura, D.; Uralil, J.; Lara-Tejero, M.; Sukhan, A. et al. (1998): Supramolecular structure of the Salmonella typhimurium type III protein secretion system. In *Science* 280 (5363), pp. 602–605. DOI: 10.1126/science.280.5363.602.
- Kubori, T.; Sukhan, A.; Aizawa, S. I.; Galán, J. E. (2000): Molecular characterization and assembly of the needle complex of the Salmonella typhimurium type III protein secretion system. In *Proceedings of the National Academy of Sciences of the United States of America* 97 (18), pp. 10225–10230. DOI: 10.1073/pnas.170128997.
- Kubori, Tomoko; Galán, Jorge E. (2003): Temporal regulation of salmonella virulence effector function by proteasome-dependent protein degradation. In *Cell* 115 (3), pp. 333–342. DOI: 10.1016/s0092-8674(03)00849-3.
- Külzer, Simone; Petersen, Wiebke; Baser, Avni; Mandel, Katharina; Przyborski, Jude M. (2013): Use of self-assembling GFP to determine protein topology and compartmentalisation in the Plasmodium

- falciparum-infected erythrocyte. In *Molecular and biochemical parasitology* 187 (2), pp. 87–90. DOI: 10.1016/j.molbiopara.2012.11.004.
- Laemmli, U. K. (1970): Cleavage of structural proteins during the assembly of the head of bacteriophage T4. In *Nature* 227 (5259), pp. 680–685. DOI: 10.1038/227680a0.
- Landgraf, Dirk; Okumus, Burak; Chien, Peter; Baker, Tania A.; Paulsson, Johan (2012): Segregation of molecules at cell division reveals native protein localization. In *Nature methods* 9 (5), pp. 480–482. DOI: 10.1038/nmeth.1955.
- Lara-Tejero, María; Kato, Junya; Wagner, Samuel; Liu, Xiaoyun; Galán, Jorge E. (2011): A sorting platform determines the order of protein secretion in bacterial type III systems. In *Science* 331 (6021), pp. 1188–1191. DOI: 10.1126/science.1201476.
- LaRock, Christopher N.; Cookson, Brad T. (2012): The Yersinia virulence effector YopM binds caspase-1 to arrest inflammasome assembly and processing. In *Cell host & microbe* 12 (6), pp. 799–805. DOI: 10.1016/j.chom.2012.10.020.
- LaRock, Doris L.; Chaudhary, Anu; Miller, Samuel I. (2015): Salmonellae interactions with host processes. In *Nature reviews. Microbiology* 13 (4), pp. 191–205. DOI: 10.1038/nrmicro3420.
- Larson, Matthew H.; Gilbert, Luke A.; Wang, Xiaowo; Lim, Wendell A.; Weissman, Jonathan S.; Qi, Lei S. (2013): CRISPR interference (CRISPRi) for sequence-specific control of gene expression. In *Nature protocols* 8 (11), pp. 2180–2196. DOI: 10.1038/nprot.2013.132.
- Lavander, Moa; Sundberg, Lena; Edqvist, Petra J.; Lloyd, Scott A.; Wolf-Watz, Hans; Forsberg, Ake (2003): Characterisation of the type III secretion protein YscU in Yersinia pseudotuberculosis. YscU cleavage--dispensable for TTSS but essential for survival. In *Advances in experimental medicine and biology* 529, pp. 109–112. DOI: 10.1007/0-306-48416-1_20.
- Lee, Hye-Young; Lee, So Eui; Woo, Jongchan; Choi, Doil; Park, Eunsook (2018): Split Green Fluorescent Protein System to Visualize Effectors Delivered from Bacteria During Infection. In *Journal of visualized experiments : JoVE* (135). DOI: 10.3791/57719.
- Lee, V. T.; Anderson, D. M.; Schneewind, O. (1998): Targeting of Yersinia Yop proteins into the cytosol of HeLa cells: one-step translocation of YopE across bacterial and eukaryotic membranes is dependent on SycE chaperone. In *Molecular microbiology* 28 (3), pp. 593–601. DOI: 10.1046/j.1365-2958.1998.00822.x.
- Lee, V. T.; Schneewind, O. (1999): Type III machines of pathogenic yersiniae secrete virulence factors into the extracellular milieu. In *Molecular microbiology* 31 (6), pp. 1619–1629. DOI: 10.1046/j.1365-2958.1999.01270.x.
- Lee, Wei Lin; Grimes, Jonathan M.; Robinson, Robert C. (2015): Yersinia effector YopO uses actin as bait to phosphorylate proteins that regulate actin polymerization. In *Nature structural & molecular biology* 22 (3), pp. 248–255. DOI: 10.1038/nsmb.2964.
- Leung, K. Y.; Reisner, B. S.; Straley, S. C. (1990): YopM inhibits platelet aggregation and is necessary for virulence of Yersinia pestis in mice. In *Infection and immunity* 58 (10), pp. 3262–3271.

- Lewis, Jennifer D.; Lee, Amy; Ma, Wenbo; Zhou, Huanbin; Guttman, David S.; Desveaux, Darrell (2011): The YopJ superfamily in plant-associated bacteria. In *Molecular plant pathology* 12 (9), pp. 928–937. DOI: 10.1111/j.1364-3703.2011.00719.x.
- Li, Bin; Zhao, Weiyu; Luo, Xiao; Zhang, Xinfu; Li, Chenglong; Zeng, Chunxi; Dong, Yizhou (2017): Engineering CRISPR-Cpf1 crRNAs and mRNAs to maximize genome editing efficiency. In *Nature biomedical engineering* 1 (5). DOI: 10.1038/s41551-017-0066.
- Li, Kai; Wang, Gang; Andersen, Troels; Zhou, Pingzhu; Pu, William T. (2014a): Optimization of genome engineering approaches with the CRISPR/Cas9 system. In *PloS one* 9 (8), e105779. DOI: 10.1371/journal.pone.0105779.
- Li, Xiaoyang; Yang, Qinghua; Tu, Haitao; Lim, Zijie; Pan, Shen Q. (2014b): Direct visualization of Agrobacterium-delivered VirE2 in recipient cells. In *The Plant journal : for cell and molecular biology* 77 (3), pp. 487–495. DOI: 10.1111/tpj.12397.
- Li, Yifan; Lin, Zhenquan; Huang, Can; Zhang, Yan; Wang, Zhiwen; Tang, Ya-Jie et al. (2015): Metabolic engineering of Escherichia coli using CRISPR-Cas9 mediated genome editing. In *Metabolic engineering* 31, pp. 13–21. DOI: 10.1016/j.ymben.2015.06.006.
- Liang, Liya; Liu, Rongming; Garst, Andrew D.; Lee, Thomas; Nogué, Violeta Sánchez I.; Beckham, Gregg T.; Gill, Ryan T. (2017): CRISPR Enabled Trackable genome Engineering for isopropanol production in Escherichia coli. In *Metabolic engineering* 41, pp. 1–10. DOI: 10.1016/j.ymben.2017.02.009.
- Ling, Kun; Doughman, Renee L.; Firestone, Ari J.; Bunce, Matthew W.; Anderson, Richard A. (2002): Type I gamma phosphatidylinositol phosphate kinase targets and regulates focal adhesions. In *Nature* 420 (6911), pp. 89–93. DOI: 10.1038/nature01082.
- Liss, Viktoria; Barlag, Britta; Nietschke, Monika; Hensel, Michael (2015): Self-labelling enzymes as universal tags for fluorescence microscopy, super-resolution microscopy and electron microscopy. In *Scientific reports* 5, p. 17740. DOI: 10.1038/srep17740.
- Liu, Fu-Tong; Rabinovich, Gabriel A. (2005): Galectins as modulators of tumour progression. In *Nature reviews. Cancer* 5 (1), pp. 29–41. DOI: 10.1038/nrc1527.
- Liu, Fu-Tong; Yang, Ri-Yao; Hsu, Daniel K. (2012): Galectins in acute and chronic inflammation. In *Annals of the New York Academy of Sciences* 1253, pp. 80–91. DOI: 10.1111/j.1749-6632.2011.06386.x.
- Lloyd, S. A.; Norman, M.; Rosqvist, R.; Wolf-Watz, H. (2001): Yersinia YopE is targeted for type III secretion by N-terminal, not mRNA, signals. In *Molecular microbiology* 39 (2), pp. 520–531. DOI: 10.1046/j.1365-2958.2001.02271.x.
- Los, G. V.; Darzins, A.; Karassina, N.; Zimprich, C., Learish, R.; McDougall, M. G.; Encell, L. P. et al. (2005): HaloTag interchangeable labeling technology for cell imaging, protein capture and immobilization. In *Promega Cell Notes* (11), pp. 2–6.
- Lundqvist, Magnus; Thalén, Niklas; Volk, Anna-Luisa; Hansen, Henning Gram; Otter, Eric von; Nygren, Per-Åke et al. (2019): Chromophore pre-maturation for improved speed and sensitivity of split-GFP monitoring of protein secretion. In *Scientific reports* 9 (1), p. 310. DOI: 10.1038/s41598-018-36559-x.

- Lunelli, Michele; Lokareddy, Ravi Kumar; Zychlinsky, Arturo; Kolbe, Michael (2009): IpaB-IpgC interaction defines binding motif for type III secretion translocator. In *Proceedings of the National Academy of Sciences of the United States of America* 106 (24), pp. 9661–9666. DOI: 10.1073/pnas.0812900106.
- Luqmani, R. A.; Dawes, P. T. (1986): Yersinia arthritis with erythema nodosum. In *Postgraduate Medical Journal* 62 (727), p. 405.
- Ma, Ka-Wai; Ma, Wenbo (2016): YopJ Family Effectors Promote Bacterial Infection through a Unique Acetyltransferase Activity. In *Microbiology and molecular biology reviews : MMBR* 80 (4), pp. 1011–1027. DOI: 10.1128/MMBR.00032-16.
- Ma, L.; Cantley, L. C.; Janmey, P. A.; Kirschner, M. W. (1998): Corequirement of specific phosphoinositides and small GTP-binding protein Cdc42 in inducing actin assembly in Xenopus egg extracts. In *The Journal of cell biology* 140 (5), pp. 1125–1136. DOI: 10.1083/jcb.140.5.1125.
- Ma, Wenbo; Dong, Frederick F. T.; Stavrinides, John; Guttman, David S. (2006): Type III effector diversification via both pathoadaptation and horizontal transfer in response to a coevolutionary arms race. In *PLoS genetics* 2 (12), e209. DOI: 10.1371/journal.pgen.0020209.
- Madigan, Michael T.; Martinko, John M. (Eds.) (2009): Brock Mikrobiologie. With assistance of Michael T. Madigan, John M. Martinko, Thomas D. Brock, Thomas Lazar, Michael Thomm. Pearson Studium. München [u.a.].
- Maejima, Ikuko; Takahashi, Atsushi; Omori, Hiroko; Kimura, Tomonori; Takabatake, Yoshitsugu; Saitoh, Tatsuya et al. (2013): Autophagy sequesters damaged lysosomes to control lysosomal biogenesis and kidney injury. In *The EMBO journal* 32 (17), pp. 2336–2347. DOI: 10.1038/emboj.2013.171.
- Malaga, Wladimir; Perez, Esther; Guilhot, Christophe (2003): Production of unmarked mutations in mycobacteria using site-specific recombination. In *FEMS microbiology letters* 219 (2), pp. 261–268. DOI: 10.1016/S0378-1097(03)00003-X.
- Mansilla Pareja, María E.; Bongiovanni, Antonino; Lafont, Frank; Colombo, María I. (2017): Alterations of the Coxiella burnetii Replicative Vacuole Membrane Integrity and Interplay with the Autophagy Pathway. In *Frontiers in cellular and infection microbiology* 7, p. 112. DOI: 10.3389/fcimb.2017.00112.
- Marketon, Melanie M.; DePaolo, R. William; DeBord, Kristin L.; Jabri, Bana; Schneewind, Olaf (2005): Plague bacteria target immune cells during infection. In *Science* 309 (5741), pp. 1739–1741. DOI: 10.1126/science.1114580.
- Marlovits, Thomas C.; Kubori, Tomoko; Lara-Tejero, María; Thomas, Dennis; Unger, Vinzenz M.; Galán, Jorge E. (2006): Assembly of the inner rod determines needle length in the type III secretion injectisome. In *Nature* 441 (7093), pp. 637–640. DOI: 10.1038/nature04822.
- Marlovits, Thomas C.; Kubori, Tomoko; Sukhan, Anand; Thomas, Dennis R.; Galán, Jorge E.; Unger, Vinzenz M. (2004): Structural insights into the assembly of the type III secretion needle complex. In *Science* 306 (5698), pp. 1040–1042. DOI: 10.1126/science.1102610.
- Marshall, J. G.; Booth, J. W.; Stambolic, V.; Mak, T.; Balla, T.; Schreiber, A. D. et al. (2001): Restricted accumulation of phosphatidylinositol 3-kinase products in a plasmalemmal subdomain during Fc gamma

- receptor-mediated phagocytosis. In *The Journal of cell biology* 153 (7), pp. 1369–1380. DOI: 10.1083/jcb.153.7.1369.
- Matteï, Pierre-Jean; Faudry, Eric; Job, Viviana; Izoré, Thierry; Attree, Ina; Dessen, Andréa (2011): Membrane targeting and pore formation by the type III secretion system translocon. In *The FEBS journal* 278 (3), pp. 414–426. DOI: 10.1111/j.1742-4658.2010.07974.x.
- McDonald, Christine; Vacratsis, Panayiotis O.; Bliska, James B.; Dixon, Jack E. (2003): The yersinia virulence factor YopM forms a novel protein complex with two cellular kinases. In *The Journal of biological chemistry* 278 (20), pp. 18514–18523. DOI: 10.1074/jbc.M301226200.
- McGhie, Emma J.; Hume, Peter J.; Hayward, Richard D.; Torres, Jaume; Koronakis, Vassilis (2002): Topology of the Salmonella invasion protein SipB in a model bilayer. In *Molecular microbiology* 44 (5), pp. 1309–1321. DOI: 10.1046/j.1365-2958.2002.02958.x.
- McIntosh, Anne; Meikle, Lynsey M.; Ormsby, Michael J.; McCormick, Beth A.; Christie, John M.; Brewer, James M. et al. (2017): SipA Activation of Caspase-3 Is a Decisive Mediator of Host Cell Survival at Early Stages of Salmonella enterica Serovar Typhimurium Infection. In *Infection and immunity* 85 (9). DOI: 10.1128/IAI.00393-17.
- McNally, Alan; Thomson, Nicholas R.; Reuter, Sandra; Wren, Brendan W. (2016): 'Add, stir and reduce': Yersinia spp. as model bacteria for pathogen evolution. In *Nature reviews. Microbiology* 14 (3), pp. 177–190. DOI: 10.1038/nrmicro.2015.29.
- McPhee, Joseph B.; Mena, Patricio; Bliska, James B. (2010): Delineation of regions of the Yersinia YopM protein required for interaction with the RSK1 and PRK2 host kinases and their requirement for interleukin-10 production and virulence. In *Infection and immunity* 78 (8), pp. 3529–3539. DOI: 10.1128/IAI.00269-10.
- Mejía, Edison; Bliska, James B.; Viboud, Gloria I. (2008): Yersinia controls type III effector delivery into host cells by modulating Rho activity. In *PLoS Pathogens* 4 (1), e3. DOI: 10.1371/journal.ppat.0040003.
- Mey, A.; Leffler, H.; Hmama, Z.; Normier, G.; Revillard, J. P. (1996): The animal lectin galectin-3 interacts with bacterial lipopolysaccharides via two independent sites. In *Journal of immunology (Baltimore, Md. : 1950)* 156 (4), pp. 1572–1577.
- Michiels, T.; Cornelis, G. R. (1991): Secretion of hybrid proteins by the Yersinia Yop export system. In *Journal of bacteriology* 173 (5), pp. 1677–1685. DOI: 10.1128/jb.173.5.1677-1685.1991.
- Michiels, T.; Wattiau, P.; Brasseur, R.; Ruyschaert, J. M.; Cornelis, G. (1990): Secretion of Yop proteins by Yersiniae. In *Infection and immunity* 58 (9), pp. 2840–2849.
- Mikhaylova, Marina; Cloin, Bas M. C.; Finan, Kieran; van den Berg, Robert; Teeuw, Jalmar; Kijanka, Marta M. et al. (2015): Resolving bundled microtubules using anti-tubulin nanobodies. In *Nature communications* 6, p. 7933. DOI: 10.1038/ncomms8933.
- Miletic, Sean; Goessweiner-Mohr, Nikolaus; Marlovits, Thomas C. (2019): The Structure of the Type III Secretion System Needle Complex. In *Current topics in microbiology and immunology*. DOI: 10.1007/82_2019_178.

- Miller, V. L.; Bliska, J. B.; Falkow, S. (1990): Nucleotide sequence of the *Yersinia enterocolitica* ail gene and characterization of the Ail protein product. In *Journal of bacteriology* 172 (2), pp. 1062–1069. DOI: 10.1128/jb.172.2.1062-1069.1990.
- Miller, V. L.; Falkow, S. (1988): Evidence for two genetic loci in *Yersinia enterocolitica* that can promote invasion of epithelial cells. In *Infection and immunity* 56 (5), pp. 1242–1248.
- Milne-Davies, Bailey; Helbig, Carlos; Wimmi, Stephan; Cheng, Dorothy W. C.; Paczia, Nicole; Diepold, Andreas (2019): Life After Secretion-*Yersinia enterocolitica* Rapidly Toggles Effector Secretion and Can Resume Cell Division in Response to Changing External Conditions. In *Frontiers in microbiology* 10, p. 2128. DOI: 10.3389/fmicb.2019.02128.
- Minamino, T.; MacNab, R. M. (2000): FliH, a soluble component of the type III flagellar export apparatus of *Salmonella*, forms a complex with FliI and inhibits its ATPase activity. In *Molecular microbiology* 37 (6), pp. 1494–1503. DOI: 10.1046/j.1365-2958.2000.02106.x.
- Mitsunobu, Hitoshi; Teramoto, Jun; Nishida, Keiji; Kondo, Akihiko (2017): Beyond Native Cas9: Manipulating Genomic Information and Function. In *Trends in biotechnology* 35 (10), pp. 983–996. DOI: 10.1016/j.tibtech.2017.06.004.
- Mittal, Rohit; Peak-Chew, Sew-Yeu; McMahon, Harvey T. (2006): Acetylation of MEK2 and I kappa B kinase (IKK) activation loop residues by YopJ inhibits signaling. In *Proceedings of the National Academy of Sciences of the United States of America* 103 (49), pp. 18574–18579. DOI: 10.1073/pnas.0608995103.
- Mojica, F. J. M.; Díez-Villaseñor, C.; García-Martínez, J.; Almendros, C. (2009): Short motif sequences determine the targets of the prokaryotic CRISPR defence system. In *Microbiology (Reading, England)* 155 (Pt 3), pp. 733–740. DOI: 10.1099/mic.0.023960-0.
- Mojica, Francisco J. M.; Díez-Villaseñor, César; García-Martínez, Jesús; Soria, Elena (2005): Intervening sequences of regularly spaced prokaryotic repeats derive from foreign genetic elements. In *Journal of molecular evolution* 60 (2), pp. 174–182. DOI: 10.1007/s00239-004-0046-3.
- Mota, Luís Jaime; Sorg, Isabel; Cornelis, Guy R. (2005): Type III secretion: the bacteria-eukaryotic cell express. In *FEMS microbiology letters* 252 (1), pp. 1–10. DOI: 10.1016/j.femsle.2005.08.036.
- Mounier, J.; Bahrani, F. K.; Sansonetti, P. J. (1997): Secretion of *Shigella flexneri* Ipa invasins on contact with epithelial cells and subsequent entry of the bacterium into cells are growth stage dependent. In *Infection and immunity* 65 (2), pp. 774–782.
- Mueller, C. A.; Broz, P.; Cornelis, G. R. (2008): The type III secretion system tip complex and translocon. In *Molecular microbiology* 68 (5), pp. 1085–1095. DOI: 10.1111/j.1365-2958.2008.06237.x.
- Mueller, Catherine A.; Broz, Petr; Müller, Shirley A.; Ringler, Philippe; Erne-Brand, Françoise; Sorg, Isabel et al. (2005): The V-antigen of *Yersinia* forms a distinct structure at the tip of injectisome needles. In *Science* 310 (5748), pp. 674–676. DOI: 10.1126/science.1118476.
- Mühlenkamp, Melanie; Oberhettinger, Philipp; Leo, Jack C.; Linke, Dirk; Schütz, Monika S. (2015): *Yersinia* adhesin A (YadA)--beauty & beast. In *International journal of medical microbiology : IJMM* 305 (2), pp. 252–258. DOI: 10.1016/j.ijmm.2014.12.008.

- Mukherjee, Sohini; Keitany, Gladys; Li, Yan; Wang, Yong; Ball, Haydn L.; Goldsmith, Elizabeth J.; Orth, Kim (2006): Yersinia YopJ acetylates and inhibits kinase activation by blocking phosphorylation. In *Science* 312 (5777), pp. 1211–1214. DOI: 10.1126/science.1126867.
- Muyldermans, Serge (2013): Nanobodies: natural single-domain antibodies. In *Annual review of biochemistry* 82, pp. 775–797. DOI: 10.1146/annurev-biochem-063011-092449.
- Nans, Andrea; Kudryashev, Mikhail; Saibil, Helen R.; Hayward, Richard D. (2015): Structure of a bacterial type III secretion system in contact with a host membrane in situ. In *Nature communications* 6, p. 10114. DOI: 10.1038/ncomms10114.
- Nauth, Theresa; Huschka, Franziska; Schweizer, Michaela; Bosse, Jens B.; Diepold, Andreas; Failla, Antonio Virgilio et al. (2018): Visualization of translocons in Yersinia type III protein secretion machines during host cell infection. In *PLoS Pathogens* 14 (12), e1007527. DOI: 10.1371/journal.ppat.1007527.
- Neyt, C.; Cornelis, G. R. (1999): Role of SycD, the chaperone of the Yersinia Yop translocators YopB and YopD. In *Molecular microbiology* 31 (1), pp. 143–156. DOI: 10.1046/j.1365-2958.1999.01154.x.
- Niebuhr, Kirsten; Giuriato, Sylvie; Pedron, Thierry; Philpott, Dana J.; Gaits, Frédérique; Sable, Julia et al. (2002): Conversion of PtdIns(4,5)P₂ into PtdIns(5)P by the *S. flexneri* effector IpgD reorganizes host cell morphology. In *The EMBO journal* 21 (19), pp. 5069–5078. DOI: 10.1093/emboj/cdf522.
- Nieminen, Julie; St-Pierre, Christian; Bhaumik, Pampa; Poirier, Françoise; Sato, Sachiko (2008): Role of galectin-3 in leukocyte recruitment in a murine model of lung infection by *Streptococcus pneumoniae*. In *Journal of immunology (Baltimore, Md. : 1950)* 180 (4), pp. 2466–2473. DOI: 10.4049/jimmunol.180.4.2466.
- Nordfelth, R.; Wolf-Watz, H. (2001): YopB of *Yersinia enterocolitica* is essential for YopE translocation. In *Infection and immunity* 69 (5), pp. 3516–3518. DOI: 10.1128/IAI.69.5.3516-3518.2001.
- Norris, F. A.; Wilson, M. P.; Wallis, T. S.; Galyov, E. E.; Majerus, P. W. (1998): SopB, a protein required for virulence of *Salmonella dublin*, is an inositol phosphate phosphatase. In *Proceedings of the National Academy of Sciences of the United States of America* 95 (24), pp. 14057–14059. DOI: 10.1073/pnas.95.24.14057.
- O'Boyle, Nicky; Connolly, James P. R.; Roe, Andrew J. (2018): Tracking elusive cargo: Illuminating spatio-temporal Type 3 effector protein dynamics using reporters. In *Cellular microbiology* 20 (1). DOI: 10.1111/cmi.12797.
- Odorizzi, G.; Babst, M.; Emr, S. D. (2000): Phosphoinositide signaling and the regulation of membrane trafficking in yeast. In *Trends in biochemical sciences* 25 (5), pp. 229–235. DOI: 10.1016/s0968-0004(00)01543-7.
- Oellerich, Mark F.; Jacobi, Christoph A.; Freund, Sandra; Niedung, Katy; Bach, Alexandra; Heesemann, Jürgen; Trülsch, Konrad (2007): *Yersinia enterocolitica* infection of mice reveals clonal invasion and abscess formation. In *Infection and immunity* 75 (8), pp. 3802–3811. DOI: 10.1128/IAI.00419-07.
- Oh, Jee-Hwan; van Pijkeren, Jan-Peter (2014): CRISPR-Cas9-assisted recombineering in *Lactobacillus reuteri*. In *Nucleic acids research* 42 (17), e131. DOI: 10.1093/nar/gku623.

- Olsson, Jan; Edqvist, Petra J.; Bröms, Jeanette E.; Forsberg, Ake; Wolf-Watz, Hans; Francis, Matthew S. (2004): The YopD translocator of *Yersinia pseudotuberculosis* is a multifunctional protein comprised of discrete domains. In *Journal of bacteriology* 186 (13), pp. 4110–4123. DOI: 10.1128/JB.186.13.4110-4123.2004.
- Orth, K.; Xu, Z.; Mudgett, M. B.; Bao, Z. Q.; Palmer, L. E.; Bliska, J. B. et al. (2000): Disruption of signaling by *Yersinia* effector YopJ, a ubiquitin-like protein protease. In *Science* 290 (5496), pp. 1594–1597. DOI: 10.1126/science.290.5496.1594.
- Pai, C. H.; Mors, V. (1978): Production of enterotoxin by *Yersinia enterocolitica*. In *Infection and immunity* 19 (3), pp. 908–911.
- Pallen, M. J.; Dougan, G.; Frankel, G. (1997): Coiled-coil domains in proteins secreted by type III secretion systems. In *Molecular microbiology* 25 (2), pp. 423–425. DOI: 10.1046/j.1365-2958.1997.4901850.x.
- Palmer, L. E.; Hobbie, S.; Galán, J. E.; Bliska, J. B. (1998): YopJ of *Yersinia pseudotuberculosis* is required for the inhibition of macrophage TNF- α production and downregulation of the MAP kinases p38 and JNK. In *Molecular microbiology* 27 (5), pp. 953–965. DOI: 10.1046/j.1365-2958.1998.00740.x.
- Paquette, Nicholas; Conlon, Joseph; Sweet, Charles; Rus, Florentina; Wilson, Lindsay; Pereira, Andrea et al. (2012): Serine/threonine acetylation of TGF β -activated kinase (TAK1) by *Yersinia pestis* YopJ inhibits innate immune signaling. In *Proceedings of the National Academy of Sciences of the United States of America* 109 (31), pp. 12710–12715. DOI: 10.1073/pnas.1008203109.
- Park, Eunsook; Lee, Hye-Young; Woo, Jongchan; Choi, Doil; Dinesh-Kumar, Savithamma P. (2017): Spatiotemporal Monitoring of *Pseudomonas syringae* Effectors via Type III Secretion Using Split Fluorescent Protein Fragments. In *The Plant cell* 29 (7), pp. 1571–1584. DOI: 10.1105/tpc.17.00047.
- Patel, Samir; Wall, Daniel M.; Castillo, Antonio; McCormick, Beth A. (2019): Caspase-3 cleavage of *Salmonella* type III secreted effector protein SifA is required for localization of functional domains and bacterial dissemination. In *Gut microbes* 10 (2), pp. 172–187. DOI: 10.1080/19490976.2018.1506668.
- Pavlidis, Dimitrios E.; Filter, Matthias; Buschulte, Anja (2019): Application of data science in risk assessment and early warning. In *EFSA* 17, p. 4835. DOI: 10.2903/j.efsa.2019.e170908.
- Pawel-Rammingen, U. von; Telepnev, M. V.; Schmidt, G.; Aktories, K.; Wolf-Watz, H.; Rosqvist, R. (2000): GAP activity of the *Yersinia* YopE cytotoxin specifically targets the Rho pathway: a mechanism for disruption of actin microfilament structure. In *Molecular microbiology* 36 (3), pp. 737–748. DOI: 10.1046/j.1365-2958.2000.01898.x.
- Paz, Irit; Sachse, Martin; Dupont, Nicolas; Mounier, Joelle; Cederfur, Cecilia; Enninga, Jost et al. (2010): Galectin-3, a marker for vacuole lysis by invasive pathogens. In *Cellular microbiology* 12 (4), pp. 530–544. DOI: 10.1111/j.1462-5822.2009.01415.x.
- Pedelacq, Jean-Denis; Cabantous, Stéphanie (2019): Development and Applications of Superfolder and Split Fluorescent Protein Detection Systems in Biology. In *International journal of molecular sciences* 20 (14). DOI: 10.3390/ijms20143479.

- Pédelacq, Jean-Denis; Cabantous, Stéphanie; Tran, Timothy; Terwilliger, Thomas C.; Waldo, Geoffrey S. (2006): Engineering and characterization of a superfolder green fluorescent protein. In *Nature biotechnology* 24 (1), pp. 79–88. DOI: 10.1038/nbt1172.
- Penna, Thereza Christina Vessoni; Ishii, Marina; Junior, Adalberto Pessoa; Cholewa, Olivia (2004): Thermal stability of recombinant green fluorescent protein (GFPuv) at various pH values. In *Applied biochemistry and biotechnology* 113-116, pp. 469–483. DOI: 10.1385/abab:114:1-3:469.
- Pepe, J. C.; Miller, V. L. (1993): Yersinia enterocolitica invasin: a primary role in the initiation of infection. In *Proceedings of the National Academy of Sciences of the United States of America* 90 (14), pp. 6473–6477. DOI: 10.1073/pnas.90.14.6473.
- Pepe, J. C.; Wachtel, M. R.; Wagar, E.; Miller, V. L. (1995): Pathogenesis of defined invasion mutants of Yersinia enterocolitica in a BALB/c mouse model of infection. In *Infection and immunity* 63 (12), pp. 4837–4848.
- Perkovic, Mario; Kunz, Michael; Endesfelder, Ulrike; Bunse, Stefanie; Wigge, Christoph; Yu, Zhou et al. (2014): Correlative light- and electron microscopy with chemical tags. In *Journal of structural biology* 186 (2), pp. 205–213. DOI: 10.1016/j.jsb.2014.03.018.
- Persson, C.; Carballeira, N.; Wolf-Watz, H.; Fällman, M. (1997): The PTPase YopH inhibits uptake of Yersinia, tyrosine phosphorylation of p130Cas and FAK, and the associated accumulation of these proteins in peripheral focal adhesions. In *The EMBO journal* 16 (9), pp. 2307–2318. DOI: 10.1093/emboj/16.9.2307.
- Persson, C.; Nordfelth, R.; Andersson, K.; Forsberg, A.; Wolf-Watz, H.; Fällman, M. (1999): Localization of the Yersinia PTPase to focal complexes is an important virulence mechanism. In *Molecular microbiology* 33 (4), pp. 828–838. DOI: 10.1046/j.1365-2958.1999.01529.x.
- Peterson, Scott N.; Kwon, Keehwan (2012): The HaloTag: Improving Soluble Expression and Applications in Protein Functional Analysis. In *Current chemical genomics* 6, pp. 8–17. DOI: 10.2174/1875397301206010008.
- Pettersson, J.; Holmström, A.; Hill, J.; Leary, S.; Frithz-Lindsten, E.; Euler-Matell, A. von et al. (1999): The V-antigen of Yersinia is surface exposed before target cell contact and involved in virulence protein translocation. In *Molecular microbiology* 32 (5), pp. 961–976. DOI: 10.1046/j.1365-2958.1999.01408.x.
- Petukhov, Michael; Tatsu, Yoshiro; Tamaki, Kazuyo; Murase, Sachiko; Uekawa, Hiroko; Yoshikawa, Susumu et al. (2009): Design of stable alpha-helices using global sequence optimization. In *Journal of peptide science : an official publication of the European Peptide Society* 15 (5), pp. 359–365. DOI: 10.1002/psc.1122.
- Pha, Khavong; Navarro, Lorena (2016): Yersinia type III effectors perturb host innate immune responses. In *World journal of biological chemistry* 7 (1), pp. 1–13. DOI: 10.4331/wjbc.v7.i1.1.
- Phan, Jason; Lee, Kyeong; Cherry, Scott; Tropea, Joseph E.; Burke, Terrence R.; Waugh, David S. (2003): High-resolution structure of the Yersinia pestis protein tyrosine phosphatase YopH in complex with a phosphotyrosyl mimetic-containing hexapeptide. In *Biochemistry* 42 (45), pp. 13113–13121. DOI: 10.1021/bi030156m.

- Pierson, D. E.; Falkow, S. (1993): The ail gene of *Yersinia enterocolitica* has a role in the ability of the organism to survive serum killing. In *Infection and immunity* 61 (5), pp. 1846–1852.
- Pitman, Derek J.; Banerjee, Shounak; Macari, Stephen J.; Castaldi, Christopher A.; Crone, Donna E.; Bystroff, Christopher (2015): Exploring the folding pathway of green fluorescent protein through disulfide engineering. In *Protein science : a publication of the Protein Society* 24 (3), pp. 341–353. DOI: 10.1002/pro.2621.
- Plagens, André; Richter, Hagen; Charpentier, Emmanuelle; Randau, Lennart (2015): DNA and RNA interference mechanisms by CRISPR-Cas surveillance complexes. In *FEMS microbiology reviews* 39 (3), pp. 442–463. DOI: 10.1093/femsre/fuv019.
- Pollard, Thomas D.; Borisy, Gary G. (2003): Cellular motility driven by assembly and disassembly of actin filaments. In *Cell* 112 (4), pp. 453–465. DOI: 10.1016/s0092-8674(03)00120-x.
- Porath, J.; Carlsson, J.; Olsson, I.; Belfrage, G. (1975): Metal chelate affinity chromatography, a new approach to protein fractionation. In *Nature* 258 (5536), pp. 598–599. DOI: 10.1038/258598a0.
- Pourcel, C.; Salvignol, G.; Vergnaud, G. (2005): CRISPR elements in *Yersinia pestis* acquire new repeats by preferential uptake of bacteriophage DNA, and provide additional tools for evolutionary studies. In *Microbiology (Reading, England)* 151 (Pt 3), pp. 653–663. DOI: 10.1099/mic.0.27437-0.
- Poyraz, Omer; Schmidt, Holger; Seidel, Karsten; Delissen, Friedmar; Ader, Christian; Tenenboim, Hezi et al. (2010): Protein refolding is required for assembly of the type three secretion needle. In *Nature structural & molecular biology* 17 (7), pp. 788–792. DOI: 10.1038/nsmb.1822.
- Prasher, D. C.; Eckenrode, V. K.; Ward, W. W.; Prendergast, F. G.; Cormier, M. J. (1992): Primary structure of the *Aequorea victoria* green-fluorescent protein. In *Gene* 111 (2), pp. 229–233. DOI: 10.1016/0378-1119(92)90691-h.
- Prehna, Gerd; Ivanov, Maya I.; Bliska, James B.; Stebbins, C. Erec (2006): *Yersinia* virulence depends on mimicry of host Rho-family nucleotide dissociation inhibitors. In *Cell* 126 (5), pp. 869–880. DOI: 10.1016/j.cell.2006.06.056.
- Prentice, M. B.; James, K. D.; Parkhill, J.; Baker, S. G.; Stevens, K.; Simmonds, M. N. et al. (2001): *Yersinia pestis* pFra shows biovar-specific differences and recent common ancestry with a *Salmonella enterica* serovar Typhi plasmid. In *Journal of bacteriology* 183 (8), pp. 2586–2594. DOI: 10.1128/JB.183.8.2586-2594.2001.
- Pujol, Céline; Bliska, James B. (2005): Turning *Yersinia* pathogenesis outside in: subversion of macrophage function by intracellular yersiniae. In *Clinical immunology (Orlando, Fla.)* 114 (3), pp. 216–226. DOI: 10.1016/j.clim.2004.07.013.
- Puylaert, J. B. (1986): Mesenteric adenitis and acute terminal ileitis: US evaluation using graded compression. In *Radiology* 161 (3), pp. 691–695. DOI: 10.1148/radiology.161.3.3538138.
- Pyne, Michael E.; Moo-Young, Murray; Chung, Duane A.; Chou, C. Perry (2015): Coupling the CRISPR/Cas9 System with Lambda Red Recombineering Enables Simplified Chromosomal Gene Replacement in *Escherichia coli*. In *Applied and environmental microbiology* 81 (15), pp. 5103–5114. DOI: 10.1128/AEM.01248-15.

Qi, Lei S.; Larson, Matthew H.; Gilbert, Luke A.; Doudna, Jennifer A.; Weissman, Jonathan S.; Arkin, Adam P.; Lim, Wendell A. (2013): Repurposing CRISPR as an RNA-guided platform for sequence-specific control of gene expression. In *Cell* 152 (5), pp. 1173–1183. DOI: 10.1016/j.cell.2013.02.022.

Quan, Jiayuan; Tian, Jingdong (2011): Circular polymerase extension cloning for high-throughput cloning of complex and combinatorial DNA libraries. In *Nature protocols* 6 (2), pp. 242–251. DOI: 10.1038/nprot.2010.181.

Rabinovich, Gabriel A.; Toscano, Marta A. (2009): Turning 'sweet' on immunity: galectin-glycan interactions in immune tolerance and inflammation. In *Nature reviews. Immunology* 9 (5), pp. 338–352. DOI: 10.1038/nri2536.

Radics, Julia; Königsmaier, Lisa; Marlovits, Thomas C. (2014): Structure of a pathogenic type 3 secretion system in action. In *Nature structural & molecular biology* 21 (1), pp. 82–87. DOI: 10.1038/nsmb.2722.

Raina, Kanak; Noblin, Devin J.; Serebrenik, Yevgeniy V.; Adams, Alison; Zhao, Connie; Crews, Craig M. (2014): Targeted protein destabilization reveals an estrogen-mediated ER stress response. In *Nature chemical biology* 10 (11), pp. 957–962. DOI: 10.1038/nchembio.1638.

Rameh, L. E.; Tolia, K. F.; Duckworth, B. C.; Cantley, L. C. (1997): A new pathway for synthesis of phosphatidylinositol-4,5-bisphosphate. In *Nature* 390 (6656), pp. 192–196. DOI: 10.1038/36621.

Ries, Jonas; Kaplan, Charlotte; Platonova, Evgenia; Eghlidi, Hadi; Ewers, Helge (2012): A simple, versatile method for GFP-based super-resolution microscopy via nanobodies. In *Nature methods* 9 (6), pp. 582–584. DOI: 10.1038/nmeth.1991.

Riordan, Kelly E.; Schneewind, Olaf (2008): YscU cleavage and the assembly of Yersinia type III secretion machine complexes. In *Molecular microbiology* 68 (6), pp. 1485–1501. DOI: 10.1111/j.1365-2958.2008.06247.x.

Roblin, Pierre; Dewitte, Frédérique; Villeret, Vincent; Biondi, Emanuele G.; Bompard, Coralie (2015): A Salmonella type three secretion effector/chaperone complex adopts a hexameric ring-like structure. In *Journal of bacteriology* 197 (4), pp. 688–698. DOI: 10.1128/JB.02294-14.

Rock, Jeremy M.; Hopkins, Forrest F.; Chavez, Alejandro; Diallo, Marieme; Chase, Michael R.; Gerrick, Elias R. et al. (2017): Programmable transcriptional repression in mycobacteria using an orthogonal CRISPR interference platform. In *Nature microbiology* 2, p. 16274. DOI: 10.1038/nmicrobiol.2016.274.

Rodrigues, Cristina D.; Enninga, Jost (2010): The 'when and whereabouts' of injected pathogen effectors. In *Nature methods* 7 (4), pp. 267–269. DOI: 10.1038/nmeth0410-267.

Rohatgi, Rajat; Ho, Hsin-yi Henry; Kirschner, Marc W. (2000): Mechanism of N-Wasp Activation by Cdc42 and Phosphatidylinositol 4,5-Bisphosphate. In *The Journal of cell biology* 150 (6), pp. 1299–1310.

Romano, Fabian B.; Tang, Yuzhou; Rossi, Kyle C.; Monopoli, Kathryn R.; Ross, Jennifer L.; Heuck, Alejandro P. (2016): Type 3 Secretion Translocators Spontaneously Assemble a Hexadecameric Transmembrane Complex. In *The Journal of biological chemistry* 291 (12), pp. 6304–6315. DOI: 10.1074/jbc.M115.681031.

Romei, Matthew G.; Boxer, Steven G. (2019): Split Green Fluorescent Proteins: Scope, Limitations, and Outlook. In *Annual review of biophysics* 48, pp. 19–44. DOI: 10.1146/annurev-biophys-051013-022846.

- Roppenser, Bernhard; Röder, Anja; Hentschke, Moritz; Ruckdeschel, Klaus; Aepfelbacher, Martin (2009): *Yersinia enterocolitica* differentially modulates RhoG activity in host cells. In *Journal of cell science* 122 (Pt 5), pp. 696–705. DOI: 10.1242/jcs.040345.
- Rosenzweig, Jason A.; Weltman, Gabriela; Plano, Gregory V.; Schesser, Kurt (2005): Modulation of *Yersinia* type three secretion system by the S1 domain of polynucleotide phosphorylase. In *The Journal of biological chemistry* 280 (1), pp. 156–163. DOI: 10.1074/jbc.M405662200.
- Rosner, B. M.; Stark, K.; Höhle, M.; Werber, D. (2012): Risk factors for sporadic *Yersinia enterocolitica* infections, Germany 2009-2010. In *Epidemiology and infection* 140 (10), pp. 1738–1747. DOI: 10.1017/S0950268811002664.
- Rosner, Bettina M.; Stark, Klaus; Werber, Dirk (2010): Epidemiology of reported *Yersinia enterocolitica* infections in Germany, 2001-2008. In *BMC public health* 10, p. 337. DOI: 10.1186/1471-2458-10-337.
- Rosner, Bettina M.; Werber, Dirk; Höhle, Michael; Stark, Klaus (2013): Clinical aspects and self-reported symptoms of sequelae of *Yersinia enterocolitica* infections in a population-based study, Germany 2009-2010. In *BMC infectious diseases* 13, p. 236. DOI: 10.1186/1471-2334-13-236.
- Rosqvist, R.; Forsberg, A.; Wolf-Watz, H. (1991): Intracellular targeting of the *Yersinia* YopE cytotoxin in mammalian cells induces actin microfilament disruption. In *Infection and immunity* 59 (12), pp. 4562–4569.
- Rosqvist, R.; Magnusson, K. E.; Wolf-Watz, H. (1994): Target cell contact triggers expression and polarized transfer of *Yersinia* YopE cytotoxin into mammalian cells. In *The EMBO journal* 13 (4), pp. 964–972.
- Ross, Julia A.; Plano, Gregory V. (2011): A C-terminal region of *Yersinia pestis* YscD binds the outer membrane secretin YscC. In *Journal of bacteriology* 193 (9), pp. 2276–2289. DOI: 10.1128/JB.01137-10.
- Roth, Michael G. (2004): Phosphoinositides in constitutive membrane traffic. In *Physiological reviews* 84 (3), pp. 699–730. DOI: 10.1152/physrev.00033.2003.
- Rothbauer, Ulrich; Zolghadr, Kourosh; Tillib, Sergei; Nowak, Danny; Schermelleh, Lothar; Gahl, Anja et al. (2006): Targeting and tracing antigens in live cells with fluorescent nanobodies. In *Nature methods* 3 (11), pp. 887–889. DOI: 10.1038/nmeth953.
- Roushan, Mohammad Reza; Zeeuw, Milou A. M. de; Hooykaas, Paul J. J.; van Heusden, Gerard Paul H. (2018): Application of phiLOV2.1 as a fluorescent marker for visualization of *Agrobacterium* effector protein translocation. In *The Plant journal : for cell and molecular biology* 96 (3), pp. 685–699. DOI: 10.1111/tpj.14060.
- Rouvoit, C. Lambert de; Sluiter, C.; Cornelis, G. R. (1992): Role of the transcriptional activator, VirF, and temperature in the expression of the pYV plasmid genes of *Yersinia enterocolitica*. In *Molecular microbiology* 6 (3), pp. 395–409. DOI: 10.1111/j.1365-2958.1992.tb01483.x.
- Rühl, Sebastian; Broz, Petr (2015): Caspase-11 activates a canonical NLRP3 inflammasome by promoting K(+) efflux. In *European journal of immunology* 45 (10), pp. 2927–2936. DOI: 10.1002/eji.201545772.
- Ryndak, Michelle B.; Chung, Hachung; London, Erwin; Bliska, James B. (2005): Role of predicted transmembrane domains for type III translocation, pore formation, and signaling by the *Yersinia*

- pseudotuberculosis YopB protein. In *Infection and immunity* 73 (4), pp. 2433–2443. DOI: 10.1128/IAI.73.4.2433–2443.2005.
- Saarikangas, Juha; Zhao, Hongxia; Lappalainen, Pekka (2010): Regulation of the actin cytoskeleton-plasma membrane interplay by phosphoinositides. In *Physiological reviews* 90 (1), pp. 259–289. DOI: 10.1152/physrev.00036.2009.
- Sahl, Steffen J.; Hell, Stefan W.; Jakobs, Stefan (2017): Fluorescence nanoscopy in cell biology. In *Nature reviews. Molecular cell biology* 18 (11), pp. 685–701. DOI: 10.1038/nrm.2017.71.
- Sano, H.; Hsu, D. K.; Yu, L.; Apgar, J. R.; Kuwabara, I.; Yamanaka, T. et al. (2000): Human galectin-3 is a novel chemoattractant for monocytes and macrophages. In *Journal of immunology (Baltimore, Md. : 1950)* 165 (4), pp. 2156–2164. DOI: 10.4049/jimmunol.165.4.2156.
- Sarantis, Helen; Balkin, Daniel M.; Camilli, Pietro de; Isberg, Ralph R.; Brumell, John H.; Grinstein, Sergio (2012): Yersinia entry into host cells requires Rab5-dependent dephosphorylation of PI(4,5)P₂ and membrane scission. In *Cell host & microbe* 11 (2), pp. 117–128. DOI: 10.1016/j.chom.2012.01.010.
- Sauvonnet, Nathalie; Pradet-Balade, Bérengère; Garcia-Sanz, Jose A.; Cornelis, Guy R. (2002): Regulation of mRNA expression in macrophages after Yersinia enterocolitica infection. Role of different Yop effectors. In *The Journal of biological chemistry* 277 (28), pp. 25133–25142. DOI: 10.1074/jbc.M203239200.
- Schaake, Julia; Drees, Anna; Grüning, Petra; Uliczka, Frank; Pisano, Fabio; Thiermann, Tanja et al. (2014): Essential Role of Invasin for Colonization and Persistence of Yersinia enterocolitica in Its Natural Reservoir Host, the Pig. In *Infection and immunity* 82 (3), pp. 960–969. DOI: 10.1128/IAI.01001-13.
- Schesser, K.; Frithz-Lindsten, E.; Wolf-Watz, H. (1996): Delineation and mutational analysis of the Yersinia pseudotuberculosis YopE domains which mediate translocation across bacterial and eukaryotic cellular membranes. In *Journal of bacteriology* 178 (24), pp. 7227–7233.
- Schesser, K.; Spiik, A. K.; Dukuzumuremyi, J. M.; Neurath, M. F.; Pettersson, S.; Wolf-Watz, H. (1998): The yopJ locus is required for Yersinia-mediated inhibition of NF-kappaB activation and cytokine expression: YopJ contains a eukaryotic SH2-like domain that is essential for its repressive activity. In *Molecular microbiology* 28 (6), pp. 1067–1079. DOI: 10.1046/j.1365-2958.1998.00851.x.
- Schlumberger, Markus C.; Müller, Andreas J.; Ehrbar, Kristin; Winnen, Brit; Duss, Iwan; Stecher, Bärbel; Hardt, Wolf-Dietrich (2005): Real-time imaging of type III secretion: Salmonella SipA injection into host cells. In *Proceedings of the National Academy of Sciences of the United States of America* 102 (35), pp. 12548–12553. DOI: 10.1073/pnas.0503407102.
- Schmid-Burgk, Jonathan L.; Gaidt, Moritz M.; Schmidt, Tobias; Ebert, Thomas S.; Bartok, Eva; Hornung, Veit (2015): Caspase-4 mediates non-canonical activation of the NLRP3 inflammasome in human myeloid cells. In *European journal of immunology* 45 (10), pp. 2911–2917. DOI: 10.1002/eji.201545523.
- Schmidt, G.; Sehr, P.; Wilm, M.; Selzer, J.; Mann, M.; Aktories, K. (1997): Gln 63 of Rho is deamidated by Escherichia coli cytotoxic necrotizing factor-1. In *Nature* 387 (6634), pp. 725–729. DOI: 10.1038/42735.
- Schoberle, Taylor J.; Chung, Lawton K.; McPhee, Joseph B.; Bogin, Ben; Bliska, James B. (2016): Uncovering an Important Role for YopJ in the Inhibition of Caspase-1 in Activated Macrophages and

- Promoting *Yersinia pseudotuberculosis* Virulence. In *Infection and immunity* 84 (4), pp. 1062–1072. DOI: 10.1128/IAI.00843-15.
- Schreiner, Madeleine; Niemann, Hartmut H. (2012): Crystal structure of the *Yersinia enterocolitica* type III secretion chaperone SycD in complex with a peptide of the minor translocator YopD. In *BMC structural biology* 12, p. 13. DOI: 10.1186/1472-6807-12-13.
- Schroeder, Gunnar N.; Hilbi, Hubert (2007): Cholesterol is required to trigger caspase-1 activation and macrophage apoptosis after phagosomal escape of *Shigella*. In *Cellular microbiology* 9 (1), pp. 265–278. DOI: 10.1111/j.1462-5822.2006.00787.x.
- Selle, Kurt; Barrangou, Rodolphe (2015): Harnessing CRISPR-Cas systems for bacterial genome editing. In *Trends in microbiology* 23 (4), pp. 225–232. DOI: 10.1016/j.tim.2015.01.008.
- Shao, Feng; Vacratsis, Panayiotis O.; Bao, Zhaoqin; Bowers, Katherine E.; Fierke, Carol A.; Dixon, Jack E. (2003): Biochemical characterization of the *Yersinia* YopT protease: cleavage site and recognition elements in Rho GTPases. In *Proceedings of the National Academy of Sciences of the United States of America* 100 (3), pp. 904–909. DOI: 10.1073/pnas.252770599.
- Sharan, Shyam K.; Thomason, Lynn C.; Kuznetsov, Sergey G.; Court, Donald L. (2009): Recombineering: a homologous recombination-based method of genetic engineering. In *Nature protocols* 4 (2), pp. 206–223. DOI: 10.1038/nprot.2008.227.
- Shayegani, M.; DeForge, I.; McGlynn, D. M.; Root, T. (1981): Characteristics of *Yersinia enterocolitica* and related species isolated from human, animal, and environmental sources. In *Journal of Clinical Microbiology* 14 (3), pp. 304–312.
- Shenkerman, Yael; Elharar, Yifat; Vishkautzan, Marina; Gur, Eyal (2014): Efficient and simple generation of unmarked gene deletions in *Mycobacterium smegmatis*. In *Gene* 533 (1), pp. 374–378. DOI: 10.1016/j.gene.2013.09.082.
- Shu, Xiaokun; Lev-Ram, Varda; Deerinck, Thomas J.; Qi, Yingchuan; Ramko, Ericka B.; Davidson, Michael W. et al. (2011): A genetically encoded tag for correlated light and electron microscopy of intact cells, tissues, and organisms. In *PLoS biology* 9 (4), e1001041. DOI: 10.1371/journal.pbio.1001041.
- Simonet, M.; Falkow, S. (1992): Invasin expression in *Yersinia pseudotuberculosis*. In *Infection and immunity* 60 (10), pp. 4414–4417.
- Singh, Atul K.; Carette, Xavier; Potluri, Lakshmi-Prasad; Sharp, Jared D.; Xu, Ranfei; Prsic, Sladjana; Husson, Robert N. (2016): Investigating essential gene function in *Mycobacterium tuberculosis* using an efficient CRISPR interference system. In *Nucleic acids research* 44 (18), e143. DOI: 10.1093/nar/gkw625.
- Singh, Vijay; Wang, Shenliang; Chan, Ke Min; Clark, Spencer A.; Kool, Eric T. (2013): Genetically encoded multispectral labeling of proteins with polyfluorophores on a DNA backbone. In *Journal of the American Chemical Society* 135 (16), pp. 6184–6191. DOI: 10.1021/ja4004393.
- Skrzypek, E.; Cowan, C.; Straley, S. C. (1998): Targeting of the *Yersinia pestis* YopM protein into HeLa cells and intracellular trafficking to the nucleus. In *Molecular microbiology* 30 (5), pp. 1051–1065. DOI: 10.1046/j.1365-2958.1998.01135.x.

- Song, Houhui; Niederweis, Michael (2007): Functional expression of the Flp recombinase in *Mycobacterium bovis* BCG. In *Gene* 399 (2), pp. 112–119. DOI: 10.1016/j.gene.2007.05.005.
- Sorg, Joseph A.; Blaylock, Bill; Schneewind, Olaf (2006): Secretion signal recognition by YscN, the *Yersinia* type III secretion ATPase. In *Proceedings of the National Academy of Sciences of the United States of America* 103 (44), pp. 16490–16495. DOI: 10.1073/pnas.0605974103.
- Sory, M. P.; Boland, A.; Lambermont, I.; Cornelis, G. R. (1995): Identification of the YopE and YopH domains required for secretion and internalization into the cytosol of macrophages, using the *cyaA* gene fusion approach. In *Proceedings of the National Academy of Sciences of the United States of America* 92 (26), pp. 11998–12002. DOI: 10.1073/pnas.92.26.11998.
- Sory, M. P.; Cornelis, G. R. (1994): Translocation of a hybrid YopE-adenylate cyclase from *Yersinia enterocolitica* into HeLa cells. In *Molecular microbiology* 14 (3), pp. 583–594. DOI: 10.1111/j.1365-2958.1994.tb02191.x.
- Stagge, Franziska; Mitronova, Gyuzel Y.; Belov, Vladimir N.; Wurm, Christian A.; Jakobs, Stefan (2013): SNAP-, CLIP- and Halo-tag labelling of budding yeast cells. In *PloS one* 8 (10), e78745. DOI: 10.1371/journal.pone.0078745.
- Straley, S. C.; Bowmer, W. S. (1986): Virulence genes regulated at the transcriptional level by Ca²⁺ in *Yersinia pestis* include structural genes for outer membrane proteins. In *Infection and immunity* 51 (2), pp. 445–454.
- Straley, S. C.; Cibull, M. L. (1989): Differential clearance and host-pathogen interactions of YopE- and YopK- YopL- *Yersinia pestis* in BALB/c mice. In *Infection and immunity* 57 (4), pp. 1200–1210.
- Straley, S. C.; Perry, R. D. (1995): Environmental modulation of gene expression and pathogenesis in *Yersinia*. In *Trends in microbiology* 3 (8), pp. 310–317. DOI: 10.1016/s0966-842x(00)88960-x.
- Straley, S. C.; Plano, G. V.; Skrzypek, E.; Haddix, P. L.; Fields, K. A. (1993): Regulation by Ca²⁺ in the *Yersinia* low-Ca²⁺ response. In *Molecular microbiology* 8 (6), pp. 1005–1010. DOI: 10.1111/j.1365-2958.1993.tb01644.x.
- Strobel, E.; Heesemann, J.; Mayer, G.; Peters, J.; Müller-Wehrich, S.; Emmerling, P. (2000): Bacteriological and Serological Findings in a Further Case of Transfusion-Mediated *Yersinia enterocolitica* Sepsis. In *Journal of Clinical Microbiology* 38 (7), pp. 2788–2790.
- Sun, Jin-Peng; Wu, Li; Fedorov, Alexander A.; Almo, Steven C.; Zhang, Zhong-Yin (2003): Crystal structure of the *Yersinia* protein-tyrosine phosphatase YopH complexed with a specific small molecule inhibitor. In *The Journal of biological chemistry* 278 (35), pp. 33392–33399. DOI: 10.1074/jbc.M304693200.
- Swarts, Daan C.; van der Oost, John; Jinek, Martin (2017): Structural Basis for Guide RNA Processing and Seed-Dependent DNA Targeting by CRISPR-Cas12a. In *Molecular cell* 66 (2), 221-233.e4. DOI: 10.1016/j.molcel.2017.03.016.
- Sweet, Charles R.; Conlon, Joseph; Golenbock, Douglas T.; Goguen, Jon; Silverman, Neal (2007): YopJ targets TRAF proteins to inhibit TLR-mediated NF- κ B, MAPK and IRF3 signal transduction. In *Cellular microbiology* 9 (11), pp. 2700–2715. DOI: 10.1111/j.1462-5822.2007.00990.x.

- Tan, Sue Zanne; Reisch, Christopher R.; Prather, Kristala L. J. (2018): A Robust CRISPR Interference Gene Repression System in *Pseudomonas*. In *Journal of bacteriology* 200 (7). DOI: 10.1128/JB.00575-17.
- Tardy, F.; Homblé, F.; Neyt, C.; Wattiez, R.; Cornelis, G. R.; Ruyschaert, J. M.; Cabiaux, V. (1999): *Yersinia enterocolitica* type III secretion-translocation system: channel formation by secreted Yops. In *The EMBO journal* 18 (23), pp. 6793–6799. DOI: 10.1093/emboj/18.23.6793.
- Tengel, Tobias; Sethson, Ingmar; Francis, Matthew S. (2002): Conformational analysis by CD and NMR spectroscopy of a peptide encompassing the amphipathic domain of YopD from *Yersinia*. In *European journal of biochemistry* 269 (15), pp. 3659–3668. DOI: 10.1046/j.1432-1033.2002.03051.x.
- Terebiznik, Mauricio R.; Vieira, Otilia V.; Marcus, Sandra L.; Slade, Andrea; Yip, Christopher M.; Trimble, William S. et al. (2002): Elimination of host cell PtdIns(4,5)P₂ by bacterial SigD promotes membrane fission during invasion by *Salmonella*. In *Nature cell biology* 4 (10), pp. 766–773. DOI: 10.1038/ncb854.
- Thomason, Lynn C.; Sawitzke, James A.; Li, Xintian; Costantino, Nina; Court, Donald L. (2014): Recombineering: genetic engineering in bacteria using homologous recombination. In *Current protocols in molecular biology* 106, 1.16.1-39. DOI: 10.1002/0471142727.mb0116s106.
- Thurston, Teresa L. M.; Wandel, Michal P.; Muhlinen, Natalia von; Foeglein, Agnes; Randow, Felix (2012): Galectin 8 targets damaged vesicles for autophagy to defend cells against bacterial invasion. In *Nature* 482 (7385), pp. 414–418. DOI: 10.1038/nature10744.
- Tian, Pingfang; Wang, Jia; Shen, Xiaolin; Rey, Justin Forrest; Yuan, Qipeng; Yan, Yajun (2017): Fundamental CRISPR-Cas9 tools and current applications in microbial systems. In *Synthetic and systems biotechnology* 2 (3), pp. 219–225. DOI: 10.1016/j.synbio.2017.08.006.
- Traenkle, Bjoern; Emele, Felix; Anton, Roman; Poetz, Oliver; Haeussler, Ragna S.; Maier, Julia et al. (2015): Monitoring interactions and dynamics of endogenous beta-catenin with intracellular nanobodies in living cells. In *Molecular & cellular proteomics : MCP* 14 (3), pp. 707–723. DOI: 10.1074/mcp.M114.044016.
- Trasak, Claudia; Zenner, Gerhardt; Vogel, Annette; Yüsekdog, Gülnihal; Rost, René; Haase, Ilka et al. (2007): *Yersinia* protein kinase YopO is activated by a novel G-actin binding process. In *The Journal of biological chemistry* 282 (4), pp. 2268–2277. DOI: 10.1074/jbc.M610071200.
- Treille, Georges-Félix; Yersin, Alexandre (1894): La peste bubonique à Hong Kong. In *Ville Congrès international d'hygiène et de démographie. Budapest, Hongrie*, pp. 310–311. Available online at <https://hal-pasteur.archives-ouvertes.fr/pasteur-00442093/document>.
- Tripal, Philipp; Bauer, Michael; Naschberger, Elisabeth; Mörtinger, Thomas; Hohenadl, Christine; Cornali, Emmanuelle et al. (2007): Unique features of different members of the human guanylate-binding protein family. In *Journal of interferon & cytokine research : the official journal of the International Society for Interferon and Cytokine Research* 27 (1), pp. 44–52. DOI: 10.1089/jir.2007.0086.
- Troisfontaines, Paul; Cornelis, Guy R. (2005): Type III secretion: more systems than you think. In *Physiology (Bethesda, Md.)* 20, pp. 326–339. DOI: 10.1152/physiol.00011.2005.

Trülzsch, Konrad; Oellerich, Mark F.; Heesemann, Jürgen (2007): Invasion and dissemination of *Yersinia enterocolitica* in the mouse infection model. In *Advances in experimental medicine and biology* 603, pp. 279–285. DOI: 10.1007/978-0-387-72124-8_25.

Trülzsch, Konrad; Roggenkamp, Andreas; Aepfelbacher, Martin; Wilharm, Gottfried; Ruckdeschel, Klaus; Heesemann, Jürgen (2003): Analysis of chaperone-dependent Yop secretion/translocation and effector function using a mini-virulence plasmid of *Yersinia enterocolitica*. In *International journal of medical microbiology : IJMM* 293 (2-3), pp. 167–177. DOI: 10.1078/1438-4221-00251.

Trülzsch, Konrad; Sporleder, Thorsten; Igwe, Emeka I.; Rüssmann, Holger; Heesemann, Jürgen (2004): Contribution of the major secreted yops of *Yersinia enterocolitica* O:8 to pathogenicity in the mouse infection model. In *Infection and immunity* 72 (9), pp. 5227–5234. DOI: 10.1128/IAI.72.9.5227-5234.2004.

Tseng, Tsai-Tien; Tyler, Brett M.; Setubal, João C. (2009): Protein secretion systems in bacterial-host associations, and their description in the Gene Ontology. In *BMC Microbiology* 9 Suppl 1, S2. DOI: 10.1186/1471-2180-9-S1-S2.

Ungewickell, Alexander; Hugge, Christopher; Kisseleva, Marina; Chang, Shao-Chun; Zou, Jun; Feng, Yucheng et al. (2005): The identification and characterization of two phosphatidylinositol-4,5-bisphosphate 4-phosphatases. In *Proceedings of the National Academy of Sciences of the United States of America* 102 (52), pp. 18854–18859. DOI: 10.1073/pnas.0509740102.

Valencia Lopez, Maria Jose; Schimmeck, Hanna; Gropengießer, Julia; Middendorf, Lukas; Quitmann, Melanie; Schneider, Carola et al. (2019): Activation of the macroautophagy pathway by *Yersinia enterocolitica* promotes intracellular multiplication and egress of yersiniae from epithelial cells. In *Cellular microbiology* 21 (9), e13046. DOI: 10.1111/cmi.13046.

van Engelenburg, Schuyler B.; Palmer, Amy E. (2008): Quantification of real-time *Salmonella* effector type III secretion kinetics reveals differential secretion rates for SopE2 and SptP. In *Chemistry & biology* 15 (6), pp. 619–628. DOI: 10.1016/j.chembiol.2008.04.014.

van Engelenburg, Schuyler B.; Palmer, Amy E. (2010): Imaging type-III secretion reveals dynamics and spatial segregation of *Salmonella* effectors. In *Nature methods* 7 (4), pp. 325–330. DOI: 10.1038/nmeth.1437.

van Pelt, W.; Wit, M. A. S. de; Wannet, W. J. B.; Ligtvoet, E. J. J.; Widdowson, M. A.; van Duynhoven, Y. T. H. P. (2003): Laboratory surveillance of bacterial gastroenteric pathogens in The Netherlands, 1991-2001. In *Epidemiology and infection* 130 (3), pp. 431–441.

Vasta, Gerardo R. (2009): Roles of galectins in infection. In *Nature reviews. Microbiology* 7 (6), pp. 424–438. DOI: 10.1038/nrmicro2146.

Vergne, Isabelle; Chua, Jennifer; Lee, Hwang-Ho; Lucas, Megan; Belisle, John; Deretic, Vojo (2005): Mechanism of phagolysosome biogenesis block by viable *Mycobacterium tuberculosis*. In *Proceedings of the National Academy of Sciences of the United States of America* 102 (11), pp. 4033–4038. DOI: 10.1073/pnas.0409716102.

Vergunst, Annette C.; van Lier, Miranda C. M.; den Dulk-Ras, Amke; Stüve, Thomas A. Grosse; Ouwehand, Anette; Hooykaas, Paul J. J. (2005): Positive charge is an important feature of the C-terminal transport

signal of the VirB/D4-translocated proteins of *Agrobacterium*. In *Proceedings of the National Academy of Sciences of the United States of America* 102 (3), pp. 832–837. DOI: 10.1073/pnas.0406241102.

Viboud, G. I.; Bliska, J. B. (2001): A bacterial type III secretion system inhibits actin polymerization to prevent pore formation in host cell membranes. In *The EMBO journal* 20 (19), pp. 5373–5382. DOI: 10.1093/emboj/20.19.5373.

Viboud, Gloria I.; Bliska, James B. (2005): *Yersinia* outer proteins: role in modulation of host cell signaling responses and pathogenesis. In *Annual review of microbiology* 59, pp. 69–89. DOI: 10.1146/annurev.micro.59.030804.121320.

Viboud, Gloria I.; Mejía, Edison; Bliska, James B. (2006): Comparison of YopE and YopT activities in counteracting host signalling responses to *Yersinia pseudotuberculosis* infection. In *Cellular microbiology* 8 (9), pp. 1504–1515. DOI: 10.1111/j.1462-5822.2006.00729.x.

Virant, David; Traenkle, Bjoern; Maier, Julia; Kaiser, Philipp D.; Bodenhöfer, Mona; Schmees, Christian et al. (2018): A peptide tag-specific nanobody enables high-quality labeling for dSTORM imaging. In *Nature communications* 9 (1), p. 930. DOI: 10.1038/s41467-018-03191-2.

Wagner, Samuel; Königsmaier, Lisa; Lara-Tejero, María; Lefebvre, Matthew; Marlovits, Thomas C.; Galán, Jorge E. (2010): Organization and coordinated assembly of the type III secretion export apparatus. In *Proceedings of the National Academy of Sciences of the United States of America* 107 (41), pp. 17745–17750. DOI: 10.1073/pnas.1008053107.

Waldo, G. S.; Standish, B. M.; Berendzen, J.; Terwilliger, T. C. (1999): Rapid protein-folding assay using green fluorescent protein. In *Nature biotechnology* 17 (7), pp. 691–695. DOI: 10.1038/10904.

Wang, He; Avican, Kemal; Fahlgren, Anna; Erttmann, Saskia F.; Nuss, Aaron M.; Dersch, Petra et al. (2016): Increased plasmid copy number is essential for *Yersinia* T3SS function and virulence. In *Science* 353 (6298), pp. 492–495. DOI: 10.1126/science.aaf7501.

Wang, Jianchang; Wang, Jinfeng; Li, Ruiwen; Shi, Ruihan; Liu, Libing; Yuan, Wanzhe (2018a): Evaluation of an incubation instrument-free reverse transcription recombinase polymerase amplification assay for rapid and point-of-need detection of canine distemper virus. In *Journal of virological methods* 260, pp. 56–61. DOI: 10.1016/j.jviromet.2018.07.007.

Wang, Tong; Wang, Min; Zhang, Qingwen; Cao, Shiyang; Li, Xiang; Qi, Zhizhen et al. (2019): Reversible Gene Expression Control in *Yersinia pestis* by Using an Optimized CRISPR Interference System. In *Applied and environmental microbiology* 85 (12). DOI: 10.1128/AEM.00097-19.

Wang, Xiaogang; Hybiske, Kevin; Stephens, Richard S. (2018b): Direct visualization of the expression and localization of chlamydial effector proteins within infected host cells. In *Pathogens and disease* 76 (2). DOI: 10.1093/femspd/fty011.

Wang, Xiaoying; Parashar, Kaustubh; Sitaram, Ananya; Bliska, James B. (2014): The GAP activity of type III effector YopE triggers killing of *Yersinia* in macrophages. In *PLoS Pathogens* 10 (8), e1004346. DOI: 10.1371/journal.ppat.1004346.

Warawa, J.; Finlay, B. B.; Kenny, B. (1999): Type III secretion-dependent hemolytic activity of enteropathogenic *Escherichia coli*. In *Infection and immunity* 67 (10), pp. 5538–5540.

- Wattiau, P.; Bernier, B.; Deslée, P.; Michiels, T.; Cornelis, G. R. (1994): Individual chaperones required for Yop secretion by *Yersinia*. In *Proceedings of the National Academy of Sciences of the United States of America* 91 (22), pp. 10493–10497. DOI: 10.1073/pnas.91.22.10493.
- Wauters, G.; Le Minor, L.; Chalon, A. M. (1971): Antigènes somatiques et flagellaires des *Yersinia enterocolitica*. In *Annales de l'Institut Pasteur* 120 (5), pp. 631–642.
- Wiedmaier, Nina; Müller, Steffen; Köberle, Martin; Manncke, Birgit; Krejci, Juliane; Autenrieth, Ingo B.; Bohn, Erwin (2008): Bacteria induce CTGF and CYR61 expression in epithelial cells in a lysophosphatidic acid receptor-dependent manner. In *International journal of medical microbiology : IJMM* 298 (3-4), pp. 231–243. DOI: 10.1016/j.ijmm.2007.06.001.
- Wilharm, Gottfried; Lehmann, Verena; Krauss, Kristina; Lehnert, Beatrix; Richter, Susanna; Ruckdeschel, Klaus et al. (2004): *Yersinia enterocolitica* type III secretion depends on the proton motive force but not on the flagellar motor components MotA and MotB. In *Infection and immunity* 72 (7), pp. 4004–4009. DOI: 10.1128/IAI.72.7.4004-4009.2004.
- Wille, Thorsten; Barlag, Britta; Jakovljevic, Vladimir; Hensel, Michael; Sourjik, Victor; Gerlach, Roman G. (2015): A gateway-based system for fast evaluation of protein-protein interactions in bacteria. In *PloS one* 10 (4), e0123646. DOI: 10.1371/journal.pone.0123646.
- Wilson, I. A.; Niman, H. L.; Houghten, R. A.; Chersonson, A. R.; Connolly, M. L.; Lerner, R. A. (1984): The structure of an antigenic determinant in a protein. In *Cell* 37 (3), pp. 767–778. DOI: 10.1016/0092-8674(84)90412-4.
- Woestyn, S.; Sory, M. P.; Boland, A.; Lequenne, O.; Cornelis, G. R. (1996): The cytosolic SycE and SycH chaperones of *Yersinia* protect the region of YopE and YopH involved in translocation across eukaryotic cell membranes. In *Molecular microbiology* 20 (6), pp. 1261–1271. DOI: 10.1111/j.1365-2958.1996.tb02645.x.
- Wolters, Manuel; Boyle, Erin C.; Lardong, Kerstin; Trülzsch, Konrad; Steffen, Anika; Rottner, Klemens et al. (2013): Cytotoxic necrotizing factor-Y boosts *Yersinia* effector translocation by activating Rac protein. In *The Journal of biological chemistry* 288 (32), pp. 23543–23553. DOI: 10.1074/jbc.M112.448662.
- Wolters, Manuel; Zobiak, Bernd; Nauth, Theresa; Aepfelbacher, Martin (2015): Analysis of *Yersinia enterocolitica* Effector Translocation into Host Cells Using Beta-lactamase Effector Fusions. In *Journal of visualized experiments : JoVE* (104). DOI: 10.3791/53115.
- Wong, Ka-Wing; Isberg, Ralph R. (2003): Arf6 and phosphoinositol-4-phosphate-5-kinase activities permit bypass of the Rac1 requirement for beta1 integrin-mediated bacterial uptake. In *The Journal of experimental medicine* 198 (4), pp. 603–614. DOI: 10.1084/jem.20021363.
- Wren, Brendan W. (2003): The yersiniae - a model genus to study the rapid evolution of bacterial pathogens. In *Nature reviews. Microbiology* 1 (1), pp. 55–64. DOI: 10.1038/nrmicro730.
- Xu, Tao; Li, Yongchao; He, Zhili; van Nostrand, Joy D.; Zhou, Jizhong (2017): Cas9 Nickase-Assisted RNA Repression Enables Stable and Efficient Manipulation of Essential Metabolic Genes in *Clostridium cellulolyticum*. In *Frontiers in microbiology* 8, p. 1744. DOI: 10.3389/fmicb.2017.01744.

- Yamano, Takashi; Nishimasu, Hiroshi; Zetsche, Bernd; Hirano, Hisato; Slaymaker, Ian M.; Li, Yinqing et al. (2016): Crystal Structure of Cpf1 in Complex with Guide RNA and Target DNA. In *Cell* 165 (4), pp. 949–962. DOI: 10.1016/j.cell.2016.04.003.
- Yan, Mei-Yi; Yan, Hai-Qin; Ren, Gai-Xian; Zhao, Ju-Ping; Guo, Xiao-Peng; Sun, Yi-Cheng (2017): CRISPR-Cas12a-Assisted Recombineering in Bacteria. In *Applied and environmental microbiology* 83 (17). DOI: 10.1128/AEM.00947-17.
- Yang, Qinghua; Li, Xiaoyang; Tu, Haitao; Pan, Shen Q. (2017): Agrobacterium-delivered virulence protein VirE2 is trafficked inside host cells via a myosin XI-K-powered ER/actin network. In *Proceedings of the National Academy of Sciences of the United States of America* 114 (11), pp. 2982–2987. DOI: 10.1073/pnas.1612098114.
- Yao, Ruilian; Di Liu; Jia, Xiao; Zheng, Yuan; Liu, Wei; Xiao, Yi (2018): CRISPR-Cas9/Cas12a biotechnology and application in bacteria. In *Synthetic and systems biotechnology* 3 (3), pp. 135–149. DOI: 10.1016/j.synbio.2018.09.004.
- Yao, Tony; Meccas, Joan; Healy, James I.; Falkow, Stanley; Chien, Yueh-hsiu (1999): Suppression of T and B Lymphocyte Activation by a *Yersinia pseudotuberculosis* Virulence Factor, YopH. In *The Journal of experimental medicine* 190 (9), pp. 1343–1350.
- Young, Alexandra M.; Minson, Michael; McQuate, Sarah E.; Palmer, Amy E. (2017): Optimized Fluorescence Complementation Platform for Visualizing Salmonella Effector Proteins Reveals Distinctly Different Intracellular Niches in Different Cell Types. In *ACS infectious diseases* 3 (8), pp. 575–584. DOI: 10.1021/acsinfecdis.7b00052.
- Young, Briana M.; Young, Glenn M. (2002): Evidence for targeting of Yop effectors by the chromosomally encoded Ysa type III secretion system of *Yersinia enterocolitica*. In *Journal of bacteriology* 184 (20), pp. 5563–5571. DOI: 10.1128/JB.184.20.5563-5571.2002.
- Young, G. M.; Badger, J. L.; Miller, V. L. (2000): Motility is required to initiate host cell invasion by *Yersinia enterocolitica*. In *Infection and immunity* 68 (7), pp. 4323–4326. DOI: 10.1128/iai.68.7.4323-4326.2000.
- Yu, D.; Ellis, H. M.; Lee, E. C.; Jenkins, N. A.; Copeland, N. G.; Court, D. L. (2000): An efficient recombination system for chromosome engineering in *Escherichia coli*. In *Proceedings of the National Academy of Sciences of the United States of America* 97 (11), pp. 5978–5983. DOI: 10.1073/pnas.100127597.
- Yu, Fei; Finley, Russell L.; Raz, Avraham; Kim, Hyeong-Reh Choi (2002): Galectin-3 translocates to the perinuclear membranes and inhibits cytochrome c release from the mitochondria. A role for synexin in galectin-3 translocation. In *The Journal of biological chemistry* 277 (18), pp. 15819–15827. DOI: 10.1074/jbc.M200154200.
- Zetsche, Bernd; Gootenberg, Jonathan S.; Abudayyeh, Omar O.; Slaymaker, Ian M.; Makarova, Kira S.; Essletzbichler, Patrick et al. (2015): Cpf1 is a single RNA-guided endonuclease of a class 2 CRISPR-Cas system. In *Cell* 163 (3), pp. 759–771. DOI: 10.1016/j.cell.2015.09.038.
- Zhang, Yongdeng; Lara-Tejero, María; Bewersdorf, Jörg; Galán, Jorge E. (2017): Visualization and characterization of individual type III protein secretion machines in live bacteria. In *Proceedings of the*

- National Academy of Sciences of the United States of America* 114 (23), pp. 6098–6103. DOI: 10.1073/pnas.1705823114.
- Zhang, Yue; Barbieri, Joseph T. (2005): A leucine-rich motif targets *Pseudomonas aeruginosa* ExoS within mammalian cells. In *Infection and immunity* 73 (12), pp. 7938–7945. DOI: 10.1128/IAI.73.12.7938-7945.2005.
- Zhang, Yue; Romanov, Galina; Bliska, James B. (2011): Type III secretion system-dependent translocation of ectopically expressed Yop effectors into macrophages by intracellular *Yersinia pseudotuberculosis*. In *Infection and immunity* 79 (11), pp. 4322–4331. DOI: 10.1128/IAI.05396-11.
- Zhang, Yue; Ting, Adrian T.; Marcu, Kenneth B.; Bliska, James B. (2005): Inhibition of MAPK and NF-kappa B pathways is necessary for rapid apoptosis in macrophages infected with *Yersinia*. In *Journal of immunology (Baltimore, Md. : 1950)* 174 (12), pp. 7939–7949. DOI: 10.4049/jimmunol.174.12.7939.
- Zhang, Z. Y. (1995): Kinetic and mechanistic characterization of a mammalian protein-tyrosine phosphatase, PTP1. In *The Journal of biological chemistry* 270 (19), pp. 11199–11204. DOI: 10.1074/jbc.270.19.11199.
- Zhang, Z. Y.; Clemens, J. C.; Schubert, H. L.; Stuckey, J. A.; Fischer, M. W.; Hume, D. M. et al. (1992): Expression, purification, and physicochemical characterization of a recombinant *Yersinia* protein tyrosine phosphatase. In *The Journal of biological chemistry* 267 (33), pp. 23759–23766.
- Zhao, Juping; Sun, Yicheng (2018): CRISPR-Cas12a-Assisted Recombineering in *Yersinia pestis*. In Ruifu Yang (Ed.): *Yersinia Pestis Protocols*, vol. 20. Singapore: Springer Singapore (Springer Protocols Handbooks), pp. 165–172.
- Zhou, Honglin; Monack, Denise M.; Kayagaki, Nobuhiko; Wertz, Ingrid; Yin, Jianpin; Wolf, Beni; Dixit, Vishva M. (2005): *Yersinia* virulence factor YopJ acts as a deubiquitinase to inhibit NF-kappa B activation. In *The Journal of experimental medicine* 202 (10), pp. 1327–1332. DOI: 10.1084/jem.20051194.
- Zilkenat, Susann; Franz-Wachtel, Mirita; Stierhof, York-Dieter; Galán, Jorge E.; Macek, Boris; Wagner, Samuel (2016): Determination of the Stoichiometry of the Complete Bacterial Type III Secretion Needle Complex Using a Combined Quantitative Proteomic Approach. In *Molecular & cellular proteomics : MCP* 15 (5), pp. 1598–1609. DOI: 10.1074/mcp.M115.056598.
- Zlokarnik, G.; Negulescu, P. A.; Knapp, T. E.; Mere, L.; Burres, N.; Feng, L. et al. (1998): Quantitation of transcription and clonal selection of single living cells with beta-lactamase as reporter. In *Science* 279 (5347), pp. 84–88. DOI: 10.1126/science.279.5347.84.
- Zwack, Erin E.; Feeley, Eric M.; Burton, Amanda R.; Hu, Baofeng; Yamamoto, Masahiro; Kanneganti, Thirumala-Devi et al. (2017): Guanylate Binding Proteins Regulate Inflammasome Activation in Response to Hyperinjected *Yersinia* Translocon Components. In *Infection and immunity* 85 (10). DOI: 10.1128/IAI.00778-16.

8. Table of figures

| | |
|--|----|
| Figure 1 Structure of type three secretion system..... | 10 |
| Figure 2 A structure and size comparison of conventional and advanced visualization approaches..... | 25 |
| Figure 3 Cas12a-crRNA in complex with its dsDNA target. | 28 |
| Figure 4 Schematic of the strains expressing Halo, SNAP, CLIP, and split-GFP tagged effector Yops..... | 34 |
| Figure 5 Effect of tagging YopH with Halo, SNAP and CLIP on expression, secretion, cytotoxicity and translocation..... | 38 |
| Figure 6 Comparison of effector protein visualization using antibody staining and self-labeling enzyme tags. | 41 |
| Figure 7 Complementation of GFP11 labeled mRFP-Rab5 and GFP1-10 as proof of principle..... | 42 |
| Figure 8 Effect of split-GFP tagging YopE on protein secretion from <i>Yersinia</i> strains compared to the wild type..... | 43 |
| Figure 9 YopE-GFP11 visualization in the cytosol of the host. | 45 |
| Figure 10 GFP complementation after pTTSS+YopE-GFP11 infection in live imaging. | 46 |
| Figure 11 Tag insertion positions for YopB and YopD in the host cell membrane..... | 46 |
| Figure 12 Effect of GFP11 insertion in YopD and YopB on expression, secretion, cytotoxicity, translocation and immunofluorescence staining. | 49 |
| Figure 13 Lack of GFP signal at split-GFP tagged pore proteins..... | 50 |
| Figure 14 Effect of ALFA-tag insertion in YopD on expression, secretion, translocation, cytotoxicity and protein interaction. | 52 |
| Figure 15 Immunofluorescence staining of YopD-ALFA with the anti-ALFA nanobody in infected cells.... | 54 |
| Figure 16 Live imaging of pore formation using nanobody staining for ALFA tagged YopD..... | 55 |
| Figure 17 Analysis of signal appearance of PLC δ -PH prior to YopD-ALFA detection. | 57 |
| Figure 18 Analysis of galectin-3 signal appearance relative to YopD-ALFA detection. | 59 |
| Figure 19 Comparison of double stranded HDR fragment and single stranded oligo for insertion of a tag into YopB and YopD..... | 99 |

9. List of tables

| | |
|--|-----|
| Table 1 Overview of experimental results using tagged <i>Yersinia</i> outer proteins | 33 |
| Table 2 Efficiency of CRISPR-Cas12a assisted recombineering in <i>Y. enterocolitica</i> | 48 |
| Table 3 Devices | 72 |
| Table 4 Technical data for the Laser-Scanning-microscope (Leica TCS SP8 X) | 73 |
| Table 5 Technical data for the spinning disk microscope (Visitron SD-TIRF) | 74 |
| Table 6 Disposables | 75 |
| Table 7 Kits, enzymes, reagents | 76 |
| Table 8 Buffer composition | 77 |
| Table 9 Primary antibodies..... | 78 |
| Table 10 Secondary antibodies | 79 |
| Table 11 Nanobodies, dyes and labeling substrates | 79 |
| Table 12 Growth media for the cultivation of <i>Y. enterocolitica</i> | 80 |
| Table 13 Antibiotics and additives for the cultivation and selection of <i>Y. enterocolitica</i> | 80 |
| Table 14 Growth media for the cultivation of eukaryotic cells | 80 |
| Table 15 Expression plasmids..... | 81 |
| Table 16 Primer and sequences | 82 |
| Table 17 <i>Yersinia enterocolitica</i> strains..... | 85 |
| Table 18 Eukaryotic cells | 88 |
| Table 19 Software..... | 88 |
| Table 20 Phusion PCR reaction mix..... | 94 |
| Table 21 Phusion thermocycler program | 94 |
| Table 22 GoTaq G2 PCR reaction mix..... | 94 |
| Table 23 GoTaq G2 thermocycler program | 95 |
| Table 24 Restriction enzyme digest..... | 95 |
| Table 25 Ligation | 96 |
| Table 26 Composition of a 10% acrylamide SDS-PAGE mini gel | 104 |

10. Abbreviations

| Abbreviation | Meaning |
|--------------------|--|
| °C | degree celsius |
| μF | microfarrad |
| μg | microgram |
| μl | microliter |
| μm | micrometer |
| μM | micromolar |
| 4Cys | tetracysteine hairpin loop |
| A | adenine |
| aa | amino acid |
| Ail | attachment invasion locus |
| Amp | ampicillin |
| APS | ammonium persulfate |
| Arf6 | adenosine diphosphate ribosylation factor 6 |
| Arp2/3 | actin-related proteins 2/3 |
| ATP | adenosine triphosphate |
| BFP | blue fluorescent protein |
| bla | β-lactamase |
| bp | base pair |
| BSA | bovine serum albumin |
| C | cytosine |
| CaCl ₂ | calcium chloride |
| Cas | CRISPR-associated protein |
| CCD-camera | charge-coupled device camera |
| CCF2AM | coumarin cephalosporin fluorescein |
| Cdc42 | cell division cycle 42 GTP binding protein |
| cDNA | copy DNA |
| CDR2 | complementary-determining region 2 |
| cm | centimeter |
| CM | chloramphenicol |
| CNF-1 | cytotoxic necrotising factor 1 |
| CNF-Y | <i>Yersinia</i> cytotoxic necrotising factor |
| cpDHFR | circularly permuted bacterial dihydrofolate reductase |
| CRD | carbohydrate-recognition domain |
| CRISPR | clustered regularly interspaced short palindromic repeats |
| crRNA | CRISPR RNA |
| CyA | cyclase A |
| DAPI | 4',6-diamidino-2-phenylindole |
| ddH ₂ O | double distilled water |
| DDX3 | DEAD box helicase 3 |
| DMEM | Dulbecco's modified eagle's medium |
| DMSO | dimethyl sulfoxide |
| DNA | deoxyribonucleic acid |
| dNTP | deoxyribonucleotide triphosphate (dATP, dCTP, dGTP, dTTP) |
| dsDNA | double stranded DNA |
| EDTA | ethylenediamine tetra-acetic acid |
| EFSA | European Food Safety Authority |
| eGFP | Enhanced GFP |
| EGTA | ethylene glycol-bis(β-aminoethyl ether)-N,N,N',N'-tetraacetic acid |
| et al. | and others (lat.: „et alteri“) |

| | |
|-----------|--|
| EtOH | ethanol |
| Fab | fragment-antigen-binding domain |
| F-actin | filamentous actin |
| FAE | follicle-associated epithelium |
| FAK | focal adhesion kinase |
| FCS | fetal calf serum |
| Flag | peptide sequence DYKDDDDK |
| FIAsH | fluorescein based biarsenical dye |
| fwd | forward |
| FyB | Fyn-binding protein |
| G | guanine |
| g | gram |
| <i>g</i> | relative centrifugal force |
| GAP | GTPase activating protein |
| GBP | guanylate-binding proteins |
| GDP | guanosine diphosphate |
| GEF | guanine nucleotide exchange factor |
| GFP | green fluorescent protein |
| GFP11 | 11 th beta strand of GFP |
| GFP1-10 | beta strands 1-10 of GFP |
| GST | glutathione-S-transferase |
| GTP | guanosine 5-triphosphate |
| h | hour |
| HA | hemagglutinin, peptide sequence YPYDVPDYA |
| HDR | homology directed repair |
| Hom | Homology arm |
| HPI | high pathogenicity island |
| HRP | horseradish peroxidase |
| IF | immunofluorescence |
| Ig | immunoglobulin |
| IL | interleukin |
| Inpp5b | inositol polyphosphate-5-phosphatase B |
| IPTG | isopropyl β -D-1-thiogalactopyranoside |
| Kan | kanamycin |
| kDa | kilo Dalton |
| L | liter |
| LB | lysogeny broth (Luria-Bertani) |
| LCR | low calcium response |
| LcrV | low calcium response protein V |
| LOV | light, oxygen and voltage-sensing domain |
| LPS | lipopolysaccharide |
| LRRs | leucine-rich-repeats |
| M | molar |
| mA | milliampere |
| MACS | magnetic cell sorting system |
| MAP | mitogen activated protein |
| MAPK | mitogen activated protein kinase |
| MAPKAP-K1 | MAPK-activated protein kinase-1 |
| M-cells | microfold cells |
| MDa | megadalton |
| mg | milligram |
| min | minute |
| ml | millilitre |

| | |
|---------------------|--|
| mM | millimolar |
| mm | millimeter |
| MOI | multiplicity of infection |
| mRNA | messenger-RNA |
| ms | millisecond |
| NADPH | nicotinamide adenine dinucleotide phosphate |
| Nb | nanobody |
| NbALFA | nanobody against the ALFA-tag |
| NFκB | nuclear factor 'kappa-light-chainenhancer' of activated B-cells |
| ng | nanogram |
| NHEJ | non-homologous end joining |
| NLRP3 | nucleotide-binding domain, leucine-rich-containing family, pyrin domain-containing-3 |
| nM | nanomolar |
| nm | nanometer |
| N-WASP | neural Wiskott-Aldrich syndrome protein |
| OD | optical density |
| ORCL | Lowe oculocerebrorenal syndrome protein |
| p130 ^{Cas} | Crk-associated substrate |
| PAGE | polyacrylamide gel electrophoresis |
| PAM | protospacer adjacent motive |
| PBS | phosphate buffered saline |
| PCR | polymerase chain reaction |
| PFA | paraformaldehyde |
| pH | power of /potential for hydrogen |
| PH | pleckstrin homology (PH) domain |
| PhoA | alkaline phosphatase |
| PI(3)K | phosphatidylinositol-3-kinase |
| PI(3)P | phosphatidylinositol-3-phosphate |
| PI(3,4,5)P3 | phosphatidylinositol-3,4,5-triphosphate |
| PI(4)P | phosphatidylinositol-4-phosphate |
| PI(4,5)P2 | phosphatidylinositol-4,5-bisphosphate |
| PI(5)P | phosphatidylinositol-5-phosphate |
| PIP(5)K | phosphoinositol-4-phosphate-5-kinase |
| PKN2 | protein kinase N2 |
| PLA2 | phospholipase A2 |
| PLC | phospholipase C |
| pM | picomolar |
| pmol | picomol |
| PMSF | phenylmethylsulfonyl fluoride |
| Pop | <i>Pseudomonas</i> outer protein |
| PP | Peyer's patches |
| PRK | protein kinase C-related kinases |
| PVDF | polyvinylidene difluoride membrane |
| pYV | <i>Yersinia</i> virulence plasmid |
| Rab | Ras-associated binding |
| Rac | Ras-related C3 botulinum toxin substrate |
| rev | reverse |
| RFP | red fluorescent protein |
| RhoA | Ras homolog gene family, member A |
| RNA | ribonucleic acid |
| rpm | revolutions per minute |
| RSK | ribosomal S6 kinase |
| RT | room temperature |

| | |
|----------|---|
| s | second |
| SD | standard deviation |
| SDS | sodium dodecylsulfate |
| SDS-PAGE | SDS-polyacrylamide-gelelektrophoresis |
| RSK1 | p90 ribosomal S6 kinase 1 or MAPKAP-K1 |
| sfGFP | superfolder GFP |
| SKAP-HOM | human src kinase associated phosphoprotein 2 |
| SPI | <i>Salmonella</i> pathogenicity island |
| Spt | spectinomycin |
| SRE | serum response element |
| ssDNA | single stranded DNA |
| SV40 | simian virus 40 |
| T | thymine |
| T4SS | type four secretion system |
| TAE | Tris-acetate-EDTA |
| Taq | <i>Thermus aquaticus</i> |
| TBS | Tris buffered saline |
| TBS-T | TBS with Tween-20 |
| TCA | trichloroacetic acid |
| TEM | transmission electron microscopy |
| TEMED | N,N,N',N'-tetramethyl ethylenediamine |
| TMR | tetramethylrhodamine |
| tracrRNA | transactivating crRNA |
| Tris | Tris-(hydroxymethyl)aminomethane |
| TTSS | type three secretion system |
| U | uracil |
| UKE | Universitätsklinikum Hamburg-Eppendorf |
| UV | ultraviolet |
| V | volt |
| v/v | volume per volume |
| VHH | variable heavy domain of heavy chain antibody or nanobody |
| w/v | weight per volume |
| WB | Western blot |
| Xcell | extracellular |
| YadA | <i>Yersinia</i> adhesin A |
| Ymt | <i>Yersinia</i> murine toxin |
| Yop | <i>Yersinia</i> outer proteins/ <i>Yersinia</i> effector proteins |
| YpkA | <i>Yersinia</i> protein kinase A |
| Ysc | <i>Yersinia</i> secretion |
| Yst | <i>Yersinia</i> stable toxin |
| α | anti- |
| Ω | Ohm |

11. Acknowledgement

An dieser Stelle möchte ich mich bei allen bedanken, die direkt oder indirekt zum Abschluss dieser Arbeit beigetragen haben. Dank eurer Unterstützung habe ich es bis hierher geschafft.

Mein erster Dank geht an meinen Doktorvater Prof. Dr. Martin Aepfelbacher, der mich in meinem Projekt mit kritischen Fragen und einem großen Erfahrungsschatz immer wieder auf den richtigen Weg gebracht hat. Einen sehr großen Anteil an meiner Arbeit hat auch Manuel. Vielen Dank für die unzähligen tollen Ideen, die Unterstützung, die unerschütterliche Motivation und das intensive Korrekturlesen. Ohne dich wäre das alles so viel schwieriger gewesen!

Allgemein geht ein ganz großer Dank an die alten und neuen Mitglieder meiner phantastischen Mibi-Familie, die mir geholfen haben die ganzen Unwägbarkeiten zu überstehen und bis hierher durchzuhalten. Vielen Dank für die großartige Ablenkung und den ein oder anderen denkwürdigen Freitag! Zunächst danke ich natürlich den Mitgliedern meiner Arbeitsgruppe. Dabei möchte ich besonders Aileen erwähnen die mich einen Großteil der Zeit begleitet hat – Dank dir gab es immer ein offenes Ohr und nie einen langweiligen Tag im Labor! Aber ich möchte auch nicht Franzi, Theresa und Marie vergessen, die immer einen guten Tipp parat hatten und mir geholfen haben mich in der UKE-Welt zurecht zu finden. Vielen Dank, dass ihr mich so toll aufgenommen habt und euer Wissen bereitwillig mit mir geteilt habt. Vielen Dank auch an Claudia für ihre fachliche Hilfe, ihre zuverlässige Organisation im Labor und die vielen netten Gespräche. Danken möchte ich auch Laura dafür uns style-technisch immer wieder zu überraschen und das jetzt auch noch mit einer süßen Mini-Laura Ausgabe. Bedanken möchte ich mich auch bei den guten Seelen unserer Arbeitsgruppe Astrid und Dorte, die es mit ihrer Wärme und ihrem Witz doch ab und an geschafft haben ein bisschen mehr Niveau in den Laden zu bringen. Besonders zu erwähnen sind Alex und Gunnar, die es geschafft haben mir zu helfen auch an stressigen Tagen die Welt nicht zu ernst zu nehmen. Vielen Dank für die unendliche Menge an Quatsch, die mir den Alltag versüßt! I also want to thank Sahaja for her incredible empathy, her refreshing innocence and many fits of laughter after too much coffee and sugar. Thanks for the encouragement and kind words and keeping me company with our crazy labmates. Ein großer Dank geht auch an die Jungs und Mädels der anderen Labore für die beste Gesellschaft und die absurdesten Themen beim Mittagessen und Kaffeetrinken. Danken möchte ich unserem alten Hasen Manja, die trotz ihrer grummeligen Art ganz viel Herz mitbringt und jeder Party das „gewisse Extra“ verleiht, unserem neuen Hasen Marie, die uns alle zuverlässig mit Gebäck versorgt und auch Vero für ihre unfassbar leuchtenden Augen beim Anblick von Süßwaren und ihrer stets positiven Art. Vielen Dank auch an Dennis für die viel zu starken Drinks und die großartigste Kombination aus bravem Mädchen und Ghetto die mir bisher begegnet ist und Tabea, die mich wie kein anderer motiviert die nötige Bewegung zu

bekommen aber auch immer für ein ausführliches Essen zu haben ist. Ich möchte auch Andi und Paul danken für jeden Quatsch zu haben zu sein und endlich etwas männliche Unterstützung in unsere Mittagessensrunde zu bringen. Danke auch an unsere verrückten Mediziner Henning, Hannes und Ben dafür, dass sie sich in unsere Biologenrunde getraut haben. Ganz besonders möchte ich Samira danken immer für mich da zu sein, ob es darum geht ein paar Tränen zusammen zu vergießen oder auch den ein oder anderen Schnaps zu viel zu trinken – beides hab' ich in den letzten Jahren gebraucht!

Auch ein großes Dankeschön an alle Ehemaligen, die ich jetzt nicht erwähnt habe, unsere netten UKE Mitarbeiter, die uns die Arbeit in den Laboren ermöglichen sowie Virgilio und Bernd von der UMIF, die mit viel Herz und Sorgfalt unsere wunderbaren Mikroskope am Laufen halten.

Danken möchte ich auch meinen Freunden außerhalb des Labors aus Schulzeiten, dem Studium in Göttingen und Brisbane oder der Hamburger Zeit. Vielen Dank für die großen und kleinen Abenteuer, eure phantastische Gesellschaft und die stete Unterstützung und Aufmunterung.

Ein besonderer Dank geht an Clemens. Du hast viel mitmachen müssen in der vergangenen Zeit, aber durch deine besonnene Art konntest du mich doch immer wieder beruhigen. Vielen Dank für deine Unterstützung, die nötige Verbindung zur Realität und die exzellente kulinarische Versorgung, die doch so manchen Tag retten konnte!

Schließlich möchte ich mich noch bei meiner Familie bedanken, die mich immer unterstützt hat und für mich da war.

12. Lebenslauf

Lebenslauf wurde aus datenschutzrechtlichen Gründen entfernt.

13. Eidesstattliche Versicherung

Ich versichere ausdrücklich, dass ich die Arbeit selbständig und ohne fremde Hilfe verfasst, andere als die von mir angegebenen Quellen und Hilfsmittel nicht benutzt und die aus den benutzten Werken wörtlich oder inhaltlich entnommenen Stellen einzeln nach Ausgabe (Auflage und Jahr des Erscheinens), Band und Seite des benutzten Werkes kenntlich gemacht habe.

Ferner versichere ich, dass ich die Dissertation bisher nicht einem Fachvertreter an einer anderen Hochschule zur Überprüfung vorgelegt oder mich anderweitig um Zulassung zur Promotion beworben habe.

Ich erkläre mich einverstanden, dass meine Dissertation vom Dekanat der Medizinischen Fakultät mit einer gängigen Software zur Erkennung von Plagiaten überprüft werden kann.

Hamburg, Juni 2020

Maren Rudolph